LEABHARLANN CHOLÁISTE NA TRÍONÓIDE, BAILE ÁTHA CLIATH | TRINITY COLLEGE LIBRARY DUBLIN
Ollscoil Átha Cliath | The University of Dublin

Terms and Conditions of Use of Digitised Theses from Trinity College Library Dublin

Copyright statement

All material supplied by Trinity College Library is protected by copyright (under the Copyright and Related Rights Act, 2000 as amended) and other relevant Intellectual Property Rights. By accessing and using a Digitised Thesis from Trinity College Library you acknowledge that all Intellectual Property Rights in any Works supplied are the sole and exclusive property of the copyright and/or other IPR holder. Specific copyright holders may not be explicitly identified. Use of materials from other sources within a thesis should not be construed as a claim over them.

A non-exclusive, non-transferable licence is hereby granted to those using or reproducing, in whole or in part, the material for valid purposes, providing the copyright owners are acknowledged using the normal conventions. Where specific permission to use material is required, this is identified and such permission must be sought from the copyright holder or agency cited.

Liability statement

By using a Digitised Thesis, I accept that Trinity College Dublin bears no legal responsibility for the accuracy, legality or comprehensiveness of materials contained within the thesis, and that Trinity College Dublin accepts no liability for indirect, consequential, or incidental, damages or losses arising from use of the thesis for whatever reason. Information located in a thesis may be subject to specific use constraints, details of which may not be explicitly described. It is the responsibility of potential and actual users to be aware of such constraints and to abide by them. By making use of material from a digitised thesis, you accept these copyright and disclaimer provisions. Where it is brought to the attention of Trinity College Library that there may be a breach of copyright or other restraint, it is the policy to withdraw or take down access to a thesis while the issue is being resolved.

Access Agreement

By using a Digitised Thesis from Trinity College Library you are bound by the following Terms & Conditions. Please read them carefully.

I have read and I understand the following statement: All material supplied via a Digitised Thesis from Trinity College Library is protected by copyright and other intellectual property rights, and duplication or sale of all or part of any of a thesis is not permitted, except that material may be duplicated by you for your research use or for educational purposes in electronic or print form providing the copyright owners are acknowledged using the normal conventions. You must obtain permission for any other use. Electronic or print copies may not be offered, whether for sale or otherwise to anyone. This copy has been supplied on the understanding that it is copyright material and that no quotation from the thesis may be published without proper acknowledgement.

Investigating the Function Of Sorting Nexin 8 And Chemokines In Niemann Pick Type C Disease

Gillian Muirhead

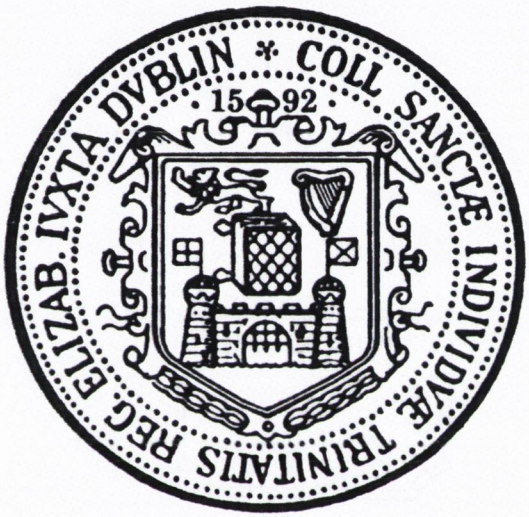

Transfer thesis submitted to University of Dublin, Trinity College

For the degree of Doctorate of Philosophy

January 2013

Supervisor: Professor Kumlesh K Dev
Institute of Neuroscience
Dept of Physiology
Trinity College Dublin

TRINITY COLLEGE
2 4 MAY 2013
LIBRARY DUBLIN

Thesis 10052

I. DECLARATION

I declare that this thesis has not been submitted for a degree at this or any other university and it is entirely my own work.

I agree to deposit this thesis in the University's open access institutional repository or allow the library to do so on my behalf, subject to Irish Copyright legislation and Trinity College Library conditions of use and acknowledgement.

Gillian Muirhead 24/01/13

Gillian Muirhead

ii. Acknowledgements

To those who know me, it will come as no surprise that this acknowledgements section took some time to write. I can do blunt, brash and (in my opinion) funny, but heartfelt and emotional are not qualities that I would be associated with, so please bear with me!

Initially I would like to thank my supervisor Professor Kumlesh Dev for putting his faith in me and hiring me three years ago. Not only have I learnt a lot under your leadership, but I have gained a new name by which I am now known by more than my own..... Miss Gillian Burnside. I would also like to thank all the staff of TCIN and the Department of Physiology both past and present for all their hard work, especially Lesley Penney, Ann Connick, Alice Jordan, Quentin Commerford, Ciaran Connelly, Gillian Roddie and Lisa Beattie. I would also like to thank Mark and the other staff members of Trinity College Bioresources for their assistance over the last three years. I would also like to thank our collaborators; Dr Stuart Cobb's Lab in Glasgow for their patience in helping generate my lentivirus. I would also like to thank Health Research Board Ireland for my funding. Without everybody's effort the work in this thesis would not have been possible.

I would like to thank all the KKD lab members past and present for their help and support, Priyanka Dutta, Grandpa Deb, Graham Sheridan, Marika Doucet, Ola Rutowska and Kara O'Connell and apologise for any of my science related rages that you may have encountered. A special thanks goes to Adam Pritchard for not only being a good brain to pick, but also being a good friend. My lunchtimes will not be the same without a pig and heifer salad and some QI chat. I would like to thank my student Isabelle for her input into this work, and for vastly improving my French (yes, three sentences was a vast improvement!). The last member of the KKD lab I have to thank is Fiona. We may have begun as lab mates and quickly moved on to drinking buddies, then progressed to house-mates but I know we will continue to be lifelong friends. Your friendship and support over the last two years, through the ups and the downs, the cheese and wine boldness and onezie fun was vital for the completion of this thesis (and for the retention of my sanity).

Words cannot express how thankful I am for the support of my family, without you I would not be where I am today. I would like to thank my brother Alan (and his wife Lesley) for setting an example of how hard work and intelligence can breed success. I would also like to thank my good-looking Auntie

Joyce for always helping me see the best in a bad situation, and for always being able to make me laugh. To Mum, you have been there when I needed you most, always with words of encouragement and love. Thank you for showing me how to be a strong and independent woman (girl power!). And Dad, your financial and moral support, friendship, love and bad jokes have been indispensible in getting me to this point in my education, thank you, from the bottom of my heart.

Now to thank one **Dr** Luke Healy, I don't even know where to begin. From our very first trip to the Wescht coast, you have taken me into your friendship and your family; whom I also have to thank for their support in my time here. You are a truly unique person who looks on life with an attitude of positivity and adventure, qualities that have helped generate countless memories in our time together during our PhDs. It is with no exaggeration that I say without your love, support and understanding (and presents of my favourite sweets) this thesis would not have happened.

Finally, I would like to thank everyone that I have had the pleasure of befriending in my time in Dublin. You have all helped to make this fair city a place that I call home. The three years I have spent here have been some of the most memorable of my life, even if I never quite got a hang of the accent.

TABLE OF CONTENTS

I. DECLARATION 1
II. ACKNOWLEDGEMENTS 2
III. LIST OF FIGURES 8
IV. ABSTRACT 11
V. ABBREVIATIONS 12

CHAPTER 1. INTRODUCTION **14**

1.1.0 NIEMANN PICK DISEASE 15
1.1.1 NIEMANN PICK DISEASE IS A NEURODEGENERATIVE DISEASE 15
1.1.2 NIEMANN PICK PROTEINS ARE MUTATED IN NPC DISEASE 15
1.1.3 NPC DIAGNOSIS AND CURRENT THERAPIES 16
1.1.4 ANIMAL MODELS OF NPC ARE AVAILABLE 19
1.2.0 INFLAMMATION AND NEURODEGENERATION 22
1.2.1 NEURONAL ANATOMY 22
1.2.2 ASTROCYTES SENSE NEURONAL ACTIVITY 22
1.2.3 MICROGLIA ARE CNS RESIDENT IMMUNE CELLS 23
1.2.4 GLIAL ACTIVATION, LEUKOCYTE INFILTRATION AND OXIDATIVE STRESS INFLUENCE NEURODEGENERATION 23
1.3.0 STEROL HOMEOSTASIS 25
1.3.1 LIPIDS AND CHOLESTEROL PLAY A CRUCIAL ROLE WITHIN THE CNS 25
1.3.2 U18666A IS A VERSATILE TOOL FOR INVESTIGATING CHOLESTEROL METABOLISM 26
1.3.3 THE SREBP PATHWAY CONTROLS CHOLESTEROL HOMEOSTASIS 30
1.3.4 INSIGS REGULATE SREBP TRAFFICKING 31
1.3.5 SNX8 IS A NOVEL ACTIVATOR OF THE SREBP PATHWAY 31
1.4.0 THE SORTING NEXIN FAMILY 32
1.4.1 THE SORTING NEXIN FAMILY IS INVOLVED IN SORTING AND TRAFFICKING 32
1.4.2 THE SNX-BAR FAMILY ARE A DISTINCT SUB-GROUP OF SORTING NEXINS 34
1.5.0 THE IMPORTANCE OF DOMAINS 34
1.5.1 THE BAR DOMAIN IS INVOLVED IN MEMBRANE CURVATURE 34
1.5.2 THE PX DOMAIN TARGETS PI MOTIFS IN CELL MEMBRANES 37
1.5.3 SORTING NEXIN 8 IS A MEMBER OF THE SNX-BAR SUB-FAMILY 37
1.6.0 THE CYCLE OF INTERNALISATION 38
1.6.1 ENDOCYTOSIS AND INTRACELLULAR SORTING ARE CRITICAL CELLULAR PROCESSES 38
1.6.2 THE RETROMER COMPLEX CONTROLS RETROGRADE SORTING 42
1.7.0 AIMS AND HYPOTHESIS 45
1.7.1 PROJECT AIMS AND HYPOTHESIS 45

CHAPTER 2. MATERIALS AND METHODS **47**

2.0.0 MATERIALS AND EQUIPMENT 48
2.1.0 METHODS 52
2.1.1 MOLECULAR BIOLOGY 52
2.1.2 BACTERIAL COMPETENT CELL PREPARATION 52

2.1.3 Heat shock transformation and plasmid DNA extraction 52
2.1.4 Polymerase Chain Reaction and restriction digestion 53
2.1.5 Dephosphorylation, Ligation and Transformation 53
2.2.0 Biochemistry 54
2.2.1 SDS - Poly Acrylamide Gel Electrophoresis and Western Blotting 54
2.3.0 Heterologous And Primary Cell Culture 55
2.3.1 Organotypic Hippocampal And Cerebellar Slice Cultures 55
2.3.2 Organotypic Hippocampal and Cerebellar Slice Staining 55
2.3.3 Coverslip, Plate and Flask Preparation for Primary Cell Culture 56
2.3.4 Brain Dissection For Primary Cultures 56
2.3.5 Astrocyte Culture 56
2.3.6 Neuronal Culture And Treatments 57
2.3.7 Primary Cell Line Staining 58
2.3.8 HEK 293T Cell Culture and shRNA Transfection 59
2.4.0 Lentivirus Preparation 59
2.4.1 HEK 293T Cell Preparation 59
2.4.2 Transfection Of Lentiviral Plasmids And Collection of Viral Particles 59
2.5.0 Immuno Assays 60
2.5.1 Cytokine Array 60
2.5.2 Analysis Of Chemokine Release By ELISA 61
2.6.0 mRNA Analysis by reverse transcriptase polymerase chain reaction 61
2.6.1 RNA Extraction 61
2.6.2 Reverse Transcription For cDNA Synthesis 62
2.6.3 cDNA Amplification By RT-PCR 62
2.6.4 PCR Quantification 62
2.7.0 Computational And Statistical Analysis 63
2.7.1 Western Blot and Cytokine Array Quantification 63
2.7.2 Quantification Of Myelination In Cerebellar Slices 63

Chapter 3. Generation And Characterisation Of SNX8 Lentivirus 66

3.1.0 Aims And Hypothesis 67
3.2.0 Abstract 68
3.3.0 Introduction 69
3.3.1 Lentiviruses Are Efficient Molecular Tools 69
3.3.2 The Retroviral Life Cycle Allows High Transfection 69
3.3.3 Components Of The Lentivirus System 70
3.3.4 Why Clone SNX8 Into A Lentiviral Vector? 71
3.4.0 Results 73
3.4.1 Preparation of the Insert and Vector 73
3.4.2 HEK 293T Cell Transfection Confirmation 73
3.4.3 GFP-SNX8 Lentiviral Transfection in Neurons 74
3.4.4 GFP-SNX8 Lentiviral Transfection in Neurons Survival Assay 74

3.5.0 Discussion 85
3.5.1 Summary Of Results 85
3.5.2 Comparing Viral Vector Transduction Systems For Use In The CNS 85
3.5.3 Lentiviral Mediated Gene Therapy For Parkinson's Disease 86
3.5.4 Lentiviral Mediated Gene Therapy For Alzheimer's Disease 87
3.5.5 Lentiviral Systems For Use In Lysosomal Storage Disorders 88
3.5.6 Moving On To The Next Chapter 88

Chapter 4. Investigating And Manipulating SNX8 Expression 90

4.1.0 Aims And Hypothesis 91
4.2.0 Abstract 92
4.3.0 Introduction 93
4.3.1 The Function Of The Sorting Nexin Family 93
4.3.2 The Role Of BAR Domain Sorting Nexins Within the CNS 93
4.3.3 The Role Of PX Domain Sorting Nexins Within the CNS 94
4.3.4 The Role Of Other Domain Containing SNXs In The CNS 95
4.3.5 The Proposed Role Of SNX8 Within The CNS 95
4.4.0 Results 98
4.4.1 SNX8 Expression in HEK 293T Cells is Downregulated by shRNA Interference 98
4.4.2 SNX8 is Expressed in Rat Tissues 98
4.4.3 SNX8 is Differentially Expressed in Hippocampal and Cerebellar Slice Cultures 99
4.4.4 SNX8 Is Differentially Expressed In Hippocampal And Cerebellar Dissociated Culutres 99
4.4.5 SNX8 Is Not Expressed In Glial Cells 99
4.4.6 SNX8 Levels Are Unchanged In Neurons Following Treatment With Cholesterol 100
4.4.7 Mevinolin Treatment Causes A Decrease In SNX8 Expression In Neurons 100
4.4.8 Treatment With U18666A Results In A Decrease In SNX8 Expression In Neurons 101
4.4.9 GFP-SNX8 Localisation Is Not Altered In Differing Cholesterol Environments 101
4.4.10 GFP-SNX8 Overexpression Does Not Alter Cholesterol Content In Normal Conditions 101
4.4.11 U18666A Mediated Cholesterol Accumulation Is Not Altered By GFP-SNX8 Overexpression 102
4.4.12 GFP-SNX8 Overexpression Does Not Alter Cholesterol Content In The Presence Of Mevinolin 102
4.4.13 GFP-SNX8 Overexpression Decreases Cholesterol Levels In High Cholesterol Conditions 103
4.5.0 Discussion 118
4.5.1 SNX8 Is Widely Expressed Within The Rat CNS 118
4.5.2 Differential Expression Of SNX8 In Neuronal Subsets 118
4.5.3 SNX8 Expression Is Restricted To Neurons, Not Glia 119
4.5.4 SNX8 Expression Is Reduced In Low Cholesterol Environments 119
4.5.5 SNX8 Overexpression Alters Cholesterol Localisation 120

Chapter 5. Investigating The Chemokine Profile of U18666A Treatment 121

5.1.0 Aims And Hypothesis 122
5.2.0 Abstract 123
5.3.0 Introduction 124
5.3.1 Cytokines And Chemokines Are Involved In Neuroinflammation 124

5.3.2 The Role Of LIX (CXCL5) In Chemotaxis And Disease 125
5.3.3 The Production Of Cytokines/Chemokines Due To Toll Like Receptor Stimulation 125
5.3.4 Neuroinflammation Has Been Implicated In Niemann Pick Type C Disease 126
5.4.0 Results 131
5.4.1 Mixed Cortical Primary Cultures are Comprised of 68% Neurons 131
5.4.2 U18666A Treatment Increases Chemokine Release From Neuronal Cultures 131
5.4.3 U18666A Treatment Increases CXC and CCL Chemokine Release 132
5.4.4 U18666A Treatment Increases LIX Release In A Time And Concentration Dependent Manner 132
5.4.5 Analysis of U18666A treatment on cell survival 133
5.4.6 U18666A Mediated Release Of LIX Is Astrocyte Independent 134
5.4.7 The Statin Mevinolin Reverses U18666A Increases In mRNA Levels Of CXC Chemokines 134
5.4.8 The Statin Mevinolin Reverses The U18666A-Mediated Increase In LIX Release 135
5.4.9 U18666A Mediated LIX Release Is Coupled To NFκB Signalling 136
5.4.10 U18666A Treatment Causes Demyelination In Cerebellar Slice Cultures 136
5.5.0 Discussion 150
5.5.1 U18666A Treatment Increases Levels Of Chemokine In Neuronal Cultures 150
5.5.2 U18666A Treatment Causes Time And Concentration Dependant Changes In LIX Levels 151
5.5.3 Astrocytes Do Not Increase Levels Of LIX In Response To U18666A 152
5.5.4 U18666A Induced Increases In mRNA Of LIX/IP-10 Were Reversed With Mevinolin Treatment 153
5.5.5 U18666A Stimulated The NFκB Pathway 154
5.5.6 U18666A Treatment Causes Significant Demyelination Of Cerebellar Neurons 154
Chapter 6. Discussion 156
6.1.0 Discussion 157
6.1.1 Opening Remarks 157
6.1.2 Is Differential SNX8 Expression Indicative Of Differences In Function? 157
6.1.3 Low And Accumulated Cholesterol Decreases SNX8 Expression; Implications For NPC 158
6.1.4 Does SNX8 Overexpression In High Cholesterol Conditions Cause Changes in Trafficking? 159
6.1.5 Why Are Chemokine Levels Increased In A Neuronal Model Of NPC Disease? 159
6.1.6 How May An Increase In Levels Of LIX Be Linked To Neurodegeneration? 160
6.1.7 Which CNS Cell Type Is Contributing To U18666A Mediated LIX Release? 161
6.1.8 Why Is NFκB Signalling Activated By U18666A In Neurons? 161
6.1.9 How Does Statin Treatment Decrease Chemokine mRNA Synthesis? 162
6.2.0 Closing Remarks 162
Bibliography 166

III. List Of Figures

Chapter 1. Introduction

1.1 Niemann Pick Disease Type C Features 17

1.2 NPC Proteins 18

1.3 U18666A Structure And Function 21

1.4 Cholesterol Synthesis And Metabolism 28

1.5 Cholesterol Movement Within The CNS 29

1.6 SREBP Pathway 33

1.7 Sorting Nexin Subfamilies 35

1.8 Sorting Nexin BAR Family 36

1.9 SNX8 Predicted Secondary Structure 39

1.10 Mammalian SNX8 Alignment 40

1.11 SNX8 And SNX1 Alignment 41

1.12 Intracellular Trafficking And Retrograde Transport 43

1.13 The Effects Of SNX8 Knockdown On Shiga And Ricin Toxin Trafficking 44

Chapter 2. Materials And Methods

2.1 Summary Of Antibodies Used In Immunohistochemistry 51

2.2 Cloning Flow Chart 64

2.3 List Of Primers Used In Cloning 65

Chapter 3. Generation And Characterisation Of SNX8 Lentivirus

3.1 Retroviral Life Cycle 72

3.2 Original SNX8 Insert From Commercial Vector 75

3.3 pEGFP-C2-SNX8 Cloning: Mammalian Vector 76

3.4 pLL4.0-GFP-SNX8 Cloning: Lentiviral Vector 77

3.5 Agarose Gel Confirmations Of pEGFP-C2-SNX8 and pLL4.0-GFP-SNX8 Cloning 78

3.6 Sequence Verification For pEGFP-C2-SNX8 Cloning 79

3.7 Sequence Verification For pLL4.0-GFP-SNX8 80

3.8 HEK 293T Cell Transfection Confirmations For pLL4.0-GFP-SNX8 plasmid 81

3.9 GFP-SNX8 Expression In Neurons Is Primarily Perinuclear 82
3.10 Biochemical Confirmation Of SNX8 Lentiviral Overexpression 83
3.11 Lentivirus Transfection Does Not Affect Cell Survival 84

Chapter 4. Investigation And Manipulation Of SNX8 Expression

4.1 Summary Of The Function Of Sorting Nexins Within The CNS 97
4.2 shRNA InterFerence Of SNX8 Expression In HEK 293T Cells 104
4.3 Western Blot Of SNX8 Expression Profile 105
4.4 Hippocampal And Cerebellar Slice Staining 106
4.5 Hippocampal And Cerebellar Dissociated Culture Staining 107
4.6 Astrocytes Do Not Express SNX8 108
4.7 Microglia Do Not Express SNX8 109
4.8 Excess Cholesterol Does Not Change SNX8 Expression In Neurons 110
4.9 Mevinolin; A Statin Causes Decreased SNX8 Expression In Neurons 111
4.10 U18666A Treatment Causes A Decrease In SNX8 Expression In Neurons 112
4.11 GFP-SNX8 Localisation Is Not Altered In Differing Cholesterol Environments 113
4.12 GFP-SNX8 Transfection Does Not Affect Cholesterol Levels Under Normal Conditions 114
4.13 U18666A Mediated Cholesterol Accumulation Is Not Altered By SNX8 Overexpression 115
4.14 In Low Cholesterol Conditions GFP-SNX8 Expression Does Not Alter Cholesterol Levels 116
4.15 SNX8 Overexpression Alters Cholesterol Localisation In A High Cholesterol Environment 117

Chapter 5. Investigating The Chemokine Profile Of U18666A Treatment

5.1 CC Receptors And Ligands 128
5.2 CXC Receptors And Ligands 129
5.3 Chemokine Receptor Activation And Signalling 130
5.4 Mixed Cortical Primary Cultures Are Comprised Of 68% Neurons 137
5.5 U18666A Causes Changes In Chemoline Levels In Mixed Cultures 138
5.6 U18666A Causes An Increase In CXCR2 Activating Chemokine Release In Mixed Cultures 139
5.7 U18666A Causes An Increase In CXCR3 Activating Chemokine Release In Mixed Cultures 140
5.8 U18666A Causes An Increase In CCL Chemokines In Mixed Cultures 141
5.9 U18666A Treatment Causes Increases In LIX Release From Mixed Cultures 142

5.10 Cell Survival Is Affected By U18666A In A Time And Concentration Dependent Manner 143
5.11 Determination Of The Purity Of Astrocyte Cultures 144
5.12 LIX Release From Astrocytes Is Not Increased By U18666A 145
5.13 U18666A Treatment Causes Changes In CXC Chemokine mRNA Levels 146
5.14 LIX Release From Mixed Cultures Is Modulated In Differing Cholesterol Environments 147
5.15 U18666A Treatment Of Neurons Causes Phosphorylation And Reduction Of IκBα 148
5.16 U18666A Treatment Causes Demyelination In Cerebellar Slices 149
5.17 U18666A Mediated LIX Release Hypothesis 155

Chapter 6. Discussion

6.1 Hypothesis Of SNX8 Expression And SREBP Function 164
6.2 The Function Of SNX8 And LIX In A Cellular Model Of NPC Disease 165

IV. ABSTRACT

It was shown that SNX8 (sorting nexin 8), a member of the sorting nexin super-family, plays a role in regulating the SREBP pathway (sterol regulatory element binding protein) of cholesterol homeostasis. Members of the SNX family are involved in intracellular trafficking and sorting of protein cargoes. It is hypothesised that SNX8 plays a role in synaptic transmission and its aberrant function may result in neurodegenerative disorders. To elucidate the role of SNX8 in neuronal function, the expression profile was investigated within the central nervous system using both slice cultures and dissociated primary cultures of neurons and glia. Here, the expression profile of SNX8 within the central nervous system and localisation in neuronal cells is reported (**Results 2**). This information was used to investigate the function of SNX8 via its over expression using a lentiviral-mediated delivery system (**Results 1**). Cholesterol homeostasis is also upset in Niemann Pick Type C Disease (NPC). it was recently shown that NSAID treatment reduced symptoms and delayed disease progression in a mouse model of NPC disease. The compound U18666a is widely used to mimic the cholesterol accumulation observed in NPC disease. We treated neuronal cultures with U18666a and investigated the inflammatory profile that resulted, hereby elucidating the inflammatory aspect of NPC disease (**Results 3**). Based on these novel findings it is hoped to further understand the impact of aberrant cholesterol homeostasis on brain function.

V. ABBREVIATIONS

The following abbreviations have been used in this thesis;

°C:	Degree Celsius
µF:	Microfarad
µg:	Microgram
µl:	Microliter
Aβ:	Beta Amyloid
AD:	Alzheimer's Disease
amp:	Ampicillin
ApoE:	Apolipoprotein E
Arf:	ADP ribosylation factor
APP:	Amyloid precursor protein
AR:	Androgen receptor
ATP:	Adenosine triphosphate
BAR:	Bin-Amphiphyin-Rvs
BACE1:	Beta-Site APP cleaving enzyme 1
BBB:	Blood-brain barrier
bHLH-zip:	Basic helix-loop-helix leucine zipper
bp:	Basepair(s)
CD11b:	Cluster of differentiation molecule 11b
CDEC:	Cardiac-derived endothelial cells
CHO:	Chinese hamster ovary
CINC:	Cytokine-Induced Neutrophil Chemoattractant
CNS:	Central nervous system
COPII:	Coatamer protein complex II
CREB:	cAMP response element-binding
CSF:	Cerebrospinal fluid
C-term:	C terminus
DIG-1:	Drosophila disc large tumour suppressor 1
DMSO:	Di-methyl sulfoxide
dNTP:	deoxyribonucletide tri-phosphate
DRG:	Dorsal root ganglion
EAE:	Experimental autoimmune encephalitis
EDTA:	Ethylene diamine tetraacetic acid
EGTA:	Ethylene glycol tetraacetic acid
ER:	Endoplasmic reticulum
ESCERT:	Endosomal sorting complex required for transport complexes
FADD:	Fas-associated protein with death domain
GABA:	γ-aminobutyric acid
GAD67:	GABA producing enzyme 67
GALC:	β-galactocerebrosidase
GCP-2:	Granulocute chemotactic protein-2
GFAP:	Glial fibrillary acidic protein
GFP:	Green fluorescent protein
GPCR:	G-protein coupled receptor
GRO:	Growth regulated oncogene
HEK 293T:	Human Embryonic Kidney 293
HEPES:	4-(2-hydroxyethyl)-1-piperazineethanesulfonic acid
HMG-CoA:	3-hydroxy-3-methylglutaryl co-enzyme A
hr:	Hour(s)
HSV:	Herpes simplex virus
Insig:	Insulin induced genes
kan:	Kanamycin
kD:	Kilodalton
kV:	Kilovolts
LDL:	Low density lipoprotein
LV:	Lentivirus
IL:	Interleukin
IκBα:	Inhibitor of NFκB
IKK:	IκB kinase
IP-10:	Interferon gamma-induced protein -10
IP_3:	Inositol (1,4,5) triphosphate
LBD:	Lewy Body Disease
LIX:	LPS induced CXC chemokine
LPS:	Lipopolysaccharide
lt:	Litre
M:	Molar
mA:	Milliampere
MBP:	Myelin basic protein
mg:	Milligram
MIG:	Monokine Induced by Gamma interferon
min:	Minute(s)
MIP:	Macrophage inflammatory protein
ml:	Millilitre
MLV:	Mouse leukaemia virus
mM:	Millimolar
MPR:	Mannose-6 phosphate receptor
MS:	Multiple Sclerosis
NADPH:	nicotinamide adenine dinucleotide phosphate-oxidase
NAP-2:	Neutrophil activating peptide-2
NFκB:	nuclear factor kappa-light-chain-enhancer of activated B cells
NFTs:	Neurofibrillary tangles
ng:	Nanogram
NK:	Natural killer

NMDA:	N-methyl-d-aspartate
NPC:	Niemann Pick Type C Disease
NR2C:	NMDA receptor 2C
NSAID:	Non-steroidal anti-inflammatory drug
OD:	Optical density
$P40^{phox}$:	Neutrophil cytosolic factor 4
PAGE:	Poly acrylamide gel electrophoresis
PCR:	Polymerase chain reaction
PD:	Parkinson's disease
PDZ:	PSD95/DlgA/ZO-1
pg:	Picogram
PGC-1α:	Peroxisome proliferator-activated
PI:	Propridium iodide
PICK1:	Protein interacting C kinase
PKC:	Protein kinase C
PSD95:	Post synaptic density protein 95
PtdIns3P:	Phosphatidylinositol 3-phosphate
PX:	Phosphoinositide-binding domain
rAAV:	Recombinant adono-associated virus
rAd:	Recombinant adenovirus
RANTES:	Regulated upon activation, normal T-cell expressed possibly secreted
Ras:	Rat sarcoma
RGS:	Regulators of G-protein signalling
RIP:	Receptor interacting protein
ROS:	Reactive oxygen species
rpm:	Revolution per minute
S1P:	Sphingosine-1-phosphate
SCAP:	SREBP cleavage activating protein
SCID:	Severe Combined Immunodeficiency Disease
SDS:	Sodium dodecyl sulphate
sec:	Second
SH3:	SRC homology domain
S1P/S2P:	Site 1/2 protease
SMLV:	Synaptic-like microvesicles
SNX:	Sorting Nexin
soln:	Solution
SphK:	Sphingosine kinase
SREBP:	Sterol Regulatory Element Binding Protein
SSD:	Sterol sensing domain
TGN:	Transgolgi network
TLR:	Toll like receptor
TNF-α:	Tumour necrosis factor α
TNFRp55:	Tumour necrosis factor receptor p55
TRADD:	TNF receptor-associated death domain
U18666a:	3-β-[2-(Diethylamino)ethoxy]-androst-5-en-17-one
V:	Volts
Vps:	Vacuolar protein sorting proteins
VSVG:	Vesicular stomatitis virus glycoprotein
x g:	Relative centrifugal force
Ω:	Ohm

CHAPTER 1. INTRODUCTION

1.1.0 NIEMANN PICK DISEASE

1.1.1 NIEMANN PICK DISEASE IS A NEURODEGENERATIVE DISEASE

Niemann Pick Disease (NP) is a fatal, autosomal recessive neurodegenerative disease, caused by abnormalities in lipid trafficking and storage (Tang et al., 2009). The disease can be classified into three distinct groups; types A-C. Patients suffering from Type A and B have a mutation in the gene coding for sphingomyelinase, an enzyme that when mutated causes lipids to accumulate in the lysosomes of numerous tissues (Vanier and Millat, 2003). Type A and B patients differ from each other in their manifestations; type A patients suffer both neurological and visceral involvement, where as patients with Type B only suffer from the latter. Niemann Pick Type C (NPC) is caused by the mutation of different genes (NPC1 and NPC2), but the patients share the Type A symptoms, only with less pronounced peripheral effects (Vanier and Millat, 2003). NPC is a rare disease, presenting in approximately 1 of 150,000 of European births (Vanier and Millat, 2003). NPC disease itself can be further categorised into four groups, depending on the age of onset; perinatal, infantile, adolescent (classical) and adult (Wraith et al., 2009). Classical NPC disease accounts for 60-70% of all cases. Neurological effects are evident from 3-5 years of age, with fine motor control difficulties and intellectual impairment being the first symptoms to present. The symptoms increase in severity with time and though some patients survive into their thirties most die in their teenage years (**Figure 1.1**) (Solomon et al., 2005).

1.1.2 NIEMANN PICK PROTEINS ARE MUTATED IN NPC DISEASE

Mutations in the NPC1 gene, which codes for NPC1 protein accounts for ~ 95% of all NPC cases, mutations of the NPC2 gene are less common and account for the remainder (Millard et al., 2005). The NPC1 gene maps to chromosome 18q11 and more than 260 mutations in the gene have been recorded (Karten et al., 2009). The gene codes for a transmembrane protein of 1278 amino acids in length with 13 transmembrane domains (**Figure 1.2a**) (Millard et al., 2005). NPC1 protein is located primarily within the membrane of late endosomes, and is ubiquitously expressed throughout mammalian tissues (Walkley and Suzuki, 2004). NPC1 contains a functional sterol sensing domain (SSD) (**Figure 1.2c**), implying it plays a role in sterol homeostasis (Millard et al., 2005). Notably, NPC1 protein is located in endosomes and endosomal storage of lipids (primarily unesterified cholesterol) is upset when NPC1 is mutated. The NPC2 gene maps to chromosome 14q24.3 and encodes for a soluble lysosomal glycoprotein of 151 amino acid residues endogenously expressed in all tissues

(Pentchev et al., 1984) (**Figure 1.2b**). NPC2 contains a cholesterol binding domain, which allows it to transport cholesterol between different membranes (Walkley and Suzuki, 2004). The cholesterol binding domain has the ability to bind other general lipids, which may explain why mutated NPC2 is more detrimental than mutated NPC1 (Wraith et al., 2009). Mutations in either of these proteins lead to changes in cell morphology both centrally and peripherally, due to the accumulation of lipids in lysosomal or late endosomal compartments. Neuronal storage defects followed by neurodegeneration, golgi apparatus fragmentation, ectopic dendritogenesis, spheroid and meganeurite formation, demyelination and the development of neurofibrillary tangles (NFTs) have all been observed (Walkley and Suzuki, 2004).

1.1.3 NPC Diagnosis And Current Therapies

The presentation of symptoms differs between NPC patients (**Figure 1.1**) and is widely dependent on the age of onset of the disease (Tang et al., 2009). Diagnosis can therefore be difficult and can be delayed long after the initial signs of onset of disease. This delay is detrimental to the neurological symptoms of NPC disease, as studies have shown that once neuronal dysfunction has reached symptomatic levels pathological changes may be irreversible (Yanjanin NM, 2009). Histopathic analysis of bone marrow aspirate and tissue samples from the patient can confirm a diagnosis of NPC disease. To give a succinct diagnosis and to differentiate between the other forms of Niemann Pick disease sphingomyelinase activity levels within leukocytes may be measured; normal levels would indicate NPC disease over the other two variants (Tang et al., 2009). Molecular genetic testing for mutations of the NPC1 and NPC2 genes are also a reliable way of confirming the subtype of the disease (Wraith et al., 2009). Until recently NPC was untreatable, though treatment of the symptoms was manageable pharmacologically. Anti-convulsants were used to treat seizures, anticholinergics to control dystonia and antidepressants for the treatment of cataplexy (Wraith and Imrie, 2009). Animal studies using neurosteroids and cholesterol binding agents have been shown to successfully decrease the severity and slow the onset of the disease (Liu et al., 2009; Mellon et al., 2008). Allopregnanolone is a neurosteroid (**Figure 1.3c**), known to positively modulate all $GABA_A$ receptor isoforms. In a mouse model of NPC disease allopregnanelone treatment was found to reduce cholesterol accumulation and inflammation and enhance myelination and lysosomal function (Liao et al., 2009). In addition, Miglustat has recently been approved as a treatment for NPC disease, and is the only current therapy (Pineda et al., 2009). Miglustat (**Figure 1.3d**) is a small iminosugar molecule that competitively inhibits the enzyme glucosylceramide synthase which in turn inhibits the synthesis of glycosphingolipids (Platt et al., 1994). Miglustat was initially developed to treat Type

FEATURE	EXPLANATION
Spacticity	Stiffness and tightness of muscles
Dystonia	Sustained muscle contractions cause repetitive movements
Ataxia	Lack of coordinated muscle movement
Dysarthria	Difficulty speaking
Dysphagia	Difficulty swallowing
Supranuclear gaze palsy	Difficulty moving eyes
Progressive Dementia	Decreasing cognitive function
Psychosis	Loss of contact with reality (may manifest itself as hallucinations/delusions)
Seizure	Due to abnormal transmission in the brain
Hepatosplenomegaly	Simultaneous enlargement of liver and spleen

FIGURE 1.1 NIEMANN PICK DISEASE TYPE C FEATURES. Symptoms of patients with Niemann Pick Type C Disease; patients may suffer from any of the above.

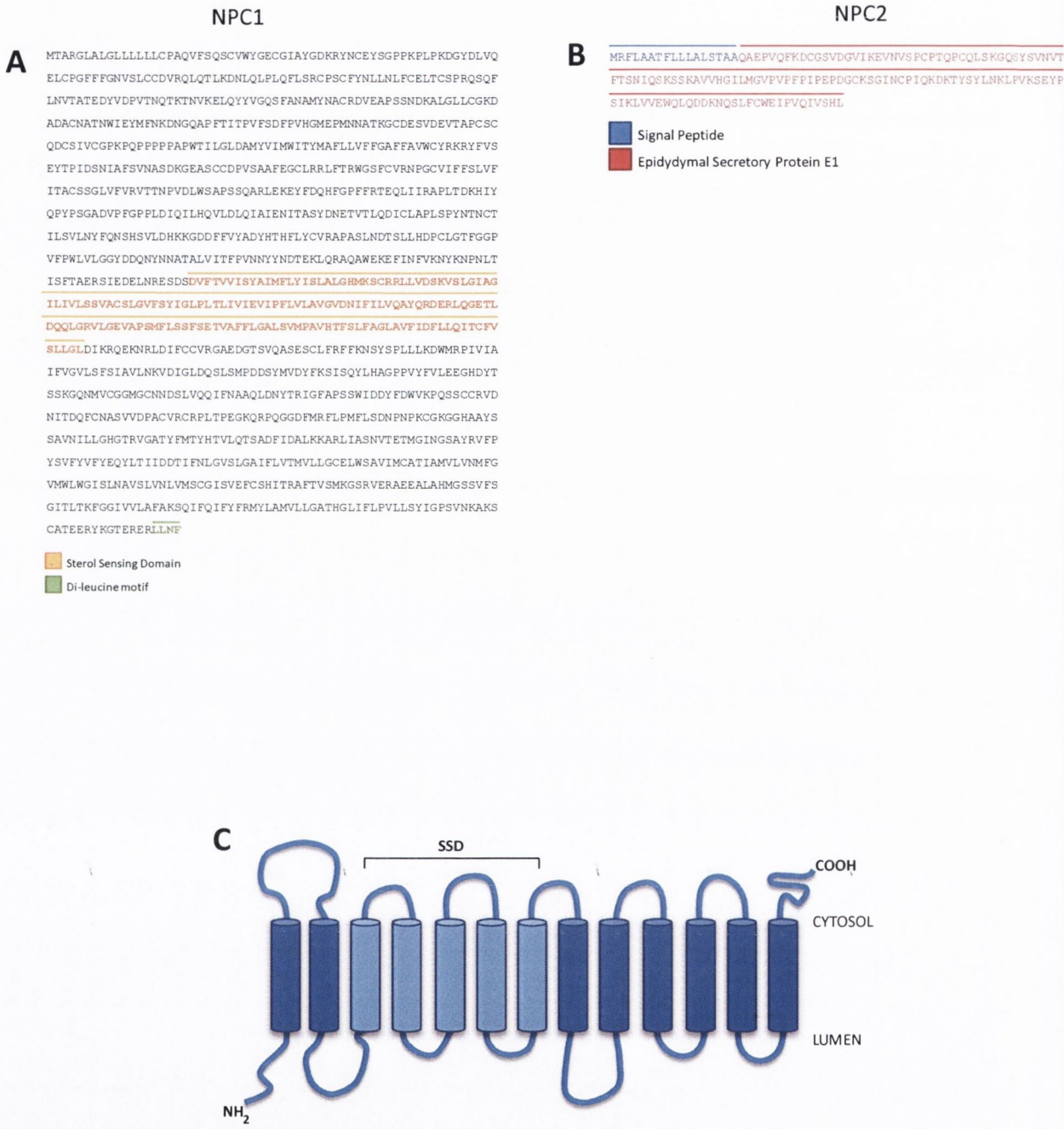

FIGURE 1.2 NPC PROTEINS. A. Amino acid sequence of human NPC1 protein with sterol sensing domain highlighted in orange and the di-leucine motif highlighted in green. **B.** Amino acid sequence of human NPC2 protein with signal peptide sequence highlighted in blue and epididymal secretory protein E1 sequence highlighted in red. **C.** Schematic of NPC1 secondary structure, showing the 13 transmembrane domains, and the sterol sensing domain (light blue).

the synthesis of glycosphingolipids (Platt et al., 1994). Miglustat was initially developed to treat Type 1 Gaucher Disease but studies with NPC 1 cell culture models showed Migulstat was able to cross the blood brain barrier and inhibit the accumulation of cholesterol. Further studies with both murine and feline NPC models showed a delayed progression of the illness and prolonged survival in Miglustat treated animals when compared to control (Zervas et al., 2001). In a long term clinical trial Miglustat treatment was found to stabilize the neurological manifestations of the disease in paediatric, juvenile and adult onset disease. Disease progression dropped from +0.11 score units/year on the disability score pre-treatment to -0.01 during treatment (Pineda et al., 2009). Miglustat offers the advantage of halting the advancement of NPC disease but it cannot reverse disease pathology.

1.1.4 Animal Models of NPC Are Available

A spontaneous occurring mutation causing Niemann Pick Type C Disease was first observed in a colony of mice in New York in 1976 (Adachi et al., 1976). Since then spontaneous forms of the disease have been identified in other animals, such as feline NPC Disease (Brown et al., 1994). Other organisms have been genetically manipulated to create models of the disease, for example a model for NPC disease has been created in the nematode *Caenorhabditis elegans* by mutating homologous forms of the human NPC1 and NPC2 genes, individually and also in double mutant form (Sym et al., 2000). Deletion mutations caused a frameshift truncation of each of the proteins. *C. elegans* cannot synthesise cholesterol endogenously, thus their environment must be supplemented with sterols for viability. Wild type worms were found to survive in the absence of cholesterol, but their first progeny died as larvae. The *npc1* and *npc1-npc2* double mutants however died at the larval stage. Other defects were noted in these mutant animals; they displayed slower development during embryogenesis and larval stages were significantly increased beyond wild type limits. This developmental shift was not noted in the *npc2* single mutant. The *npc1* and *npc1-npc2* double mutants were also observed to lay large numbers of premature eggs. In addition the *npc1-npc2* double mutants were observed to form Dauer larvae inappropriately (Sym et al., 2000). Dauer larvae are specially formed in harsh conditions such as starvation, high temperature or overcrowding. This phenotype was observed to form when sensory neurons were laser ablated in wild type worms (Bargmann and Horvitz, 1991) suggesting a link between the NPC proteins and sensory neuron function. Drosophila models of NPC disease have also been engineered. Unlike the human form, the Drosophila genome encodes two NPC1 genes (*dnpc1a*, *dnpc1b*) and eight NPC2 genes. Alblation of two of these *dnpc2* genes was found to cause neurodegeneration and eventual premature death

(Huang et al., 2007). The *dnpc1a* knock out mutant drosophila died before they reached maturation due to defects in steroid hormone production. Rescue of hormone synthesis allowed progression to adulthood, when, like in the human disease, drosophila showed progressive motor defects and shortened life span. Cholesterol was seen to accumulate within the retina and brain (particularly cultured neurons) of the *dnpc1a* mutant (Huang et al., 2007). Multivesicular organelles were also noted to develop within the brain prior to the onset of neurodegeneration. Targeted expression of wild-type *dnpc1a* within neurons reversed this degeneration and when expressed in glia was seen to lengthen the life span back to that of wild type animals (Phillips et al., 2008). NPC disease spontaneously occurs via autosomal recessive mutation in felines, with the first breeding colony established in 1989. Morphologically and biochemically these cats show similarities to the human form of NPC disease (Munana et al., 1994). Clinically the cats suffer from hepatosplenomegaly, body tremor, ataxia and dysmetria and usually die before reaching 10 months of age. Within the CNS the brains of the cats weigh almost two times that of control litter mates presumably due to cholesterol accumulation. Cerebellar purkinje neurons were observed to accumulate unesterified cholesterol as well as other lipids, before cellular degeneration and death (Brown et al., 1994). Abnomal dendrite outgrowth was also observed on cortical pyramidal neurons. The gene responsible for the disease has been mapped to be an orthologue of human NPC1 (Somers et al., 2003). The morphological changes exhibited in NPC disease are mirrored in two commonly used murine models of NPC disease. In addition to the feline model, BALB/c npc^{nih} and C57BLKsJ mice both posess mutated NPC1 protein (Karten et al., 2005). A mouse model of NPC2 mutated protein is also available and is very similar to the afore mentioned models (Loftus et al., 1997). The BALB/c npc^{nih} mice display abnormal development from approximately four weeks of age, they follow the human phenotype with progressive decline in cognitive and motor function ending with death due to lack of feeding at about 70-80 days. The brain of the mutant mice is smaller than control animals, with atrophy visible in the cerebellum and midbrain regions. Progressive neurodegeneration particularly of the purkinje neurons is a common feature of the mutant animals as is widespread de-myelination. The only human feature that the mouse model does not share is the formation of NFTs (Loftus et al., 1997).

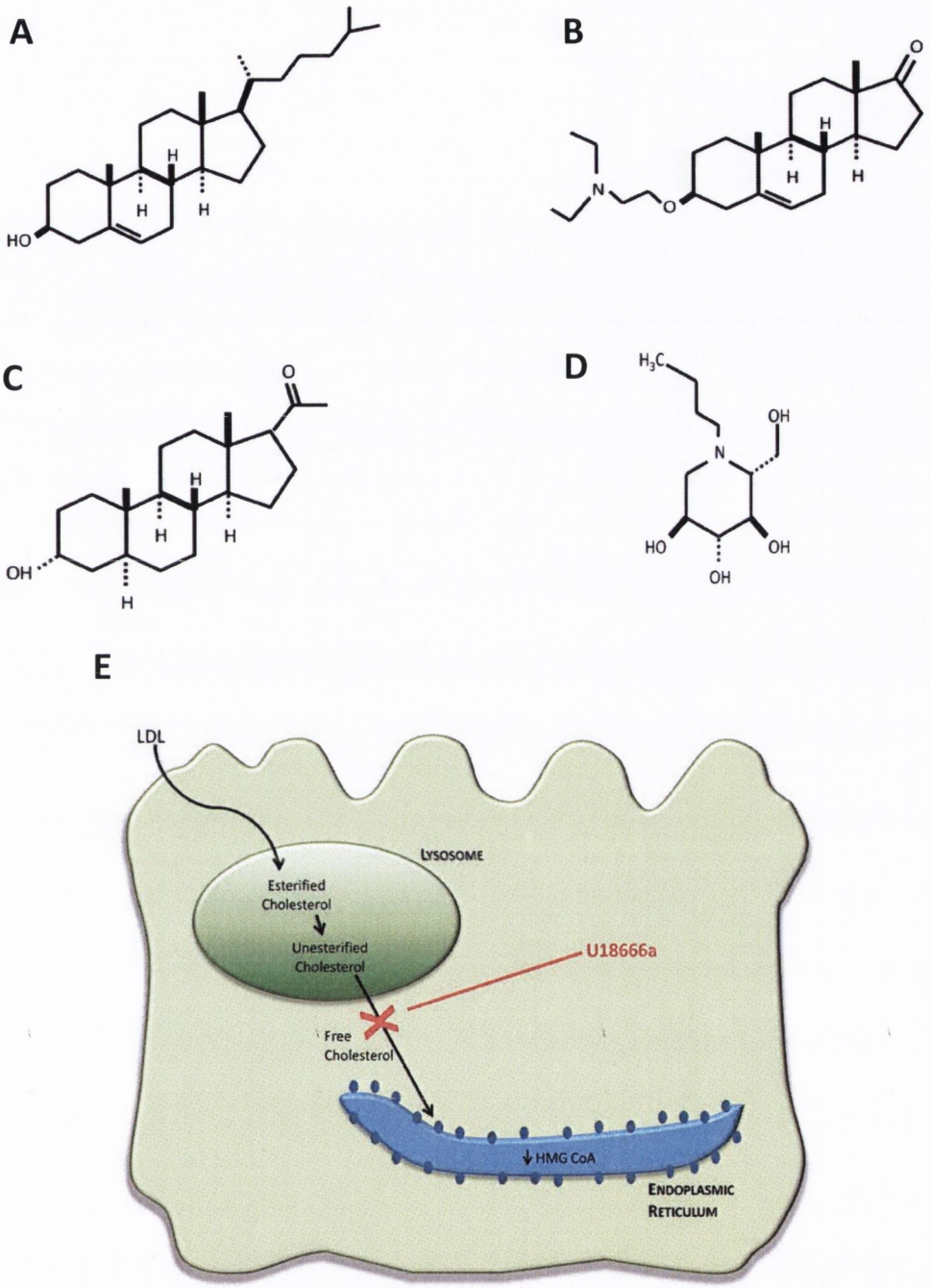

FIGURE 1.3. U18666A STRUCTURE AND FUNCTION. Chemical structure of **A.** cholesterol. **B.** Chemical U18666a (3-β-[2-(Diethylamino)ethoxy]androst-5-en-17-one), showing the amphipathic cation amine structure, and conservation of similar groups to cholesterol. **C.** Allopregnanolone. **D.** Miglustat. **E.** Diagram showing the proposed mechanism of U18666a action on cholesterol trafficking. LDL is taken into the lysosome and converted into esterified cholesterol, then to unesterified cholesterol. Free cholesterol is then released from the lysosome to decrease HMGCoA activity. U18666a blocks cholesterol egression from the lysosome.

1.2.0 Inflammation And Neurodegeneration

1.2.1 Neuronal Anatomy

Within the human brain there are around 100 billion neurons, and almost ten times as many glia. There are four types of glia within the CNS; astrocytes, microglia, oligodendrocytes and ependymal cells. Neurons carry signals both electrically and chemically via action potentials and neurotransmitter release at the synapse, and glia are traditionally seen as supportive cells for this neuronal function (Choiard and Salecker, 2004). Neurons are the fundamental signaling cell type within the CNS, as they are able to transmit signals over long distances due to their unique structure. A typical neuron consists of a cell body (soma), dendrites and an axon. The soma extends out into numerous dendrites which in turn branch multiple times (known as the dendritic tree). Only one axon extends from every neuron, action potentials initiate electrical signals at the axon hillock which travel down the length of the axon. At the synapse the electrical impulse triggers the release of neurotransmitters presynaptically into the synaptic cleft, which are uptaken by receptors on the post synaptic surface of the dendrite of another neuron (Klug et al., 2012). It is by this electro-chemical signaling that neural networks are able to communicate. Neurons are post-mitotic, therefore cannot proliferate (aside from restricted areas of neurogenesis in the hippocampus and olfactory bulb), therefore when neuroral death occurs, no new neurons can be generated, resulting in the neuronal deficits observed in neurodegenerative diseases (Herrup and Yang, 2007).

1.2.2 Astrocytes Sense Neuronal Activity

Astrocytes are stellate cells with varying numbers of processes giving them their characteristic star shape (He and Sun, 2007). They are structurally, physically and biochemically diverse which is reflected in their broad spectrum of functions. Astrocytes can be distinguished by their expression of the intermediate filament protein glial fibrillary acidic protein (GFAP), now an established cell-specific marker. This glial cell type have been implicated in a large number of vital processes in the brain; their processes extend into synapses, nodes of Ranvier and are major components of the BBB (Bacci et al., 1999; Paolinelli et al., 2011; Perea and Araque, 2010). Initially thought to only provide structural support to synapses, recent studies have shown astrocytes to be active participants in synaptic transmission (Ciet et al., 2001). Astrocytes are capable of 'sensing' neuronal activity through the wide range of ion channels and neurotransmitter receptors that decorate the plasma membrane of these cells Neuronal differentiation, maturation, survival and neurite outgrowth are

processes that are all influenced by the release of various growth factors from astrocytes (Ransom and Ransom, 2012).

1.2.3 Microglia Are CNS Resident Immune Cells

Microglia are immune cells localised entirely within the CNS, and they are responsible for removing toxic substances that emerge from within the CNS, or that enter it by permeating the BBB (Perry, 2007; Soriano and Piva, 2008). They are monocyte-lineage cells and share many characteristics with macrophages, which perform a similar role in the periphery. Microglia can exist in several functional states, which correspond loosely with a particular morphological phenotype. Ramified microglia extend processes into their immediate surroundings allowing them to survey the extracellular space for any changes in the normally highly-stable CNS microenvironment. Microglia displaying such a phenotype are said to be in a "resting" state and lack the ability to present antigens to peripheral T-cells. Their cell bodies are immobile while the cells continuously release a variety of neurotrophic and anti-inflammatory cytokines including IL-4 and IL-10 (Block et al., 2007). These cytokines help to maintain a healthy environment to support neuronal growth and survival. The detection of an insult i.e. neurotoxin, pathogen-associated molecular pattern (PAMP), cell debris or cytokine, can induce an alteration in the phenotypic and functional state of microglia. Following stimulation, microglia adopt a more amoeboid morphology, a process often accompanied by the upregulation of cell surface membrane proteins which facilitate functions ranging from antgen presentation to phagocytosis (Block et al., 2007; Lynch, 2009). In addition to these phenotypic changes, activated microglia typically exhibit upregulated transcription of genes coding for pro-inflammatory cytokines and a corresponding increase in the secretion of such molecules. This feature of activated microglia allows them to propagate the pro-inflammatory signal by activating nearby microglia and other immune cells and establishing a inflammatory environment in the CNS (Perry, 2007; Soriano and Piva, 2008).

1.2.4 Glial Activation, Leukocyte Infiltration And Oxidative Stress Influence Neurodegeneration

The CNS displays unique structural and functional features, such as the presence of a blood-brain barrier (BBB), blood-cerebrospinal fluid (CSF) barrier, an immunotolerised environment and the lack of regular lymphoid drainage (Ransohoff and Brown, 2012). These qualities act concurrently to limit inflammatory damage in an environment with limited regenerative capacity. In some pathological

situations of inflammation (such as multiple sclerosis) the BBB integrity is breached, and activated lymphocytes, monocytes or neutrophils can infiltrate the CNS. Other neurodegenerative diseases such as Alzheimer's disease involve an inflammatory response mainly regulated by intrinsic immune cells (microglia in particular) (Takata and Kitamura, 2012). Leukocyte infiltration is stimulated by chemokines and involves the interaction of these cell types with various cell adhesion molecules (in particular selectins) to mediate leukocyte tethering and rolling along the endothelial surface. The activated leukocyte then adheres strongly to the endothelium via interaction with other adhesion molecules, which is mediated by chemokines (Laudanna et al., 2002). Cerebrovascular endothelial cells have been observed to themselves produce chemokines (Glabinski and Ransohoff, 1999). These cells transport chemokines to the luminal surface where they are presented to leukocytes, stimulating leukocyte infiltration. Most infiltrating leukocytes accumulate within the perivascular space, though in some conditions the cells continue to infiltrate brain structures. Glial activation can also contribute to leukocyte infiltration (Grace et al., 2011). When the innate immune system is activated, microglia and astrocytes become transformed into an activated state (Jones et al., 1997). In this form these glia release inflammatory mediators such as cytokines (immunomodulators) and chemokines (leukocyte chemoattractants) which further exacerbates the neuroinflammatory state. Sandhoff's disease is a lysosomal storage disorder exhibiting a neurodegenerative pathology. In this disease the macrophage/microglia population were found to be active before detection of neuronal apoptosis and this inflammatory response was further compounded by leukocyte infiltration from the periphery mediated by the chemokine MIP-1α (Wu and Proia, 2004).

The neurodegeneration seen in NPC disease has been linked to apoptosis caused by the up-regulation of genes involved in the tumour necrosis factor-α (TNF-α) death pathway namely – Caspase-8, FADD (Fas-associated protein with death domain), TNFRp55 (tumour necrosis factor receptor-55), TRADD (TNF receptor-associated death domain), and RIP (receptor interacting protein) (Wu et al., 2005). TNF-α mRNA was found to be present almost 50 fold in the cerebellum of *NPC1*$^{-/-}$ mice when compared to age matched controls (Wu et al., 2005). Both neurons and astrocytes shared this increase in TNF-α expression. The neurosteroid allopregnanolone was seen to reduce purkinje neurodegeneration, decrease glial cell activation and increase life span in a mouse model of NPC disease (Griffin et al., 2004). The benefits of this treatment have been linked to the production of anti-oxidants *in vitro* (Zampieri et al., 2009). This was also highlighted in an earlier study showing delayed onset of symptoms in a mouse model of NPC disease following antioxidant (vitamin E) treatment (Bascunan-Castillo et al., 2004).

1.3.0 STEROL HOMEOSTASIS

1.3.1 LIPIDS AND CHOLESTEROL PLAY A CRUCIAL ROLE WITHIN THE CNS

The biosynthesis of cholesterol (**Figure 1.4**) is a highly regulated process resulting in the formation of vital steroids and bile salts. A high proportion of the body's cholesterol is contained within the CNS; (almost 25% of the total body cholesterol) (Valenza, 2006), and 20% of this total brain cholesterol is intracellular (Xie et al., 2003). Cholesterol homeostasis within the CNS is completely independent from the periphery as it is unable to cross the blood-brain barrier (Bjorkhem and Meaney, 2004). Numerous studies have been performed to determine the role of cholesterol in vascular and liver cell types, but comparatively less is known of the role of cholesterol within the cells of the CNS. Cholesterol is a key component of biological membranes and plays a vital role in myelin synthesis, synaptogenesis, membrane trafficking and signal transduction (Dietschy and Turley, 2004). It has also been shown that alongside the structural aspects of cholesterol, cellular processes such as endosomal trafficking and transport of synaptic vesicles also depends on cholesterol biosynthesis (Thiele et al., 2000). Cholesterol is a polar lipid and when accumulated it is toxic to its host cell, thus disruption to the synthesis, metabolism and trafficking of cholesterol is involved in many neurological diseases, such as NPC disease (Karten et al., 2002), Alzheimer's disease (Koudinov and Koudinova, 2001) and Huntington's disease (Vance et al., 2005).

Neural cholesterol is primarily unesterified and plays a key role in many structural aspects of brain morphology; it is an integral component of the myelin sheath and is also highly concentrated in the plasma membranes of neurons and astrocytes (Snipes and Orfali, 1998). The highest level of cholesterol synthesis within the CNS occurs during development when myelination is in progress, with oligodendrocytes producing the majority of the lipid (Dietschy and Turley, 2004). During development neurons also endogenously synthesise cholesterol within the cell body and it is transported to the distal axons for synaptogenesis and axonal outgrowth (Karten et al., 2002). After reaching maturation neurons reduce this synthesis and become dependent on the supply of exogenous cholesterol from glial cells (Quan et al., 2003). In the mature CNS cholesterol is primarily synthesised by oligodendrocytes and astrocytes, to a level of almost 3 fold of that in neurons (Bjorkhem and Meaney, 2004). The cholesterol synthesised within oligodendrocytes is used for the formation of myelin in the surrounding myelin sheaths, whilst the majority of cholesterol synthesised in astrocytes has been hypothesised to be transferred to neurons (**Figure 1.5**) via interaction with the low density lipoprotein receptor (LDLR) (which recognises apolipoprotein E (ApoE)). In support of this hypothesis it has been shown that ApoE containing lipoproteins isolated

from culture medium containing astrocytes can increase axonal extension when added to rat retinal ganglion cells (Hayashi et al., 2004). Neither ApoE nor cholesterol alone stimulated axonal growth indicating that the growth effects are mediated directly by ApoE/cholesterol released from astrocytes. Lipoproteins from astrocytes have also been implicated in the promotion of synaptogenesis in rat retinal ganglion neurons, by increasing intracellular cholesterol levels (Mauch et al., 2001). Thus both endogenous and glial supplied cholesterol are important in neuronal function. Cholesterol is enriched in synaptic membranes, and influences synaptic function. Within a neuronal cell line, cholesterol has been identified to directly bind to both synaptophysin and synaptotagmin at the synapse, and cholesterol depletion was found to block the release of synaptic-like microvesicles (SLMVs) (Thiele et al., 2000). SNARE complexes (Soluble NSF Attachment Protein Receptor) and fusion pore formation are also cholesterol dependent (Cho et al., 2007; Tong et al., 2009) suggesting cholesterol is criticial for correct neuronal function.

Recently it has been found that statins, a commonly prescribed drug to lower circulating cholesterol levels, have proved beneficial for the prevention of Alzheimer's disease (Fonseca et al., 2010). Statins inhibit 3-hydroxy-3-methylglutaryl co-enzyme A (HMG-CoA) reductase, which catalyses the synthesis of mevalonate, thus limiting cholesterol synthesis (**Figure 1.4**)(Mailman et al., 2011). In cultured neurons statin treatment has been observed to increase α-secretase cleavage of APP (amyloid precursor protein), alongside reduced tau hyperphosphorylation (Fan et al., 2001). Reduced NFT formation and amyloid deposition has also been observed in Alzheimer's disease patients treated with statins (Fassbender et al., 2001). However, as cholesterol is critical to correct synaptic function, long term exposure of neurons to statins may affect synaptic transmission, in particular chronic exposure of neurons to the statin lovastatin was found to decrease neurite density, reduce synaptic number and impair vesicle exocytosis (Mailman et al., 2011).

1.3.2 U18666A Is A Versatile Tool For Investigating Cholesterol Metabolism

U18666a (3-β-[2-(Diethylamino)ethoxy]androst-5-en-17-one) is an amphipathic steroid (**Figure 1.3b**) first synthesised along with other di-alkyl-amino-ethyl esters in 1951 (Cavallini and Massarani, 1951). The compound was first put into large scale synthesis in 1963 to investigate it's capacity to inhibit the synthesis of cholesterol as a treatment for heart disease (Phillips and Avigan, 1963) but research was stopped when in animal studies the compound was found to cause the formation of cataracts (Cenedella and Bierkamper, 1979). Despite this, U18666a has played a vital role in understanding intracellular cholesterol trafficking and synthesis. U18666a has been shown to indirectly inhibit the

LDL mediated block of HMGCoA reductase activity (Panini et al., 1984). It does this by blocking the release of free cholesterol from lysosomes, blocking the trafficking to the plasma membrane and the endoplasmic reticulum (**Figure 1.3e**). The treatment of cells with U18666a causes cholesterol to accumulate within the lysosomal compartment, and the addition of LDL does not over-come the block of cholesterol egression (Liscum and Faust, 1989). Cellular structure is affected as membrane lipids are condensed and cells have also been observed to undergo apoptosis following treatment with U18666a. The exact mechanism by which U18666a exerts this effect is unknown, though its effects are concentration dependent, and independent of the pH of the lysosome, cytoskeleton integrity and protein synthesis (Cenedella, 1980). In addition, U18666a treatment also alters the mannose 6-phosphate receptor trafficking pathway, and increases intracellular calcium levels (Ikeda et al., 2005).

Importantly, the actions of U18666a may be dependent on regulation of NPC1 protein. The transport of NPC1 protein is altered when cholesterol is accumulated in the lysosome by U18666a treatment, and NPC1 mRNA levels increase (Watari et al., 2000). Mutant NPC cells treated with U18666a showed no further increase in cholesterol accumulation, whereas knock-in of the protein restored U18666a capacity to sequester cholesterol in the lysosome (Sugimoto et al., 2001). U18666a treatment is now used as a means of creating a cellular model of NPC disease. Primary neuronal cultures treated chronically with U18666a showed apoptotic cell death, not necrosis (Koh and Cheung, 2006). This programmed cell death has been linked with activation of calpains and caspases after 72 hours of 1 μg/ml U18666a treatment. Caspase-12 was seen to be elevated at an earlier time point than calpain and other caspases (Koh et al., 2006a). Pro-caspase-12 is found primarily in the endoplasmic reticulum (ER), thus U18666a mediated neuronal apoptosis may be initiated by ER stress. Chronic U18666a treatment has also been found to result in an increase in reactive oxygen species (ROS) production, leading to oxidative stress (Koh et al., 2006b). This finding correlates with the finding that NPC mouse brains show mitochondrial dysfunction and ATP deficiency (Yu et al., 2005). Alzheimer 's disease pathology also shows increases in oxidative stress markers, where anti-oxidant therapy has been used as treatment (Koh and Cheung, 2006). High cholesterol levels are also correlated with the risk of AD, and statins have been seen to be beneficial in reducing symptoms (Koh et al., 2006b). This coupled with the fact that U18666a treatment leads to increased Aβ40 and Aβ42 (amyloid beta) levels in primary cortical neurons demonstrates a further link between NPC and AD (Koh et al., 2006b). Lastly, microarray analysis following U18666a treatment showed changes in expression of proteins involved in protein folding and trafficking, regulation of transcription, lipid metabolism and transport and responses to cell death (Koh and Cheung, 2006) This change in

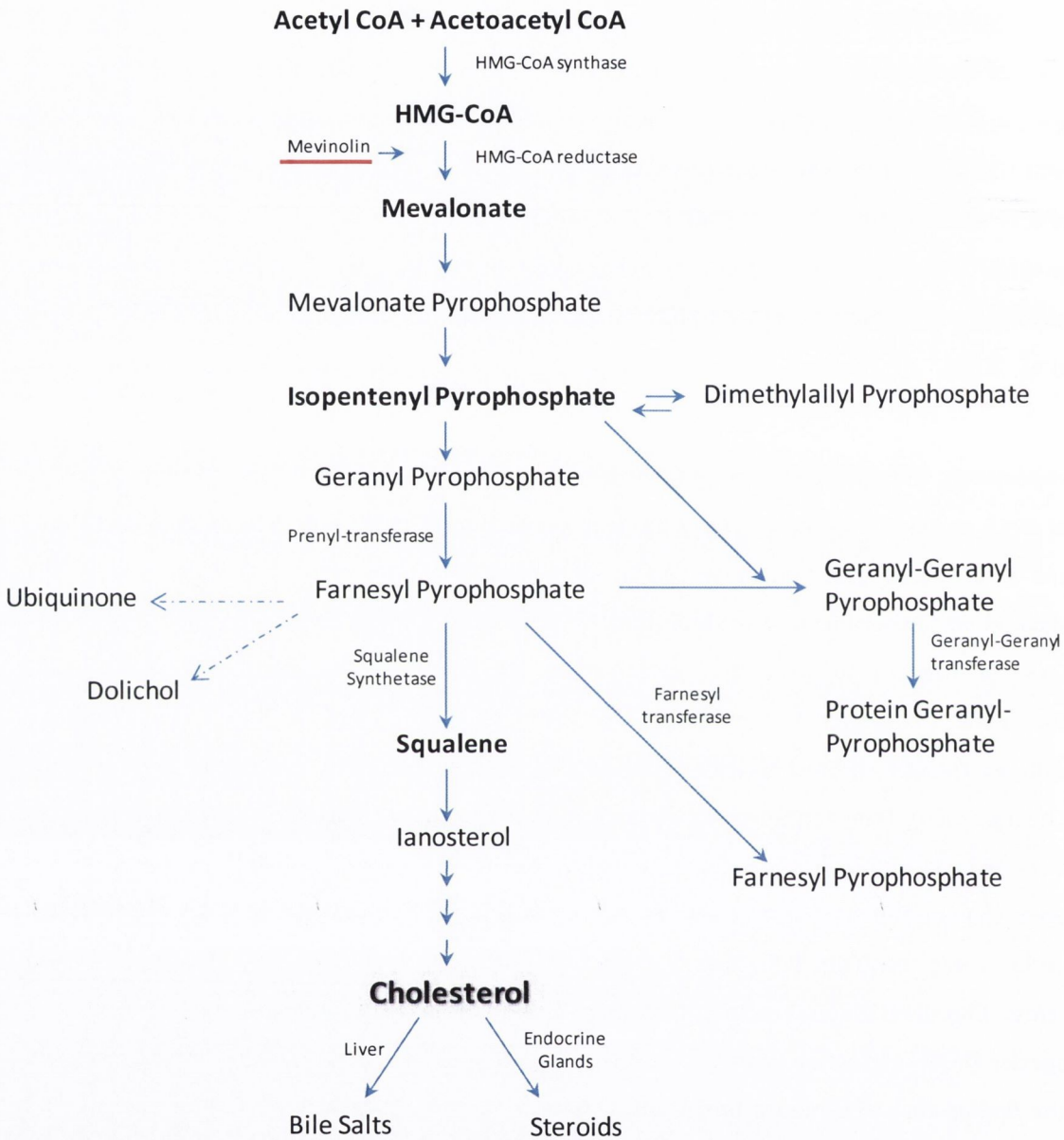

FIGURE 1.4. CHOLESTEROL SYNTHESIS AND METABOLISM. Cholesterol is synthesised peripherally and within the CNS by the same pathway. There are five major steps in the pathway (shown in bold); acetyl-CoA is converted to HMG-CoA, then to mevalonate, this is then converted to isopentyl pyrophosphate, which in turn is changed into squalene. Finally, squalene is converted to cholesterol (Sato and Takano, 1995).

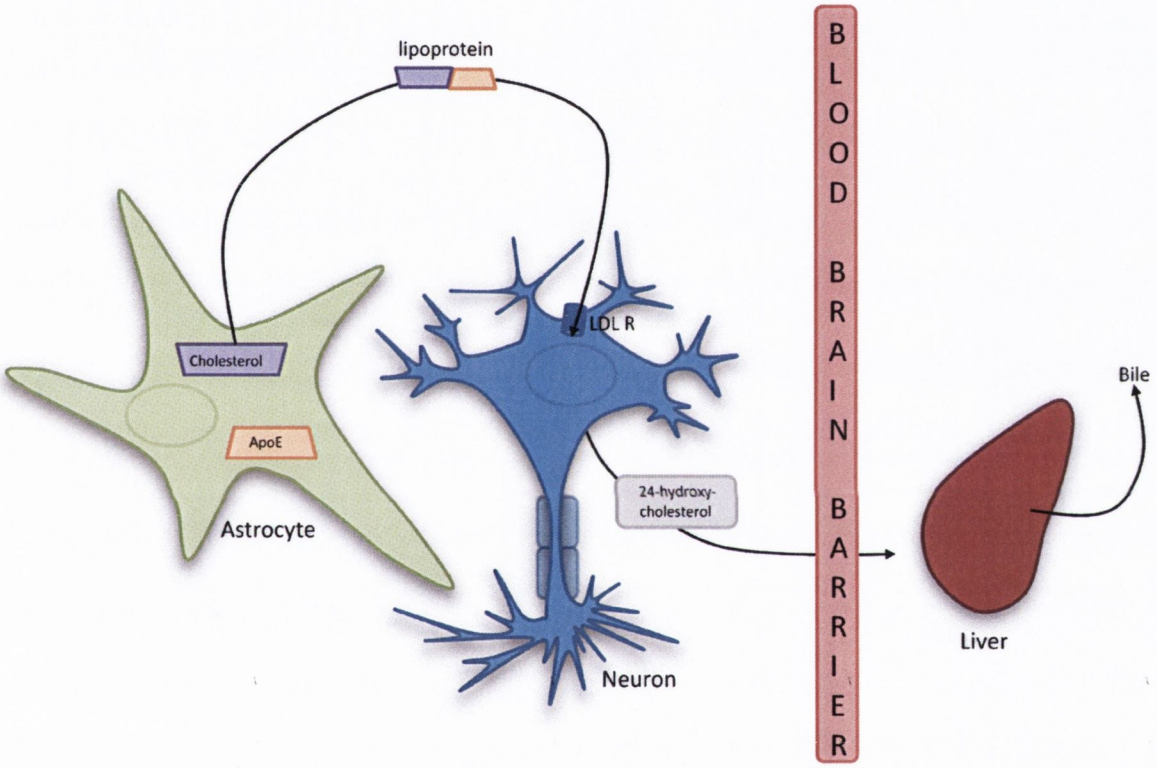

FIGURE 1.5. CHOLESTEROL MOVEMENT WITHIN THE CNS. In the mature CNS astrocytes are a major source of cholesterol. This cholesterol is combined with ApoE to form glial derived lipoprotein, which is transported to neurons, and hypothesised to enter neurons by interaction with a member of the LDLR family. Excess cholesterol is metabolised to 24-hydroxy-cholesterol which (due to the loss of a side chain) can pass through the BBB. The cholesterol metabolite travels in the plasma to the liver where it is excreted in bile.

genetic profile correlates with a similar study to investigate susceptibility factors for AD (Serretti et al., 2005).

1.3.3 The SREBP Pathway Controls Cholesterol Homeostasis

As cholesterol is a vital component of normal cell structure and function, it is highly regulated via an important and somewhat complex pathway; the SREBP (Sterol regulatory element binding protein) pathway. SREBPs are membrane spanning proteins anchored in the ER which act as transcription factors for genes that regulate the synthesis and metabolism of cholesterol. The main function of the SREBP pathway is to activate and transport (transcriptionally active) SREBP isoforms to the nucleus where they can exert their effects on DNA transcription, which involves many other interacting proteins (Rawson, 2003). The mammalian genome contains two genes for SREBP that code for three different isoforms; SREBP-1a, SREBP-1c and SREBP-2. As yet no differentiation in function has been observed between these isoforms thus, here after the term SREBP will be used to refer to all three isoforms. SREBPs are basic helix-loop-helix leucine-zipper (bHLH-zip) transcription factors and have two membrane spanning helices that anchor the protein to the ER, where it is transcriptionally inactive (Bengoechea-Alonso and Ericsson, 2007). When the demand for cholesterol within the cell rises, a sterol sensing domain containing protein, SCAP (SREBP-cleavage-activating protein), interacts with the carboxy terminus of SREBP and chaperones SREBP to the golgi via uptake into COPII vesicles (coatamer protein complex II positive vesicles) (Nohturfft et al., 2000). Once the SREBP/SCAP complex has entered the golgi; in order for SREBP to be activated it needs to be cleaved from the membrane. This is facilitated by interaction with two proteases S1P and S2P (site 1 and site 2 protease). S1P cleaves SREBP at the intracellular loop, separating the bHLH-zip domain from the other inactive component, but retaining the protein in the membrane. S2P (an intermembrane cleaving protease, similar to presenilin (involved cleaving APP in AD) then cleaves the bHLH-zip section at the amino terminal site of the transmembrane location. This frees the SREBP transcription factor element from the membrane and allowing nuclear transport to stimulate the transcription of genes that lead to enhanced overall cholesterol levels in the cell (Bengoechea-Alonso and Ericsson, 2007)(summarised in **Figure 1.6**).

1.3.4 Insigs Regulate SREBP Trafficking

The SREBP pathway is part of a feedback loop, and during high cholesterol levels, the pathway can be modulated to inhibit SREBP activation. When cholesterol is present in high quantity it binds to the sterol sensing domain of SCAP, causing a conformational change, inhibiting its ability to bind with proteins in the COPII vesicles. Thus, SREBP is not translocated to the Golgi thus is not cleaved into its active form and therefore cannot activate the transcription of the SREBP target genes (**Figure 1.6**). The SREBP pathway is also negatively modulated by a group of proteins called Insigs (insulin induced genes). Insig-1 is a protein found in the ER regardless of the presence of sterols (Yang et al., 2002). Though it is almost 60% homologous with Insig-1, Insig-2 is not transcriptionally activated by SREBP, and needs a baseline level of sterol present in order to be active. It has been shown that overexpression of Insig-1 blocks the SREBP pathway by inhibiting the SCAP/SREBP complex from leaving the ER, even in low cholesterol states (**Figure 1.6**) (Yang et al., 2002). Insig-1 is a target gene of SREBP, thus SREBP and Insig-1 act to negatively regulate each other. The conformational change in SCAP following interaction with cholesterol encourages Insig to anchor SCAP in the membrane of the ER. The presence of sterols diminishes the ubiquitination and degradation of Insig-1, thus in high cholesterol levels Insig is bound preferentially to SCAP (Bengoechea-Alonso and Ericsson, 2007). When cholesterol levels decrease, the interaction is less favourable, Insig detaches from SCAP and the SCAP/SREBP complex is free to move towards the Golgi, Insig-1 is ubiquitinated and degraded thus reducing its inhibitory effects (Yang et al., 2002). Insigs are also involved in the HMG CoA regulation of sterol homeostasis. HMG CoA reductase is a sterol sensor and is the rate limiting factor in the synthesis of sterols; it too is activated by SREBP (Hua et al., 1996). The presence of sterols stimulates the degradation of HMG CoA reductase. Insig-1 has been found to interact with the sterol sensing domain of HMG CoA reductase stimulating the degredation of the enzyme, thus decreasing cholesterol production (Sever et al., 2003). Therefore, Insigs negatively regulate two modulators of the SREBP cholesterol pathway; SCAP and HMG CoA.

1.3.5 SNX8 Is A Novel Activator Of The SREBP Pathway

We have previously shown that the SREPB pathway is modulated by a variety of molecules (Chatterjee et al, 2009). A genome wide cDNA over expression screen of 10,000 sequences was performed to find possible SREBP modulators as determined by the transcription of a luciferase gene driven from an SREBP specific promoter (Chatterjee et al., 2009). The initial hits were verified using biological assays, and 27 activators and 40 repressors of the SREBP pathway were identified. One activator identified was the protein SNX8 (sorting nexin 8), a member of the sorting nexin family of

proteins. It was found that when both Insig and SNX8 were co-overexpressed in CHO (Chinese hamster ovary) cells, SNX8 could overcome the Insig mediated block on the SREBP pathway and trigger the production of cholesterol (Chatterjee et al., 2009). In fact, SNX8 overcame the Insig block to a greater extent than SCAP, the endogenous activator of the pathway. The SNX family have been identified to modulate endocytosis and endosomal sorting alongside various trafficking events (Johannes and Wunder, 2011), and more recently were found to form retromer complexes in retrograde sorting (Rojas et al., 2007). Therefore, it is possible that SNX8 may regulate SREBP activity via regulation of trafficking. As cholesterol homeostasis is vital for correct neuronal function, and SNX8 regulates the SREBP pathway, it is important to further investigate the role of SNX8 in brain function and diseases of the CNS such as NPC disease.

1.4.0 THE SORTING NEXIN FAMILY

1.4.1 THE SORTING NEXIN FAMILY IS INVOLVED IN SORTING AND TRAFFICKING

Members of the sorting nexin (SNX) family are classified by the presence of a PX domain (phosphoinositide-binding structural domain) (Johannes and Wunder, 2011). As PX domains function by binding PtdIns3P (phosphatidylinositol 3-phosphate), the sorting nexins are mostly found in the phosphoinositide rich areas of the endosomal system where they influence endocytosis, endosomal sorting and signalling (Braun et al., 2010). A subsection of the SNX family contain only a PX domain (SNX^{PX} proteins), and as yet possess no other characterised domains (Wang et al., 2010). Another sub section of the family also contain a BAR (Bin, amphiphysin, Rvs) domain. A third sub-family can be made up of SNX members that contain other characterised domains such as SH3 domains (SRC homology domain), PDZ domains ((post synaptic density protein (PSD95), drosophila disc large tumor suppressor (Dig1), zonula occludens-1 protein (zo-1)) or RGS domains (regulators of g protein signalling) (**Figure 1.7**). The PX and PX-BAR members of the family are amongst the most researched members of the SNX family (**Figure 1.8**). Though many of the SNXs have yet to be characterised in detail, their functions can be inferred by the domains they contain. As more is discovered about the function of the sorting nexin family, they are increasingly being found to play a role in disease such as Alzheimers Disease (Zhao et al., 2012).

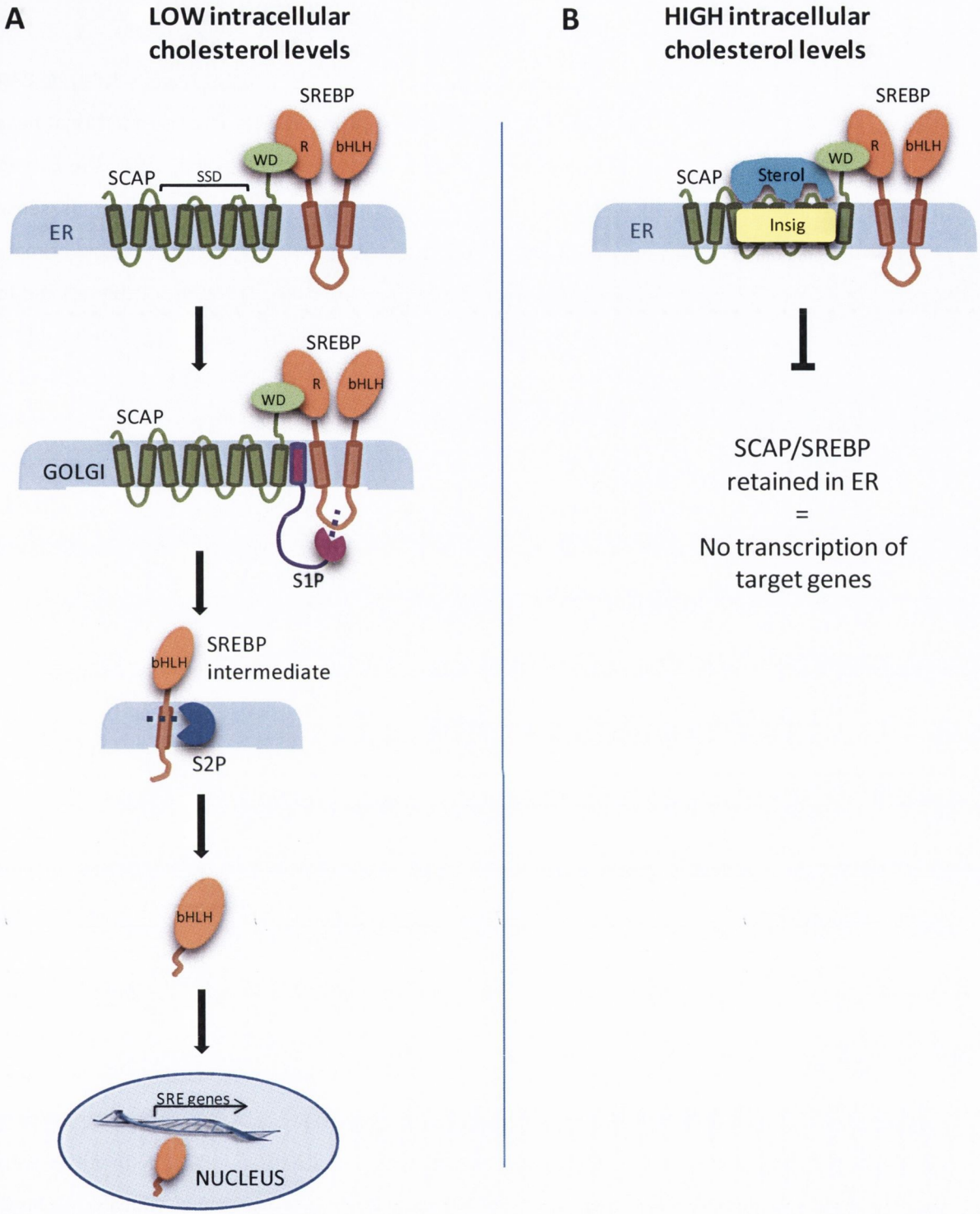

FIGURE 1.6. SREBP PATHWAY SUMMARY. A Low cholesterol levels are sensed by the sterol sensing domain (SSD) of SCAP which interacts with SREBP and shuttles it from the ER to the Golgi. In the Golgi S1P enzymes cleave SREBP at its intraluminal loop. The intermediate SREBP is in turn cleaved by S2P (an intramembrane cleavage enzyme) which releases the activated form of SREBP allowing transport to the nucleus and transcription of genes that upregulate cholesterol homeostasis. **B** High cholesterol levels are sensed by the SSD of SCAP, which triggers an interaction with Insig. This interaction retains the SCAP/SREBP complex in the ER and thus prevents SREBP cleavage, thus inhibiting the production of cholesterol.

1.4.2 The SNX-BAR Family Are A Distinct Sub-Group of Sorting Nexins

There are 12 mammalian proteins that contain both the PX and BAR domains (**Figure 1.8b**). N-BAR domains (BAR domains with an additional N-terminal amphipathic helix) insert the additional helix into membranes causing the membrane to curve more, this shape is then stabilised by the curved shape of the BAR domain (**Figure 1.8c**). Thus not only do BAR containing SNX proteins sense membrane curvature they also induce it (McMahon and Gallop, 2005). Subtle differences in primary sequence between different BAR containing SNXs can target them to specific areas of the cell and to specific subcellular locations. For example SNX1 preferentially binds to PtdIns(4,5)P_2 (phosphoinositide 4, 5-phosphate) which is present in greatest quantity in the plasma membrane. In contrast, SNX9 prefers to bind to Ptd(3,5)P_2 (phosphoinositide 3, 5-phosphate) which is a component of the early endosome (Carlton et al., 2004; Yarar et al., 2007). The high level of specificity may also be caused by hetero or homo dimerisation of BAR containing SNXs. SNX1 and SNX2 have already been described to participate in the retromer complex, thus by combining the different properties of two heteromeric SNX-BARs different functions may be possible.

1.5.0 The Importance of domains

1.5.1 The BAR domain Is Involved In Membrane Curvature

The BAR domain is a protein dimer domain comprised of three α helices, which form a banana shape, with positive residues lining its inner façade, encouraging interaction with the lipid bilayer (Peter et al., 2004) (**Figure 1.8c**). BAR containing proteins such as PICK1 (Protein Interacting with C Kinase), amphyphysin and the endothelins are found throughout eukaryotic genomes and are functionally important in pathways such as endocytosis, exocytosis, cell division, apoptosis and regulation of transcription (Frost et al., 2009). The BAR domain was first crystallised from Drosophila amphiphysin, members of which family are known to be involved in early endocytosis, by assisting the formation of curved membranes (tubulate membranes) (Bhatia et al., 2009). Similarities were also noted between amphyphysin and the GTPase binding domain of Arfaptin 2, which binds small GTPases such as members of the Ras (rat sarcoma) and Arf (ADP ribosylation factor) families which are known to regulate intracellular transport, cytoskeleton rearrangement and cargo uptake (Dawson et al., 2006). BAR domains tend to dock with curved membranes of a radius of approximately 15 nm, and are therefore thought to be sensors of membrane curvature (McMahon and Gallop, 2005). This quality may be due to the contour of the BAR domain and the specific arrangements of the residues within the docking area (Zimmerberg and McLaughlin, 2004).

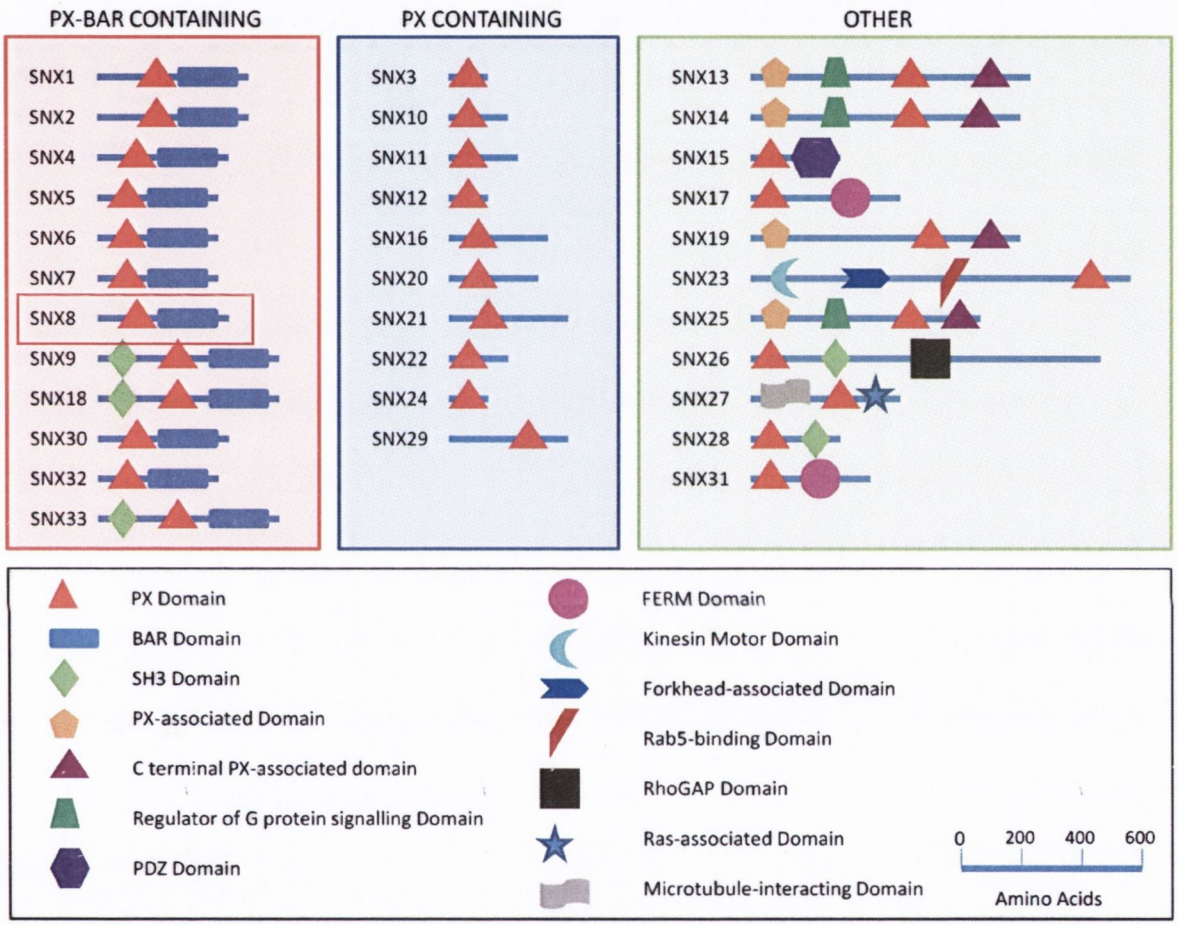

FIGURE 1.7. SORTING NEXIN SUBFAMILIES. The blue box top right contains members of the sorting nexin family that contain only the PX domain. The red box top left contains members of the PX-BAR domain containing sub-family of sorting nexins of which SNX8 is a member (shown in bold).

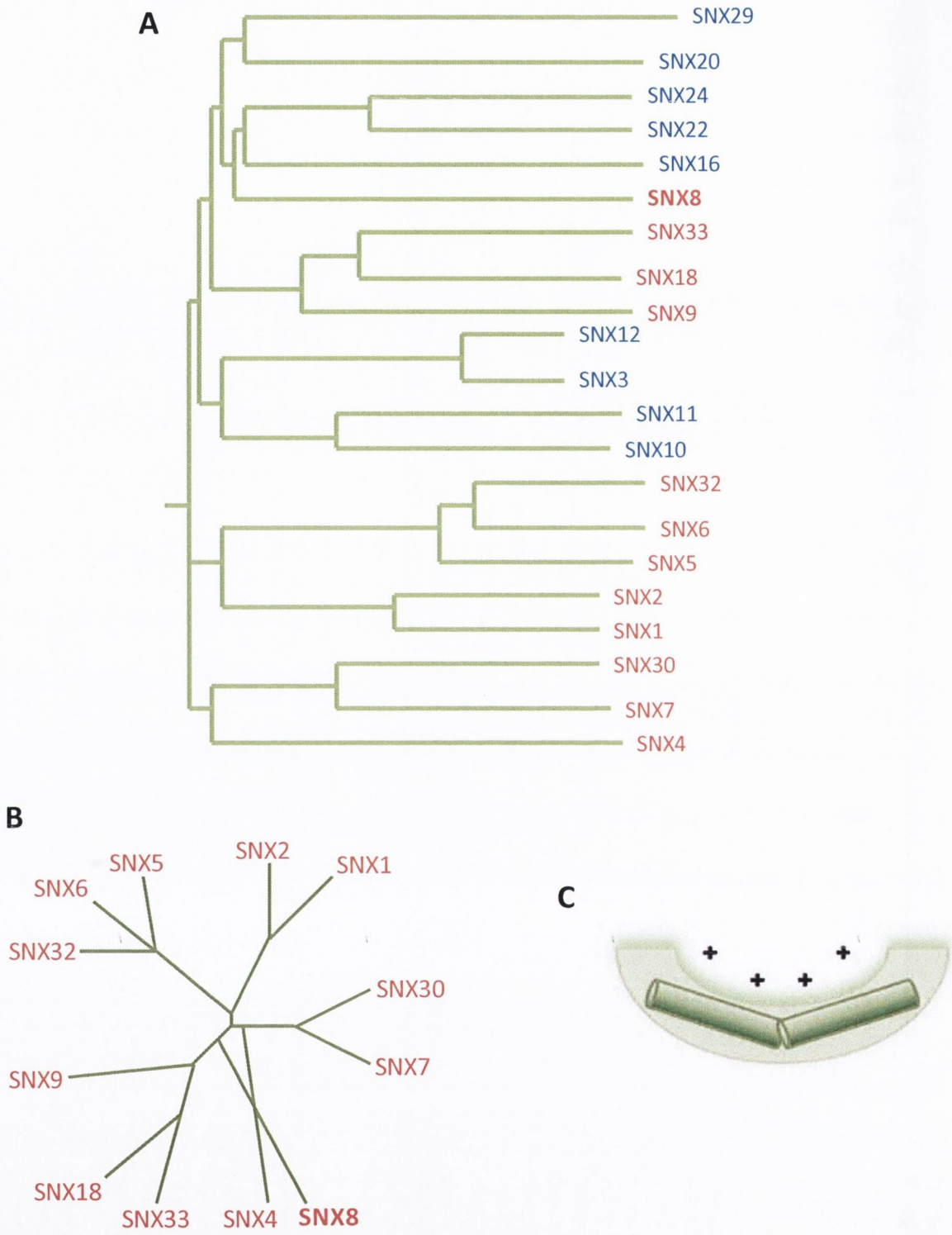

FIGURE 1.8. THE SORTING NEXIN BAR FAMILY. A. The diagram shows a rooted phylogenic tree for the PX BAR and PX containing sorting nexin family members (blue writing shows members of the PX containing SNX family; red writing shows members of the SNX BAR family with SNX8 in bold). **B.** Unrooted phylogenic tree showing all the members of the SNX BAR family, with SNX8 in bold. SNX8 appears to be most closely related to SNX9, SNX18, SNX33 and SNX4. **C.** Dimerisation of BAR domains leads to the formation of a banana shaped curve, + signs indicate the basic charged residues on the concave façade, encouraging interaction with curved membranes.

Electrostatic interactions between the positive residues of the BAR domain and the negatively charged lipids of membranes such as PtdIns(4,5)P_2 also encourage interaction between the protein and membranes (Dawson et al., 2006). BAR domains are also said to stabilise membrane curvature both *in vitro* and *in vivo*; deforming/tubulating membranes for example in the process of vesicle budding (Bhatia et al., 2009).

1.5.2 The PX domain Targets PI motifs In Cell Membranes

Phosphoinositides (PI's) are phosphorylated phosphatidylinositol molecules that regulate various cellular processes. They act as recognition and docking sites for proteins containing a PI recognition domain such as the PX domain (Cozier et al., 2002). The PX domain is found in almost 50 mammalian proteins that regulate membrane trafficking in the endocytic pathway (such as phospholipases and sorting nexins). Sorting nexins make up the majority of these proteins, all 33 members contain a PX domain now referred to as the SNX-PX domain (Seet and Hong, 2006). The sequence of the PX domain is similar in all members, where the structure is highly conserved. One particular PX domain containing protein $p40^{phox}$ (neutrophil cytosolic factor 4; a regulatory component of NADPH-oxide synthesis), shows an N terminal three stranded β sheet and three α helices arranged to form a pocket for PtdIns(3)P interaction (Bravo et al., 2001). Substituting conserved residues in this lipid binding pocket allows different PtdIns to interact with different PX containing proteins in a specific manner (Cozier et al., 2002). The presence of the PX domain does not guarantee that the protein will bind to PtdInsP's; in particular the SNX1 PX domain alone is unable to target to endosomal membranes (Zhong et al., 2002). It was found that the correct localisation was only observed when SNX1 was able to dimerize with itself, via its C terminal BAR domain. Thus BAR domains and PX domains work in tandem in SNXs to allow correct localisation to endosomes, and therefore accurate trafficking.

1.5.3 Sorting Nexin 8 Is A Member Of The SNX-BAR Sub-Family

Sorting nexin 8 (SNX8) contains a C terminal BAR domain as well as the obligatory PX domain, and is a member of the SNX-BAR subfamily of sorting nexins. SNX8 is a protein of 465 amino acid residues, with the PX and BAR domains together accounting for approximately 320 amino acids of its length (**Figure 1.9**). The amino acid sequence of SNX8 is highly conserved between mammals (**Figure 1.10**) and its role appears evolutionary conserved. The yeast homologue of SNX8, (Mvp1p) is known to be involved in endosomal sorting (Ekena and Stevens, 1995). The secondary structure of SNX8 is

unknown. Until very recently the exact function of SNX8 was also unknown. SNX8 does share similar sequence homology with SNX1 (**Figure 1.11**) (Dyve et al., 2009). SNX8 is thought to be involved in endosome to Golgi transport as a component of the retromer complex. Using toxins that highjack the retrograde transport network, SNX8 has been shown to share the function of SNX1. Specifically, it has been shown that GFP tagged SNX8 co-localised with known members of the mammalian retromer complex at the TGN of HeLa (Henrietta Lacks) cells, implicating SNX8 as a new member of the retromer, or at least in having an interaction with the complex (Dyve et al., 2009). The siRNA mediated knockdown of SNX8 increased the trafficking of Shiga toxin to the TGN, where siRNA-SNX8 only marginally decreased the trafficking of Ricin toxin (Dyve et al., 2009) (**Figure 1.13**). This led to the hypothesis that SNX8 acts to negatively regulate the retrograde sorting of Shiga toxin via interaction with the retromer complex, and that SNX8 may regulate the trafficking of specific proteins (due to its differential effects on both toxins) (Dyve et al., 2009).

1.6.0 THE CYCLE OF INTERNALISATION

1.6.1 ENDOCYTOSIS AND INTRACELLULAR SORTING ARE CRITICAL CELLULAR PROCESSES

The endocytic system is a crucial pathway in the sorting of various membrane related proteins, playing roles in, for example, receptor signalling and nutrient uptake (Ryan, 2006). The fate of a protein being trafficked depends on different interactions between sorting motifs within the membrane spanning proteins of the endosomal system and machinery that interacts with the sorting motifs (Bonanomi et al., 2006). A protein that is endocytosed from the membrane via clathrin coated endocytosis will be trafficked to one of three destinations; it can be (i) recycled back to the plasma membrane, (ii) the Trans-golgi newtwork (TGN) or (iii) a lysosome for degradation (Ryan, 2006). Protein trafficking is a highly dynamic process of kinesin and dynein transfer between vesicular structures positioned at key places in the cell governed by interactions with the cytoskeleton (Bowers and Stevens, 2005). Firstly cargo proteins such as receptors are endocytosed and once the vesicle uncoats it fuses with the early endosome, which are generally spaced widely throughout the intracellular environment. Early endosomes then mature into late endosomes which are located closer to the nucleus. Early endosomes mature by fusing together and thus increasing their surface area, at which point the tubular formation of early endosomes is lost. Endosomal pH also decreases due to interaction with vacuolar ATP-ase (Conibear and Stevens, 1998). Cargo proteins may also become included in many small luminal vesicles, which is why late endosomes are

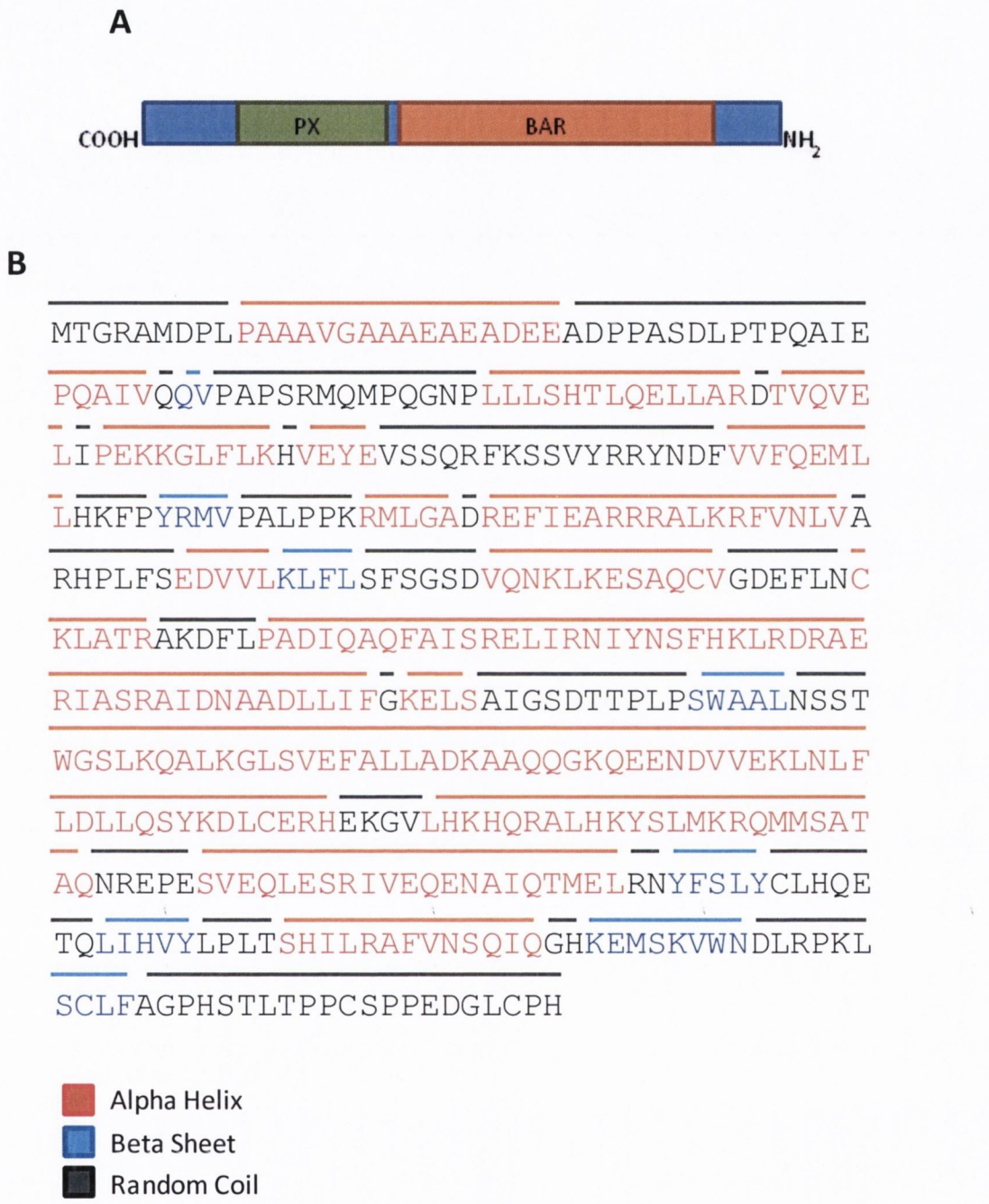

FIGURE 1.9. SNX8 PREDICTED SECONDARY STRUCTURE. A. SNX8 protein structure, showing both PX and BAR domains. **B.** As little is known of the structure of SNX8, SDSC Biology Workbench 3.2 Software (GOR4 program) was used to predict the position of helices (red), sheets (blue) and coils (grey). It appears SNX8 is primarily composed of alpha helices.

```
SNX8_Rat        MTGRAMDPLPSPAVAAAAEAEADEEADPPATGPQTSQVTEWRNLD-----
SNX8_Mouse      MTGRAMDPLPSPAVAAAAEAEADEEADPPATGPRTSQVTEWRALD-----
SNX8_Human      MTGRAMDPLPAAAVGAAAEAEADEEADPPASDLPTPQAIEPQAIVQQVPA
                **********:.**.***************:.  *.*. * : :

SNX8_Rat        PRRMQMPQGNPLLLSYTLQELLAKDTVQVELIPEKKGLFLKHVEYEVSSQ
SNX8_Mouse      PGRMQMPQGNPLLLSYTLQELLAKDTVQVELIPEKKGLFLKHVEYEVSSQ
SNX8_Human      PSRMQMPQGNPLLLSHTLQELLARDTVQVELIPEKKGLFLKHVEYEVSSQ
                * ************:*******:*************************

SNX8_Rat        RFKSSVYRRYNDFVVFHEVLLHKFPYRMVPALPPKRVLGADREFIEGRRR
SNX8_Mouse      RFKSSVYRRYNDFVVFHEVLLHKFPYRMVPALPPKRVLGADREFIEGRRR
SNX8_Human      RFKSSVYRRYNDFVVFQEMLLHKFPYRMVPALPPKRMLGADREFIEARRR
                ****************:*:*****************:*********.***

SNX8_Rat        ALKRFINLVARHPPFSEDVLLKLFLSFSGSDVQHK-KEAAQCVGDEFTNC
SNX8_Mouse      ALKRFINLVARHPPFSEDVLLKLFLSFSGSDVQHKLKEAAQCVGDEFMNC
SNX8_Human      ALKRFVNLVARHPLFSEDVVLKLFLSFSGSDVQNKLKESAQCVGDEFLNC
                *****:******* *****:*************:* **:******** **

SNX8_Rat        KLAARAKDFLPADIQTQFAMSRELIRNVYNSFYKLRDRAERIASRAIDNA
SNX8_Mouse      KLAARAKDFLPADIQTQFAMSRELIRNVYNSFYKLRDRAERIASRAIDNA
SNX8_Human      KLATRAKDFLPADIQAQFAISRELIRNIYNSFHKLRDRAERIASRAIDNA
                ***:***********:***:*******:****:*****************

SNX8_Rat        ADLLIFGKELRQVTLALGSDTTPLPSWAALHLSTWGSLKQALKGLSVEFA
SNX8_Mouse      ADLLIFGKELS----ALGSDTTPLPSWAALHLSTWGSLKQALKGLSVEFA
SNX8_Human      ADLLIFGKELS----AIGSDTTPLPSWAALNSSTWGSLKQALKGLSVEFA
                **********     *:*************: ******************

SNX8_Rat        LLADKAAQQGKKEENDVVEKLNLFLDLLQSYKDLCERHEKGVLHKHQRAL
SNX8_Mouse      LLADRAAQQGKKEENDVVEKLNLFLDLLQSYKDLCERHEKGVLHKHQRAL
SNX8_Human      LLADKAAQQGKQEENDVVEKLNLFLDLLQSYKDLCERHEKGVLHKHQRAL
                ****:******:****************************************

SNX8_Rat        HKYGLMKRQMMSA-AHGREPESVEQLESRIVEQENVIQTMELRNYFSLYC
SNX8_Mouse      HKYGLMKRQMMSA-AHGREPESVEQLESRIVEQENVIQTMELRNYFSLYC
SNX8_Human      HKYSLMKRQMMSATAQNREPESVEQLESRIVEQENAIQTMELRNYFSLYC
                ***.********* *:.*****************.**************

SNX8_Rat        LHQETQLVHVYLPLTSHILGAFVNSQIQGHKEMSKVWNDLKPKLSCLFAG
SNX8_Mouse      LHQETQLVHVYLPLTSHILGAFVNSQIQGHKEMSKVWNDLKPKLSCLFAG
SNX8_Human      LHQETQLIHVYLPLTSHILRAFVNSQIQGHKEMSKVWNDLRPKLSCLFAG
                *******:*********** ********************:*********

SNX8_Rat        PHSVLTPPRSPQEDGMCPH
SNX8_Mouse      PHSVLTPPRSPQEDGVCPH
SNX8_Human      PHSTLTPPCSPPEDGLCPH
                ***.**** ** ***:***
```

FIGURE 1.10. MAMMALIAN SNX8 ALIGNMENT. Amino acid sequence alignment of SNX8 between rat, (NP_001099382.1) mouse (NP_758481.1), and human (DQ895722.2), showing that the SNX8 sequence is highly conserved between all three species. * denotes a single, fully conserved residue, : denotes conservation of strong groups, . denotes conservation of weak groups, - denotes no consensus. (SDSC biology workbench 3.2 software was used (CLUSTALW program)).

```
SNX8_Human   -MTG----RAMDPLPAAAVGAAAEAEADEEADPP---ASDLPTPQAIEPQ
SNX1_Human   MASGGGGCSASERLPPPFPGLEPESEGAAGGSEPEAGDSDTEGEDIFTGA
               :*     * : **..  *  .*:*.   .. *    **    : :

SNX8_Human   AIVQQVPAP----SRMQMPQGNP-----LLLSHTLQELLARDTVQVELIP
SNX1_Human   AVVSKHQSPKITTSLLPINNGSKENGIHEEQDQEPQDLFADATVELSLDS
             *:*.:  :*    * : : :*.         .:  *:*:*  **::.* .

SNX8_Human   EKKG--LFLKHVEYEVSSQRFKSSVYRRYNDFVVFQEMLLHKFPYRMVPA
SNX1_Human   TQNNQKKVLAKTLISLPPQEATNSSKPQPTYEELEEEEQEDQFDLTVGIT
              ::.   .* :.  .:..*. ..*   : .   : :*   .:*   :  :

SNX8_Human   LPPKR-----------MLGADREFIEARRRALKR-FVNLVARHPLFSED
SNX1_Human   DPEKIGDGMNAYVAYKVTTQTSLPLFRSKQFAVKRRFSDFLGLYEKLSEK
              * *                :.  ::.::: *:** * :::. :  :**.

SNX8_Human   VVLKLFLSFSGSDVQNKLKESAQCVGDEFLNCKLATRAKDFLPADIQAQF
SNX1_Human   HSQNGFIVPPPPEKSLIGMTKVKVGKEDSSSAEFLEKRRAALERYLQRIV
               : *:  . .: .     ..:   ::  ..::  : :  *   :*  .

SNX8_Human   AISRELIRNIYNSFHKLRDRAERIASRAIDNAADLLIFGKELSAIGSDTT
SNX1_Human   NHPTMLQDPDVREFLEKEELPRAVGTQTLSGAGLLKMFNKATDAVSKMTI
             .  *     ..* : .: .. :.::::..*. * :*.*  .*:.. *

SNX8_Human   PLP----------------SWAALNSSTWGSLKQALKGLSVEFALLADK
SNX1_Human   KMNESDIWFEEKLQEVECEEQRLRKLHAVVETLVNHRKELALNTAQFAKS
              :                 .      :.  :* :  * *::: * :*..

SNX8_Human   AAQQGKQEEN-DVVEKLNLFLDLLQSYKDLCERHEKGVLHKHQRALHKYS
SNX1_Human   LAMLGSSEDNTALSRALSQLAEVEEKIEQLHQEQANNDFFLLAELLSDY-
              *  *..*:*  : . *. : :: :. ::* :.: :. :.   . * .*

SNX8_Human   LMKRQMMSATAQNREPESVEQLESRIVEQENAIQTMELRNYFSLYCLHQE
SNX1_Human   IRLLAIVRAAFDQRMKTWQRWQDAQATLQKKREAEARLLWANKPDKLQQA
             :    :: *: ::*     .  ::: . *::     .*    .   *:*

SNX8_Human   TQLIHVYLPLTSHILRAFVNSQIQGHKEMSKVWNDLRPKLSCLFAGPHST
SNX1_Human   KDEILEWESRVTQYERDFERISTVVRKEVIRFEKEKSKDFKNHVIKYLET
             .: *  : . .::  * * . .   :**: :. ::   .:.  .    .*

SNX8_Human   LTPPCSPPE---DGLCPH-----
SNX1_Human   LLYSQQQLAKYWEAFLPEAKAIS
             *  . .      :.: *.
```

FIGURE 1.11. SNX8 AND SNX1 ALIGNMENT. Amino acid sequence alignment of SNX1 and SNX8, showing that the SNX8 sequence is highly conserved between each protein. * denotes a single, fully conserved residue, : denotes conservation of strong groups, . denotes conservation of weak groups, - denotes no consensus.(SDSC biology workbench 3.2 software was used (CLUSTALW program)).

also referred to as multivesicular bodies. At this stage, receptors for example are stripped from their ligands and proteins can be tagged with ubiquitin. From the late endosome, cargo proteins in the luminal vesicles can travel to the lysosome. In order for this to occur the late endosome fuses with the lysosome and delivers the cargo proteins into the lumen. ESCERT (endosomal sorting complex required for transport complexes) detect the ubiquitin tagged proteins and degrade them (pathway (1) in **Figure 1.12**). The trafficking of proteins back to the plasma membrane involves the trafficking to the recycling endosomes and then insertion back into the plasma membrane. This is the case for many G protein coupled receptors (GPCRs), for fast turn around in their signalling cascade (pathway (2) in **Figure 1.12**). The TGN is an important site in the sorting pathway; transport of cargo proteins from endosomes to this organelle is known as retrograde transport and is mediated by the formation and interaction of retromer complexes (pathway (3) in **Figure 1.12**).

1.6.2 The Retromer Complex Controls Retrograde Sorting

SNX8 has recently been suggested to regulate retrograde sorting. The TGN forward pathway involves the packaging and sorting of cargo proteins formed in the ER and transported through the Golgi (Griffiths and Simons, 1986), where as the retrograde or reverse pathway involving the transport of proteins from the endosome to the TGN is less well known. Retrograde transport is known to occur with some receptor types, namely the MPR (mannose 6-phosphate receptor) in mammals. The newly produced ligand binds at the TGN and the receptor-ligand complex is packaged into vesicles and transported to endosomes. Here the change in environment causes ligand dissociation which is then transported to the lysosome where it is converted into its active form. The receptor is then trafficked back to the TGN to allow a cyclic process (Bonifacino and Rojas, 2006). Bacterial and plant toxins such as Shiga and Ricin toxin respectively have been observed to highjack cellular machinery including the retrograde pathway to allow them to be endocytosed and transported to their target area within the cell to exert their noxious effects (Dyve et al., 2009). Importantly, SNX8 appears to inhibit trafficking of Shiga toxin to the TGN where siRNA SNX8 intereference increased shiga toxin transport. The retromer complex is the cellular machinery responsible for the transport of many proteins through this pathway. Five Vps proteins (vacuolar protein sorting proteins) that form a retromer complex in *S. cerevisiae* have been found to regulate the trafficking of pro-carboxypeptidase Y from the TGN to the endosome (Bowers and Stevens, 2005). These proteins include Vps5, 17, 26, 29 and 35. Mutation of any one of these proteins resulted in the incorrect sorting of pro-carboxypeptidase Y. There are human homologues of these yeast retromer proteins of

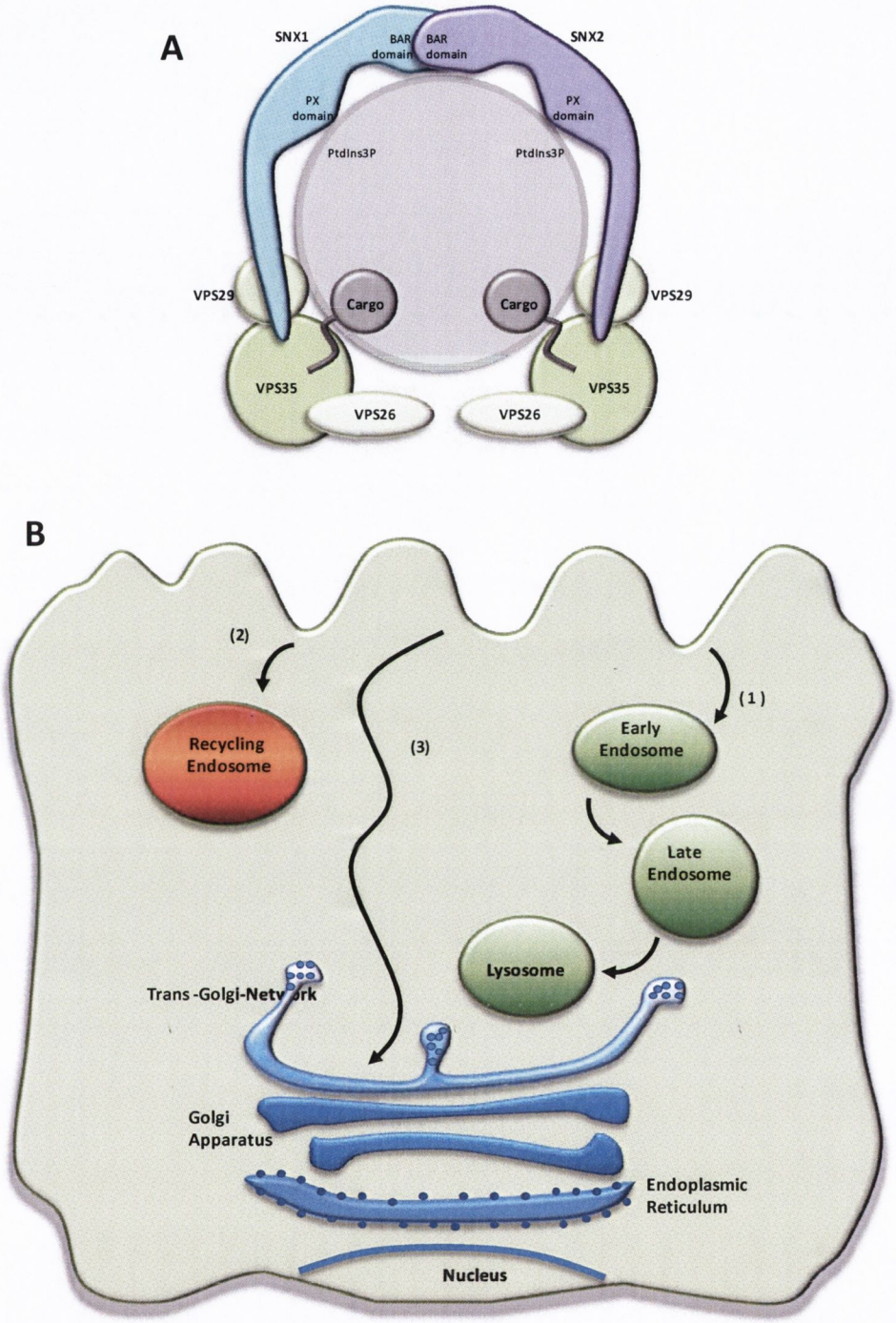

FIGURE 1.12. INTRACELLULAR TRAFFICKING AND RETROGRADE TRANSPORT. A. Structure of the retromer complex. **B.** Internalisation of protein (for example a receptor) can follow one of three primary routes. **(1)** Degradation - The protein could be endocytosed and trafficked to the early endosome, which matures into the late endosome and the contents taken to the lysosome where they are degraded. **(2)** Recycling - The protein could be endocytosed and trafficked to the recycling endosome where in the case of a receptor it is stripped of it's ligand and then trafficked back to the plasma membrane. **(3)** Retrograde – The protein is endocytosed as route one, but instead of being taken to the lysosome to be degraded it is trafficked to the trans-golgi network where it is retained long term.

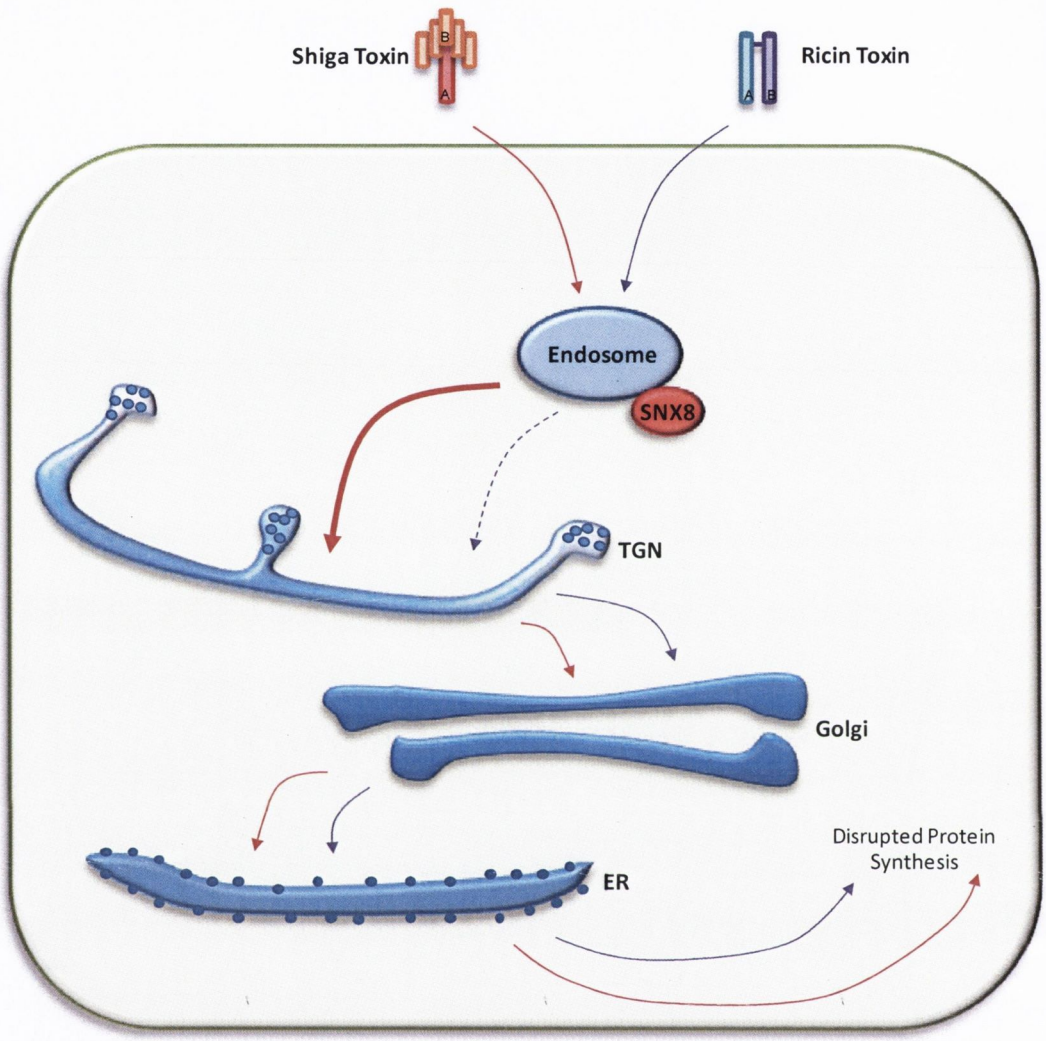

FIGURE 1.13. THE EFFECTS OF SNX8 KNOCKDOWN ON SHIGA AND RICIN TOXIN TRAFFICKING. Ricin and Shiga toxin are both endocytosed and undergo retrograde transport via the endosome, to the trans-golgi-network, then to the golgi complex, and finally to the endoplasmic reticulum, where the A subunit separates from the B moiety. The A subunit then enters the cytoplasm where it inbibits the 60S ribosomal subunit, and therefore protein synthesis. SNX8 knockdown was found to increase shiga toxin transport to the TGN, where as ricin toxin transport was seen to be slightly decreased. SNX8 was found to be co-localised with both the early endosome and some retromer components, suggesting the differential protein trafficking is due to SNX8s role within endosomal sorting.

which sorting nexin family members are included, namely SNX1 and SNX2, in addition to VSP29, 26 and 35 (Haft et al., 2000) (**Figure 1.10**). The domain structure of the SNX family renders them necessary to target the Vps complex to the endosome (Rojas et al., 2007). This is due to the combination of both the PX domain that can interact with the correct phosphoinositide and the BAR domain that can dimerise and sense and stabilise membrane curvature. The SNX part of the retromer is involved in correct recruitment and the Vps part is the "cargo recognition complex" (Bonifacino and Rojas, 2006). The N terminal sequences of the SNX subunits bind at either side of the Vps complex suggesting the complex binds in a parallel line along the endosomal membrane. Thus the complex may form a coat around structures such as the tubular extensions from the endosome (Hierro et al., 2007). These extensions tubulate further with retromer interaction and are trafficked towards the TGN, instead of the default lysosomal pathway.

Sortilin is a mammalian homologue of Vps10 and is hypothesised to be trafficked from the endosome to TGN via the retromer system (Mari et al., 2008). A short sequence in the cytosolic tail was found to interact with the retromer complex in a recent study using co-immunoprecipitation assays. This interaction was necessary for the successful retrograde transport of sortilin (Seaman, 2007). In addition to SNX8 other sorting nexins have been identified to interact with the retromer complex, for example SNX3 confer a higher level of specificity of cargo recognition by binding to both the retromer and to a conserved sequence in the c-terminal tail of the iron transporter Fet3-Ftr1 (Strochlic et al., 2007). This interaction is essential for the homeostasis of iron levels, primarily by ensuring the correct recycling of the transporter between the plasma membrane, endosome and TGN. Recently retromer dysfunction has been implicated in neurodegenerative disease. Retromer levels have been observed to be lower in some brain regions of Alzheimer's patients (Small et al., 2005). siRNA interference of the Vps35 component of the retromer complex was found to increase Aβ peptide levels, reduce the frequency of APP transport, and enlarge early endosomes (Bhalla et al., 2012). Taken together, these reports clearly indicate a role for several family members of SNXs, inclusing SNX8 as playing vital roles in protein cargo transport via the retromer complex.

1.7.0 Aims And Hypothesis

1.7.1 Project Aims And Hypothesis

Indications are that SNX8 is involved both in retrograde sorting and the regulation of the SREBP pathway (Chatterjee et al., 2009; Dyve et al., 2009). As cholesterol homeostasis plays a crucial role in

neurodegenerative diseases, such as NPC disease, the aim of this project was to explore the function of SNX8 within the CNS environment. Specifically, initially the aim was to explore SNX8 expression within the CNS, and then modulate this expression using a lentiviral system to overexpress a GFP tagged SNX8 construct. The function of SNX8 will be investigated in three differing cholesterol conditions, (i) statin mediated low cholesterol levels, (ii) high cholesterol levels and (iii) U18666a mediated lysosomally accumulated cholesterol (a cellular model of NPC disease). Finally, the inflammatory profile of U18666a treated neurons was investigated, with the hope to gain insight into the neuroinflammatory aspect of NPC disease.

It was hypothesised that SNX8 is expressed within the CNS, and this expression may be modulated in differing cholesterol environments. Lentiviral mediated GFP-SNX8 overexpression may also alter cholesterol conditions within neurons, and if so, SNX8 gene therapy may be useful in altering cholesterol related disorders, such as NPC disease and Alzheimer's disease within the CNS. In addition, we hypothesise that U18666a treatment may elicit immune responses from CNS resident cells, leading to further characterisation of the inflammatory aspects of NPC disease. Specific changes in chemokine or cytokine levels may highlight a novel target for manipulation with the aim of treating the inflammatory symptoms observed in NPC disease.

CHAPTER 2. MATERIALS AND METHODS

2.0.0 MATERIALS AND EQUIPMENT

MOLECULAR BIOLOGY

2-mercaptoethanol (31350010-20ml, Gibco) • 2-propanol (I9516-500ml, Sigma) • Agar (BP1423-500g, Fisher) • Agarose (BP1356-100g) • Agarose Low Melting Point (BP165-25g) • Ampicillin (A9518-25g) • Calcium chloride (C3306-100g, Sigma) • Calf intestinal alkaline phosphatase (CIP) and buffer 3 (MO290L, New England Biolabs) • D-(+)-glucose (G8270-1kg, Sigma) • Ethanol (E7023-500ml, Sigma) • ExACTgene 1kb DNA ladder (BP2578100-1ml, Fisher) • GelRed (41003-1ml, Biotium) • Gene pulser cuvettes (1652089, Bio-Rad) • Glycerol (G2289-500ml, Sigma) • IP-10 PCR Primer (Rn01413889_g1, Applied Biosystems) • Kanamycin (60615-5g, Sigma) • Kpn1 restriction enzyme (10899186001, Roche) • LIX ELISA (DY543, R+D Systems) • LIX PCR primer (Rn01441604_m1, Applied Biosystems) • Luria Bertani (LB) Broth (BP1426-2kg, Sigma) • Magnesium chloride (M2670-100g, Sigma) • Magnesium sulphate (M2643-500g, Sigma) • Nhe1 restriction enzyme (10885843001, Roche) • Nucleospin RNA II kit (NC9581114, Fisher) • Plasmid Midi Kit (12143, Qiagen) • Plasmid Maxi Kit (12163, Qiagen) • QIAprep Spin Miniprep Kit (12125, Qiagen) • QIAquick gel extraction kit (28704, Qiagen) • QIAquick PCR purification kit (28104, Qiagen) • Rat beta-actin PCR primer (401846, Applied biosystems) • Sma1 restriction enzyme (10220566001, Roche) • Sodium chloride (S3014-5kg, Sigma) • Subcloning efficiency DH5α competent cells and recovery medium (18265-017, Invitrogen) • T4 DNA ligase and ligase buffer (15224017, Invitrogen) • Taqman universal PCR mastermix (4304437, Applied Biosystems) • Taq polymerase with PCR reaction buffer 10x and PCR nucleotide mix (4728882001, Roche) • Tryptone (J859-500g, Amresco) • Water (W4502-1L, Sigma) • Xho1 restriction enzyme (10889194001, Roche) • XL1-blue electrocompetent cells (200228, Stratagene) •

BIOCHEMISTRY

6-aminohexanoic acid (A7824-25g, Sigma) • Acetic Acid (695092, Sigma) • Acrylamide 30% bis solution 37.5 (161-0158-500ml, Bio-Rad) • Ammonium persulfate (A3678-25g, Sigma) • Bovine serum albumin (BSA) (A9647-100g) • Brilliant blue R-250 (Coomassie blue (BPE101-25, Fisher) • Calcium chloride (C3306-100g) • cDNA archive kit (4387406, Applied biosystems) • Ethylenediaminetetraacetic acid disodium salt dihydrate (EDTA) (E5134-500g, Sigma) • Glycine (G080060-1kg, Fisher) • Hydrochlorlic acid (258148-500ml, Sigma) • Immobilon P polyvinylidene difluoride membrane (PVDF) (P2938, Sigma) Magnesium sulphate (M2643-500g, Sigma) • Methanol (M/4056/017-2.5L, Fisher) • N, N, N',N-tetramethylethylenediamine (TEMED) (T7024-25ml, Sigma) • Potassium chloride (P9541-500g, Sigma) • Potassium phosphate dibasic trihydrate (P9666-100g,

Sigma) • Precision Plus Protein Dual Colour Standards (161-0374-0.5ml, Bio-Rad) • Re-blot plus (2504, Milipore) • Sodium bicarbonate (S5761-500g, Sigma) • Sodium chloride (S3014-5kg, Sigma) • Sodium dodecyl sulphate (SDS) (L4390-500g, Sigma) • Sodium hydroxide (S8045-500g, Sigma) • Sodium phosphate dibasic heptahydrate (S9390-250g, Sigma) • Sodium Pyruvate (S8636-100ml, Sigma) • Tris Base (BP152-1kg, Fisher) • Triton X-100 (T9284-500ml, Sigma) • Tween 20 (P7949-500ml, Sigma) •

CELL CULTURE

0.2 µm single-use filter units (16534, Sartorius Stedim) • 0.25% Trypsin/EDTA solution (T4049-100ml, Sigma) • 0.4% Trypan blue solution (T8154-100ml, Sigma) • 25-OH cholesterol (707678, Sigma) • 35 mm Petri dishes (1171734, Lennox) • 4-(2-hydroxyethyl)-1-piperazineethanesulfonic acid (HEPES) (15630-056-100ml, Invitrogen) • 6-aminohexanoic acid (A7824-25g, Sigma) • B27 (17504-044-10ml, Invitrogen) • Borosilicate coverglass 13 mm diameter (631-0149, VWR) • Control shRNA plasmid A (sc-1087060, Santa Cruz) • D-(+)-glucose (G8270-1kg, Sigma) • Dimethylsulphoxide (DMSO) (D8418-250ml, Sigma) • Disposable and sterile cell scrapers (08-100-241, Fisher) • Dulbecco's modified Eagle medium (DMEM) (D6546-500ml, Sigma) • DMEM high glucose (L0104-500ml, Biosera) • DMEM-F12 (SH3000404, Fisher) • Dulbecco's PBS (14190-094-500ml, Invitrogen) • Fetal Bovine Serum (FBS) heat inactivated (S1900-500ml) • Filipin III (F4767, Sigma) • Filter paper grade 3 (1003-917, Whatman) • Formaldehyde 37% solution (5339988500ml, Sigma) • Glass coverslips 22 mm x 50 mm (MNJ-350-070P, Fisher) • HEK293T cells (American Type Culture Collection, ATCC) • Hyclone Hypure cell culture grade water (HYC-001-216G-500ml, Thermoscientific) • Laemmli (sample) buffer (161-0737-30ml, Bio-Rad) • L-glutamine (G7513-100ml, Gibco) • Lipofectamine transfection reagent (18324-012-1ml, Invitrogen) • MEM (SH3002401, Fisher) • Mevinolin (M2147, Sigma) • Microscope slides 76 mm x 26 mm (MNJ-150-030U, Fisher) • Neurobasal A medium (10888-022-500ml, Invitrogen) • Nunc 24-well plates (TKT-190-110Y, Fisher) • Nunc 6-well plates (TKT-190-110E, Fisher) • Optimem 1 reduced serum medium (11058-021-500ml, Invitrogen) • Papain (P4762-50mg, Sigma) • PBS tablets (P4417-100tab, Sigma) • Penicillin/streptomycin (P4333-100ml, Sigma) • Phosphate buffered saline (PBS) (20012-500ml Invitrogen) • Plus Reagent (11514-015-0.75ml, Invitrogen) • Polyethylene imine (PEI) (provided by Kamal Gadalla, Glasgow University) • Poly-L-lysine hydrobromide (P1399-25mg, Sigma) • Propridium iodide (NC0221356, Fisher) (Proteome Profiler Rat Cytokine Array Kit (ARY008,R+D Systems) • shRNA plasmid transfection medium (sc-108062) • shRNA plasmid transfection reagent (sc-108062, Santa Cruz) • single use filter units Millex GP (SLGP033RS, Millipore) • SNX8 shRNA plasmid (human) (sc-61595, Santa Cruz) • T-150 cm(2) cell culture flasks (430825, Corning) •T-25 cm (2) cell culture flasks (430639, Corning) • T-75 cm(2) cell

culture flasks (430641, Corning) • Thinwall ultraclear ultracentrifuge tubes (344058, Beckman) • U18666a (662015, Merk) • Vectashield mounting medium for fluorescence (H1000-10ml, Vector Laboritories) •

EQUIPMENT

Beckman Optima XL-80K ultracentrifuge • Beckman SW-28 ultracentrifuge rotor • Electropotator (Biorad) • Fujifilm LAS-3000 Intelligent Dark-box • Incubator (Binder, Mason Technology) • NanoDrop-spectrophotometer (ND-1000 V3.5, nanodrop technologies Inc., USA) • Polymerase chain reaction (PCR) machine (Applied Bioscience) • Powerpack (Biorad) • Shaker (New Brunswick Scientific E24 Incubator, Mason Technology) • Small bench centrifuge (Hermle, Mason Technology) • Sonicator (Sonics, Vibracell) • Spectrophotometer (Biophotometer, Eppendorf) • Synergy HT multimode microplate reader (BioTek, Mason) • Thermocycler (PTC-200, Peltier Thermal Cycler, MJ Research, Biosciences Ireland) • Ultraviolet (UV) transilluminator (Syngene, UK) • Water bath (UAB 12 EU, Grant)

Antibody	Host	Company	Cat. No.	WB Dilution	IF Dilution
Primary Antibodies					
Actin	mouse	ECM biosciences	AM2021	1:2000	-
Cluster of differentiation molecule 11b (CD11b)	mouse	Gift from Marina Lynch Group		-	1:500
2', 3'-cyclic nucleotide 3'-phospho-diesterase (CNPase)	mouse	Millipore	MAB326	-	1:500
Glial Fibrillary Acidic Protein (GFAP)	mouse	Millipore	MAB360	-	1:500
Green Fluorescent Protein (GFP)	rabbit	Millipore	AB3080	1:2000	1:1000
Inhibitor of NFκB (IκBα)	rabbit	ECM biosciences	IP1861	1:1000	-
Neurofillament-H	chicken	Millipore	AB5539	-	1:500
Myelin Basic Protein (MBP)	rabbit	Abcam	AB40390	-	1:500
Sorting Nexin 8 (SNX8) (d-17)	goat	Santa Cruz	SC-41939	1:400	1:200
Phosphorylated IκBα (ser32)	rabbit	Cell Signalling	2859	1:1000	-
Hoescht	-	Gift from Novartis		-	1:800
HRP-conjugated secondaries					
anti-goat	rabbit	Sigma	A4174	1:5000	-
anti-mouse	goat	Sigma	A8924	1:5000	-
anti-rabbit	donkey	GE Healthcare	NA934	1:5000	-
Dylight/Alexa secondaries					
anti-chicken Dylight 488	donkey	Jackson Imm. Res.	703-485-155	-	1:500
anti-chicken Dylight 633	donkey	Jackson Imm. Res.	711-485-152		1:500
anti-goat alexa 633	donkey	Invitrogen	A21082	-	1:500
anti-mouse dylight 488	donkey	Jackson Imm. Res.	715-485-150	-	1:500
anti-rabbit alexa 488	goat	Invitrogen	A21071	-	1:500

FIGURE 2.1. SUMMARY OF ANTIBODIES USED IN IMMUNOHISTOCHEMISTRY. Table summarising the details of antibodies used for staining and western blotting.

2.1.0 METHODS

2.1.1 MOLECULAR BIOLOGY

2.1.2 BACTERIAL COMPETENT CELL PREPARATION

Luria Bertani (LB) agar plates (10% Peptone, 5% yeast extract, 5% sodium chloride, 10% agar in H_20) were prepared by autoclaving and pouring the solution into sterile petri dishes. The plates were used to grow DH5α *E. coli* overnight at 37°C. A single colony was picked from the plate and used to inoculate 5 ml LB medium. The culture was incubated overnight with continuous shaking at 200 rpm at 37°C. Thereafter, 2 ml of the overnight bacterial culture was transferred into 200 ml of LB media and incubated with continuous shaking at 200 rpm for 2-3 hr at 37°C to reach an OD^{600} of 0.6-1.0. The 200 ml sample then was divided into 4 x 50 ml falcon tubes and centrifuged at 3,000 x g for 15 min at 4°C. The bacterial pellet was resuspended thoroughly in 20 ml ice cold 100 mM $MgSO_4$ and centrifuged at 3,000 x g for 15 min at 4°C. The pellet was then resuspended in 2 ml of ice cold 100 mM $CaCl_2$ with 15% glycerol. The suspensions were aliquoted into 50 µl (in pre-cooled 1.5 ml eppendorf tubes) and snap-chilled in liquid nitrogen. The cells were stored at -80°C until use.

2.1.3 HEAT SHOCK TRANSFORMATION AND PLASMID DNA EXTRACTION

Heat shock method of transformation was used to obtain recombinant bacterial colonies. The DH5α strain was used to yield plasmid DNA. Competent cells were removed from -80°C and thawed on ice for 15-20 min. Next, 1-2 µg of plasmid DNA was mixed with 50 µl of competent bacteria and incubated on ice for 15 min. Heat shock was applied for 90 sec by placing the tube in a water bath at 42°C then immediately transferring onto ice for 10 min. To recover the cells, 1 ml LB was added to the transformed bacteria and incubated with continuous shaking at 200 rpm for 60 min at 37°C. The cells were centrifuged at 3,000 x g for 2 min. The pellet was resuspended in 200 µl LB and spread on pre-warmed agar plates supplemented with either 50 µg/ml kanamycin or ampicillin. Plates were incubated overnight at 37°C. A single colony was used to inoculate in 5 ml of LB medium and left overnight with continuous shaking at 200 rpm at 37°C. The plasmid DNA was extracted from the bacterial culture using a plasmid mini-prep or plasmid maxi-prep kit according to manufacturer's recommendation (Qiagen).

2.1.4 Polymerase Chain Reaction and restriction digestion

The components used for polymerase chain reaction (PCR) were 20 pg DNA template, 1x PCR buffer, 10 p/mol forward and reverse primer, dNTPs (200 µM) and 1 U of DNA polymerase in a 20 µl reaction mix. After the initial denaturation (94°C for 5 min) the PCR reaction cycle was programmed as follows: denaturation (94°C for 60 sec), annealing (65°C for 60 sec) and elongation (72°C for 2 min). This cycle was repeated 30 times to achieve the desired amplification. Before ending the reaction, the elongation temperature was maintained for 10 min, at the end of 30^{th} cycle. The PCR fragments were purified using a PCR purification kit (Qiagen). The sample was then stored at -20°C until further use. The restriction digestion was performed in a reaction volume of 20 µl using 1 µg of DNA incubated with 1 U of restriction enzyme and 1x appropriate buffer at 37°C for 2 hrs. DNA fragments were run on agarose gels (1 x TBE (40 mM Tris-borate and 1 mM EDTA) and 1% agarose) alongside a DNA ladder to determine whether they were of appropriate size. Following restriction digest the fragments were purified using a gel purification kit (Qiagen).

2.1.5 Dephosphorylation, Ligation and Transformation

To restrict self-ligation, the digested and purified vector DNA was dephosphorylated by incubating in 1x CIP buffer (calf intestinal alkaline phosphatise) and 1 U of phosphatase enzyme for 1 hr at 37°C. The reaction was then deactivated by placing in a heatblock set to 70°C for 10 mins. After dephosphorylation, the vector was separated in 1% agarose gel and rescued using a gel extraction kit (Qiagen). The ligation reaction was performed with a T4 ligase kit (Invitrogen) using 200 ng of insert with 50 ng of cut vector, 1x ligation buffer and 1 U of T4 DNA ligase (total vol 20 µl). The ligation mixture was incubated overnight at 16°C. After ligation, 2 µl of ligation mixture was used to transform 40 µl XL1-Blue electro-competent cells by electroporation (1.7 kV, 200 Ω, 25 µF). The transformed cells were incubated in 1 ml of SOC medium (0.5% Yeast Extract, 2% Tryptone, 10 mM NaCl, 2.5 mM KCl, 10 mM MgCl2, 10 mM MgSO4, 20 mM Glucose) for 1.5 hr. The bacterial cells were centrifuged at 3000 g for 2mins and the pellet resuspended in 200 µl LB supplemented with either kanamycin or ampicillin (50 µg/ml). An aliquot of 100 µl cells was plated on either kanamycin or ampicillin supplemented LB agar plates. After over-night incubation, one colony was picked and used to inoculate 5 ml of LB media which was then incubated at 37°C with continuous shaking overnight. The plasmid DNA was extracted using mini-prep kit (Qiagen). Each sample was examined by PCR and restriction digestion for presence of the insert. For further verification of the successful cloning, recombinant plasmids were to Eurofins MWG Operon for DNS sequencing.

2.2.0 BIOCHEMISTRY

2.2.1 SDS - POLY ACRYLAMIDE GEL ELECTROPHORESIS AND WESTERN BLOTTING

Proteins were separated according to their respective molecular weight in poly acrylamide gels. The resolving gel was made with 10% acrylamide, 0.4 mM TRIS-HCl pH 8.8, 0.1% SDS, 0.05% APS and 0.1% TEMED. The stacking gel was made with 4% acrylamide, 0.37 mM TRIS-HCl pH 8.8, 0.1% SDS, 0.05% APS and 0.1% TEMED. The proteins were separated under constant 100 V when the samples were in stacking gel and constant 150 V when the samples entered the resolving gel. Separated proteins were viewed by western blotting. Western blotting was performed using a semi-dry transfer method. The resolved proteins were transferred to PVDF (Poly Vinylidene Difluoride) membrane (Sigma). The PVDF membrane was cut according to the size of the gel and immersed into methanol for 15 sec to activate the membrane then transferred into solution C (25 mM TRIS, 0.02% SDS, 20% methanol and 40 mM ε-amino caprionic acid) for 1 hr. Whatman papers (grade 3) were cut and two strips were dipped into each solution A (0.3M TRIS, 0.02% SDS, 20% methanol), solution B (25 mM TRIS, 0.02% SDS, 20% methanol) and solution C. The order of components for the protein transfer was arranged in the transfer unit as follows, Anode - 2x Whatman papers in Solution A, 2x Whatman papers in Solution B, PDVF membrane, SDS-PAGE, 2x Whatman papers in Solution C - Cathode. The transfer unit was run for 90 min under a constant current of 50 mA. After transfer the PDVF membrane was blocked with 5% non-fat milk or 5% BSA in PBS-T buffer (1x PBS buffer (8g of NaCl, 0.2g of KCl, 1.44g of Na_2HPO_4, 0.24g of KH_2PO_4) with 0.1% Tween-20) for 2 hr at room temperature, then incubated with primary antibody overnight at 4°C. Next, the blot was washed with PBS-T buffer for 4 x 5 min, then incubated with secondary antibody for 2 hr at room temperature. Thereafter, the blot was washed 4 x 5 min in PBS-T and visualised using Immobolin chemiluminescent HRP substrate. Blots were imaged on a Fujifilm LAS-3000 Intelligent Dark-box. For commercial blots the membrane was reactivated with 100% methanol for a few seconds then thoroughly washed with TBS-T (25 mM Tris-Cl, pH 8.0; 125 mM NaCl; 0.1% Tween 20) twice to remove residual methanol. The membrane was incubated with 5% nonfat dry milk in TBS-T for 1 hour to block non-specific antibody binding, and all steps carried out as before (with TBS-T replacing PBS-T). To strip and re-probe with a new antibody blots were placed in Re-Blot Strong Solution (Millipore) diluted 1:10 in water for 15 min, then blocked with 1% milk/TBST for 1 hour and the process of antibody incubation and development carried out as above.

2.3.0 HETEROLOGOUS AND PRIMARY CELL CULTURE

2.3.1 ORGANOTYPIC HIPPOCAMPAL AND CEREBELLAR SLICE CULTURES

Post natal day 10 Wistar rats were decapitated and the skin and skull cut away from the head. The brain was then carefully excised from the skull and placed in ice cold MEM (Minimum Essential Medium Eagle, with Earle's salts and without L-glutamine) for approximately 30 seconds. Using a razor blade, the two hemispheres were separated directly down the midline, one hemisphere was then placed back in the chilled slice media. The hippocampus was dissected by using two small spatulas to pull back the cortex from the rest of the brain, revealing the hippocampus. Using the spatula the ends of the hippocampus were gently separated from the surrounding tissue. The spatula was put under the concave face of the hippocampus and used to carefully roll out the tissue section, any excess tissue was then removed from around the separated hippocampus. The cerebellum was dissected from other brain tissue using a scalpel. The excised tissue was then transferred to the tissue chopper and sectioned into 400 micron slicesand the slices kept in MEM at 4°C for 1 hr. The slices were then separated carefully using two needle heads under a stereo microscope. The slices were plated onto membrane inserts in 6 well plates (Millipore) (5 per insert) with 1ml of culture media underneath the insert (50% Optimem, 25% HBSS, 25% FBS, 27.5 mM D-glucose, 2 mM L-glutamine, 10,000 U/ml pen/strep, 10 mM HEPES). The slices were incubated at 35.5°C, 5% CO_2 and the media was changed every 2-3 days.

2.3.2 ORGANOTYPIC HIPPOCAMPAL AND CEREBELLAR SLICE STAINING

The inserts were removed from their current 6 well plate and placed in a new plate containing 1ml ice cold PBS. Next, 1 ml of ice cold PBS was carefully pipetted onto the insert to remove any traces of media. The inserts were then placed in 1ml of 4% formaldehyde and a further 1ml pippetted on top and left for 5 mins. The inserts were then washed with ice cold PBS (2 x 5 mins). The slices were permeabilised by placing the inserts in 1ml (again with 1 ml on top of the insert) of 0.5% Triton X (in PBS) and left overnight at 4°C. The PBS wash steps were repeated. The slices were then blocked for 4 hours in 20% BSA at room temperature, followed by repetition of the PBS wash steps. The slices were then cut out from the insert and placed in 60µl of 5% BSA (on a microscope slide) with the appropriate dilution of primary antibody. The slides were placed in a slide box containing water overnight at 4°C to ensure the slices did not dry out. The cut out slices were washed in PBS for 3 x 5 mins. The secondary antibody was made up in 5% BSA and was incubated like the primary antibody for 4 hr. The PBS wash steps were then repeated. Hoescht of 1:800 dilution was made up in 5% BSA

and incubated for 1 hr. The PBS wash steps were repeated. The slices were then mounted on slides with OCT and covered with a coverslip.

2.3.3 Coverslip, Plate and Flask Preparation for Primary Cell Culture

For primary cell cultures each culture flask or 6 well plate was coated with a poly-L-lysine solution (40 µg/ml in sterile H_2O: Sigma) and left for 1 hr at 37°C. This solution was then removed and the flask washed with cell culture grade water (Invitrogen) x2 and left to dry in the laminar flow hood. For primary cell cultures grown on coverslips, borosilicate glass coverslips with a diameter of 13 mm (VWR) were sterilized prior to use by immersion in 70% methanol followed by exposure to UV light overnight. Coverslips were then coated with poly-L-lysine (40 µg/ml) for 1 hr at 37°C. The coverslips were then rinsed briefly with cell culture grade water and laid out in the laminar flow hood to air dry before being placed in 24 well-plates.

2.3.4 Brain Dissection For Primary Cultures

Postnatal one-day old female Wistar rats (supplied by the Bioresources Unit, Trinity College Dublin) were used for both the astrocyte and neuronal cultures. The pups were decapitated in accordance with The Animals Act 1986 (Scientific Procedures) Schedule I guidelines. The skull was exposed by cutting the skin from the neck down to the tip of the nose. The skull was then removed by making a sagittal cut along the level of the medial longitudinal fissure and two horizontal cuts along each side of the skull at the level of the ears. The skull was peeled back revealing the cortex which was rapidly removed with curved forceps.

2.3.5 Astrocyte Culture

Following dissection the cortices were placed in pre-warmed supplemented DMEM F12 ((Dulbecco's Modified Eagle Medium, Nutrient Mixture F-12) and 10% FBS, 1% pen/strep). The meninges were removed from the cortices using a fine straight forceps and the cortices were then cross-chopped using a sterile disposable scalpel. The tissue was incubated in the media for 20min at 37°C, then passed through a sterile nylon mesh cell strainer (40µm, BD Biosciences). This filtrate was centrifuged at 2,000 x g for 3min at room temperature. The resulting cell pellet was resuspened in pre-warmed supplemented DMEM high glucose media (10% FBS, 1% penicillin/streptomycin) and transferred into poly-L-lysine coated T75 culture flasks, usually two cortices per T75 flask. When

confluent (~ 13 days) the flasks were removed from the incubator, the caps were tightened and the flasks made air-tight with parafilm. The flasks were then shaken at 200 rpm for 3hrs at 37°C in an orbital shaker. Each flask was then tapped ~30 times and the media decanted to remove microglia (which were then transferred into a six well plate, or onto coverslips for further experiments). The remaining flasks were incubated with 2 ml trypsin-EDTA for 12mins at 37°C. Supplemented media was added to the flasks to inhibit the trypsin and the flasks were again tapped, the resulting cell suspension was collected and centrifuged at 2,000 x g for 3 min at room temperature. The pellet was resuspended in 8 ml DMEM/High Glucose, a cell count was carried out and the cells were plated at a density of 1 x 10^5 cells/ml on poly-L-lysine coated glass coverslips in 24-well plates. The cells were allowed to adhere for 3 hr after which the wells were flooded with 500µl pre-warmed supplemented DMEM/High Glucose. Cells were grown for 10 days or until confluent before treatment.

2.3.6 Neuronal Culture And Treatments

Following dissection, the cortices (detailed in section 3.5) were placed in a drop of chilled neuronal culture buffer (116mM NaCl, 5.4mM KCl, 26mM $NaHCO_3$, 1.3 $NaHPO_4$, 1mM $MgSO_47H_2O$, 1mM $CaCl_22H_2O$, 0.5mM EDTA.2Na.$2H_2O$, 25mM Glucose. pH 7.4). The cortices were then chopped using a sterile disposable scalpel. The tissue was then transferred into 2.5ml of papain solution (0.15 % in neuronal buffer) and left to incubate at 37°C for 20 min. The tissue was then transferred into 2ml of BSA solution (1 % in neuronal buffer) with care to ensure few traces of papain solution remained. The solution was triturated ~ 15 times with a fine tipped Pasteur pipette, then transferred into another 2ml of BSA solution, triturated again. This process was repeated into a third tube of BSA. The solution was then centrifuged at 3000 x g for 3 min. The BSA was decanted, with care, to ensure the pellet was not disturbed. The pellet was resuspended in 5ml pre-warmed supplemented Neurobasal-A media (Neurobasal-A media, 2% B-27, 1% glutamine). The cell suspension was left for ~5 min to allow any clumps of cells to settle to the bottom. The cell solution was then plated on poly-L coated coverslips in 24 well well plates (120 µl per well). After 1hr incubation at 37°C, 5% CO_2 the wells were flooded with 500 µl pre-warmed supplemented media. For western blotting 500 µl of the cell solution was plated in each well of a poly-L coated 6 well plate. After 1 hr incubation at 37°C, 5% CO_2 the wells were flooded with 1 ml pre-warmed supplemented media. Half of the media was changed every 3 days. Cells were grown for 7 days before treatment. Cells were treated with either 2µg/ml 25-OH cholesterol (Chang et al., 1998), 1 µg/ml U18666a (Cheung et al., 2004) or 0.25 µM mevinolin (Mailman et al., 2011) (Santa-Catalina et al., 2008).

2.3.7 Primary Cell Line Staining

The 24 well plates containing coverslips were washed with ice cold PBS for 5 min to remove any traces of media. The cells were fixed with 100% ice cold methanol for 10 min and were then washed with PBS (2 x 5 min). Following this, the cells were permeabilised with PTx buffer (0.2% Triton X in PBS) for 10 min, and then left in blocking buffer (2% BSA in PBS) for 2hrs at RT. Then, the cells were left to incubate in primary antibody (made up in blocking buffer) overnight at $4^{o}C$. The coverslips were washed in PBS (3 x 5 min) and left to incubate in secondary antibody (again made up in blocking buffer) for 2 hr at room temperature. The PBS wash step was repeated (2 x 5 min), and Hoescht (1:800 in PBS) was added to the wells for 15 min. The PBS wash step was repeated (2 x 5 min) before the coverslips were mounted using vectashield. The cells were then visualized using the confocal microscope.

Filipin staining was used to detect unesterified cholesterol accumulation in treated neurons (Maxfield and Wustner, 2012). Cells were grown on coverslips in a 24 well plate for one week, and administered with appropriate treatment. The cells were then fixed with 3% formaldehyde in PBS for 30 mins and again washed 3 times with PBS. From this stage onwards all work was carried out in the dark. DMSO (40 µl) was directly injected through the cap of the Filipin bottle (Sigma) (containing 1 mg) to give a concentration of 25mg/ml. A 1:100 dilution (in PBS) of this solution was then used as a working stock. The cells were incubated in the Filipin solution for 30 mins at RT, and then rinsed 3 times in PBS. Coverslips were mounted on glass slides using vectashield and imaged on the confocal microscope using the UV package for hoescht stain.

Propridium iodide (PI) is membrane impermeant and generally excluded from viable cells thus is commonly used for identifying dead cells. When bound to nucleic acids, the absorption maximum for PI is 535 nm and the fluorescence emission maximum is 617 nm. Following appropriate treatment neuronal cultures were washed with PBS for 5 min to remove any traces of media. The cells were then incubated in a 500nM solution of PI (diluted in PBS) for 10 min and then washed twice in PBS (5 min) to remove all unincorporated dye. Following this, cells were permeabilised with PTx buffer for 10 min, the PBS wash step was then repeated (2 x 5 min), and Hoescht (1:800 in PBS) was added to the wells for 15 min. The PBS wash steps were repeated (2 x 5 min), and the coverslips were then mounted using vectashield.

2.3.8 HEK 293T Cell Culture and shRNA Transfection

HEK 293T cells were revived from -80^{O}C by warming for ~ 1 min in a 37^{O}C water bath. Once thawed, the cells (1 ml) were added to 9 ml of pre-warmed DMEM High Glucose (supplemented with 10% FBS, 1% penicillin/streptomycin) in a T25 cell culture flask and incubated at 37^{O}C, 5% CO_2 overnight. The next day the media was changed (to remove the DMSO from freezing mixture). Once 50 – 70% confluent the cells were trypsinised and re-plated in a T75 flask. Generally the cells were split every 5-6 days once ~ 75% confluent and the media changed every 3 days.

For transfection the cells were grown overnight in a 6 well plate (in antibiotic free media) at a density of 1-2 x 10^5 cells/ml (50-70% confluent). To make up solution A; 10 µl of resuspended SNX8 (or control) shRNA plasmid DNA (1 µg) (Santa Cruz) was added to 90 µl of shRNA plasmid transfection media (Santa Cruz). For solution B; 5 µl of shRNA transfection reagent (Santa Cruz) was added to 95 µl transfection media. Solution A and B were then mixed together to form the transfection mix and incubated at RT for 30 min. The DMEM media was removed from the 6 well plate and the wells washed 2 x 2 ml transfection media. Then 0.8 ml of transfection media was added to the well, followed by 200 µl transfection mix in a drop-wise manner. The plate was then gently rotated to ensure complete dispersion of the transfection mix. The cells were incubated for 6 hours at 37^{O}C, 5% CO_2. The media was then aspirated and replaced with fresh supplemented DMEM high glucose media for 24 hrs. The cells were then fixed and stained or the lysate used for western blotting.

2.4.0 Lentivirus Preparation

2.4.1 HEK 293T Cell Preparation

HEK 293T cells were revived and cultured as previously described. To generate enough cells for sufficient lentiviral particle generation the cells were then re-plated in a T150 flask, and the trypsinisation repeated to give six T150 flasks at ~80% confluency on the day of transfection.

2.4.2 Transfection Of Lentiviral Plasmids And Collection of Viral Particles

For the transfection mix, two separate tubes were prepared. The first tube contained 42ml Optimem and 7.5 µl polyetheleneimine (PEI, transfection reagent). The second tube contained 42ml of media

and 20 µg pLP1 vector, 10 µg pLP2 vector, 10 µg VSVG and 40 µg of pLL4.0_GFP-SNX8 (or pLL4.0 empty vector). The two tubes were inverted several times to mix and then filter sterilised. Tube one (containing transfection reagent) was then added slowly drop by drop into tube two to create the transfection mix. The media was removed from six flasks of HEK 293T cells and 14 ml of the transfection mix was added to each flask and incubated for 4 hours at 37°C, 5% CO_2. The media was then removed and replaced with 30 ml supplemented DMEM and incubated for a further 48 hr. The media was then collected and replaced with fresh supplemented DMEM. The collected media was centrifuged at 3000 x g for 10 mins at 4°C to pellet cell debris, and filter sterilised. The media was then ultracentrifuged at 27,000 x g for 2 hours at 4°C. The supernatant was discarded and 2.5 ml of un-supplemented DMEM (without Fetal Bovine Serum, penicillin/streptomycin, L-glutamine or sodium pyruvate) was added to the pellet and stored overnight at 4°C. The pellet was then resuspended by pipetting up and down on ice. The next batch of media was collected from the cells and both centrifugation steps carried out as before. Again 2.5 ml of media was added to the pellet and resuspended. Both resuspended pellets were combined (30 ml total) and thoroughly mixed by pipetting on ice. The media was then loaded into an ultracentrifuge tube and spun at 27,000 x g for 2 hours at 4°C. The supernatant was discarded and the pellet placed in 100 µl PBS overnight. The pellet was then vortexed vigourously until fully resuspended. The viral particles were then aliquoted to 5 µl volumes (to prevent freeze thaw cycles) and stored at -80°C until use.

2.5.0 Immuno Assays

2.5.1 Cytokine Array

The proteome profiler antibody array for rat cytokines kit (R and D systems) provides capture and detection for 27 chemokines and cytokines. The capture antibodies are spotted in duplicate on the surface of nitrocellulose membranes. The culture media from treated neuronal cells were mixed with the cocktail of biotinylated detection antibodies and incubated with the membrane. After washing the membrane, streptavidin-HRP and chemiluminescent reagents were added sequentially, and the amount of cytokine bound was detected by developing the blots in a Fujifilm dark box. All steps of the assay were carried out according to the suppliers' instructions.

2.5.2 Analysis Of Chemokine Release By ELISA

Concentrations of LIX chemokine release was measured using a commercially available ELISA kit (R&D Systems, UK). Initially, 96-well plates were coated with anti-rat LIX capture antibody (4 µg/ml) in PBS and incubated at 4°C overnight. The plates were then washed 3 x PBS-T and blocked for 1 hour at RT with diluent (1% BSA in PBS), then washed 3 x PBS-T. Next, plates were incubated with recombinant rat LIX standard (0-4000 pg/ml in diluents) or sample for 2 hours at RT, followed by 3 x PBS-T washes. Plates were then incubated with biotinylated goat anti-rat LIX secondary antibody (75 ng/ml) in 1% BSA for 2 hours at RT, then washed 3 x PBS-T. Following this, the plates were incubated with horse radish peroxidase (HRP)-conjugated streptavidin (1:200 in 1% BSA in PBS) for 20 minutes in the dark at RT. Then plates were washed 3 x PBS-T, and substrate solution was added to each well, once the colourimetric reaction had taken place the progression was stopped by adding 1M H_2SO_4 (stop solution). Absorbance was read at 420 nm within 30 minutes of stopping the reaction. A standard curve was generated by plotting the standards and their absorbance values and the concentrations were corrected allowing for protein concentrations. Protein concentrations supernatants were expressed as pg/ml (GraphPad Prism v 5.0; GraphPad Software, USA).

2.6.0 mRNA Analysis by Reverse Transcriptase Polymerase Chain Reaction

2.6.1 RNA Extraction

Messenger RNA (mRNA) was extracted from neuronal cultures treated with either 2 µg/ml cholesterol, 1 µg/ml U18666a, mevinolin (0.25 µM), or U18666a and mevinolin combined for 3 hours. Using a nucleospin RNA II kit, cells were scraped from 6-well plates in a cell lysis buffer containing RA1 buffer and 2-mercapto-ethanol (100:1). Cell lysates were then filtered using NucleoSpin Filters, collected in an Eppendorf tubes and centrifuged (11,000 x g, 1min). Ethanol (70%, 350µl) was added to the filtrate, mixed and loaded onto NucleoSpin RNA II columns. To bind the RNA to the column, tubes were centrifuged (8,000 x g, 30s). The silica membrane was then desalinated by adding membrane desalting buffer (350µl) and centrifuging (11,000 x g, 1min) to dry the membrane. To digest the DNA, DNase reaction mixture (95µl) was added to the column and incubated at room temperature for 15min. The silica membrane was then washed and dried. RNA was eluted by adding RNase free H_20 and centrifuging (11,000 x g, 1min), the RNA concentration was then quantified using a nanoDrop-spectrophotometer.

2.6.2 Reverse Transcription For cDNA Synthesis

Total mRNA (1µg) was reverse transcribed into cDNA using high-capacity cDNA archive kit (Applied Biosystems, Darmstadt, Germany) according to the protocol provided by the manufacturer. Briefly, RNA (1µg) was added to fresh tubes containing the appropriate volume of nuclease-free H_20 to make a 25µl volume. A 2x mastermix was prepared containing the appropriate volumes of 10x RT buffer, 25x dNTPs, 10x random primer multiscribe reverse transcriptase (50U/µl). The mastermix (25µl) was added to the RNA and nuclease free H_20. Tubes were incubated for 10min at 25°C followed by 2h at 37°C on a thermocycler.

2.6.3 cDNA Amplification By RT-PCR

Real-time PCR primers were delivered as "TaqMan® Gene Expression Assays" for the mouse genes LIX (assay I.D - Rn01441604_m1) and IP-10 (assay I.D - Rn01413889_g1) (Applied Biosystems, Darmstadt, Germany). Real-time PCR was performed on Applied Biosystems ABI Prism 7300 Sequence Detection System v1.3.1in 96-well format and 25µl reaction volume per well. cDNA samples (200pg/well) were mixed with Taqman Universal PCR Mastermix (Applied Biosystems, Darmstadt, Germany) and the respective target gene assay. Mouse β-actin RNA (Applied Biosystems) was used as reference. Each sample was measured in a single RT-PCR run. Forty cycles were run with the following conditions: 2min at 50°C, 10min at 95°C and for each cycle 15s at 95 °C for denaturation and 1min at 60°C for transcription.

2.6.4 PCR Quantification

The expression of each target gene was determined using the efficiency-corrected comparative CT method. Target genes in different samples were compared to a reference gene (β-actin). These values were normalized to an endogenous control and the relative differences between samples were expressed as a ratio. Values are expressed fold change in mRNA levels (7300 real-time PCR software, Applied Biosystems, USA).

2.7.0 COMPUTATIONAL AND STATISTICAL ANALYSIS

2.7.1 WESTERN BLOT AND CYTOKINE ARRAY QUANTIFICATION

Image J software was used to quantify the signal intensity for western blots. The intensity of the target protein and loading control was ascertained by using the analyse gels section of the menu, the target protein value was then divided by the loading control and plotted using graphpad prism. The same method was used to analyse the cytokine array; the intensity of each dot was measured and the percentage difference from control was calculated, and then plotted and statistics calculated (either Students T-test or one-way ANOVA with appropriate post hoc tests) using graphpad prism version 5.0.

2.7.2 QUANTIFICATION OF MYELINATION IN CEREBELLAR SLICES

To quantify the level of myelination in cerebellar slices images were taken using the Olympus FV1000 confocal microscope. Image acquisition settings were kept the same across different treatments. Image analysis was conducted using the software package EBImage (http://www.bioconductor.org/help/bioc-views/release/bioc/html/EBImage.html) run through the statistical programming environment, R. EBImage allows analysis of red, green, and blue channels separately. Every pixel (1024 3 1024) was assigned an intensity value between 0 and 1, where 0 represents no intensity and 1 represents an intensity value of 4096 as per a 12 bit image. Neurofilament H staining (red) labels axonal processes and was used as a "mask" in order to measure the amount of MBP staining (green) co-localized with neurofilament H only, i.e., neuronal MBP staining. Fluorescence intensity thresholds were set to remove background staining. Therefore, only those pixels representing specific staining were included in the analysis. For MBP, the percentage of green pixels which were co-localized with red (neurofilament H) was calculated. This percentage was then multiplied by the average green pixel fluorescence intensity to give a single figure for neuronal MBP staining. Statistical analysis was determined by Students T-test using graphpad prism version 5.0.

Oligoname	Sequence
SNX8_SmaI_FP	5'- TTT CCC GGG ATG ACT GGC CGC GCG ATG -3' (Sma1)
SNX8_NheI_RP	5'- TTT GTC AGC CTA GTG AGG ACA CAG GCC - 3' (Nhe1)
SNX8_Xho1_FP_GFP	5' - ATA CTC GAG CAT GAC TGG CCG CGC GAT G - 3' (Xho1)
SNX8_Kpn1_RP_GFP	5' – ATA GGT ACC CTA GTG AGG ACA CAG GCC – 3' (Kpn1)

FIGURE 2.2. LIST OF PRIMERS USED FOR CLONING. These primers were used to PCR amplify the SNX8 inserts for lentivirus and mammalian cloning. The restriction enzyme sequences are underlined.

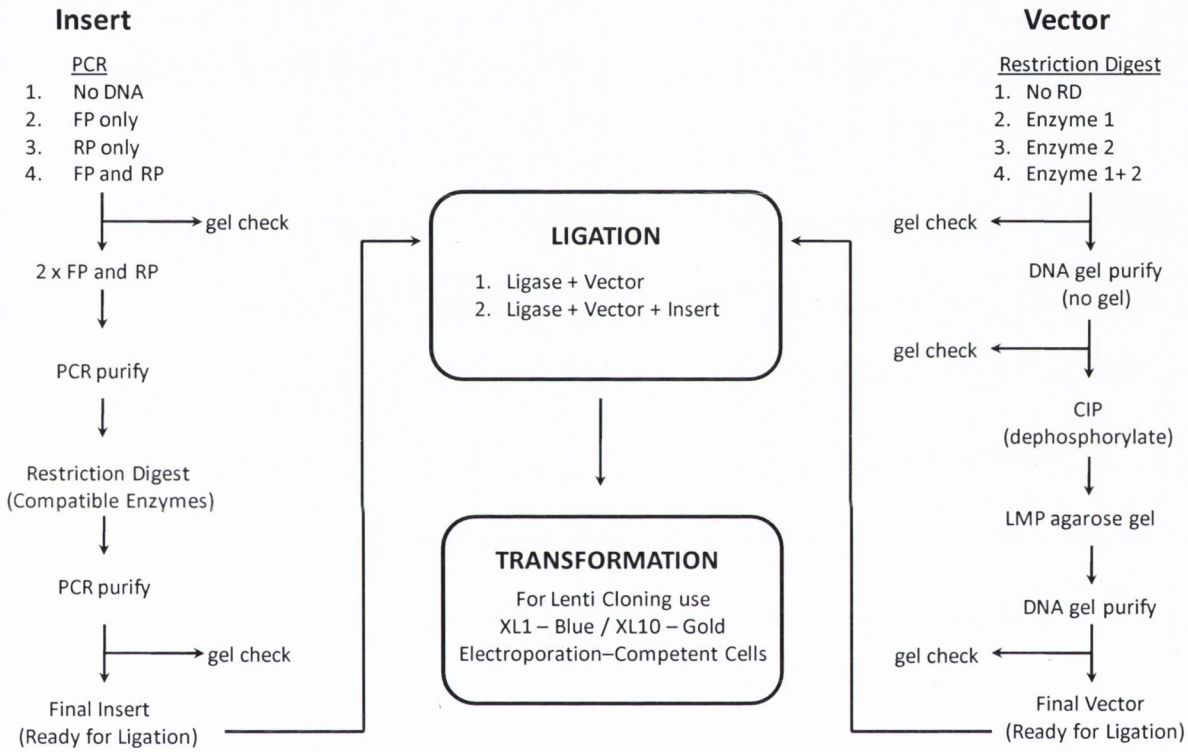

FIGURE 2.3. CLONING FLOW CHART. The chart shows the standardised procedure for cloning. The steps for preparing the insert and vector are shown, followed by ligation and transformation.

CHAPTER 3. GENERATION AND CHARACTERISATION OF SNX8 LENTIVIRUS

3.1.0 AIMS AND HYPOTHESIS

- Prepare SNX8 insert and pEGFP-C2 vector for intermediate plasmid
- Prepare GFP-SNX8 insert and pLL4.0 vector for final lentiviral plasmid
- Elucidate successful cloning via molecular methods (PCR and restriction digestion)
- Demonstrate successful cloning with DNA sequencing
- Prove plasmid is capable of transfecting cells
- Generate lentiviral particles of both GFP and GFP-SNX8
- Explore the expression profile of GFP-SNX8 lentivirus within neurons
- Investigate the effect of lentivirus transfection on cell survival

This chapter describes the manufacture of the GFP-SNX8 lentivirus. It was hypothesised that GFP-SNX8 may be expressed in neurons via a lentiviral delivery system. It was also hypothesised that this expression may be modulated in differing cholesterol environments, and visualised with ease due to the GFP tag.

3.2.0 ABSTRACT

SNX8 is a member of the PX-BAR domain containing sub-family of sorting nexins which has recently been implicated as a novel activator of the SREBP pathway (sterol regulatory element binding protein) of cholesterol homeostasis. Cholesterol is essential for neuronal synaptic transmission and plasticity at both pre- and post-synaptic densities. Other members of the SNX family are known to be involved in various stages of intracellular trafficking and sorting events. Combined, this information leads to the hypothesis that SNX8 may play a role in vesicular protein cargo trafficking and/or transport of components of the SREBP pathway, thus influencing synaptic function. In order to elucidate this lentiviral-mediated delivery system to overexpress SNX8 in cells of the CNS was designed. SNX8 was first cloned into pEGFP-C2 vector (an intermediate plasmid) to provide a GFP tag at the N terminus of the sequence. The GFP-SNX8 was then subcloned into the lentiviral vector pLL4.0. Molecular confirmation and sequencing validated the success of the cloning. Next, HEK 293T cells were transfected with the plasmid prior to generation of the lentivirus to confirm transfection efficiency. Lentiviral particles were then generated and neurons were transfected with GFP-SNX8, which showed punctuate expression of the protein in a perinuclear region, similar to plasmid transfected HEK 293T cells. The GFP-SNX8 expression also extended into the processes of neurons. Lastly, the transfection of GFP-SNX8 lentivirus was found to have no adverse effect on cell survival. These results demonstated successful cloning of the GFP-SNX8 lentivirus and validated its further use to investigate SNX8 function in neurons.

3.3.0 INTRODUCTION

3.3.1 LENTIVIRUSES ARE EFFICIENT MOLECULAR TOOLS

The development of gene vectors has lead to gene therapy in both animal and human models of disease. Small scale MLV oncoretroviral (murine leukemia virus) vectors have been used in trials to treat X-SCID in children although significant numbers developed vector related leukaemia (Cavazzana-Calvo M, 2000). This lead to the development of future generations of viral vectors with increased safety and specificity, including the popular HIV-1 based lentivirus. The retroviral family (*Retroviridae*) comprises of RNA spherical viruses up to 120 nm. Two positive RNA strands, integrase, protease and reverse transcriptase enzymes are packaged inside nucleocapsid protein, which is then surrounded by a capsid protein shell (Vogt VM, 1999). Matrix proteins surround this shell and interact with the lipid envelope containing viral envelope glycoproteins, which interact in a cell specific manner with cellular receptors on host cells. The genome of the lentivirus can be split into gag, pol and env genes. Gag encodes structural proteins, pol encodes the enzymes for ssRNA and env encodes the viral envelope. The *cis*-acting sequence of the genome is also needed for integration into the host chromosome (Coil DA, 2004). *Retroviridae* can be divided into two subtypes – simple and complex, with oncoretroviruses and lentivirus being examples of these respectively (Sakuma et al., 2012). In simple retroviruses the gag, pol and env genes are removed and the cassette containing the gene of interest or siRNA is inserted. Oncoretrovirus vectors are efficient in transfecting cells for a variety of reasons; the viral proteins have been removed, so will not elicit immune response. They can also integrate into the host genome to allow persistent gene expression. However, retroviral vectors do have their limitations. For example, they can only transduce dividing cells (Lewis PF, 1994), the virus particle is unstable, the virus also undergoes a significant level of insertional mutagenesis and low viral titres are common (Le Doux JM, 1999). Lentivirus vectors overcome some of these limitations; they are able to transduce post-mitotic cells and have a far lower rate of insertional mutagenesis (Naldini et al., 1996b). Complex lentiviral vectors are now being used to a greater extent than the simple oncoretroviruses in gene therapy (Escors D, 2010).

3.3.2 THE RETROVIRAL LIFE CYCLE ALLOWS HIGH TRANSFECTION

The life cycle via which retroviruses infect the host and hijack the cellular machinery to replicate itself can be broken down into several steps (**Figure 1**). Initially, the viral envelope binds to target

receptors on the cell surface, the envelope then fuses with the cell membrane and the viral core travels into the cytoplasm. The virus is uncoated and single stranded RNA is then reverse transcribed into double stranded DNA which is transported to the nucleus. In the nucleus the DNA is integrated into the hosts DNA allowing for long term expression of the inserted genes. The DNA then undergoes transcription and translation. (Palu et al., 2000). Unlike the natural process of the virus being packaged and the cell becoming lysed to release the generated virus in order to infect surrounding cells, lentiviruses have been generated to not stimulate the cell to enter the lytic cycle, thus infected cells do not die (Mandel et al., 2008).

3.3.3 Components Of The Lentivirus System

Different generations of lentivirus are available (from 1st to 3rd generation), which have modifications to the packaging systems. However, in general lentivirus particles are generated by cotransfection of HEK 293T cells with 3 plasmids: i) a packaging plasmid, ii) a transfer plasmid, iii) and an envelope encoding plasmid (Naldini et al., 1996a). i) The packaging plasmid expresses the enzymes and proteins necessary for the successful infection of the virus particle. The packaging plasmid has been modified so that all virulent and toxic proteins have been removed without reducing the level of virus replication (Gibbs et al., 1994). ii) The transfer plasmid expresses vector mRNA required for accurate packaging, reverse transcription, nuclear transport and host DNA integration. The gene of interest along with its promoter is also cloned into this plasmid (Naldini et al., 1996b). iii) The envelope encoding plasmid supplies the budding virus with glycoproteins for envelope formation; as the viral envelope is removed in lentiviral systems. After transient transfection of the cells the virus is collected filtered and concentrated by untracentrifugation at up to 100,000 x g (Pluta and Kacprzak, 2009).

Lentivirus can be modified in a variety of ways to increase safety and specificity. One of these techniques is the development of tissue or cell specific envelopes. Modifying viral envelope glycoproteins, allows interaction with specific receptor types on cell surfaces, thus increasing transduction specificity. This process of modifying the glycoproteins is termed pseudotyping. Lentiviral vectors are commonly pseudotyped with VSVG (vesicular stomatitis virus glycoprotein), which interacts with a ubiquitous receptor, allowing the virus to transduce several cell types. Both natural glycoproteins and genetically engineered glycoproteins are available to confer cell specific receptor interactions. Genetic manipulation of theses glycoproteins has lead to the generation of lentiviral vectors that can specifically transduce tumour cells, endothelial cells, immune cells and

bone marrow derived mesenchymal stem cells (Zhang et al., 2004). Cell and tissue specific promoters can also be used in the transfer plasmid, allowing the gene of interest to be expressed only in the target cell type (Liu et al., 2004). It is also possible to modulate the expression of the target gene by using an inducible promoter, such as the tetracycline-based induction system. This system is useful in gene therapy to control gene expression in an inducible manner (Seo et al., 2009).

3.3.4 Why Clone SNX8 Into A Lentiviral Vector?

Over expression and knock down of proteins has been used successfully to provide information on the function of many proteins. To our knowledge, this is the first study using lentiviral methods to overexpress a member of the SNX family. In order to fully investigate the role of SNX8 within the CNS, a lentiviral mediated delivery system was utilised to overexpress GFP tagged SNX8. This method is particularly useful as neurons are post-mitotic and difficult to transduce. The lentiviral system instigates transfection of the protein within all cells of the CNS (with a slight preference for neurons over glia), which in turn allows the investigation of SNX8 function within these cell types, and ultimately can elucidate SNX8 function within the retrograde and SREBP pathways.

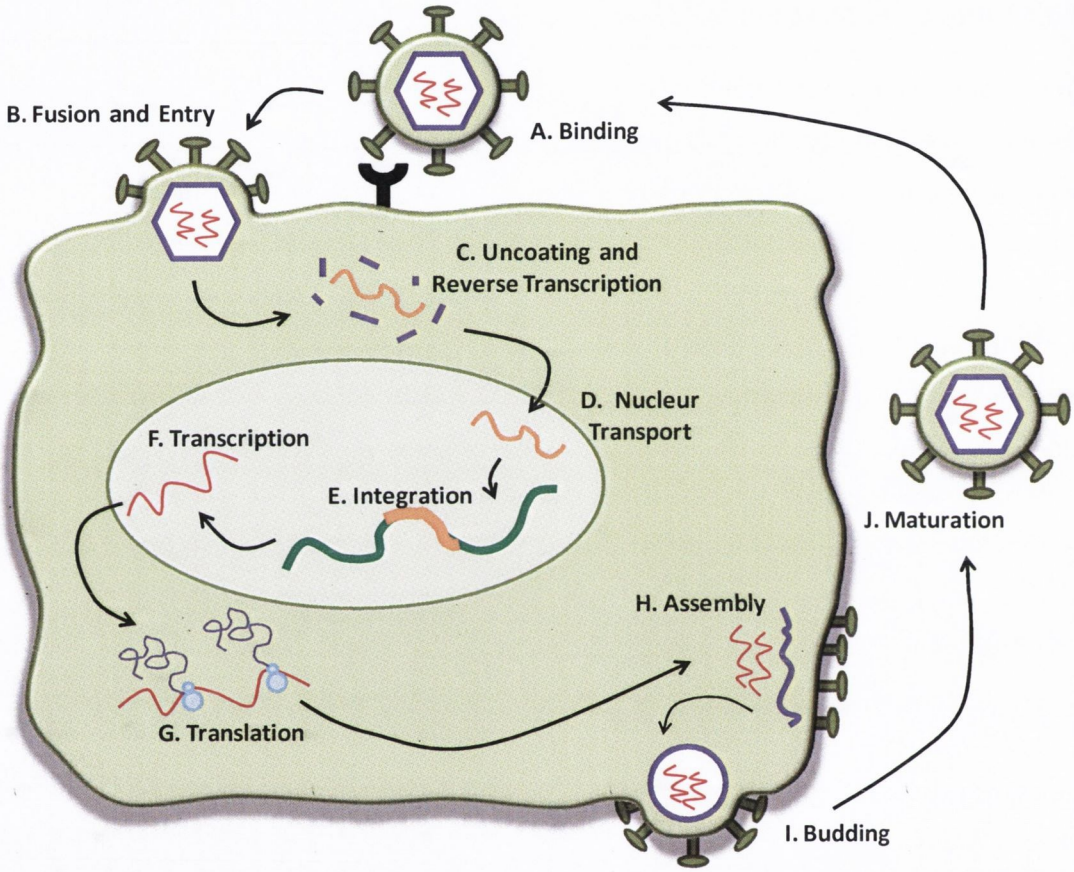

FIGURE 3.1. RETROVIRAL LIFE CYCLE. A. The viral envelope binds to target receptors on the cell surface, **B.** the envelope then fuses with the cell membrane and the viral core travels into the cytoplasm. **C.** The virus is uncoated and single stranded RNA is then reverse transcribed into double stranded DNA which is **D.** transported to the nucleus. **E.** In the nucleus the DNA is integrated into the hosts DNA allowing for long term expression of the inserted genes. **F.** The DNA then undergoes transcription and translation. **G.** The viral RNA then assembles with the viral particle and **I.** buds off from the host cell. (inhibited in lentivirus) **J.** Once mature the new virus can go on to infect other cells.

3.4.0 RESULTS

3.4.1 PREPARATION OF THE INSERT AND VECTOR

The SNX8 pENTR11 plasmid obtained from Geneservice was first characterised before use. Specifically the plasmid was verified by digestion and PCR, and then sequence verified (**Figure 3.2**). Next, primers were designed to amplify SNX8 from the pENTR211 vector by PCR (**Figure 3.3**). Once the fragment was amplified, it was PCR purified using a Qiagen kit. The fragment was then digested with appropriate restriction enzymes to allow annealing with the vector. For pEGFP-C2 the restriction sites chosen were Xho1 and Kpn1 (**Figure 3.3**) and for pLL4.0 the sites were Sma1 and Nhe1 (**Figure 3.4**). Following digestion the insert was again PCR purified, ready for ligation with the vector. Two vectors were used to express SNX8; pEGFP-C2 vector (**Figure 3.3**) for use as an intermediate mammalian expression vector, and pLL4.0 for use as a lentivirus vector (**Figure 3.4**). The cloning of SNX8 firstly into the pEGFP-C2 vector and the consecutive cloning of GFP-SNX8 into pLL4.0 generated a GFP tag at the N terminus in the lentiviral vector. An n terminal tag was desired as the BAR domain of SNX8 is at the extreme c terminus, therefore the addition of a tag at this location may inhibit the dimerisation of the BAR domain. Both vectors were prepared by digestion with the same restriction enzymes as the insert (Xho1 and Kpn1 for pEGFP-C2 and Sma1 and Nhe1 for pLL4.0). Each vector was then gel purified using a Quiagen kit and then dephosphorylated using CIP enzyme (Calf Intestinal Alkaline Phosphatase) to reduce self ligation of the vector during the ligation step. Following dephosphorylation the vectors were run on low melting point agarose gels from which they were purified, to separate the digested and undigested vector. Agarose gel confirmation was performed at all stages of the preparation to ensure the quality of the insert and vector (**Figure 3.3 and 3.4**). The insert and vector was ligated and the ligation mix was then transformed into E. coli which were plated on antibiotic supplemented plates. Colonies were selected and the DNA was then purified and PCR and digestion reactions used to confirm bands present of the correct sizes for both vectors (**Figure 5**). The DNA was finally sent for sequencing to confirm the successful cloning of SNX8 into the intermediate pEGFP-C2 plasmid and GFP-SNX8 into the final lentiviral vector (**Figure 3.6 and 3.7**).

3.4.2 HEK 293T CELL TRANSFECTION CONFIRMATION

HEK 293T cells were transfected with pLL4.0-GFP-SNX8 and empty vector pLL4.0-GFP for 24 hours to demonstrate that the vectors are capable of transfecting cells and expressing protein, before generating the lentiviral particles. pLL4.0-GFP showed ~70% transfection efficiency and showed a

ubiquitous expression of GFP throughout the cytoplasm (**Figure 3.8a**). Cells transfected with pLL4.0-GFP-SNX8 showed slightly lower transfection efficiency, with GFP-SNX8 displaying a perinuclear distribution (**Figure 3.8b**). Western blots were performed with the cell lysates of transfected cells. When the blots were probed with GFP, no band was visible in the non-transfected well. A band corresponding to the size of GFP (27 KDa) was seen in the GFP transfected well. A larger band was seen in the GFP-SNX8 transfected well (80 KDa), corresponding to the size of the fusion protein (**Figure 3.8c**). These data demonstrate the successful expression of GFP-SNX8 by the pLL4.0 vector, allowing the pLL4.0-GFP-SNX8 lentivirus to be generated.

3.4.3 GFP-SNX8 Lentiviral Transfection in Neurons

Following the generation of the GFP-SNX8 lentiviral particles, it remained to be investigated that the virus was able to successfully transduce neurons. In order to do this, neuronal cultures were transfected with both the GFP and GFP-SNX8 lentiviruses, 48 hours post transduction neurons were either imaged or western blots performed with the cell lysate. Both lentiviruses successfully transfected neurons, with 70% transfection efficiency (**Figure 3.9**). The GFP lentivirus was shown to be expressed throughout the cell including the soma and processes, and western blotting with GFP antibody indicated a band at 27 KDa (**Figure 3.10**). Images of GFP-SNX8 transfected neurons show a different expression when compared to GFP alone. SNX8 expression is seen to be expressed around the nucleus in a perinuclear manner and extending out from the soma in a punctuate pattern. Western blotting with GFP antibody indicated a band at approximately 80 KDa corresponding to the size of the GFP-SNX8 fusion protein (**Figure 3.10**).

3.4.4 GFP-SNX8 Lentiviral Transfection in Neurons Survival Assay

After concluding the GFP-SNX8 lentivirus was able to transfect cells it remained to be elucidated whether the transfection process or GFP-SNX8 itself had any effect on cell survival. Following transfection with either GFP or GFP-SNX8 lentivirus cells were fixed and stained with propridium idodide to identify dead cells and hoescht to indicate total number of cells present. When the total propridium staining was divided by the total hoescht staining, this gave a cell death ratio. Neither GFP nor GFP-SNX8 transfection had any effect on cell survival (**Figure 3.11**), with neither significantly deviating from control levels ($p>0.05$, one way ANOVA). This experiment indicates two important points; firstly the data shows lentiviral transfection does not negatively affect cell viability and secondly, overexpression of SNX8 protein is not detrimental to cell survival.

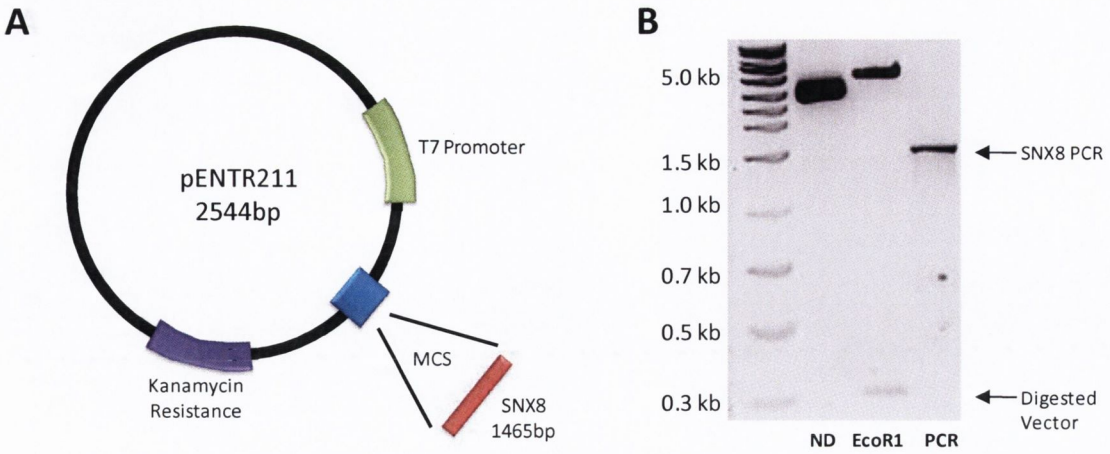

C

```
ACA TGT TCT TTC CTG CGT TAT CCC CTG ATT CTG TGG ATA ACC GTA TTA CCG CCT TTG AGT GAG CTG
ATA CCG CTC GCC GCA GCC GAA CGA CCG AGC GCA GCG AGT CAG TGA GCG AGG AAG CGG AAG AGC GCC
CAA TAC GCA AAC CGC CTC TCC CCG CGC GTT GGC CGA TTC ATT AAT GCA GCT GGC ACG ACA GGT TTC
CCG ACT GGA AAG CGG GCA GTG AGC GCA ACG CAA TTA ATA CGC GTA CCG CTA GCC AGG AAG AGT TTG
TAG AAA CGC AAA AAG GCC ATC CGT CAG GAT GGC CTT CTG CTT AGT TTG ATG CCT GGC AGT TTA TGG
CGG GCG TCC TGC CCG CCA CCC TCC GGG CCG TTG CTT CAC AAC GTT CAA ATC CGC TCC CGG CGG ATT
TGT CCT ACT CAG GAG AGC GTT CAC CGA CAA ACA ACA GAT AAA ACG AAA GGC CCA GTC TTC CGA CTG
AGC CTT TCG TTT TAT TTG ATG CCT GGC AGT TCC CTA CTC TCG CGT TAA CGC TAG CAT GGA TGT TTT
CCC AGT CAC GAC GTT GTA AAA CGA CGG CCA GTC TTA AGC TCG GGC CCC AAA TAA TGA TTT TAT TTT
GAC TGA TAG TGA CCT GTT CGT TGC AAC AAA TTG ATG AGC AAT GCT TTT TTA TAA TGC CAA CTT TGT
ACA AAA AAG CAG GCT ACC CAG CTT TCT TGT ACA AAG TTG GCA TTA TAA GAA AGC ATT GCT TAT CAA
TTT GTT GCA ACG AAC AGG TCA CTA TCA GTC AAA ATA AAA TCA TTA TTT GCC ATC CAG CTG ATA TCC
CCT ATA GTG AGT CGT ATT ACA TGG TCA TAG CTG TTT CCT GGC AGC TCT GGC CCG TGT CTC AAA ATC
TCT GAT GTT ACA TTG CAC AAG ATA AAA ATA TAT CAT CAT GAA CAA TAA AAC TGT CTG CTT ACA TAA
ACA GTA ATA CAA GGG GTG TTA TGA GCC ATA TTC AAC GGG AAA CGT CGA GGC CGC GAT TAA ATT CCA
ACA TGG ATG CTG ATT TAT ATG GGT ATA AAT GGG CTC GCG ATA ATG TCG GGC AAT CAG GTG CGA CAA
TCT ATC GCT TGT ATG GGA AGC CCG ATG CGC CAG AGT TGT TTC TGA AAC ATG GCA AAG GTA GCG TTG
CCA ATG ATG TTA CAG ATG AGA TGG TCA GAC TAA ACT GGC TGA CGG AAT TTA TGC CTC TTC CGA CCA
TCA AGC ATT TTA TCC GTA CTC CTG ATG ATG CAT GGT TAC TCA CCA CTG CGA TCC CCG GAA AAA CAG
CAT TCC AGG TAT TAG AAG AAT ATC CTG ATT CAG GTG AAA ATA TTG TTG ATG CGC TGG CAG TGT TCC
TGC GCC GGT TGC ATT CGA TTC CTG TTT GTA ATT GTC CTT TTA ACA GCG ATC GCG TAT TTC GTC TCG
CTC AGG CGC AAT CAC GAA TGA ATA ACG GTT TGG TTG ATG CGA GTG ATT TTG ATG ACG AGC GTA ATG
GCT GGC CTG TTG AAC AAG TCT GGA AAG AAA TGC ATA AAC TTT TGC CAT TCT CAC CGG ATT CAG TCG
TCA CTC ATG GTG ATT TCT CAC TTG ATA ACC TTA TTT TTG ACG AGG GGA AAT TAA TAG GTT GTA TTG
ATG TTG GAC GAG TCG GAA TCG CAG ACC GAT ACC AGG ATC TTG CCA TCC TAT GGA ACT GCC TCG GTG
AGT TTT CTC CTT CAT TAC AGA AAC GGC TTT TTC AAA AAT ATG GTA TTG ATA ATC CTG ATA TGA ATA
AAT TGC AGT TTC ATT TGA TGC TCG ATG AGT TTT TCT AAT CAG AAT TGG TTA ATT GGT TGT AAC ACT
GGC AGA GCA TTA CGC TGA CTT GAC GGG ACG GCG CAA GCT CAT GAC CAA AAT CCC TTA ACG TGA GTT
ACG CGT CGT TCC ACT GAG CGT CAG ACC CCG TAG AAA AGA TCA AAG GAT CTT CTT GAG ATC CTT TTT
TTC TGC GCG TAA TCT GCT GCT TGC AAA CAA AAA AAC CAC CGC TAC CAG CGG TGG TTT GTT TGC CGG
ATC AAG AGC TAC CAA CTC TTT TTC CGA AGG TAA CTG GCT TCA GCA GAG CGC AGA TAC CAA ATA CTG
TCC TTC TAG TGT AGC CGT AGT TAG GCC ACC ACT TCA AGA ACT CTG TAG CAC CGC CTA CAT ACC TCG
CTC TGC TAA TCC TGT TAC CAG TGG CTG CTG CCA GTG GCG ATA AGT CGT GTC TTA CCG GGT TGG ACT
CAA GAC GAT AGT TAC CGG ATA AGG CGC AGC GGT CGG GCT GAA CGG GGG GTT CGT GCA CAC AGC CCA
GCT TGG AGC GAA CGA CCT ACA CCG AAC TGA GAT ACC TAC AGC GTG AGC ATT GAG AAA GCG CCA CGC
TTC CCG AAG GGA GAA AGG CGG ACA GGT ATC CGG TAA GCG GCA GGG TCG GAA CAG GAG AGC GCA CGA
GGG AGC TTC CAG GGG GAA ACG CCT GGT ATC TTT ATA GTC CTG TCG GGT TTC GCC ACC TCT GAC TTG
AGC GTC GAT TTT TGT GAT GCT CGT CAG GGG GGC GGA GCC TAT GGA AAA ACG CCA GCA ACG CGG CCT
TTT TAC GGT TCC TGG CCT TTT GCT GGC CTT TTG CTC
XXXX - M13 Primer Sites
```

FIGURE 3.2. ORIGINAL SNX8 INSERT FROM COMMERCIAL VECTOR (PENTR211). A. Vector map for pENTR211 vector showing SNX8 insert at multuple cloning site **B.** Agarose gel picture of pENTR211. Lane 1 contains undigested vector, Lane 2 contains the cut vector with EcoR1 enzyme which digests the SNX8 containing vector twice to create a band at 0.35kb and 3.6kb in order to confirm the size of the vector. Lane 3 contains the PCR fragment of SNX8 amplified from the pENTR211 vector. **C.** The sequence of pENTR211 vector with the universal M13 primer sites shown underlined.

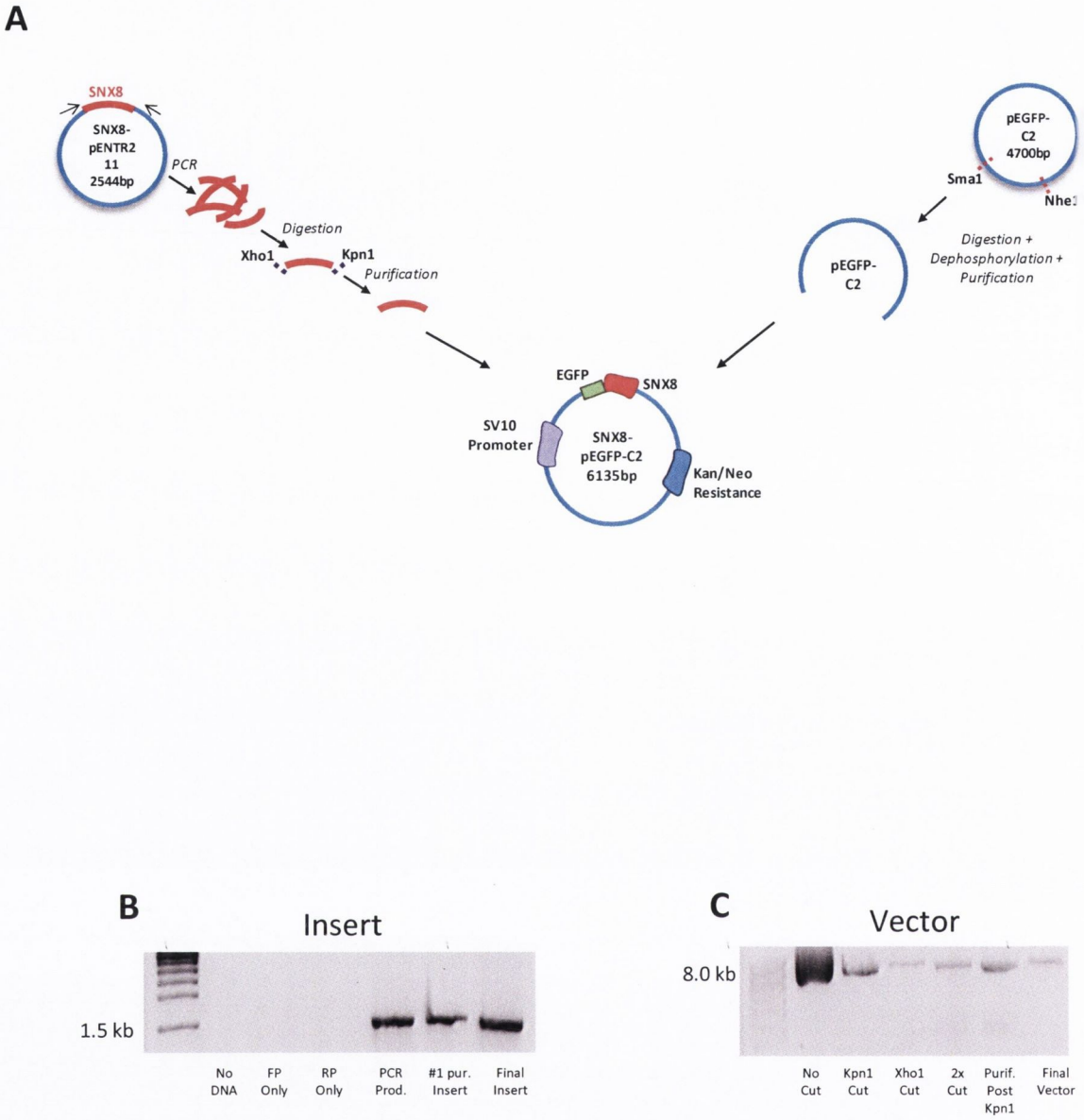

FIGURE 3.3. PEGFP-C2-SNX8 CLONING; MAMMALIAN VECTOR. A. Schematic showing cloning strategy of SNX8 insert and vector preparation for cloning. **B.** Agarose gel showing stages of cloning protocol for the SNX8 insert. No DNA, forward primer only (FP only) and reverse primer only (RP only) are negative controls. The initial PCR product is then purified (PCR prod. and #1 pur. insert) and digested with Kpn1 and Xho1, and finally purified again to create the final insert. **C.** Agarose gel showing stages of cloning protocol for the pEGFP-C2 vector.

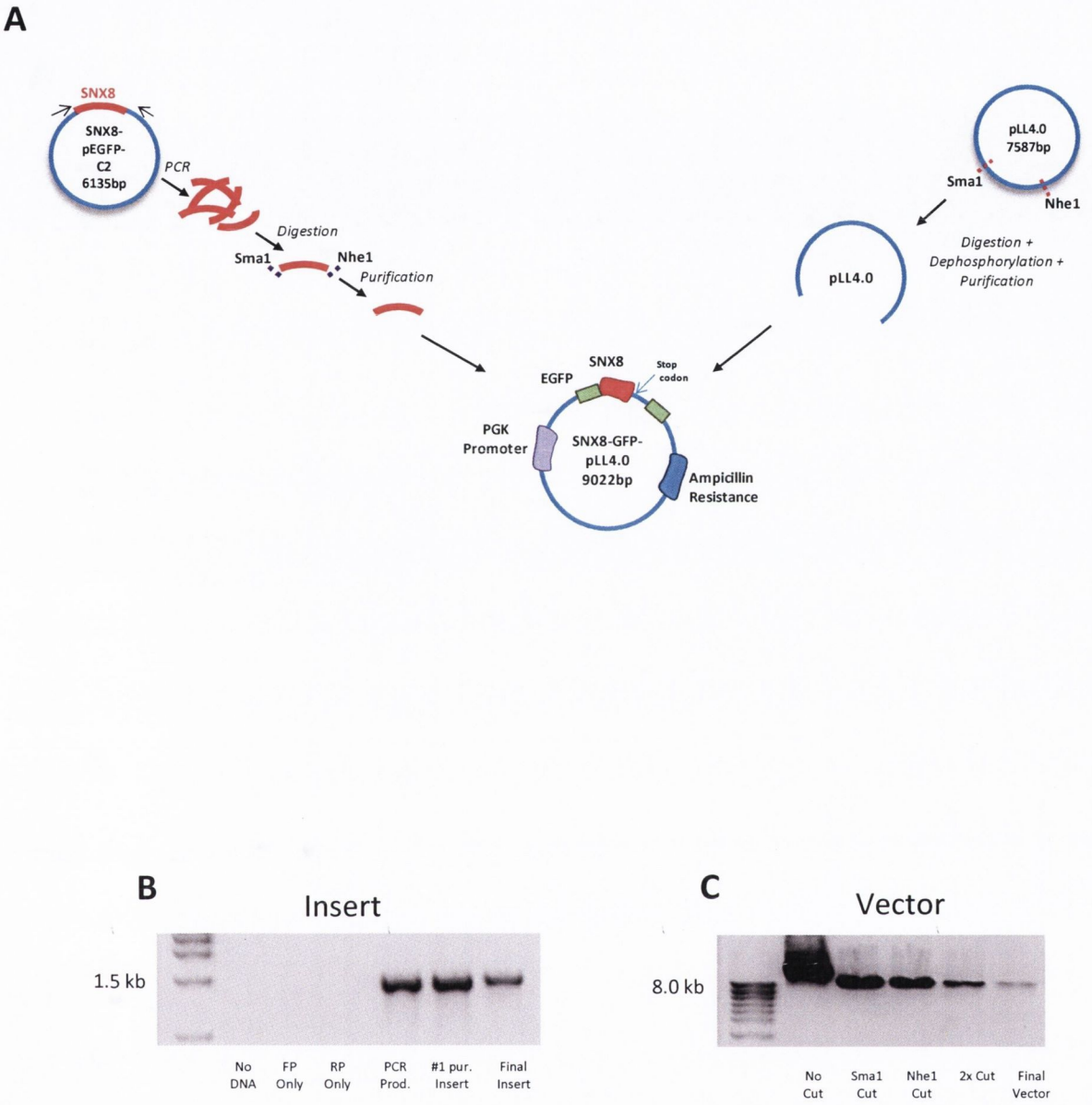

FIGURE 3.4. PLL4.0-GFP-SNX8 CLONING; LENTIVIRAL VECTOR. A. Schematic showing cloning strategy for SNX8 insert into pLL4.0 lentiviral vector **B.** Agarose gel showing stages of cloning protocol for the SNX8 insert. **C.** Agarose gel showing stages of cloning protocol for the pLL4.0 vector.

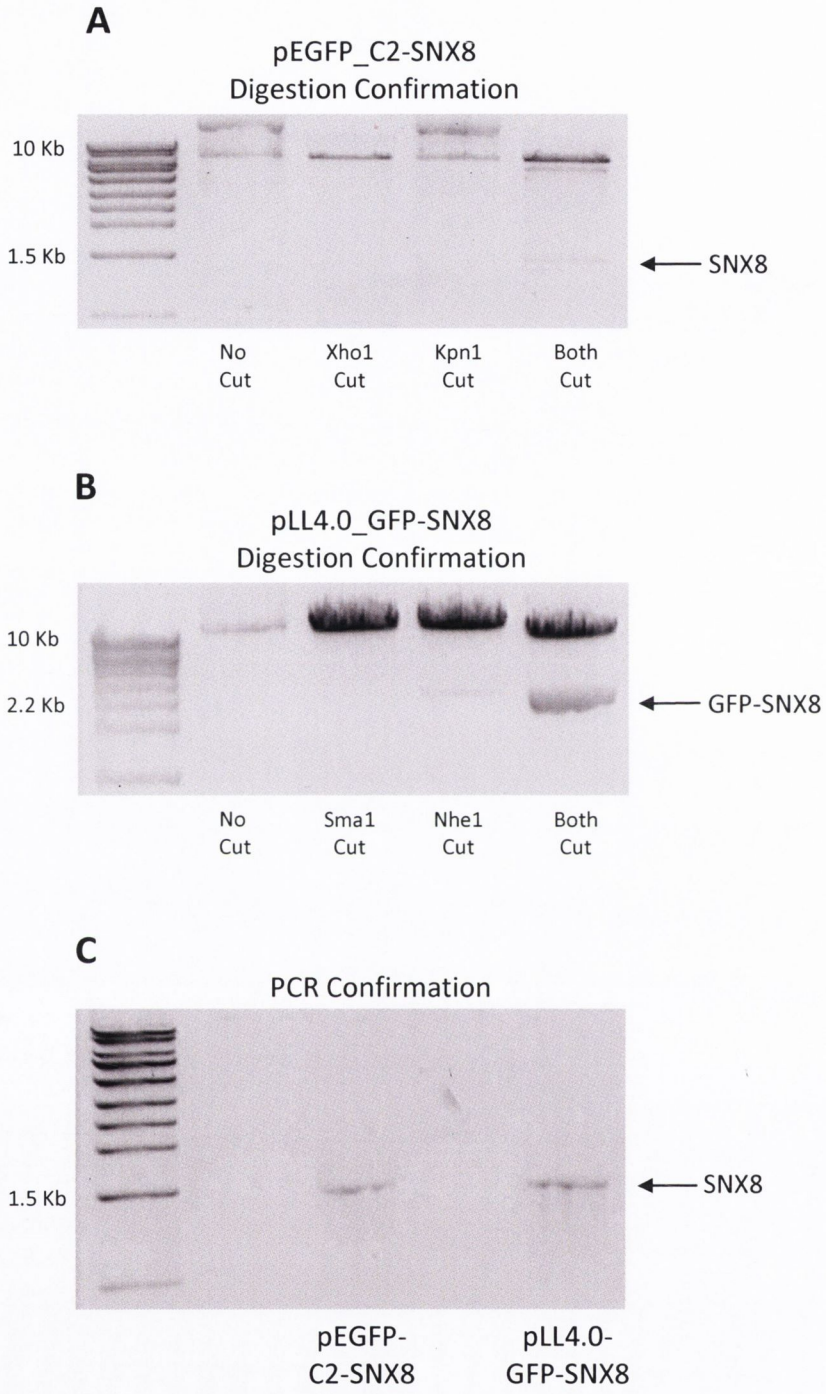

FIGURE 3.5. AGAROSE GEL CONFIRMATIONS OF PEGFP-C2-SNX8 AND PLL4.0-GFP-SNX8 CLONING. A. Digestion confirmation for **A.** pEGFP-C2-SNX8 showing presence of SNX8 insert at 1.5Kb following digestion with Xho1 and Kpn1 **B.** pLL4.0-GFP-SNX8 showing GFP-SNX8 insert at 2.2 Kb following digestion with Sma1 and Nhe1 **C.** PCR confirmation using SNX8 forward and reverse primers for both vectors, SNX8 insert was successfully amplified in both cases, deeming the cloning a success.

A

TAC AAA AAA GCA GGC TCC ACC **ATG ACT GGC CGC GCG ATG GAC CCG CTG CCC GCG GCT GCA GTC GGG GCG**
GCA GCT GAG GCG GAG GCT GAC GAG GAG GCG GAT CCC CCG GCG TCA GAT CTG CCG ACA CCC CAG GCC ATC
GAG CCC CAG GCC ATC GTG CAG CAG GTC CCA GCC CCC AGT CGA ATG CAG ATG CCG CAG GGG AAC CCG CTG
CTG CTG TCC CAC ACC CTG CAG GAG CTG CTG GCC AGG GAC ACC GTG CAG GTG GAG CTC ATT CCG GAG AAG
AAG GGC CTC TTC CTG AAG CAT GTG GAG TAT GAG GTT TCC AGC CAG CGC TTC AAG TCC TCG GTA TAC AGA
CGG TAC AAT GAC TTC GTG GTC TTC CAG GAG ATG CTC CTG CAC AAG TTC CCC TAC CGT ATG GTG CCT GCC
CTG CCA CCC AAG AGA ATG CTG GGA GCT GAC AGG GAG TTC ATC GAG GCC AGG AGG AGA GCC CTG AAG CGC
TTC GTC AAC CTG GTG GCG CGA CAC CCC CTG TTC TCC GAG GAT GTG GTC CTC AAG CTC TTC CTG TCC TTC
AGC GGC TCG GAT GTG CAG AAC AAG TTA AAG GAG TCA GCA CAG TGC GTC GGG GAC GAA TTC CTG AAC TGT
AAG CTG GCT ACC AGG GCC AAG GAC TTC CTC CCA GCT GAC ATC CAG GCT CAG TTT GCC ATC AGC CGG GAG
CTG ATC CGG AAC ATC TAC AAT AGC TTT CAC AAG CTT CGC GAC AGG GCC GAG CGG ATC GCG TCG CGG GCC
ATC GAC AAT GCG GCA GAT CTT CTC ATA TTC GGG AAG GAG CTA AGT GCA ATA GGG TCT GAC ACG ACC CCG
CTG CCC TCC TGG GCC GCT CTG AAT AGC AGC ACG TGG GGG TCC CTG AAG CAG GCT CTG AAA GGC CTG TCT
GTG GAA TTC GCG CTG CTC GCC GAC AAG GCT GCA CAA CAG GGT AAG CAG GAA GAG AAC GAC GTG GTG GAG
AAG CTG AAC CTC TTC TTG GAT CTG CTG CAG TCC TAT AAG GAC CTG TGC GAG CGG CAT GAG AAG GGC GTG
TTG CAC AAG CAC CAG CGG GCC CTG CAC AAG TAC AGC CTG ATG AAG AGG CAG ATG ATG AGC GCC ACC GCG
CAG AAC CGC GAG CCG GAG TCC GTG GAG CAG CTG GAG TCC CGC ATC GTG GAG CAG GAG AAC GCG ATT CAG
ACG ATG GAG CTG CGG AAC TAC TTC TCC CTG TAC TGC CTG CAC CAG GAG ACG CAG CTC ATC CAC GTC TAC
CTG CCC CTC ACC TCC CAC ATC CTC CGC GCC TTC GTC AAC TCT CAG ATC CAA GGG CAC AAG GAG ATG AGC
AAG GTG TGG AAC GAC CTG AGG CCC AAG CTC AGC TGC CTC TTT GCG GGA CCA CAC AGC ACC CTG ACC CCA
CCG TGC TCC CCG CCG GAG GAC GGC CTG TGT CCT CAC TGA GAC CCA GCT TTC TTG TAC

B

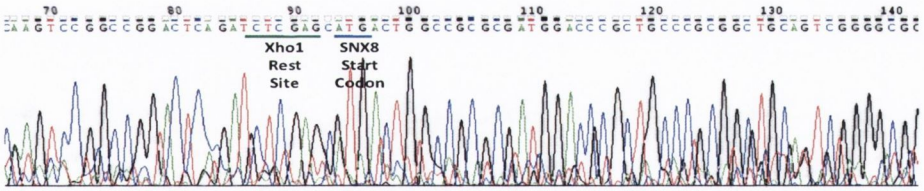

C

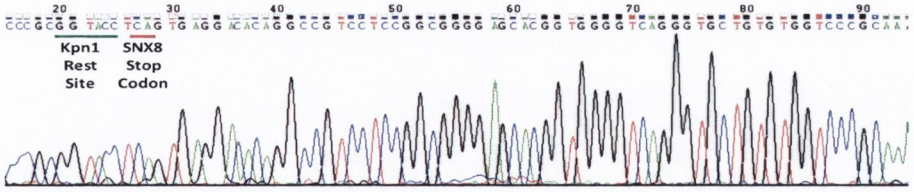

FIGURE 3.6. SEQUENCE VERIFICATION FOR PEGFP-C2-SNX8 CLONING. A. The sequence of SNX8 is shown in bold, the forward primer is shown in red, the reverse primer is shown in blue and the start and stop codons are underlined. Sequencing results showing **B.** the Xho1 restriction site (forward primer) used to clone SNX8 into pEGFP-C2 vector **C.** Kpn1 restriction site (reverse primer) used to clone SNX8 into pEGFP-C2 vector, confirming the success of the cloning.

A

```
ATG GTG AGC AAG GGC GAG GAG CTG TTC ACC GGG GTG GTG CCC ATC CTG GTC GAG CTG GAC GGC GAC GTA AAC
GGC CAC AAG TTC AGC GTG TCC GGC GAG GGC GAG GGC GAT GCC ACC TAC GGC AAG CTG ACC CTG AAG TTC ATC
TGC ACC ACC GGC AAG CTG CCC GTG CCC TGG CCC ACC CTC GTG ACC ACC CTG ACC TAC GGC GTG CAG TGC TTC
AGC CGC TAC CCC GAC CAC ATG AAG CAG CAC GAC TTC TTC AAG TCC GCC ATG CCC GAA GGC TAC GTC CAG GAG
CGC ACC ATC TTC TTC AAG GAC GAC GGC AAC TAC AAG ACC CGC GCC GAG GTG AAG TTC GAG GGC GAC ACC CTG
GTG AAC CGC ATC GAG CTG AAG GGC ATC GAC TTC AAG GAG GAC GGC AAC ATC CTG GGG CAC AAG CTG GAG TAC
AAC TAC AAC AGC CAC AAC GTC TAT ATC ATG GCC GAC AAG CAG AAG AAC GGC ATC AAG GTG AAC TTC AAG ATC
CGC CAC AAC ATC GAG GAC GGC AGC GTG CAG CTC GCC GAC CAC TAC CAG CAG AAC ACC CCC ATC GGC GAC GGC
CCC GTG CTG CTG CCC GAC AAC CAC TAC CTG AGC ACC CAG TCC GCC CTG AGC AAA GAC CCC AAC GAG AAG CGC
GAT CAC ATG GTC CTG CTG GAG TTC GTG ACC GCC GCC GGG ATC ACT CTC GGC ATG GAC GAG CTG TAC AAG TCC
GGC CGG ACT CAG ATC TCG AGC ATG ACT GGC CGC GCG ATG GAC CCG CTG CCC GCG GCT GCA GTC GGG GCG GCA
GCT GAG GCG GAG GCT GAC GAG GAG GCG GAT CCC CCG GCG TCA GAT CTG CCG ACA CCC CAG GCC ATC GAG CCC
CAG GCC ATC GTG CAG CAG GTC CCA GCC CCC AGT CGA ATG CAG ATG CCG CAG GGG AAC CCG CTG CTG CTG TCC
CAC ACC CTG CAG GAG CTG CTG GCC AGG GAC ACC GTG CAG GTG GAG CTC ATT CCG GAG AAG AAG GGC CTC TTC
CTG AAG CAT GTG GAG TAT GAG GTT TCC AGC CAG CGC TTC AAG TCC TCG GTA TAC AGA CGG TAC AAT GAC TTC
GTG GTC TTC CAG GAG ATG CTC CTG CAC AAG TTC CCC TAC CGT ATG GTG CCT GCC CTG CCA CCC AAG AGA ATG
CTG GGA GCT GAC AGG GAG TTC ATC GAG GCC AGG AGG AGA GCC CTG AAG CGC TTC GTC AAC CTG GTG GCG CGA
CAC CCC CTG TTC TCC GAG GAT GTG GTC CTC AAG CTC TTC CTG TCC TTC AGC GGC TCG GAT GTG CAG AAC AAG
TTA AAG GAG TCA GCA CAG TGC GTC GGG GAC GAA TTC CTG AAC TGT AAG CTG GCT ACC AGG GCC AAG GAC TTC
CTC CCA GCT GAC ATC CAG GCT CAG TTT GCC ATC AGC CGG GAG CTG ATC CGG AAC ATC TAC AAT AGC TTT CAC
AAG CTT CGC GAC AGG GCC GAG CGG ATC GCG TCG CGG GCC ATC GAC AAT GCG GCA GAT CTT CTC ATA TTC GGG
AAG GAG CTA AGT GCA ATA GGG TCT GAC ACG ACC CCG CTG CCC TCC TGG GCC GCT CTG AAT AGC AGC ACG TGG
GGG TCC CTG AAG CAG GCT CTG AAA GGC CTG TCT GTG GAA TTC GCG CTG CTC GCC GAC AAG GCT GCA CAA CAG
GGT AAG CAG GAA GAG AAC GAC GTG GTG GAG AAG CTG AAC CTC TTC TTG GAT CTG CTG CAG TCC TAT AAG GAC
CTG TGC GAG CGG CAT GAG AAG GGC GTG TTG CAC AAG CAC CAG CGG GCC CTG CAC AAG TAC AGC CTG ATG AAG
AGG CAG ATG ATG AGC GCC ACC GCG CAG AAC CGC GAG CCG GAG TCC GTG GAG CAG CTG GAG TCC CGC ATC GTG
GAG CAG GAG AAC GCG ATT CAG ACG ATG GAG CTG CGG AAC TAC TTC TCC CTG TAC TGC CTG CAC CAG GAG ACG
CAG CTC ATC CAC GTC TAC CTG CCC CTC ACC TCC CAC ATC CTC CGC GCC TTC GTC AAC TCT CAG ATC CAA GGG
CAC AAG GAG ATG AGC AAG GTG TGG AAC GAC CTG AGG CCC AAG CTC AGC TGC CTC TTT GCG GGA CCA CAC AGC
ACC CTG ACC CCA CCG TGC TCC CCG CCG GAG GAC GGC CTG TGT CCT CAC TTG TGA
```

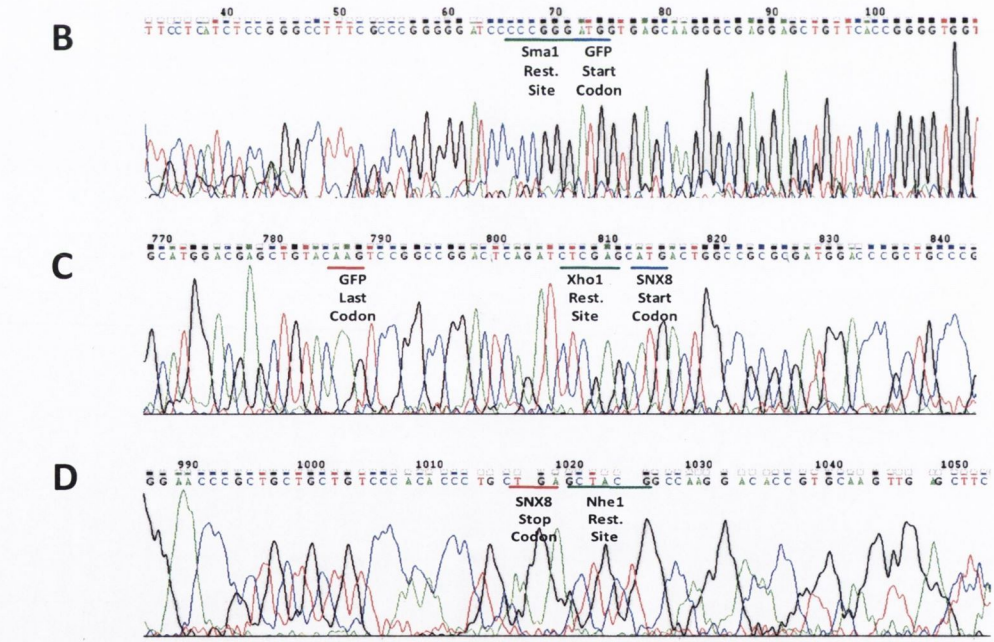

FIGURE 3.7. SEQUENCE VERIFICATION FOR PLL4.0_GFP-SNX8 CLONING. A. The GFP-SNX8 sequence inserted into the pLL4.0 vector, with the start and stop codons of GFP indicated in greeen and the start and stop codons of SNX8 indicated in red. Sequencing results showing **B.** Sma1 restriction site used to clone GFP-SNX8 **C.** the Xho1 restriction site used to clone SNX8 into the pEGFP-C2 vector and **D.** the Nhe1 restriction site next to the SNX8 stop codon. The data infers GFP-SNX8 was successfully cloned into the pLL4.0 vector.

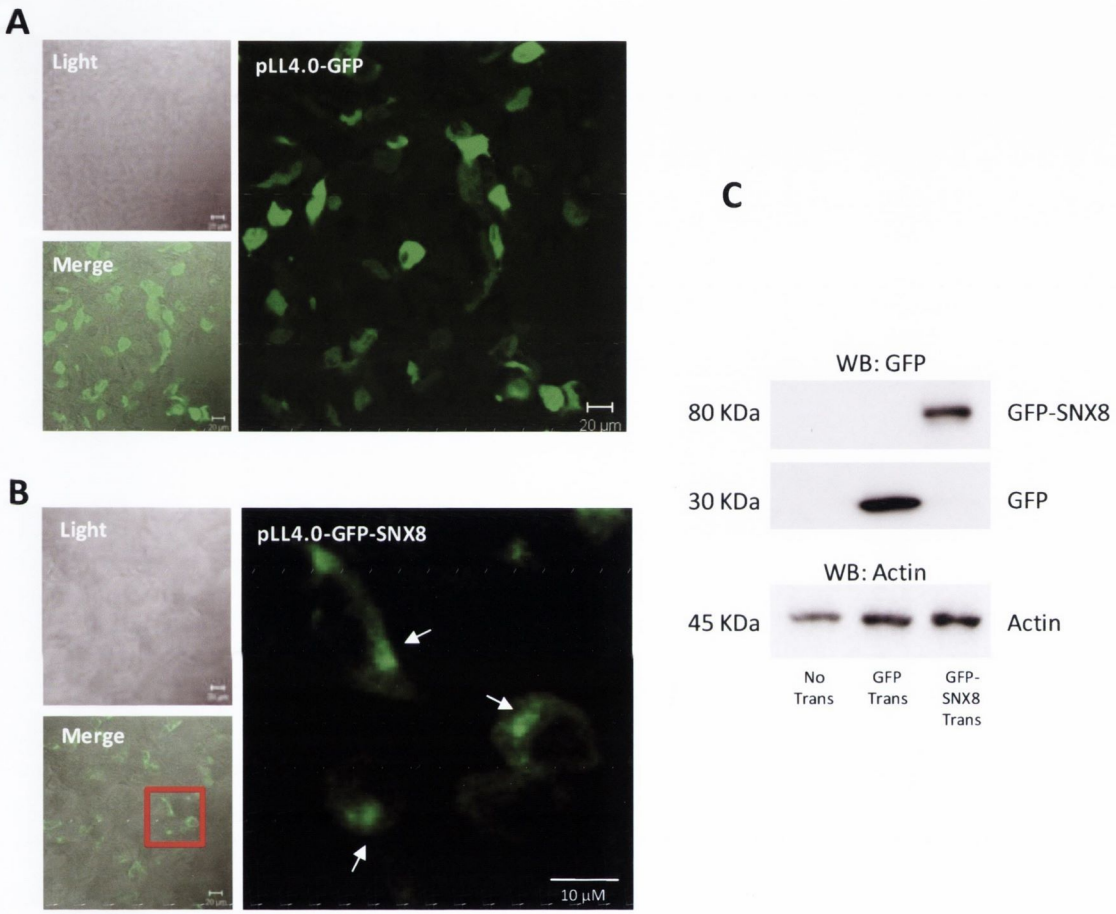

FIGURE 3.8. HEK 293T CELL TRANSFECTION CHECKS FOR PLL4.0-GFP-SNX8 PLASMID. Confocal image showing HEK 293T cells transfected with **A.** pLL4.0-GFP empty vector and **B.** pLL4.0-GFP-SNX8. The large panel shows a magnified image of the region of the red box. The tagged protein is visible in the perinuclear region of the cell, indicated by white arrows. **C.** Western blot using lysates from transfected cells, probing with GFP antibody shows no GFP signal in the non-transfected cells, a GFP signal in the pLL4.0 empty vector transfected cells at 27 KDa (middle panel) and a band at 80 KDa in the GFP-SNX8 transfected cells (top panel), corresponding to the size of the fusion protein.

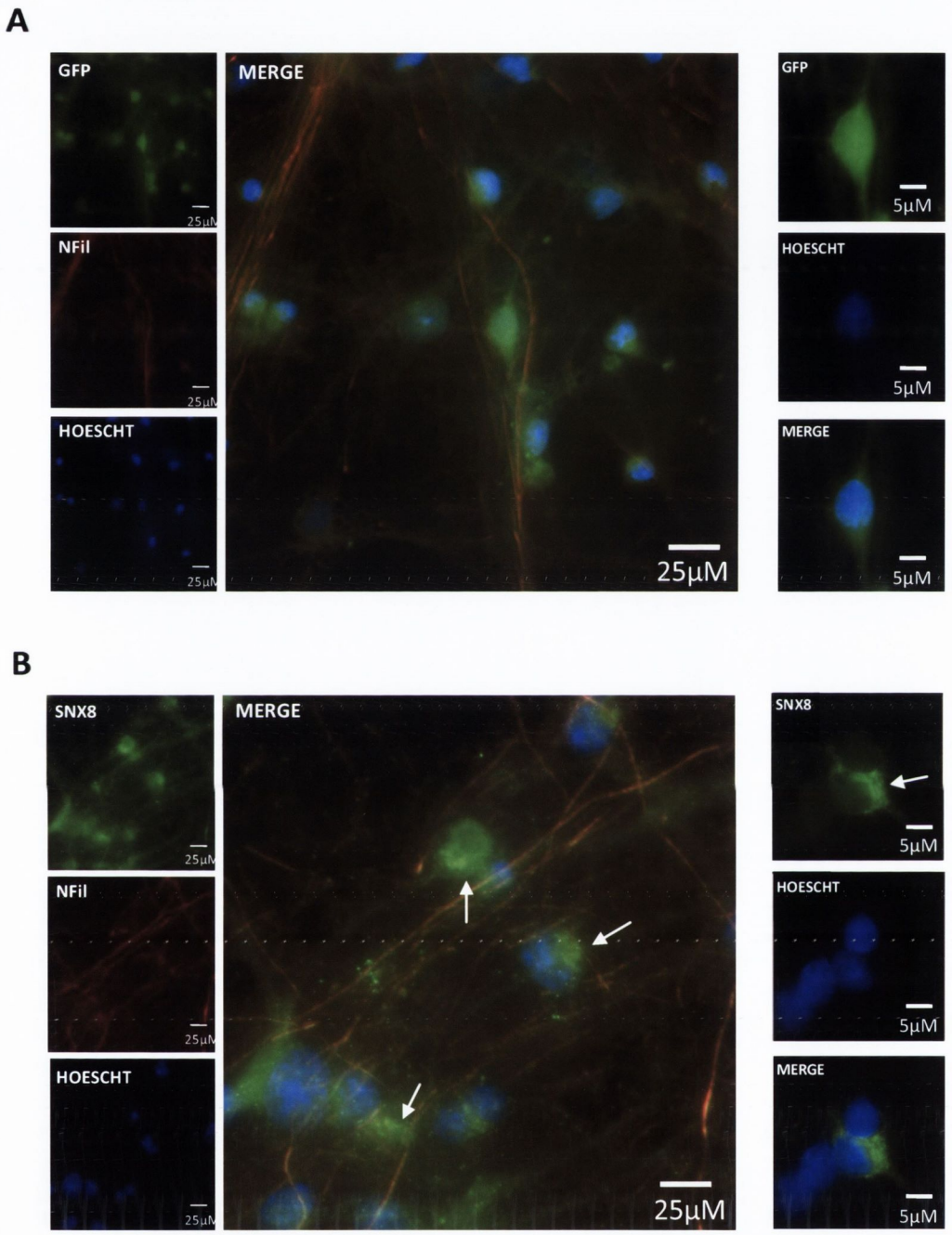

FIGURE 3.9. GFP-SNX8 EXPRESSION IN NEURONS IS PRIMARILY PERINUCLEAR. Images showing neurons transfected with **A.** GFP lentivirus, which is observed to transduce the whole cell and **B.** GFP-SNX8, which punctuate expression can be observed, as indicated by arrows. The right panels in both figures show magnified images, highlighting the differences in expression between GFP alone and GFP-SNX8.

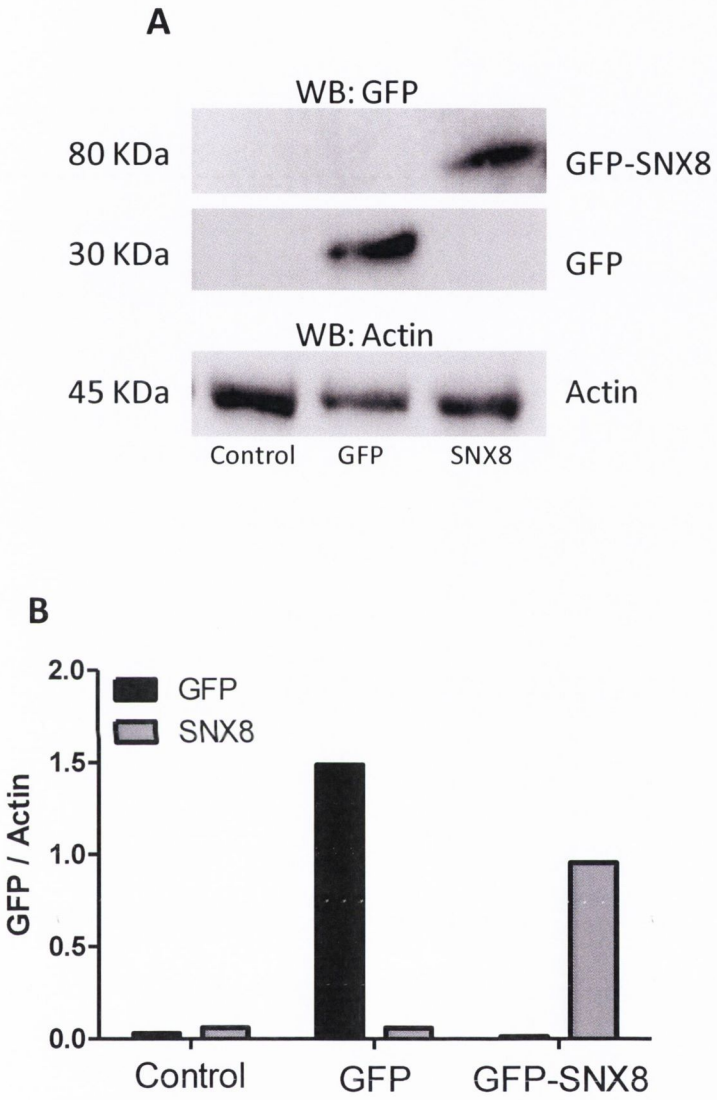

FIGURE 3.10. BIOCHEMICAL CONFIRMATION OF SNX8 LENTIVIRAL OVEREXPRESSION A. Western blot of neuron cell lysates following transfection with GFP or GFP-SNX8 using GFP antibody and Actin antibody as a loading control. The GFP-SNX8 fusion protein can be observed at 80KDa, and the GFP alone at 27KDa. **B.** Graph showing quantification of western blots, in GFP transfected cells, a GFP antibody signal is only present at 30 KDa. In GFP-SNX8 transfected cells GFP signal was only detected at 80 KDa, no signal was detected in non-transfected control cells.

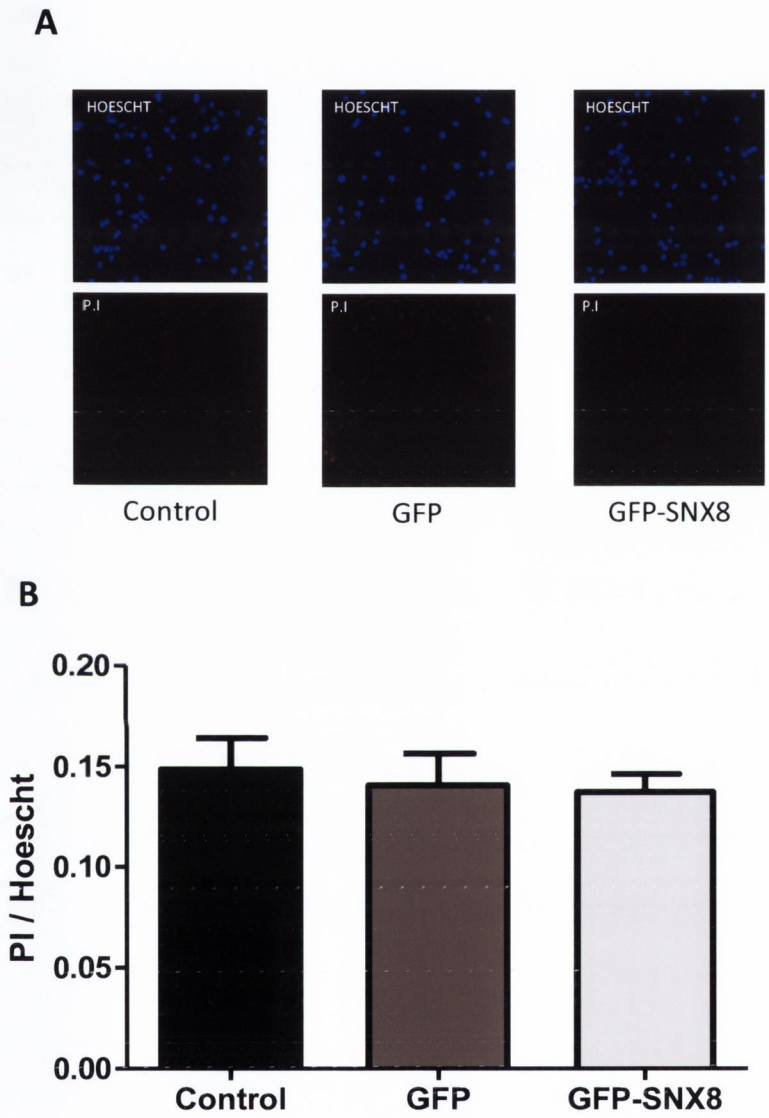

FIGURE 3.11. LENTIVIRUS TRANSFECTION DOES NOT AFFECT CELL SURVIVAL. A. Neurons were transfected with GFP and GFP-SNX8 lentivirus, after 72 hours the cells were fixed and stained with hoescht and propidium iodide to detect dead cells. **B.** The PI to hoescht ratio was calculated for each image. Transfection of neither the GFP nor the GFP-SNX8 viruses detrimentally affected cell survival. (n=4, one way ANOVA, Dunnets Post Hoc, $p > 0.05$)

3.5.0 DISCUSSION

3.5.1 SUMMARY OF RESULTS

SNX8 was cloned primarily into an intermediate plasmid (pEGFP-C2), which allowed the addition of a GFP tag to the N terminus of the protein. This fusion protein was then subcloned into a lentiviral vector (pLL4.0). Confirmation of successful cloning was then ensured by both restriction digestion and PCR studies, and by DNA sequencing. Lentiviral particles of GFP-SNX8 and GFP alone were generated and neurons were transfected with the viruses to confirm the lentiviruses were capable of transfecting these cell types and also to investigate the expression pattern of GFP-SNX8 within neurons. GFP alone successfully transfected neurons, with ubiquitous cytoplasmic expression. GFP-SNX8 lentivirus also successfully transfected neurons and in contrast to GFP showed a punctuate expression around the nucleus, with localisation also out of the soma towards the processes. Previously GFP-SNX8 has been seen to be colocalised with EEA1 (early endosome antigen 1), and also with components of the retromer; SNX1 and VPS35 (Dyve et al., 2009). This punctuate expression may be indicative of SNX8 involvement in endosomal trafficking or retrograde transport. Propridium iodide staining showed that GFP-SNX8 transfection did not adversely affect cell viability indicating that GFP-SNX8 overexpression is not neurotoxic.

3.5.2 COMPARING VIRAL VECTOR TRANSDUCTION SYSTEMS FOR USE IN THE CNS

The development of agents that deliver DNA to the brain is key to the realisation of gene therapy to treat diseases of the CNS. As the majority of cells in the CNS are post-mitotic, vectors capable of transducing quiescent cells are a necessity. Currently there are four main viral vectors that can be utilized to deliver genes; herpes simplex viruses (HSV), recombinant adenovirus (rAd), recombinant adeno-associated viruses (rAAV) and lentiviruses (Lv). There are some differences between these delivery systems, however all have been engineered to be non-replicating, therefore, can only transduce the cells they infect, so the virus does not spread. All the systems have also been adapted so they cannot enter the lytic cycle (killing the cell they infect) (Mandel et al., 2008). HSV is a very large virus, with the potential for genes up to 150kb to be inserted if all viral genes are removed (Fraefel et al., 2000). However, HSV vectors cannot support long term expression *in vivo* and are ultimately cytotoxic (Burton et al., 2005) thus are not favoured over the other viral delivery systems, such as rAd, the earliest used viral delivery system to the CNS (Le Gal La Salle et al., 1993). This system is characterised by high level transgene expression and the ability to transduce quiescent cells, including neurons and glia (Gerdes et al., 2000). Conversely, wild type viral genes remain within

these vectors illiciting host inflammatory response, and innate and adaptive immune responses have been observed within the brain (Byrnes et al., 1995). In an attempt to overcome this, newer generation vectors have been designed; "gutless" vectors have had the complete viral genome removed, but with this came a resultant decrease in transfection efficiency (Lowenstein et al., 2002). Recombinant adeno-associated viruses do not generate an immune response from the host as they have no viral genes, however to a lesser extent an immune response has been observed due to viral proteins in the capsid (Lowenstein, 2004). Aside from this, rAAVs are highly desirable for use in gene therapy within the CNS as they feature low pathogenicity, a natural latency and are replication incompetent (Mandel et al., 2008). Hundreds of genotypes of AAV have been identified, but only AAV1-10 have been engineered into vectors (Davidson et al., 2000). AAV2 is the most commonly used variation within the CNS, where it transduces neurons exclusively (Burger et al., 2005). A large proportion of the human population have circulating antibodies to AAV2, these neutralising antibodies are capable of blocking AAV transduction in the brain, indicating these delivery systems may not be the best option for large scale clinical gene therapy (Peden et al., 2004). The last category of gene delivery system is the lentiviral system, the only oncoretrovirus able to trasduce both mitotic and post-mitotic cells (Naldini and Verma, 2000). Lentiviruses are more complex than other retroviruses as they contain additional regulatory genes along with *tat* and *rev*, such as *vif* and *vpr*. These components allow a greater level of manipulation of function than other delivery systems (Naldini and Verma, 2000). Lentiviruses have been used extensively in the CNS, with a preference towards the transduction of neurons, however expression has been observed in a small percentage of glia too (Blomer et al., 1997). These data combined highlight that lentiviral vectors are the optimal viral delivery system for work within the CNS.

3.5.3 Lentiviral Mediated Gene Therapy For Parkinson's Disease

As lentiviruses can transfect post-mitotic cells, they are an attractive candidate for treating neurodegeneration. Thus far, lentiviral delivery systems have been used to investigate Parkinson's disease, Alzheimer's Disease and lysosomal storage diseases (in particular Leukodystrophy). Accumulation of the synaptic protein α-synuclein (α-syn) leading to alterations in the autophagy pathway is a hallmark of Parkinson's disease (PD) and Lewy body disease (LBD) (Wakabayashi et al., 1997). Beclin-1 is a regulator of the autophagy pathway, thus it was hypothesised overexpression of this protein may alter the disease pathology. As an example, lentivirus expressing beclin-1 was delivered to the brain of α-syn transgenic mice (Spencer et al., 2009). Neuropathological analysis demonstrated that beclin 1 lentivirus injections improved the synaptic and dendritic pathology in the

mice and reduced the accumulation of α-syn in the limbic system without any significant negative side effects. This finding was coupled with enhanced lysosomal activation and reduced alterations in the autophagy pathway. Thus, lentiviral mediated beclin 1 overexpression may present a novel therapeutic target for LBD/PD by direct or indirect interaction with the autophagy pathway. Along with endogenous protein overexpression lentiviral vectors can be used to express mutated genes. Recent evidence indicates a critical role for neuroinflammation in the pathogenesis of PD, with particular focus on TNF (tumour necrosis factor), which when inhibited can attenuate neurodegeneration (Sriram et al., 2006). Thus, another example where lentivirus has been used in PD is the use of a lentivirus encoding dominantnegativeTNF (lenti-DN-TNF). This lenti-DN-TNF was injected into the substantia nigra pars compacta (SNpc) of a mouse model of PD. Five weeks following treatment, no further loss of nigral dopaminergic neurons was observed, and microglial activation was attenuated (Harms et al., 2011), suggesting lentiviral vectors containing dominant negative form of TNF may prove a valuable mechanism for gene therapy, not only in Parkinson's Disease, but in other CNS disorders. Lentiviral vectors can also be generated which express RNA interference (RNAi), this system has also been used in models of Parkinsons disease. The loss of dopamine within the striatum in PD upregualtes GAD67 (GABA producing enzyme 67) expression within striatal neurons, changing the activity of the basal ganglia circuit (Wichmann and DeLong, 2003). In an attempt to normalise GAD67 levels, lentiviral vectors containing RNAi against GAD67 mitochondiral RNA were generated. When injected into the stiatum of a rat model of Parkinson's disease, the lentivirus successfully reduced GAD67 levels, as well as normalising the aberrant neural activity observed from the loss of dopamine (Horvath et al., 2011).

3.5.4 Lentiviral Mediated Gene Therapy For Alzheimer's Disease

In Alzheimer disease, increased beta-secretase (BACE1) activity has been associated with neurodegeneration and accumulation of amyloid precursor protein (APP) products. Thus, inactivation of BACE1 could be important in the treatment of Alzheimer disease. Lowering BACE1 levels using lentiviral vectors expressing siRNAs targeting BACE1 reduced amyloid production and the neurodegenerative and behavioral deficits in APP transgenic mice (a model of Alzheimer disease)(Singer et al., 2005). Lentiviral mediated RNA interference has also been used to deliver APP695-siRNA to hippocampal and cortical neurons of APP695 transgenic mice (AD model) in vitro. This treatment resulted in a reduction in neuronal apoptosis, possibly through the reduction of caspase-3 activity and the neuronal apoptosis pathway (Zhao et al., 2011). Lentiviral mediated protein overexpression has also been investigated as a potential therapy for AD. The endopeptidase,

neprilysin, has been implicated as a major Aβ degrading enzyme in mice and humans. Lentivirus was used to deliver this enzyme into the brain of APP transgenic mice for up to 6 months. This resulted not only in a decrese in amyloid plaque load but also reduced the levels of intracellular Aβ immunoreactivity. These reductions were associated with improved behavioral performance in the water maze and ameliorated the dendritic and synaptic pathology in the APP transgenic mice (Spencer et al., 2008).

3.5.5 Lentiviral Systems For Use In Lysosomal Storage Disorders

An interesting study investigating a lysosomal storage disorder highlights the versatility of lentiviruses in gene therapy. Leukodystrophies (a subset of lysosomal storage disorders) are rare diseases caused by defects in the genes coding for lysosomal enzymes that degrade several glycosphingolipids (Perlman and Mar, 2012). Gene therapy for leukodystrophies requires efficient distribution of the missing enzymes in CNS tissues to prevent demyelination and neurodegeneration (Lattanzi et al., 2010). Bidirectional lentiviruses were generated, initiating the expression of both the target gene (β-galactocerebrosidase, GALC) and a reporter gene, which allowed both detection of transgene distribution and enzyme activity. This enzyme GALC, is mutated in Krabbe Dissease and in the twitcher mouse model (Lattanzi et al., 2010). A single injection of the lentivirus to the external capsule (a white matter region enriched in neuronal projections) in early symptomatic twitcher mice resulted in rapid and robust expression of a functional GALC protein in the telencephalon, cerebellum, brainstem and spinal cord. This expression led to global rescue of GALC enzymatic activity, significant reduction of tissue storage and decrease of activated astroglia and microglia (Lattanzi et al., 2010). Combined this data illustrates the versatility and advantageous uses of lentiviral mediated gene delivery systems as a valuable device in the treatment of disorders of the CNS, with particular focus on the prevention of neurodegeneration.

3.5.6 Moving On To The Next Chapter

The Lv-GFP-SNX8 was generated to allow the characterisation of SNX8 function within the CNS. The expression of SNX8 can be modulated in a variety of cellular conditions, allowing useful insights into the role of the sorting nexin in both the retrograde pathway and the SREBP pathway, both of which SNX8 has been identified to influence. This chapter has shown the successful development of the

SNX8 lentivirus, the next chapter will initially explore endogenous SNX8 expression, before using the GFP-SNX8 lentivirus to further explore its protein function.

CHAPTER 4. INVESTIGATING AND MANIPULATING SNX8 EXPRESSION

4.1.0 AIMS AND HYPOTHESIS

- Demonstrate the specificity of the SNX8 antibody
- Investigate the expression profile of SNX8 within rat body tissue and CNS
- Elucidate the expression profile of SNX8 within different CNS cell types
- Explore changes in SNX8 expression in differing cholesterol environments
- Study changes in SNX8 levels and location in a cellular model of NPC disease
- Investigate the effect of SNX8 overexpression on cholesterol levels in neurons
- Use SNX8 lentivirus to visualise changes in SNX8 localisation in differing cholesterol environments

This chapter explores SNX8 expression within the CNS, and utilises the GFP-SNX8 lentivirus to modulate this expression in differing cholesterol environments. It was hypothesised that SNX8 would be expressed within specific cell types of the CNS and that expression levels or localisation may be modulated in differing cholesterol environments. It was also hypothesised that overexpression of SNX8 may alter endogenous cholesterol levels.

4.2.0 ABSTRACT

SNX8 was previously identified to overcome the Insig dependent block of the SREBP pathway of cholesterol homeostasis. Cholesterol is a vital component of the CNS, and is involved in processes such as synaptic function and myelination. Thus, the expression of SNX8 within the CNS was investigated to enable the identification of its role in this environment. SNX8 was found to be endogenously expressed in rat peripheral organs and the CNS. SNX8 was differentially expressed within neurons of hippocampal and cerebellar slice cultures, with the protein being localised primarily to the soma within cerebellar neurons and within the processes and soma in hippocampal neurons. Interestingly, SNX8 was not found to be expressed in glial cells, namely astrocytes and microglia. Next, the effect of altered cholesterol levels on SNX8 expression was examined. Protein levels were found to be unchanged in the presence of excess cholesterol, and decreased in the presence of both mevinolin (a cholesterol lowering statin), and U18666a (which causes cholesterol to accumulate within the lysosome). In the presence of excess cholesterol the overexpression of GFP-SNX8 caused redistribution and overall decrease in levels of unesterified cholesterol within neurons, indicating a differential sorting role for SNX8 in high cholesterol levels.

4.3.0 INTRODUCTION

4.3.1 THE FUNCTION OF THE SORTING NEXIN FAMILY

The sorting nexin family of proteins are implicated in endosomal sorting within many cell types due to the presence of a PX domain that targets the protein to PtdIns(3)P found in endsosomal membranes (Cullen, 2008). There are currently 33 identified members of the sorting nexin family; these members can be subdivided into three categories dependant on their domain structure. The subgroup termed the SNX^{PX} group contains only the PX domain, with no other flanking domains (Seet and Hong, 2006). The SNX^{BAR} family contain both a PX domain and a Bin, amphiphysin, Rvs (BAR) domain. As previously described the BAR domain is known to dimerise to sense and stabilise membrane curvature (Peter et al., 2004). The remaining sorting nexins form the SNX^{other} group which alongside the PX domain, contain diverse domains such as PDZ (postsynaptic density protein-95, discs-large, zona occludens-1), SH3 (Src homology 3) and RA (Ras-associated) domain (Cullen, 2008). Relatively little research has been carried out to investigate the function of sorting nexins. However, recently SNXs have been implicated in various roles within the CNS (Teasdale and Collins, 2012).

4.3.2 THE ROLE OF BAR DOMAIN SORTING NEXINS WITHIN THE CNS

It is known that sorting nexins contribute to endosomal sorting, a critical process in the tuning of neuronal function during activation and plasticity (Sadowski et al., 2009). The fact that SNXs function within the endosomal sorting pathway leads to the hypothesis that they may play a role in endocytosis and exocytosis of synaptic vesicles (Lundmark and Carlsson, 2009). SNX9 is a member of the SNX^{BAR} subfamily and its expression is increased with time within the mouse brain, confirmed by western blotting of mouse neuron cell lysate at days 3, 7, 14, and 21 of culture. In the same study, it was found that SNX9 bound to dynamin-1 and co-localised with pre-synaptic vesicle markers and regulates synaptic vesicle endocytosis. Knockdown of SNX9 caused defects in synaptic vesicle endocytosis but not exocytosis confirming that the protein is involved in specific parts of synaptic vesicle function (Shin et al., 2007). In drosophila SNX9 has been found to interact with drosophila Dock protein and influence axon guidance via Dscam (Down's syndrome cell adhesion molecule) signalling (Worby et al., 2002; Worby et al., 2001). Another member of the SNX^{BAR} subfamily, SNX18, was found to be dynamically regulated in murine developing spinal motor neurons (Nakazawa et al., 2011). Expression increased during the development of spinal neurons, then decreased with maturation. GFP tagged SNX18 was also found to be expressed in the growth cones of developing

dorsal root ganglion (DRG) neurons, indicating a role for SNX18 in axonal elongation. This study suggests that PX-BAR sorting nexins may have a critical role in the development of the central nervous system. Another SNX^{BAR} family member has been identified in a very different neuronal environment. SNX2 and the androgen receptor (AR) mRNA are both increased in song control nuclei of juvenile zebra finch males compared to females (Wu et al., 2010). It is therefore possible that both AR and SNX2 are involved in masculinization of this brain region, and the combination of these two proteins enhances the action of trophic factors within the brain (**Figure 3.1**).

4.3.3 The Role Of PX Domain Sorting Nexins Within the CNS

SNX^{PX} members have been found to be expressed in the CNS and like PX-BAR containing sorting nexins have been implicated in development and function of neurons. SNX16 has been found to control a presynaptic trafficking pathway (Rodal et al., 2011). SNX16 interacts with Nwk (Nervous Wreck - a presynaptic F-BAR/SH3 protein that regulates synaptic growth signaling in Drosophila melanogaster) to promote synaptic growth signaling via activated bone morphogenic protein receptors. In another study using a mouse neuronal cell line, SNX3 (an SNX^{PX} member) was also observed to play a role in neuronal development particularly neurogenisis and neuritogenesis (Mizutani et al., 2009). SNX3 knockdown also caused a decrease in neurite outgrowth and overexpression caused an increase in outgrowth. SNX3 mRNA was also found to be highly expressed in the mouse from embryonic stage through to adulthood (Mizutani et al., 2011). The same group have identified high expression of SNX12 (SNX^{PX} member) within the mouse CNS (Mizutani et al., 2012). In the brain SNX12 expression was found to increase during the embryonic stage and decrease after birth. SNX12 expression was restricted to neurons, with no expression observed in glial cells. Neuronal expression of SNX12 was high in post-mitotic neurons, particularly in layers II-IV of the the cerebral cortex during development. Knockdown of SNX12 was also found to attenuate neurite outgrowth. This data combined illustrates SNX12 plays a critical role in neurite formation and general development of the cerebral cortex in mice. In addition to its role in development SNX12 has been found to interact with BACE1 (beta-site APP cleaving enzyme 1) and dysregulate BACE1 endocytosis. This in turn affecting cleavage of APP (beta-amyloid precursor protein) and Abeta (beta-amyloid) production, the hallmark of AD (Alzheimer's Disease) pathology (Zhao et al., 2012). SNX12 overexpression was found to reduce levels of Abeta, soluble APPbeta and APP beta-carboxyl terminal fragments whilst SNX12 knockdown produced opposite effects. This information combined with the data that SNX12 levels are decreased in the brain of AD patients indicates SNX12 as a possible target for intervention in AD (Zhao et al., 2012) (**Figure 3.1**).

4.3.4 The Role Of Other Domain Containing SNXs In The CNS

Another SNX member has been implicated in APP processing; SNX17 (a $SNX^{PX\text{-}other}$ member) was found to colocalise with APP in early endosomes, and interact directly with APP via the cytoplasmic domain (Lee et al., 2008). Knockdown of endogenous SNX17 and overexpression of a dominant-negative mutant of SNX17 expression both reduced steady-state levels of APP with a resultant increase in Abeta production. This data led to the identification of SNX17 as a novel APP intracellular adaptor protein highly expressed in neurons (Lee et al., 2008). Other domain containing sorting nexin have also been implicated in receptor adaptation and trafficking within the CNS. For example, SNX27, one of the few PDZ domain containing sorting nexins has been found to bind to the PDZ motif of the 5-HT4a receptor and changes the trafficking of part of 5-HT4(a)R towards early endosomes (Joubert et al., 2004). It has also been discovered that SNX27 which is present in the postsynaptic compartment of hippocampal neurons is involved in learning, analgesia, and drug addiction via reducing the surface expression of G protein gated inwardly rectifying potassium channels (Lunn et al., 2007). SNX27 plays an essential role in postnatal growth and survival, targeted ablation of the SNX27 gene in mice, was embryonically lethal and caused growth retardation (Cai et al., 2011). In the same study SNX27 was identified as a novel N-Methyl-d-aspartate (NMDA) receptor 2C (NR2C) interacting protein, mediated by a c-terminal PDZ domain (SNX27) to PDZ motif (NR2C) interaction. Impaired NR2C endocytosis and overall increased NR2C expression levels in $SNX27^{(-/-)}$ neurons, indicates that SNX27 may function to regulate endocytosis and/or endosomal sorting of NR2C (Cai et al., 2011) (**Figure 3.1**).

4.3.5 The Proposed Role Of SNX8 Within The CNS

Sorting nexin function within the CNS is beginning to be better characterised. The SNX^{PX} family have been identified in neuronal development and neurite outgrowth (Mizutani et al., 2009). SNX^{other} members have also been implicated in development and via their supplementary domains have been observed to influence receptor trafficking (Cai et al., 2011). The PX-BAR containing sorting nexins like the other sorting nexins have been seen to be critical for correct development of the CNS, alongside this $SNXs^{BAR}$ have been found to regulate synaptic vesicle endocytosis and axon guidance and elongation (Nakazawa et al., 2011). Most SNXs have been found to be localised to the early endosome, due to the preferential interaction of the PX domain with PtdIns(3)P. Previous studies have shown GFP tagged SNX8 colocalised with EEA1 (an early endosome marker) and also with components of the retromer complex (Dyve et al., 2009). Furthermore, SNX8 was also identified as a positive modulator of the SREBP pathway. SNX8 overexpression was able to overcome the Insig

mediated block of the SREBP SCAP complex within the ER (Chatterjee et al., 2009). Efficient cholesterol homeostasis is critical for correct brain function, where aberrant cholesterol transport results in diseases such as Niemann Pick Type C Disease. In this disease, unesterified cholesterol accumulates within the endosomal lysosomal compartment and causes neurodegeneration and eventual cell death. We believe that SNX8 may interact with proteins within the SREBP pathway and the endosomal-lysosomal compartment to modulate cholesterol homeostasis within neurons. As sorting nexins have a diverse role within the CNS, SNX8 may be involved in a variety of cellular functions within neurons, such as neurogenesis, growth, cell death and possibly even receptor trafficking similar to other SNXs (**Figure 3.1**).

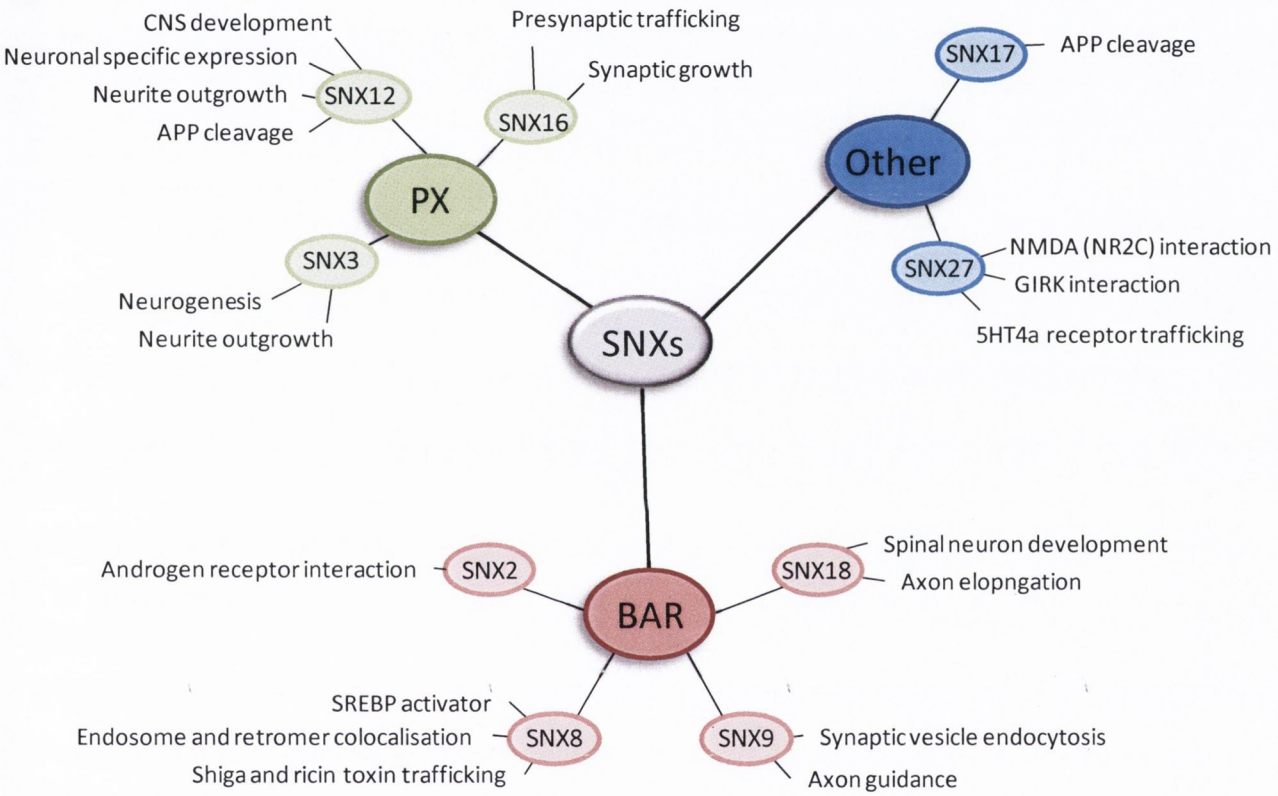

FIGURE 4.1. SUMMARY OF THE FUNCTION OF SORTING NEXINS WITHIN THE CNS. Schematic showing the sorting nexins that have been identified to have a role within the CNS. The sorting nexins are divided into their domain subfamily (PX, BAR and Other), and the particular role of each sorting nexin is summarized.

4.4.0 Results

4.4.1 SNX8 Expression in HEK 293T Cells is Downregulated by shRNA Interference

In order to first confirm the specificity of the SNX8 primary antibody, HEK 293T cells were transfected with a shRNA plasmid (Santa Cruz). The SNX8 shRNA plasmid is a pool of 3 target-specific lentiviral vector plasmids, each encoding 19-25 nucleotides (plus hairpin) shRNAs designed to knock down gene expression. A scrambled sequence shRNA plasmid was also used as a control. Following transfection the cells were fixed and stained. Confocal microscopy showed SNX8 was present endogenously in HEK 293T cells, specifically in the cell body, excluding the nucleus (**Figure 4.2a**). Transfection of the control (scrambled sequence) plasmid did not affect SNX8 protein expression (**Figure 4.2b**). In contrast, the SNX8 staining was successfully reduced by the transfection of HEK293 cells with the SNX8 shRNA plasmid (**Figure 4.2c**). The data suggests that the SNX8 primary antibody specifically targets SNX8 protein.

4.4.2 SNX8 is Expressed in Rat Tissues

A commercial nitrocellulose membrane (Imgenex) with lysates from adult rat body tissue (heart, small intestine, kidney, liver, lung, skeletal muscle, stomach, spleen, ovary and testis) was probed with SNX8 primary antibody, to validate the expression profile of SNX8 protein levels within the body (**Figure 4.3a**). The blot was then stripped and re-probed with actin primary antibody as a loading control to quantify the amount of protein present. The actin signal indicated protein levels were not standardised on the blot as claimed by the company. The SNX8 signal was very faint overall for the whole blot and bands were only present in heart and liver. When comparing the SNX8 signal to the actin signal the heart showed moderate levels of SNX8 expression. The SNX8 signal was found to be stronger than the actin signal in the liver sample, indicating high SNX8 expression.

To investigate expression and possible changes in SNX8 expression in the brain during development a commercial western blot membrane (Zyagen) with samples from differrent aged rat brain tissue lysates (embryonic day 20, postnatal day 1, weeks 1, 2 and 3, Months 1, 3, 6 and 12) was probed with SNX8 primary antibody (**Figure 4.3b**). The blot was then stripped and re-probed with actin primary antibody as a loading control to quantify the amount of protein present. SNX8 was present throughout all stages of development in the rat brain, from embryoyic stages to adulthood. Taken together, the data show that SNX8 is expressed in the brain (and likely other tissues) where high expression in the brain is first detected at the embryonic stage.

4.4.3 SNX8 is Differentially Expressed in Hippocampal and Cerebellar Slice Cultures

Following the discovery that SNX8 was present in the brain of rats throughout development, the distribution pattern within the brain was further elucidated. Hippocampal and cerebellar slice cultures were used to examine the expression of SNX8 within these brain regions. The slices were stained with SNX8 and neurofillament antibody and visualised using confocal microscopy. SNX8 was widely expressed in both hippocampal and cerebellar slices (**Figure 4.4**). When examining the CA1, CA3 and dentate gyrus SNX8 was found to be expressed in all regions (**Figure 4.4 a-d**). Similarly, SNX8 was seen to be expressed in the purkinje layer, the granule layer, the white matter of the cerebellum (**Figure 4.4 e-h**). The expression pattern of SNX8 within cerebellar neurons is different from hippocampal neurons. SNX8 expression was visible primarily in the cell body within the cerebellum, with little or no staining visible in the processes, where as staining was visible in both regions in the hippocampus.

4.4.4 SNX8 Is Differentially Expressed In Hippocampal And Cerebellar Dissociated Culutres

In order to investigate the difference in expression of SNX8 in hippocampal and cerebellar slices, dissociated cultures were stained with SNX8 antibody and neurofillament antibody, to allow further characterisation of protein localisation. In hippocampal neurons SNX8 was seen to be co-localised with neurofillament staining and was seen to be distributed throughout the cell, both in the cell body and in the processes (**Figure 4.5a**). In cerebellar neurons, SNX8 protein was localised primarily within the soma (**Figure 4.5b**). These data from dissociated cultures were in agreement with the subcellular localisation found in cerebellar and hippocamplal slice cultures. The differential localisation of SNX8 in cerebellar neurons may indicate a potential difference in the function of the protein in these neuronal subsets.

4.4.5 SNX8 Is Not Expressed In Glial Cells

After concluding SNX8 is present in the brain, particularly within neurons, it remained to be examined whether the protein was present in any other cell types of the CNS. Glial cells were cultured for 7 days then fixed and stained to investigate the expression profile of SNX8 within both astrocytes and microglia. Glial fibrillary acidic protein (GFAP) antibody was used to identify astrocytes. SNX8 staining was not observed in enriched astrocyte cultures, indicating SNX8 is not present in this cell type (**Figure 4.6a**). Cell lysates from enriched astrocyte cultures were also used in

western blots to examine SNX8 expression. No signal was detected in the samples; further confirming SNX8 is not present in astrocytes (**Figure 4.6b**). Microglia were stained with CD11b antibody as a cellular marker along with SNX8 antibody. Similar to astrocytes, SNX8 staining was not observed in microglia (**Figure 4.7a**). Furthermore, Western blot analysis with SNX8 antibody on microglia cell lysates also revealed that SNX8 was not present (**Figure 4.7b**). The low or absence of SNX8 expression in astrocytes is somewhat interesting, given the role of this cell type in cholesterol synthesis within the CNS.

4.4.6 SNX8 Levels Are Unchanged In Neurons Following Treatment With Cholesterol

Our previous data shows that SNX8 regulates the SREBP pathway (Chatterjee et al., 2009). These previous studies were conducted in heterologous cell lines. Thus, we aimed to examine if SNX8 is regulated in neurons under different cholesterol conditions. Initially, cells were treated with 2 μg/ml 25-OH cholesterol for 24 hours, to inhibit the SREBP pathway (Chang et al., 1998). Western blots of cell lysates from treated and control cells were performed with SNX8 and actin (as a loading control) antibodies to detect any changes in SNX8 expression levels in excess cholesterol conditions (**Figure 4.8a**). Quantification of the blots revealed SNX8 expression remained unchanged in the presence of excess cholesterol (n=5, Students T-test, $p>0.05$) (**Figure 4.8b**). This finding is interesting as SNX8 is known to directly stimulate the SREBP pathway, thus upregulating cholesterol production, it appears there is no direct effect of this increase in cholesterol as a feedback to then influence SNX8 levels.

4.4.7 Mevinolin Treatment Causes A Decrease In SNX8 Expression In Neurons

Statins are widely clinically used to lower cholesterol levels (Rutishauser, 2011). Following the observation that cholesterol treatment left SNX8 levels unchanged, the effects of low cholesterol on SNX8 expression was then examined. Neurons were treated with 0.25 μM mevinolin for 24 hours (Santa-Catalina et al., 2008) and the lysate processed for western blotting, with SNX8 and actin antibody (**Figure 4.9a**). These data show that mevinolin treatment decreases SNX8 expression in neurons (n=5, Students T-test, $p<0.001$) (**Figure 4.9b**), indicating that low cholesterol levels instigate a reduction in SNX8 expression, where as high cholesterol levels have no effect on SNX8 levels.

4.4.8 Treatment With U18666a Results In A Decrease In SNX8 Expression In Neurons

U18666a induces a cellular model of NPC disease by causing cholesterol accumulation within endosomes and lysosomes (cenedCenedella, 1980). The sterol sensor that that detects intracellular cholesterol levels is present in the endoplasmic reticulum (Irisawa et al., 2009). U18666a mediated cholesterol accumulation within the lysosome leads to decreased cholesterol levels at the endoplasmic reticulum, thus the sterol sensor detects that the cell is cholesterol deficient. As SNX8 expression was seen to be decreased in low cholesterol levels (mevinolin treatement), it was hypothesised SNX8 levels would also change following treatment with U18666a. Cells were treated with 1 µg/ml U18666a for 24 hours 1 µg/ml U18666a (Cheung et al., 2004) and the lysate used for western blotting with SNX8 and actin antibodies (**Figure 4.10a**). U18666a was found to significantly decrease neuronal SNX8 levels (n=5, Students T-test, $p<0.01$). These data are in agreement with the previous finding that mevinolin treatment decreased SNX8 protein expression. The data also further support the hypothesis that SNX8 levels are decreased when under conditions of accumulated cholesterol. Given that U18666a induces a cellular model of NPC disease it is possible to speculate that levels of SNX8 may change in this disease.

4.4.9 GFP-SNX8 Localisation Is Not Altered In Differing Cholesterol Environments

Following the discovery that SNX8 expression levels were decreased in low cholesterol levels but unchanged in the presence of excess cholesterol, it remained to be investigated whether the localisation of SNX8 was affected in any way in these different environments. Mixed cultures were transfected with GFP-SNX8 lentivirus. After two days the cells were then treated with either 2 µg/ml 25-OH cholesterol, 1 µg/ml U18666a or 0.25 µM mevinolin for 24 hours, then fixed and stained with hoescht to identify cell nuclei. As shown previously GFP-SNX8 was found to be localised to the soma of neurons in a punctuate expression pattern (**Figure 4.11**). The expression profile was not altered in any of the treatment groups, showing that although SNX8 expression levels are changed in low cholesterol levels, the localisation of the protein however is not altered.

4.4.10 GFP-SNX8 Overexpression Does Not Alter Cholesterol Content In Normal Conditions

It has been observed in previous experiments that changes in the cellular cholesterol environment can alter SNX8 expression. In order to further investigate the role of SNX8 in cholesterol homeostasis, neuronal culutres were transfected with GFP-SNX8 lentivirus, and fixed and stained

with Filipin III. When bound to unesterified cholesterol Filipin fluoresces, allowing the levels of cholesterol within the cell to be quantified, thus enabling the determination of whether SNX8 overexpression directly influences cholesterol levels. Under physiological cholesterol conditions the overexpression of SNX8 was not found to drastically alter the distribution of cholesterol. However, a slight increase in cell density was observed (**Figure 4.12a and b**). Quantification of the overall fluorescence from all control and GFP-SNX8 images was plotted, SNX8 overexpresion found not to significantly alter fluorescence levels. It can therefore be extrapolated that SNX8 overexpression does not alter cholesterol levels under normal conditions (**Figure 4.12c**). (n=3, Students T-test, $p>0.05$).

4.4.11 U18666a Mediated Cholesterol Accumulation Is Not Altered By GFP-SNX8 Overexpression

It is well characterised in the literature that Filipin staining can be used to visualise the U18666a mediated accumulation of cholesterol within the endosomal-lysosomal pathway of cells (Iftakhar et al., 2009). Following the finding that U18666a treatment caused decreased expression of SNX8 in neurons (**Figure 4.10**), neurons were transfected with GFP-SNX8 lentivirus for 2 days, on day 3 the trasfected neurons (or non-transfected controls) were treated with 1 μg/ml U18666a for 24 hours, then fixed and stained with Filipin before imaging. Both GFP-SNX8 transfected and non-transfected control neurons were observed to exhibit the characteristic spherical accumulation of unesterified cholesterol (**Figure 4.13a and b**). In the SNX8 transfected culture there was an increase in cell number and processes. However, following the quantification of total fluorescence it was found that there was no significant difference in total cholesterol levels after GFP-SNX8 transfection (**Figure 4.13c**) (n=3, Students T-test, $p>0.05$), indicating SNX8 overexpression had no effect on U18666a mediated cholesterol accumulation.

4.4.12 GFP-SNX8 Overexpression Does Not Alter Cholesterol Content In The Presence Of Mevinolin

It was previously observed that mevinolin (statin) treatment triggered a decrease in SNX8 expression levels in neurons (**Figure 4.9**). To further investigate the relationship between SNX8 and cholesterol in low cholesterol levels neurons were transfected with GFP-SNX8 lentivirus for 48 hours then treated with 0.25 μM mevinolin for 24 hours, and the cells fixed and stained as in the previous

experiment. Filipin staining was observed to be slightly denser following SNX8 overexpression, indicating the presence of more cell processes (**Figure 4.14a and b**). However, quantification of overall fluorescence indicated there was no change in overall cholesterol levels following GFP-SNX8 overexpression (**Figure 4.14c**) (n=3, Students T-test, $p>0.05$).

4.4.13 GFP-SNX8 Overexpression Decreases Cholesterol Levels In High Cholesterol Conditions

Following the observation that SNX8 levels were unchanged in the presence of excess cholesterol (**Figure 4.8**), whereas expression was decreased after both mevinolin and U18666a treatment (**Figures 4.9 and 4.10**), it remained to be investigated whether SNX8 overexpression could alter cholesterol levels in the presence of excess cholesterol. Neuronal cultures were transfected with GFP-SNX8 lentivirus. After two days the cells were then treated with 2 µg/ml 25-OH cholesterol for 24 hours, then fixed and stained as in previous Filipin experiments. Filipin staining revealed changes in cholesterol localisation following GFP-SNX8 transfection; cholesterol localisation was found to be punctuate, similar to a U18666a mediated phenotype (**Figure 4.15a and b**). Overall fluorescence levels were seen to decrease following GFP-SNX8 transfection, indicating SNX8 overexpression stimulates a decrease in unesterified cholesterol levels in the presence of excess cholesterol (**Figure 4.15c**). n=3, Students-t-test $p<0.05$).

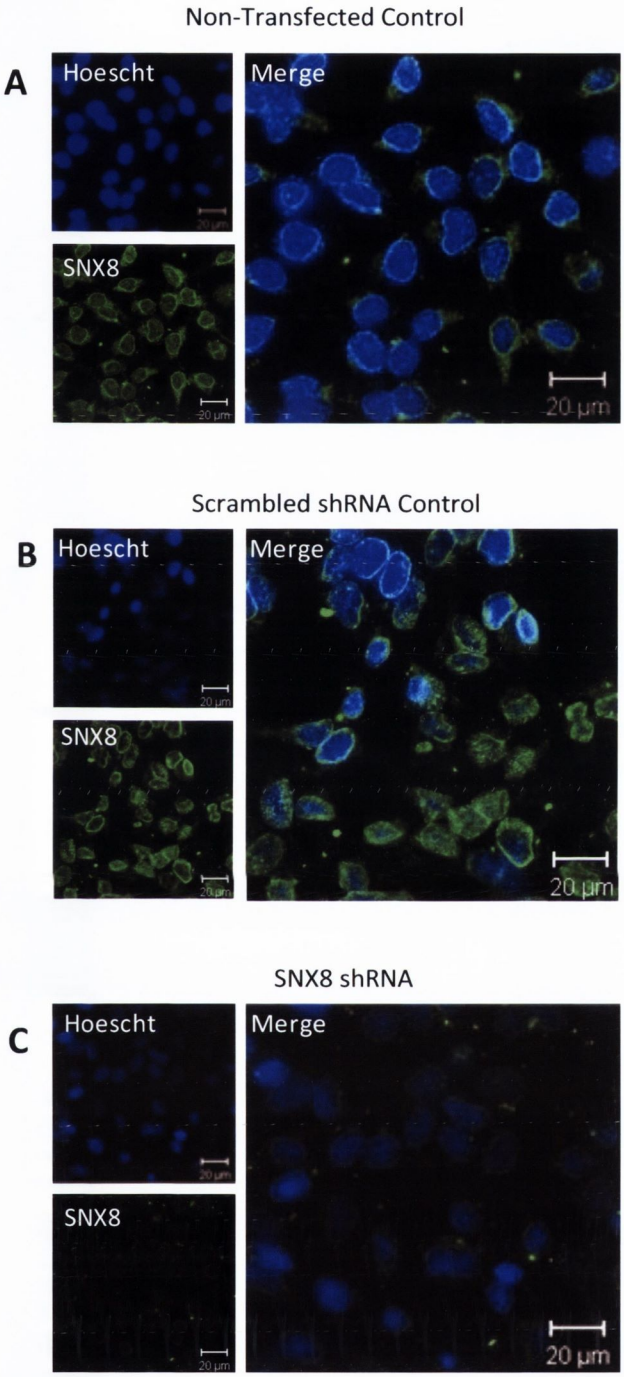

FIGURE 4.2. SHRNA INTERFERENCE OF SNX8 EXPRESSION IN HEK 293T CELLS. A SNX8 is expressed endogenously in HEK 293T cells, and can be seen to be localised throughout the cell. **B** Transfection of a shRNA plasmid containing a scrambled DNA sequence as a control did not affect SNX8 expression. **C.** Transfection of a plasmid containing shRNA targeted to SNX8 caused a decrease in SNX8 expression.

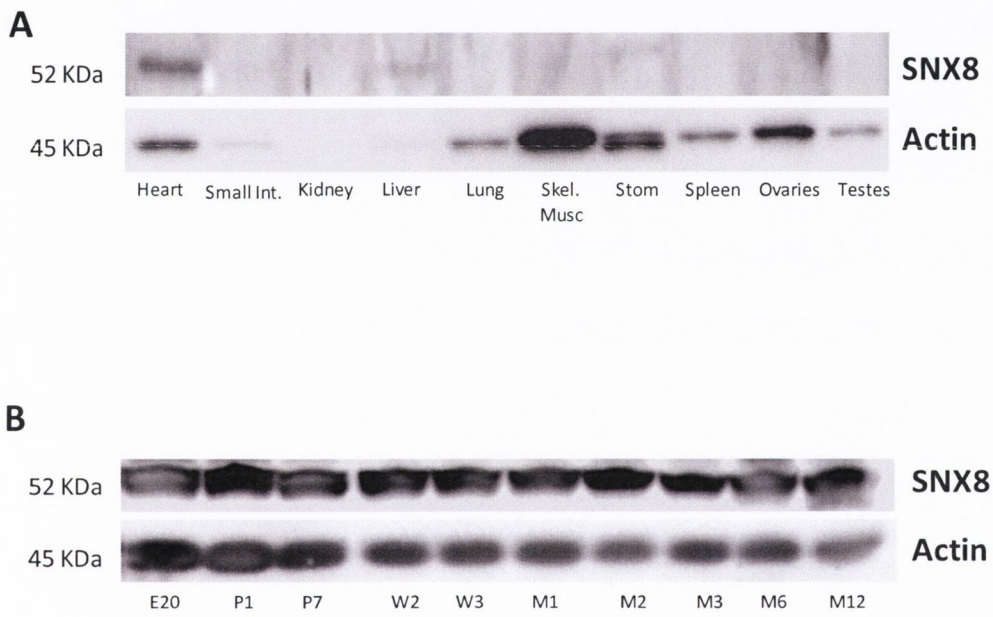

FIGURE 4.3. WESTERN BLOT OF SNX8 EXPRESSION PROFILE. A. Western blot of SNX8 expression in different rat body tissue types. The membrane was probed with SNX8 primary antibody, a faint SNX8 signal can be seen in the heart and liver tissues. The membrane was then stripped and re-probed with actin antibody. The actin signal shows protein levels were not standardised as claimed by the company. **B.** Western blot of SNX8 expression in different aged rat brain samples (embryonic day 20, postnatal day 1 and 7, weeks 2 and 3, months 1, 2, 3, 6 and 12). SNX8 protein was seen to be highly expressed at all stages of development.

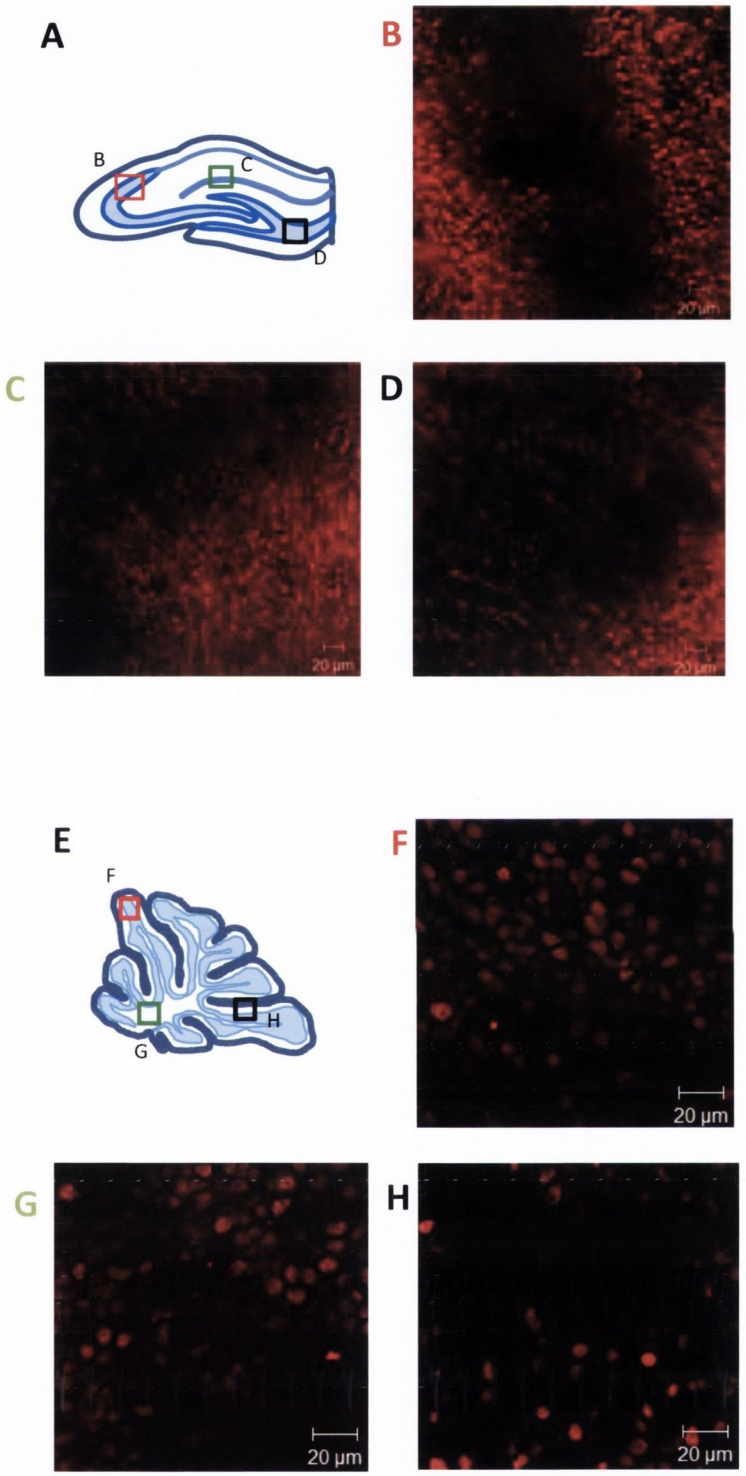

FIGURE 4.4. HIPPOCAMPAL AND CEREBELLAR SLICE STAINING. **A** Schematic diagram of hippocampal slice, showing the regions of images B-D. **B-D.** Staining with SNX8 antibody reveals that the protein is present in both the cell bodies and processes of cells throughout all regions of the hippocampus. **E** Schematic diagram of cerebellar slice, showing the regions of images E-H. **E-H.** Unlike the hippocampal staining, in the cerebellum SNX8 expression is more concentrated in the cell bodies and less so in the processes of the cells in this region.

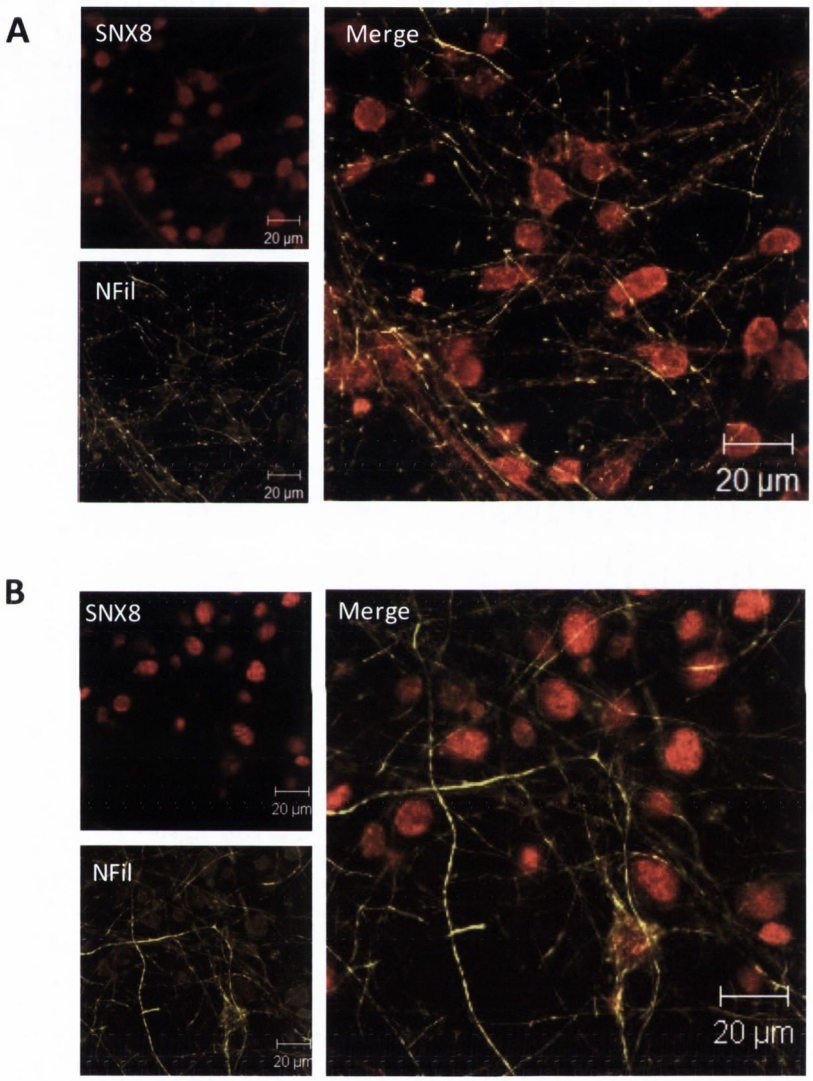

FIGURE 4.5. HIPPOCAMPAL AND CEREBELLAR DISSOCIATED CULTURE STAINING. A. SNX8 and neurofillament staining are shown in the smaller panels. In the larger panel SNX8 staining overlaps with the neurofillament staining showing SNX8 is present in hippocampal neurons, both in the cell body and in the processes. **B.** Staining of cerebellar dissociated cultures with SNX8 and neurofillament primary antibodies shows SNX8 antibody is present primarily in cell bodies, with no staining visible in the axons or dendrites.

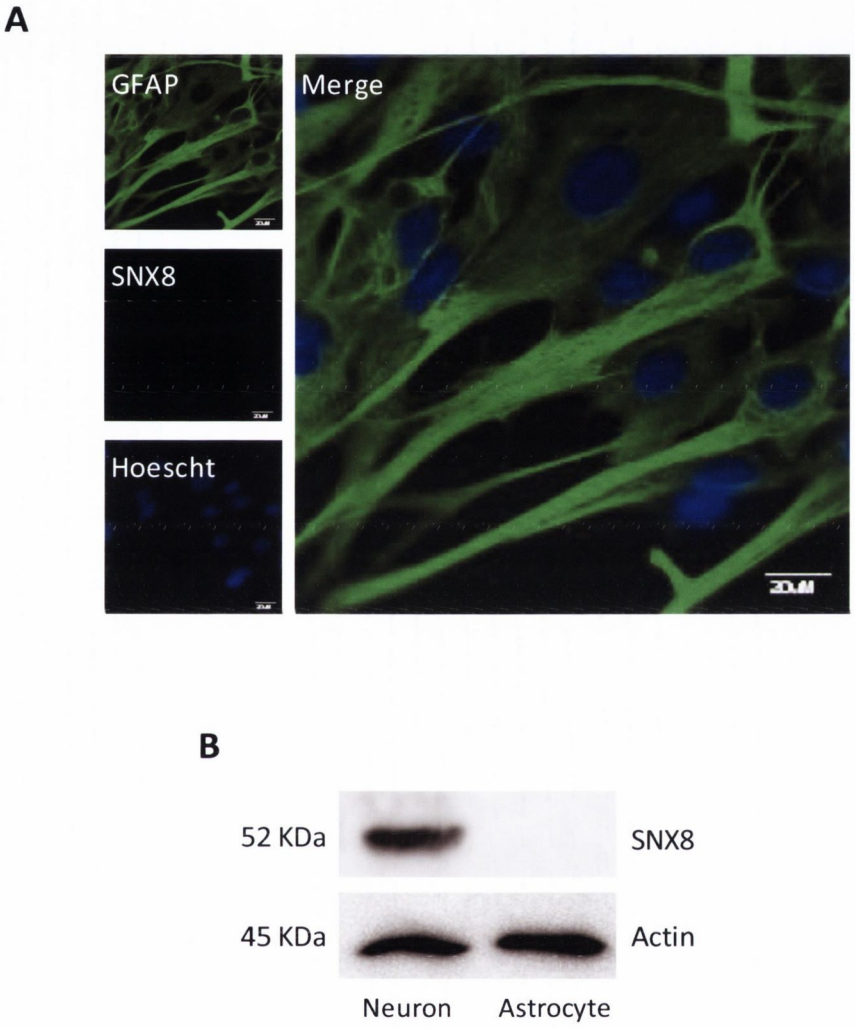

FIGURE 4.6. ASTROCYTES DO NOT EXPRESS SNX8. **A.** No SNX8 staining was observed in pure astocyte cultures, stained with GFAP as a cellular marker for astrocytes, SNX8 antibody and hoescht to identify cell nuclei. **B**. Western blot showing neuron (as positive control) and enriched astrocyte cell lysates probed with SNX8 antibody. No signal in the astrocyte sample identifies SNX8 is not expressed in this cell type.

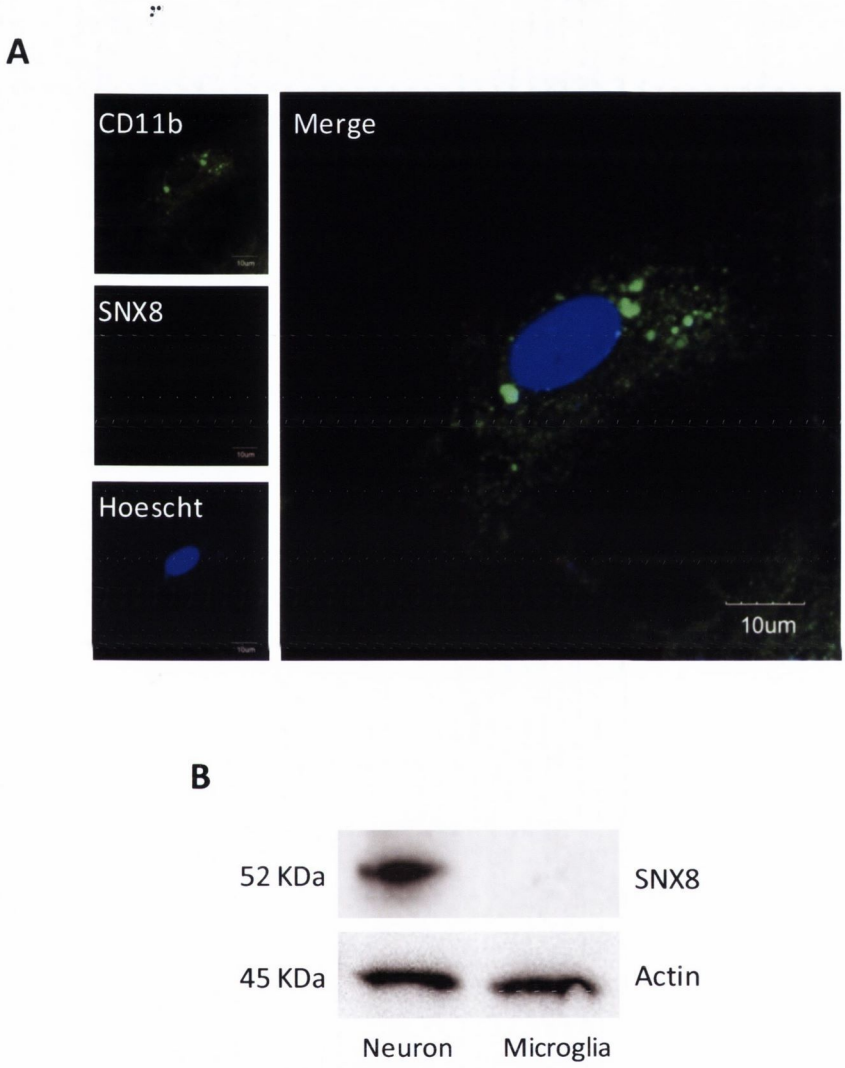

FIGURE 4.7. MICROGLIA DO NOT EXPRESS SNX8. A. No SNX8 staining was observed in microglia, stained with CD11b as a cellular marker for microglia, SNX8 antibody and hoescht to identify cell nuclei. **B.** Western blot showing neuron (as positive control) and microglia cell lysates probed with SNX8 antibody. No signal in the microglia sample identifies SNX8 is not expressed in this cell type.

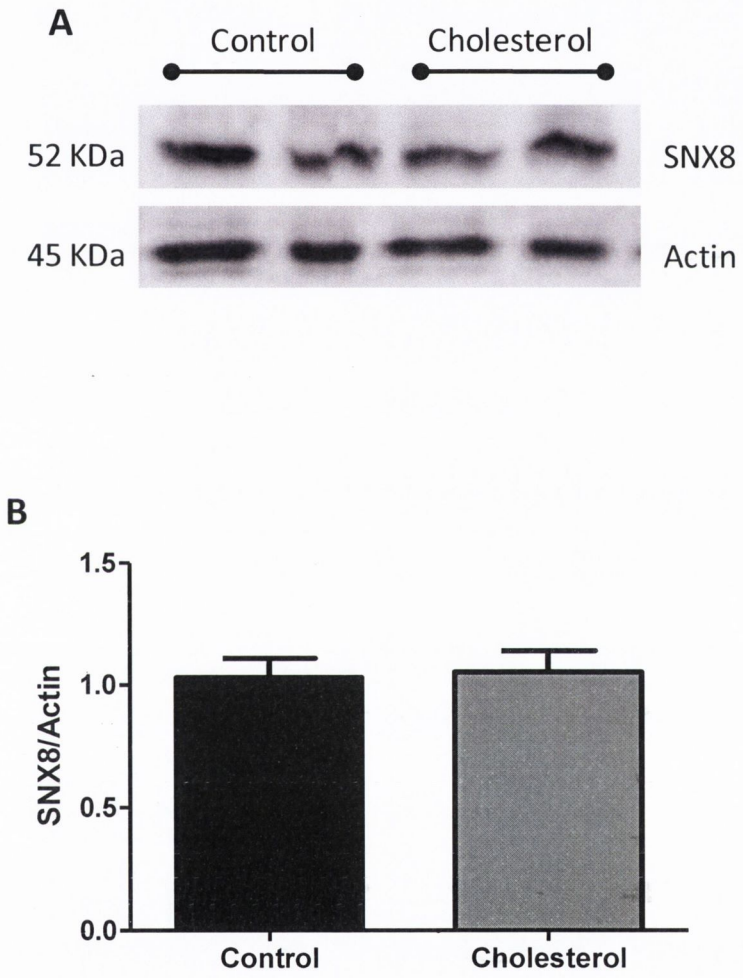

FIGURE 4.8. EXCESS CHOLESTEROL DOES NOT CHANGE SNX8 EXPRESSION IN NEURONS. A. Representative western blot showing neuronal culture lysate probed with SNX8 antibody and actin as a loading control. Neurons were treated with 2 µg/ml 25-OH cholesterol for 24 hours. **B.** Quantification of n=5 western blots showed no significant change in SNX8 expression in high cholesterol conditions (n=5, Students T-test $p>0.05$).

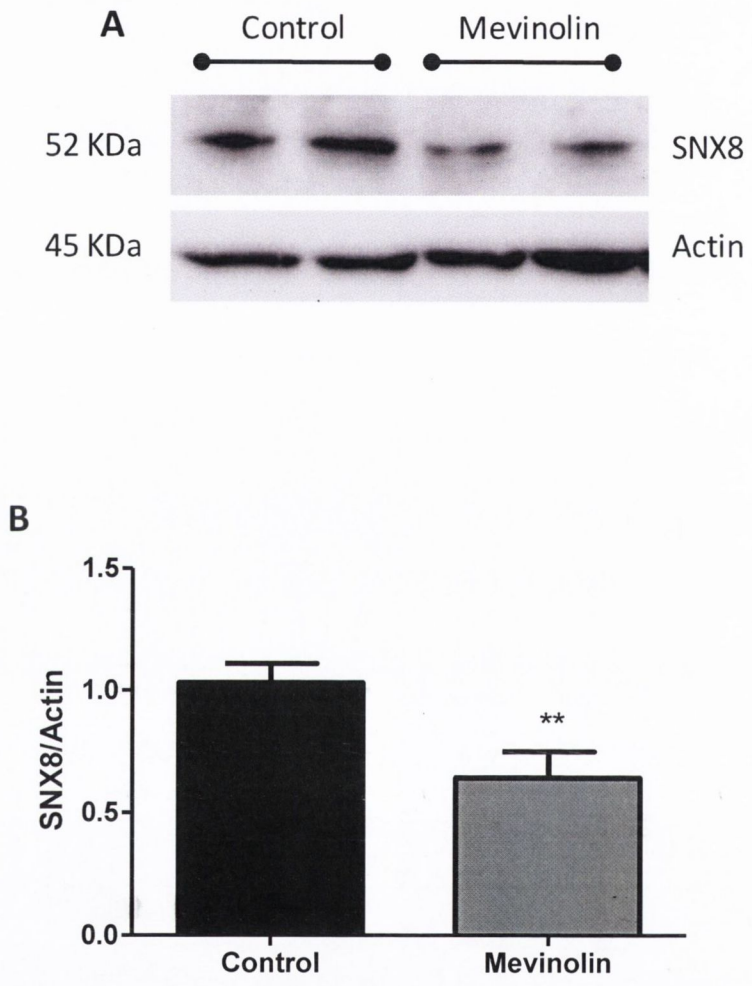

FIGURE 4.9. MEVINOLIN; A STATIN CAUSES DECREASED SNX8 EXPRESSION IN NEURONS. A. Representative western blot showing neuronal culture lysate probed with SNX8 antibody and actin as a loading control. Neurons were treated with 0.25 μM mevinolin for 24 hours. **B.** Quantification of n=5 western blots showed a significant decrease in SNX8 expression in low cholesterol conditions (n=5, Students T-test $p<0.01$).

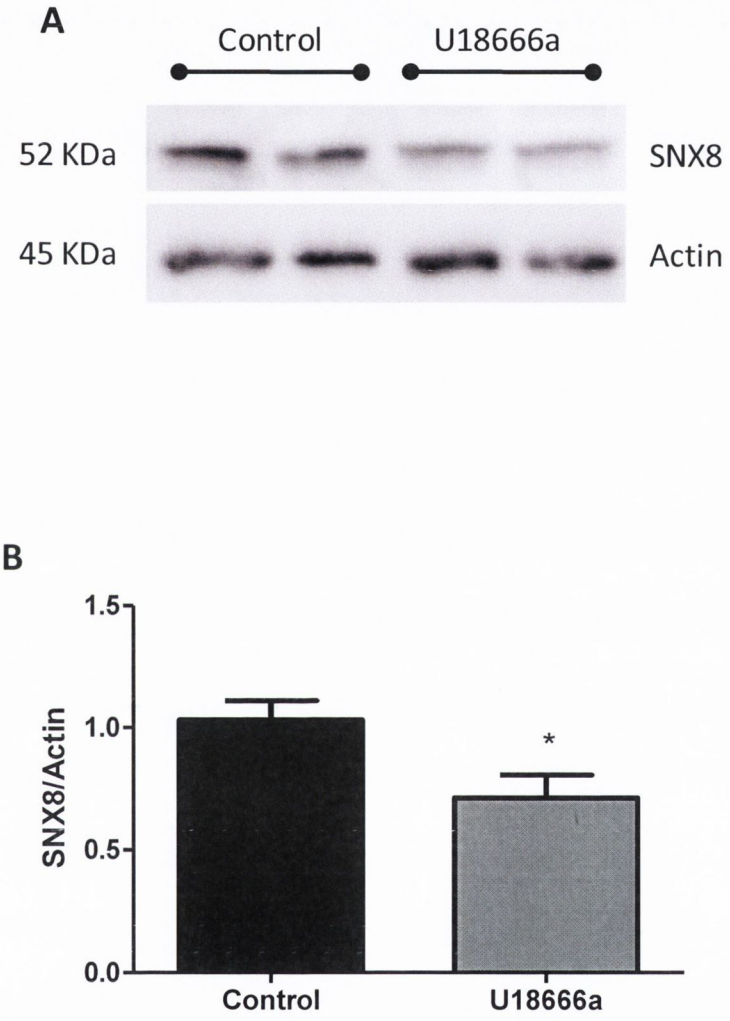

FIGURE 4.10. U18666A TREATMENT CAUSES A DECREASE IN SNX8 EXPRESSION IN NEURONS A. Representative western blot showing neuronal culture lysate probed with SNX8 antibody and actin as a loading control. Neurons were treated with 1 µg/ml U18666a for 24 hours. **B.** Quantification of n=5 western blots showed no significant change in SNX8 expression in an NPC like state (n=5, Students T-test $p>0.05$).

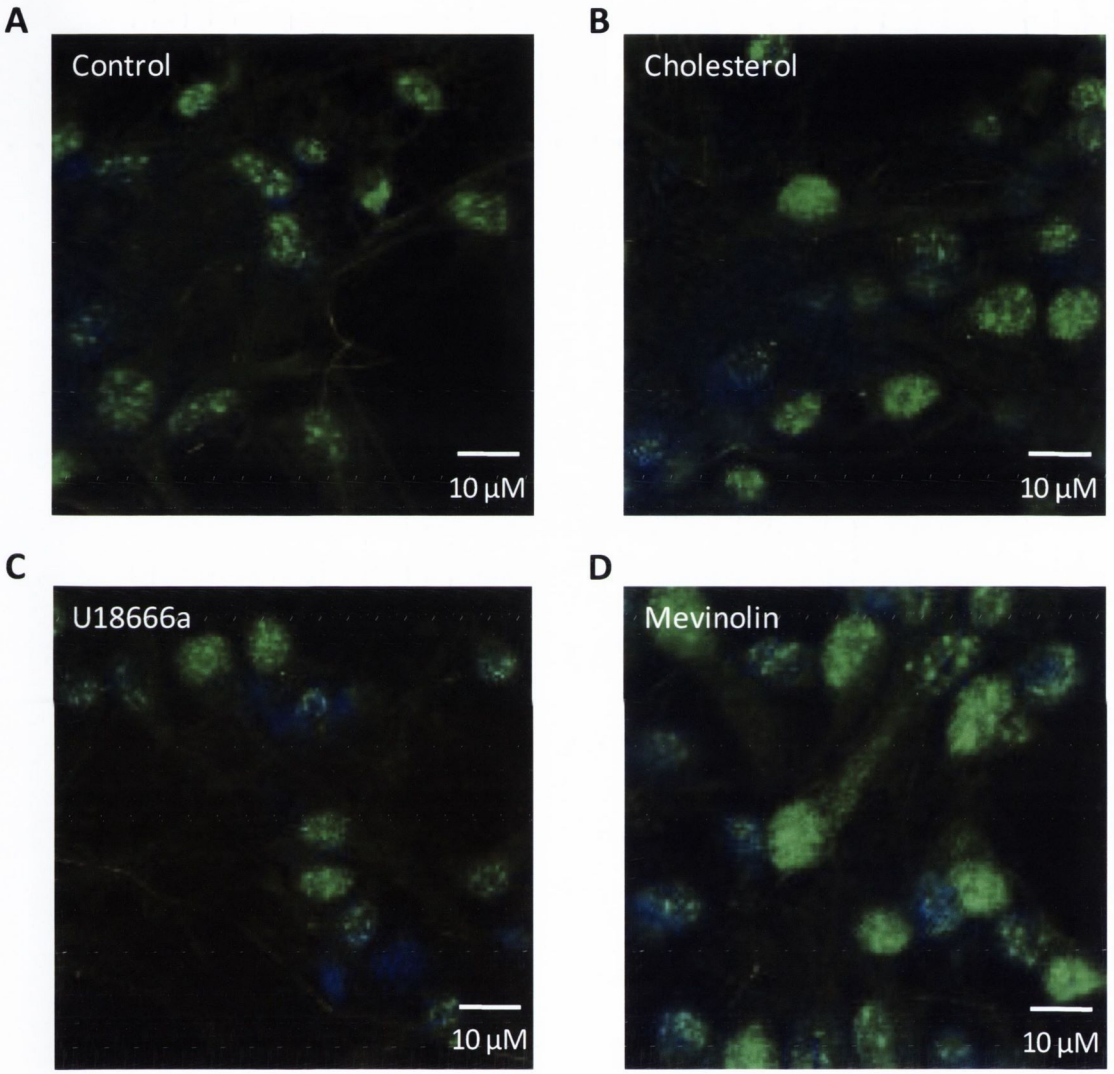

FIGURE 4.11. GFP-SNX8 LOCALISATION IS NOT ALTERED IN DIFFERING CHOLESTEROL ENVIRONMENTS. A. Neuronal culture transfected with GFP-SNX8 lentivirus, and stained with hoescht to detect nuclei. GFP-SNX8 can be observed in punctuate expression within the soma **B-D.** As in control neurons were transfected with GFP-SNX8 lentivirus then treated with either 2 µg/ml 25-OH cholesterol, 1 µg/ml U18666a or 0.25 µM mevinolin for 24 hours. GFP-SNX8 localisation is again punctuate and focused around the soma in all conditions.

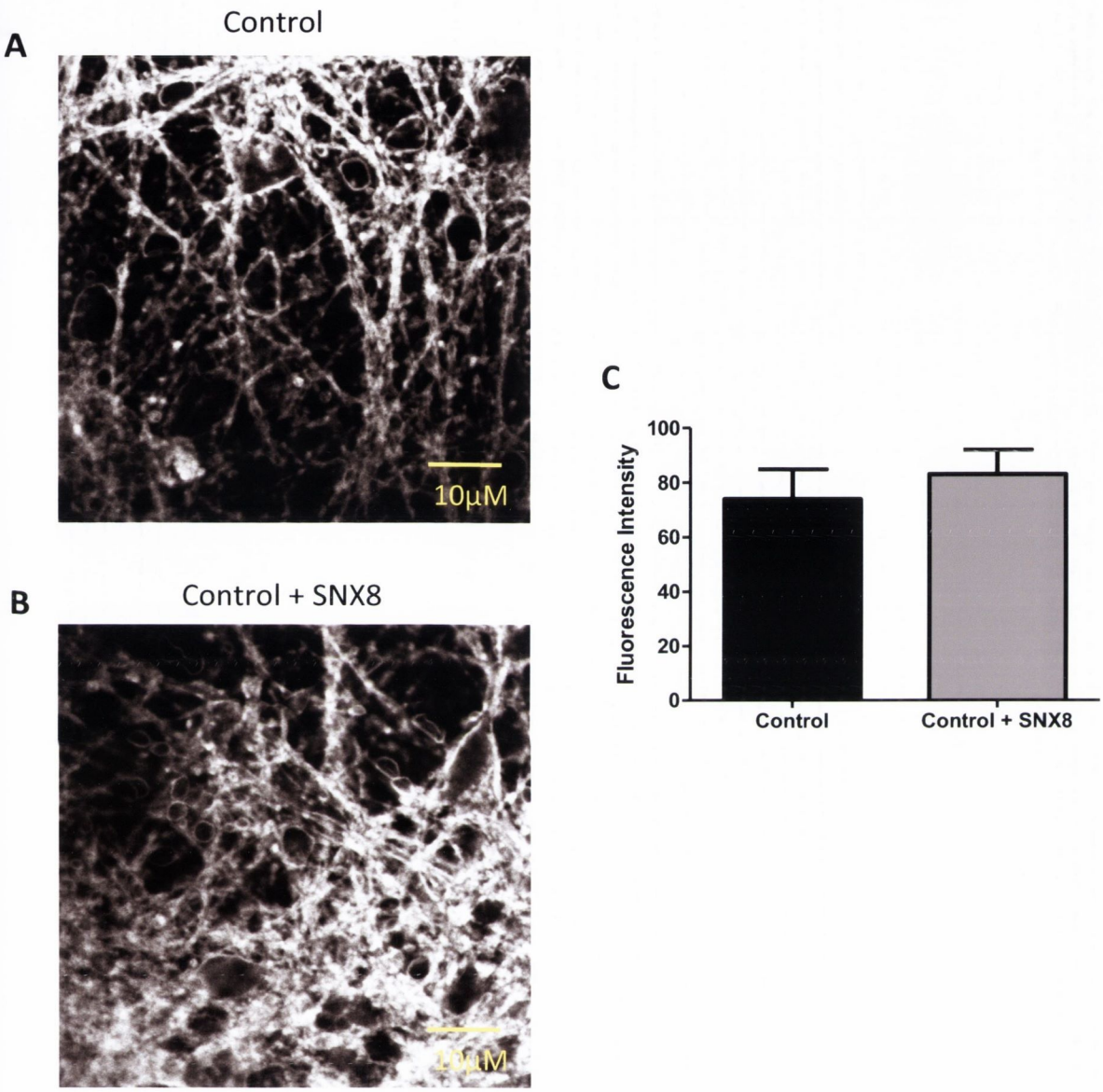

FIGURE 4.12. GFP-SNX8 TRANSFECTION DOES NOT AFFECT CHOLESTEROL LEVELS UNDER NORMAL CONDITIONS. **A.** Neuronal cultures were fixed and stained with Filipin III to detect unesterified cholesterol levels. **B.** Neuronal cultures were transfected with GFP-SNX8 lentivirus for 2 days, fixed and stained with Filipin. SNX8 transfection does not alter cholesterol levels or localization. **C.** Overall fluorescence was quantified for each image, the average was plotted. There was no difference in overall fluorescence and therefore cholesterol levels following SNX8 lenti transfection under physiological conditions. (n=3, Students T-test, $p>0.05$).

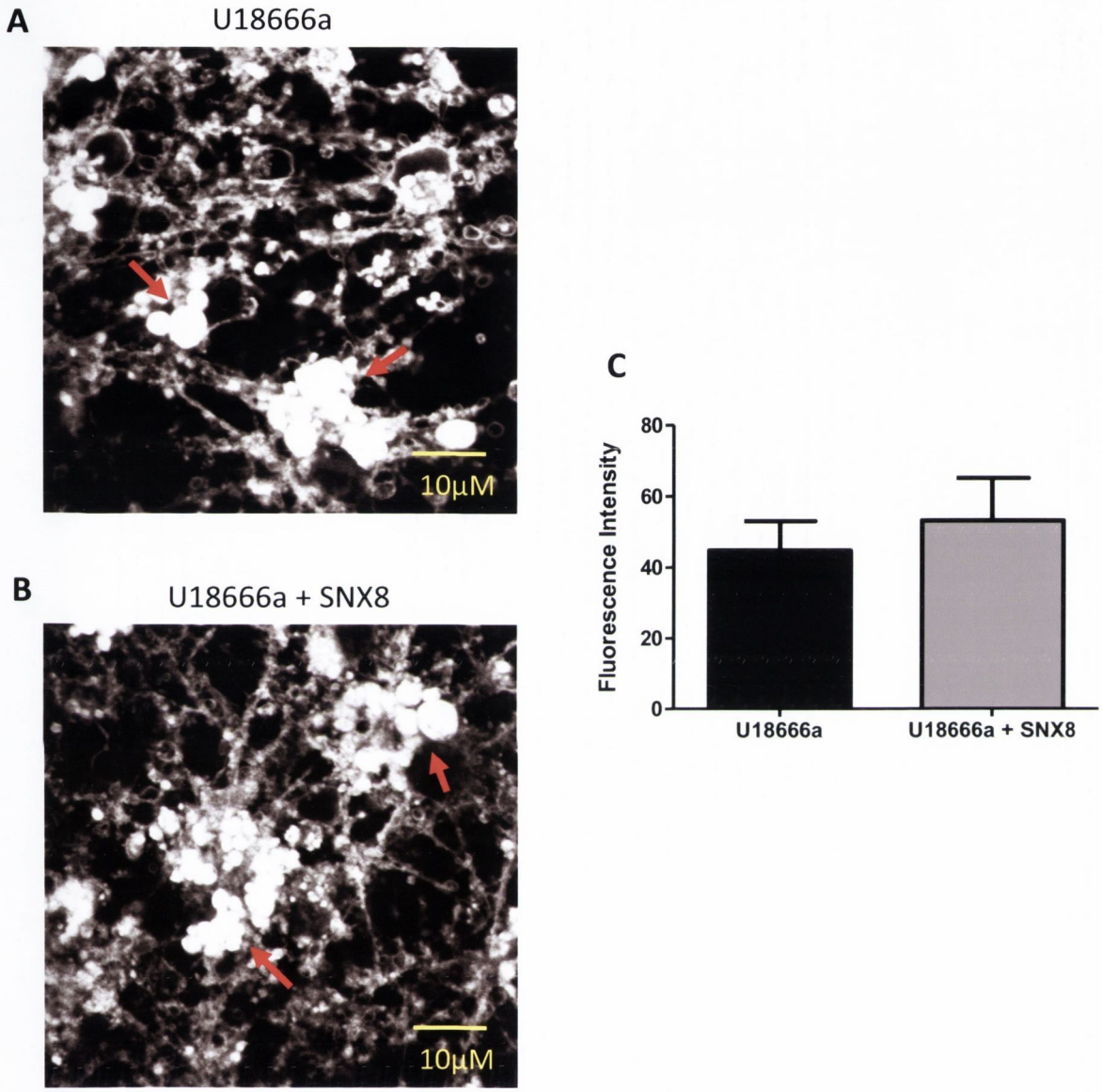

FIGURE 4.13. U18666A MEDIATED CHOLESTEROL ACCUMULATION IS NOT ALTERED BY SNX8 OVEREXPRESSION. A. Neuronal cultures were treated with 1μg/ml U18666a fixed and stained with Filipin **B.** Neuronal cultures were transfected with GFP-SNX8 lentivirus for 2 days, on day 3 cells were treated with 1μg/ml U18666a for 24 hours, fixed and stained with Filipin. SNX8 transfection does not alter the accumulation of cholesterol, indicated by arrows. **C.** Overall fluorescence was quantified for each image, the average fluorescence for all experiments was plotted. There was no difference in overall fluorescence and therefore cholesterol levels following SNX8 lenti transfection. (n=3, Students T-test, $p>0.05$).

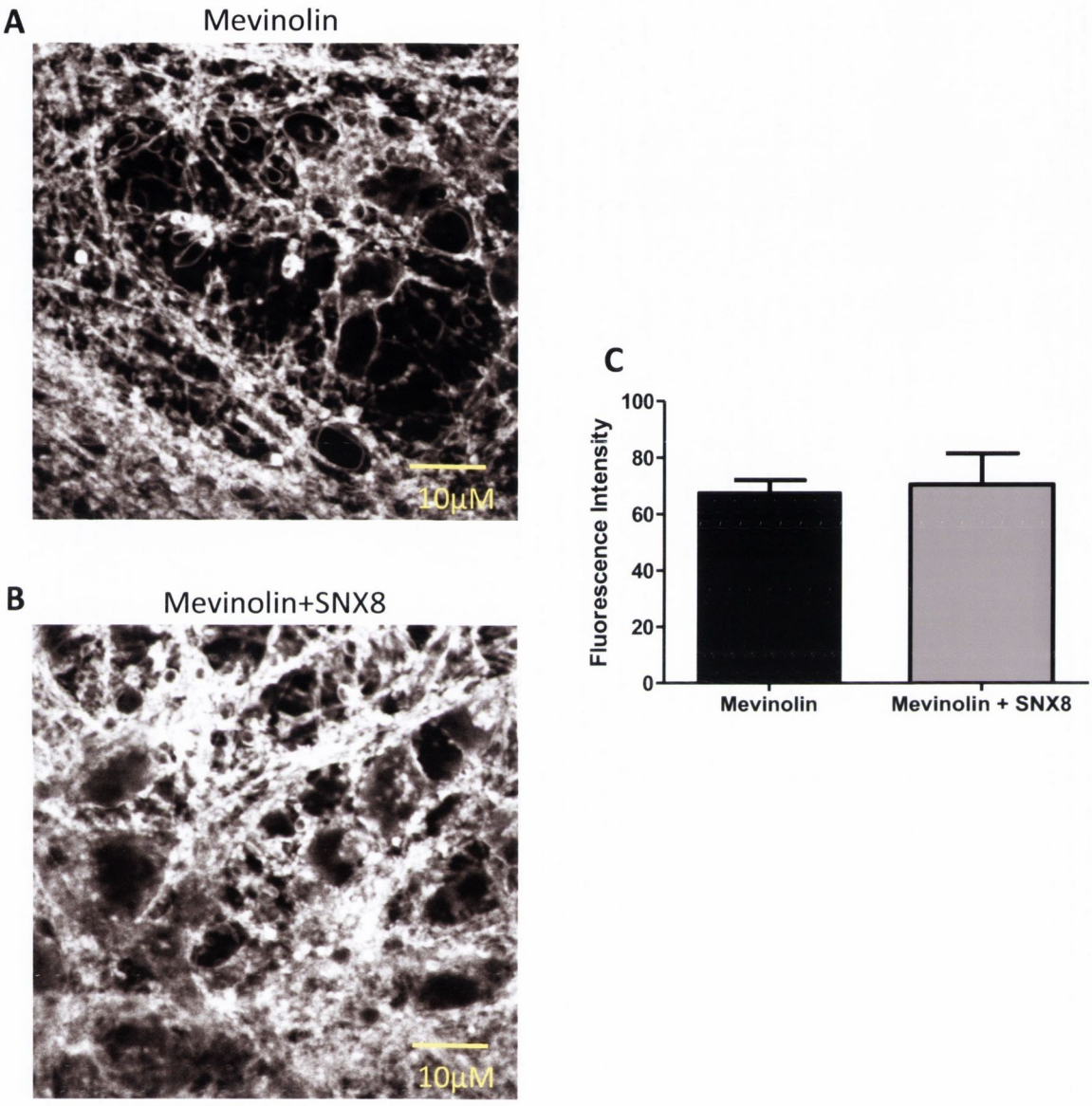

FIGURE 4.14. IN A LOW CHOLESTEROL ENVIRONMENT SNX8 OVEREXPRESSION DOES NOT ALTER CHOLESTEROL LEVELS **A.** Neuronal cultures were treated with 0.25μM mevinolin, fixed and stained with Filipin **B.** Neuronal cultures were transfected with GFP-SNX8 lentivirus for 2 days, on day 3 cells were treated with the same mevinolin dose for 24 hours, fixed and stained with Filipin. SNX8 transfection does not alter cholesterol positioning. **C.** Overall fluorescence was quantified for each image, the average fluorescence for all experiments was plotted. There was no difference in overall fluorescence and therefore cholesterol levels following SNX8 lenti transfection in low cholesterol conditions. (n=3, Students T-test, $p>0.05$).

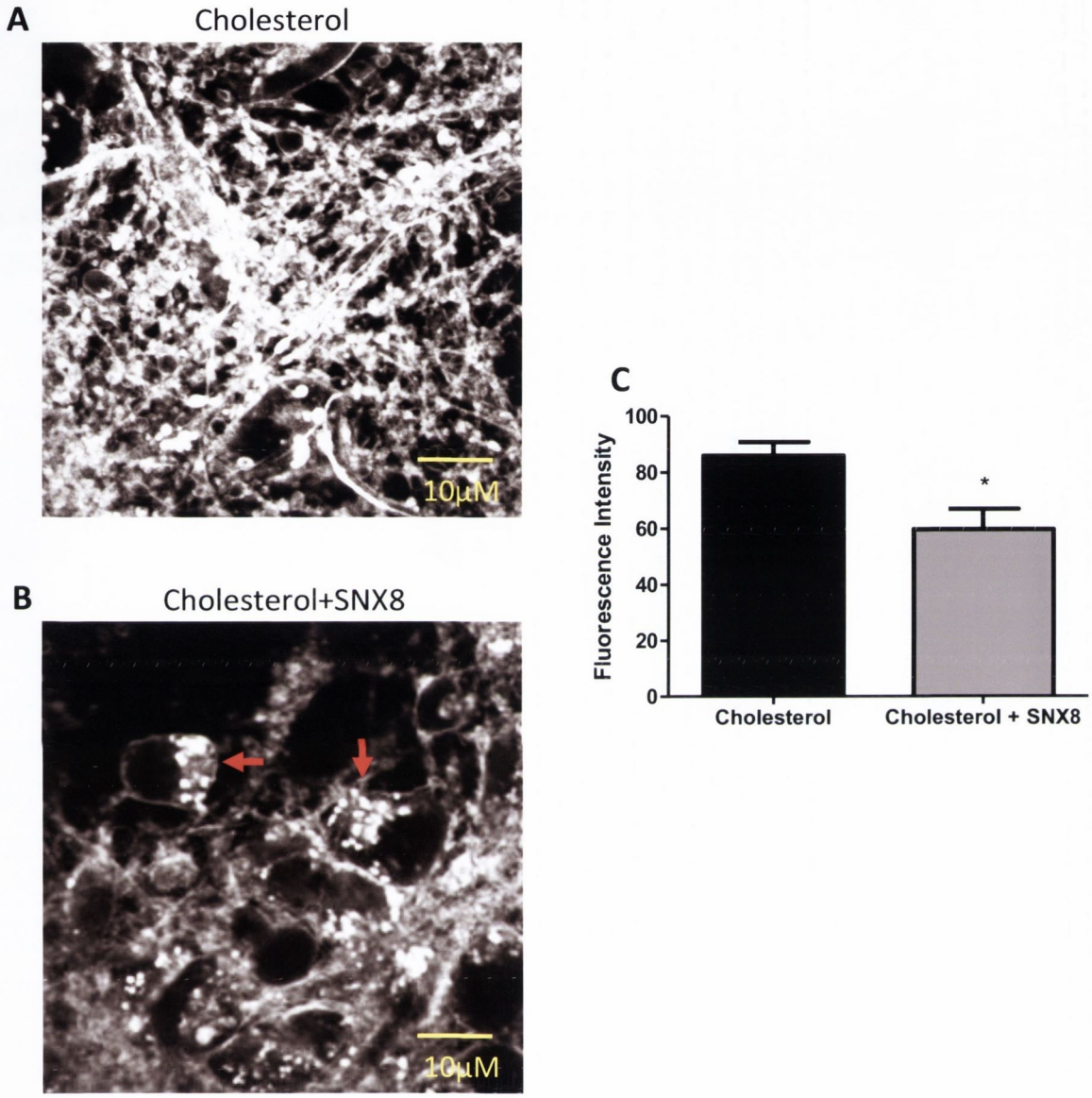

FIGURE 4.15. SNX8 OVEREXPRESSION ALTERS CHOLESTEROL LOCALISATION IN A HIGH CHOLESTEROL ENVIRONMENT A. Neuronal cultures were treated with 2μg/ml 25-OH cholesterol for 24 hours, fixed and stained with Filipin **B.** Neuronal cultures were transfected with GFP-SNX8 lentivirus for 2 days, on day 3 the same cholesterol treatment was applied. SNX8 transfection altered cholesterol positioning, with punctuate structures observed (indicated by arrows) **C.** Overall fluorescence was quantified for each image, the average fluorescence for all experiments was plotted. There was a significant decrease in overall fluorescence following SNX8 transfection indicating a decrease in cholesterol levels (n=3, students t-test, $p<0.05$).

4.5.0 Discussion

4.5.1 SNX8 Is Widely Expressed Within The Rat CNS

In order to further investigate the role of SNX8 in neuronal function and regulation of cholesterol/SREBP pathway, we initially examined the expression of SNX8. Firstly, to validate the specificity of the SNX8 antibody, shRNA directed against SNX8 was used in HEK 293T cells which were found to endogenously express SNX8. The transfection of the shRNA plasmid was found to decrease the immunostaining of SNX8 in HEK 293T cells, confirming the specificity of the antibody. Next, the expression profile of SNX8 was investigated within the body. Commercial blots were purchased that contained lysates from different rat organs (heart, small intestine, kidney, liver, lung, skeletal muscle, stomach, spleen, ovaries and testes). The membrane was probed with SNX8 primary antibody to detect the presence of SNX8 in the different tissue types. Whilst the actin levels showed non-standardised protein loading the SNX8 signal was detected in the heart and liver. When comparing the band intensities with actin, it appears that SNX8 is likely highly expressed in the liver and moderately in the heart. The high expression of SNX8 in the liver may be related to its role in cholesterol/SREBP pathway, where the liver is the major organ in cholesterol synthesis. The expression of SNX8 within the brain was next investigated. A commercial blot containing brain tissue lysates from varying aged rats (embryonic day 20, postnatal day 1 and 7, weeks 2 and 3, months 1, 2, 3, 6 and 12) was probed with SNX8 primary antibody and SNX8 protein expression was found throughout development, in the brain of embryos (E20) through to fully grown adult rats (12 months). In conclusion, this data may indicate that SNX8 expression is essential for brain function and/or development, or neuronal function, like its family members SNX9 and SNX18 (Nakazawa et al., 2011; Shin et al., 2007).

4.5.2 Differential Expression Of SNX8 In Neuronal Subsets

As SNX8 was found to be expressed in whole brain tissue, the regions and cell types of the brain were then investigated for the presence of SNX8. Hippocampal and cerebellar slice cultures were stained with SNX8 primary antibody. The staining revealed differences in SNX8 distribution within the two regions. In the cerebellum SNX8 expression was restricted to the cell body; comparatively in the hippocampus SNX8 was present both in the cell body and the processes. The staining of dissociated hippocampal and cerebellar neurons allowed further investigation of this difference in expression. SNX8 expression was visible throughout hippocampal neurons but was concentrated in

the cell bodies of cerebellar neurons. The differential localisation of SNX8 within these two subsets of neurons indicates a possible variance in the function of SNX8. Myelination of axons within the cerebellum is closely linked to cholesterol homeostasis where SNX8 may somehow modulate cholesterol homeostasis in the cerebellum. Indeed, cerebellar atrophy, in particular degeneration of purkinje neurons and demyelination of the corpus collosum occurs in NPC disease, possibly indicating differential susceptibility of neuronal subsets to cholesterol dysfunction (Higashi et al., 1993). How exactly the accumulation of cholesterol within the lysosomes of cells leads to this phenotype is yet to be elucidated.

4.5.3 SNX8 Expression Is Restricted To Neurons, Not Glia

Immunostaining of astrocyte and microglia alongside western blotting data showed SNX8 was not present in these glial cells. This data corresponds with the finding that the SNX^{PX} family member SNX12 was found to be expressed in cerebral cortex neurons, but not glia (Mizutani et al., 2012). The fact that these sorting nexins are differentially expressed in CNS cell types indicates they perform neuronal specific functions, such as synaptic vesicle endocytosis or exocytosis. SNX12 was found to be upregulated during development and be concentrated in post mitotic neurons, as well as stimulating neurite outgrowth (Mizutani et al., 2012). Our data does not show SNX8 is developmentally upregulated, but it does appear to have a neuronal restriced expression pattern in these mixed cultures indicating like SNX12, SNX8 may perform neuronal specific functions.

4.5.4 SNX8 Expression Is Reduced In Low Cholesterol Environments

Excess cholesterol conditions were found to have no effect on SNX8 expression levels as discovered by western blotting. However, treatment with both mevinolin and U18666a were found decrease SNX8 expression within neurons. These findings indicate a differential regulation of SNX8 with the interaction between SNX8 mevinolin and U18666a versus cholesterol. U18666a acts to cause the accumulation of cholesterol within the endosomal, lysosomal pathway (Cenedella, 1980). The sterol sensor for the cholesterol homeostasis is present in the endoplasmic reticulum, thus the cell cannot sense the build up of cholesterol and continues to signal to produce more (Cenedella, 2009). Mevinolin, a statin, works to lower intracellular cholesterol by inhibiting HMG CoA reductase, the rate limiting enzyme in the pathway of cholesterol synthesis. Thus both U18666a and mevinolin act to cause "low" cholesterol conditions within the cytoplasm. This decrease in cholesterol down regulates the expression of SNX8. SNX8 was previously found to overcome the Insig mediated block

of the SREBP pathway of cholesterol homeostasis, and was identified as a positive modulator of this pathway (Chatterjee et al., 2009). Therefore, the decrease in SNX8 would decrease the cleavage of SREBP, which in turn reduces the transcription of SRE genes, resulting in overall reduction in cholesterol production within the cell. SNX8 levels are unchanged in the presence of excess cholesterol; therefore it is possible SNX8 may be at its maximal expression in this condition. It is known that low cholesterol conditions cause apoptosis in neurons (Park et al., 2009). It is possible that the initial stages of apoptosis may stop the transcription and translation of SNX8. Analysis of apoptotic markers alongside SNX8 protein levels would allow for the correlation of these two processes.

4.5.5 SNX8 Overexpression Alters Cholesterol Localisation

In order to fully investigate the role of SNX8 in cholesterol homeostasis within neurons, the GFP-SNX8 lentivirus generated was utilised. Neurons were cultured and transfected with the lentivirus. Following this, cells were treated with either U18666a, mevinolin or 25-OH cholesterol thus generating four different cholesterol environments (accumulated cholesterol, low cholesterol, high cholesterol, and physiological cholesterol). Firstly, it was found SNX8 overexpression had no effect on unesterified cholesterol levels or localisation under physiological cholesterol conditions. This finding was mimicked in both U18666a treated and mevinolin treated neurons. However, in high cholesterol levels GFP-SNX8 overexpression was found to decrease Filipin staining and cause an accumulation of cholesterol within cells, much to the effect of U18666a treatment. As SNX8 has been identified as an activator of the SREBP pathway it was hypothesised that overexpression of the protein would cause an increase in cholesterol levels which was not observed in any cholesterol condition (Chatterjee et al., 2009). The observation that SNX8 overexpression can change cholesterol distribution may be better attributed to its role as a sorting protein, rather than its direct effects on the SREBP pathway. As previously discussed SNX8 knockdown was found to alter the retrograde transport of ricin and shiga toxin (Dyve et al., 2009). This differential trafficking was deemed to be due to the function of SNX8 in endosomal sorting via the retrograde pathway as SNX8 was found to be colocalised with both components. It may be hypothesised that the increase in cholesterol levels triggers a change in SNX8 sorting capabilities, and with SNX8 overexpression cholesterol becomes accumulated in lysosomes when present at high levels. This would explain why the accumulated cholesterol looks to be very similar to U18666a treated neurons. Real time imaging of movement of the GFP tagged SNX8 following differing cholesterol altering treatments would allow characterisation of the movement of SNX8, allowing the visualisation of any changes in trafficking.

CHAPTER 5. INVESTIGATING THE CHEMOKINE PROFILE OF U18666A TREATMENT

5.1.0 AIMS AND HYPOTHESIS

- Characterise the cellular composition of mixed cortical cultures
- Confirm the cholesterol accumulating actions of U18666a
- Identify changes in cytokine and chemokine levels from neurons following treatment with U18666a
- Investigate the specific changes in LIX levels following U18666a treatment
- Investigate chemokine synthesis and release in various cholesterol conditions
- Elucidate the mechanism underlying cholesterol mediated chemokine release

In this chapter the effects of U18666a on cytokine/chemokine levels were examined. The working hypothesis is that U18666a induces an NPC phenotype *in vitro* and these conditions result in a pro-inflammatory response which would result in the neurodegenerative events seen in NPC disease. The work suggests that targeting the pro-inflammatory response in NPC disease may be of potential therapeutic benefit in NPC disease.

5.2.0 ABSTRACT

Niemann Pick Disease Type C (NPC) is a fatal, autosomal recessive neurodegenerative disease, caused by mutations in either NPC1 or NPC2 proteins. Mutation of these proteins causes the accumulation of lipids (particularly cholesterol) in lysosomal or late endosomal compartments, which in turn causes changes in morphology, function and eventually leads to cell death. It has been shown in a mouse model of NPC disease that NSAID treatment not only delayed the onset of clinical signs but significantly prolonged the lifespan of the mice, demonstrating an inflammatory aspect in disease progression. Here, we report the inflammatory profile of an *in vitro* model of NPC1 disease. Neuronal cultures were treated with the compound U18666a (widely used to mimic NPC disease) and the conditioned media used in an array to identify changes in 29 different cytokines and chemokines. RANTES, IP-10, MIP-3α, CINC-1, LIX, MIG and MIP-1α levels were all seen to be significantly increased in the NPC model. Following these initial hits, the levels of LIX were further elucidated following different timepoints and concentrations of U18666a, in both mixed cultures and astrocytes. The release of LIX from mixed cultures was seen to significantly increase after 16hrs of treatment. The amount of cell death following U18666a treatment was also quantified using propridium iodine staining. U18666a treatment caused activation of the NFκB pathway, with overall levels of IκBα decreasing and pIκBα (Ser 32) levels increasing. Widespread demyelination has been observed in the cerebellum of a murine NPC model (Loftus et al., 1997). In order to investigate whether U18666a can mimic this phenotype, cerebellar slice cultures were treated with the compound and the level of myelination quantified. U18666a was found to significantly increase demyelination in this experimental paradigm. Taken together these data suggest U18666a treatment elicits an inflammatory response from neuronal cultures, and these changes may be attributed to the inflammation observed in NPC disease.

5.3.0 INTRODUCTION

5.3.1 CYTOKINES AND CHEMOKINES ARE INVOLVED IN NEUROINFLAMMATION

Cytokines are synthesised and released by immune cells and glial cells during inflammation. More than 100 cytokines have been identified, which can be broken down into five subfamilies; interleukins, chemokines, interferons, colony-stimulating factors and growth factors and TNFs (tumour necrosis factors) (Steinke and Borish, 2006). Cytokines act by binding to their specific receptor, which can also be upregulated in cases of inflammation. Most cytokines act on kinase linked receptors, regulating phosphorylation cascades and in turn gene expression. In contrast, chemokines act on G-protein coupled receptors. Chemokines derive their name from their chemoattractant properties towards leukocytes, guiding immune cells to sites of inflammation. However the function of chemokines is not limited to chemoattraction, with some chemokines also being involved in angiogenisis and development (Volin and Koch, 2011). Chemokines are characterised by their structure, specifically the positioning of N-terminal cysteine residues. In the CC subfamily (which primarily target neutrophils) the cysteine residues are positioned next to each other. In the CXC family, the two cysteines are separated by another amino acid, these members target monocytes and T cells. Recently two smaller families have been identified; the C subfamily contain only a single cysteine residue and the only member of the CXC3 chemokines is fractalkine which has three amino acids separating the cysteine residues (Steinke and Borish, 2006). As previously mentioned chemokines act on G protein coupled receptors; CCL (CC ligand) chemokines bind to CCRs (CC receptors) and CXCL (CXC ligand) chemokines bind to CXCRs (CXCR receptors) (**Figure 5.1 and 5.2**). Any given immune cell can express multiples of these receptors, with each receptor signalling through its G-protein complex, which then triggers a variety of downstream effectors. Multiple chemokine ligands can activate one chemokine receptor. Chemokine receptors are $G\alpha_i$, with the α subunit activating Src kinases, in turn activating mitogen activated protein kinases (MAPKs) and protein kinase B (PKB) (Akira et al., 1993). The $\beta\gamma$ subunit can activate at least three separate pathways, again including the MAPKs and PKB via phosphatidylinositol 3 kinase γ (PI3Kγ). PKC is activated by both Pky-2 (protein tyrosine kinase 2 β) and phospholipase C (PLC), which induces calcium influx activating a host of cellular processes (Thelen, 2001) (**Figure 5.3**). Chemokines play an important role in disease, in particular autoimmune diseases and disorders with a prominent inflammatory component, such as psoriasis, asthma and multiple sclerosis (Flier et al., 2001; Pease, 2011; Trebst et al., 2001). This chapter focuses on the release of chemokines from mixed neuronal cultures. In particular, LIX/CXCL5 release (lipopolysaccharide induced CXC chemokine) in an *in vitro* cellular model of NPC disease.

5.3.2 The Role Of LIX (CXCL5) In Chemotaxis And Disease

ELR chemokines are members of a CXC chemokine subfamily that are potent neutrophil chemoattractants, whereas non-ELR CXC chemokines have been reported to promote angiogenesis and are poor attractors of neutrophils (Bajetto et al., 2001). ELR chemokines are characterized by a tripeptide motif (glutamic acid/leucine/arganine) at their N terminal domain. Thus far, seven ELR chemokines have been identified; growth regulated oncogene-alpha (GRO-α/CXCL1), growth regulated oncogene-beta (GRO-β/CXCL2), growth regulated oncogene-gamma (GRO-γ/CXCL3), granulocyte chemokactic protein-2 (GCP-2/CXCL6), neutrophil activating peptide-two (NAP-2/CXCL7) and LIX (lipopolysaccharide induced CXC chemokine) also known as CXCL5 or ENA-78 (epithelial-cell derived neutrophil activating peptide-78). LIX was characterised as an inducible factor following stimulation of cells with the inflammatory cytokines IL-1 and TNF-α (Chang et al., 1994). Its principal role seems to be the promotion of chemotaxis of neutrophils specifically possessing angiogenic properties. LIX elicits its effects through interaction with the CXCR2 chemokine receptor (Persson et al., 2003) (**Figure 5.2**). The CXCR2 has been found to be expressed within the CNS and its activation has been previously implicated in disorders of inflammation, myelin and oligodendroglial biology (Charo and Ransohoff, 2006). A recent study on the cuprizone induced demyelination model of MS revealed that $CXCR2^{-/-}$ mice are relatively resistant to cuprizone induced demyelination, and that $CXCR2^{+}$ neutrophils are essential for cuprizone-induced demyelination (Liu et al., 2010). This information illustrates LIX (and other CXCR2 activating chemokines) may signal the initiation demyelination.

5.3.3 The Production Of Cytokines/Chemokines Due To Toll Like Receptor Stimulation

The mechanism underlying the synthesis of cytokines/chemokines in inflammation is well established and in general involves the activation of toll like receptors. There 13 toll like receptors activated by their specific ligands. In general the activation of TLR's, for example LPS/TLR4 leads to activation of the NFκB pathway and enhanced synthesis of pro-inflammatory cytokines and chemokines. NFκB is a protein complex that influences rapid changes in DNA transcription in response to cellular stressors such as ROS, TNFα and IL-1β (Chandel et al., 2000). There are five mammalian NF-κB family members that form dimers: RelA/p65, RelB, c-Rel, p50 (NF-κB1), and p52 (NF-κB2) (Sen and Smale, 2010). In the "resting" state, NFκB dimers are held inactive in the cytoplasm through association with IκB proteins (inhibitor of κB) of which there are four forms (IκBα, IκBβ, IκBε and IκBδ and Bcl-3). Inducing stimuli such as TLR receptor activation via LPS (bacterial

lipopolysacharide) triggers activation of the IKK (IκB kinase complex). This activation leads to phosphorylation, ubiquitination, and eventual degradation of IkB proteins by the proteosome. The uncoupling of IκB reveals NLS (nuclear localisation signals) present on the NFκB dimmers, which allows the protein to translocate to the nucleus, bind specific DNA sequences called response elements (RE), and promote transcription of target genes such as pro-inflammatory cytokines (Hayden and Ghosh, 2012). NFκB signalling also promotes the production of IκB, resulting in NFκB oscillations via negative feedback (Nelson et al., 2004). NFκB is known to be constitutively active in some chronic inflammatory diseases such as asthma, atherosclerosis and arthritis (Demer and Tintut, 2011; Imanifooladi et al., 2010; Loo et al., 1998). Within the CNS, NFκB can be activated by other factors such as growth factors and glutamate resulting in NFκB activation not being restricted to immune response (Meffert et al., 2003). Within the CNS NFκB has been found to play diverse roles in learning and memory and plasticity, via modulation of dendritic outgrowth and synapse function (Boersma et al., 2011; Choi et al., 2012).

5.3.4 Neuroinflammation Has Been Implicated In Niemann Pick Type C Disease

In a mouse model of a lysosomal storage disorder (Sandhoff disease (*hexb*$^{-/-}$)) non-steroidal anti-inflammatory drugs (NSAIDS) and anti-oxidant treatment improved symptoms and increased life expectancy, even if given post-macrophage infiltration into the CNS (Jeyakumar et al., 2004). Combination therapy with NSAID and miglustat to decrease sphingolipid accumulation resulted in an even greater effect. A double knock out mouse for *hexb*$^{-/-}$ (Hexosaminidase B, a lysosomal enzyme subunit) and *MIP-1α*$^{-/-}$ showed a 30% increase in life expectancy indicating chemokine induced CNS inflammation plays a role in the disease progression (Wu and Proia, 2004). NPC disease is similar to Sandhoff disease in that it involves lysosomal dysfunction. The accumulation of sphingolipids and cholesterol within the lysosome of NPC deficient cells causes neuronal death within the CNS (Higashi et al., 1993). Some studies now show NPC disease pathology may involve aspects of neuro-inflammation. Microglial and astroglial activation is visible in many regions of the NPC mouse brain, particularly in areas undergoing neurodegeneration; in cerebellum these changes occurr prior to neuronal cell death (Baudry et al., 2003). NPC1 protein was also found to be present primarily in astrocytes in the monkey brain (Patel et al., 1999). A study to investigate beneficial effects of NSAID treatment on the progression of symptoms in a mouse model of NPC disease discovered that aspirin or ibuprofen treatment not only delayed the onset of clinical signs but significantly prolonged the lifespan of the mice. Combinational therapy of these NSAIDs and miglustat (to reduce sphingolipid storage) showed an additive effect (Smith et al., 2009).

To further support the notion that the immune system is altered in NPC disease, cultured human NPC fibroblasts were observed to secrete higher interleukin-6 (IL-6) and interleukin-8 (IL-8) levels than wild-type. Increased levels of Toll-like receptor 4 (TLR4) were found to be co-localised with accumulated cholesterol within the endosomal/lysosomal compartment and siRNA knockdown of the receptor successfully decreased cytokine release (Suzuki et al., 2007). A double knockout mouse for IL-$6^{-/-}$ and $NPC^{-/-}$ showed a decrease in STAT-3 (signal transducers and activators of transcription 3) levels back to control and also significantly reduced glial activation (Suzuki et al., 2007). Another inflammatory aspect of NPC disease was identified when members of the TNF-α death pathway were up-regulated in an NPC1 mutant mouse (BALB/c *npc*^{nih}). Caspase-8, FADD (Fas-associated protein with death domain), TNFRp55 (tumour necrosis factor receptor-55), TRADD (TNF receptor-associated death domain), and RIP (receptor interacting protein) mRNA levels were all found to be upregulated in these mice. Elevated TNF-α levels were found in both neurons and astrocytes, indicating apoptotic cell death regulated by the TNF receptor superfamily (Wu et al., 2005). The compound U18666a, which mimics an NPC phenotype in RAW 264.7 cells, has also been shown to increase TNF-α release, activation of the TNF death pathway and cause apoptosis of various cell types (Iftakhar et al., 2009). The data from these studies suggests activated glia and the inflammatory mediators they release may contribute to neuronal loss in NPC disease.

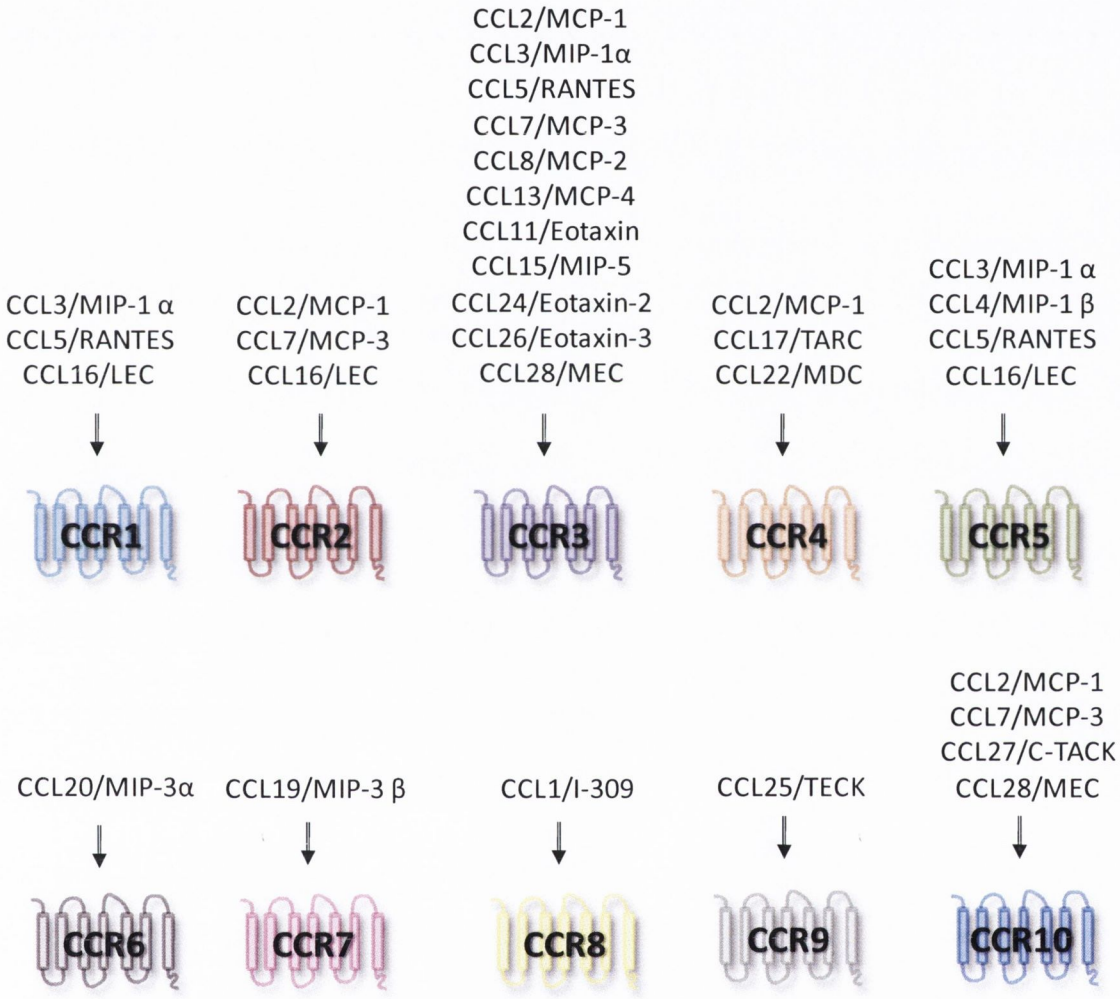

FIGURE 5.1. CC RECEPTORS AND LIGANDS. There are ten CC receptors. Multiple chemokines can bind to the same receptor and trigger intracellular responses, for example the CCR3 receptor has at least 11 known ligands, including members of the MCP and Eotaxin families. CCR6-9 however only have one known ligand as yet.

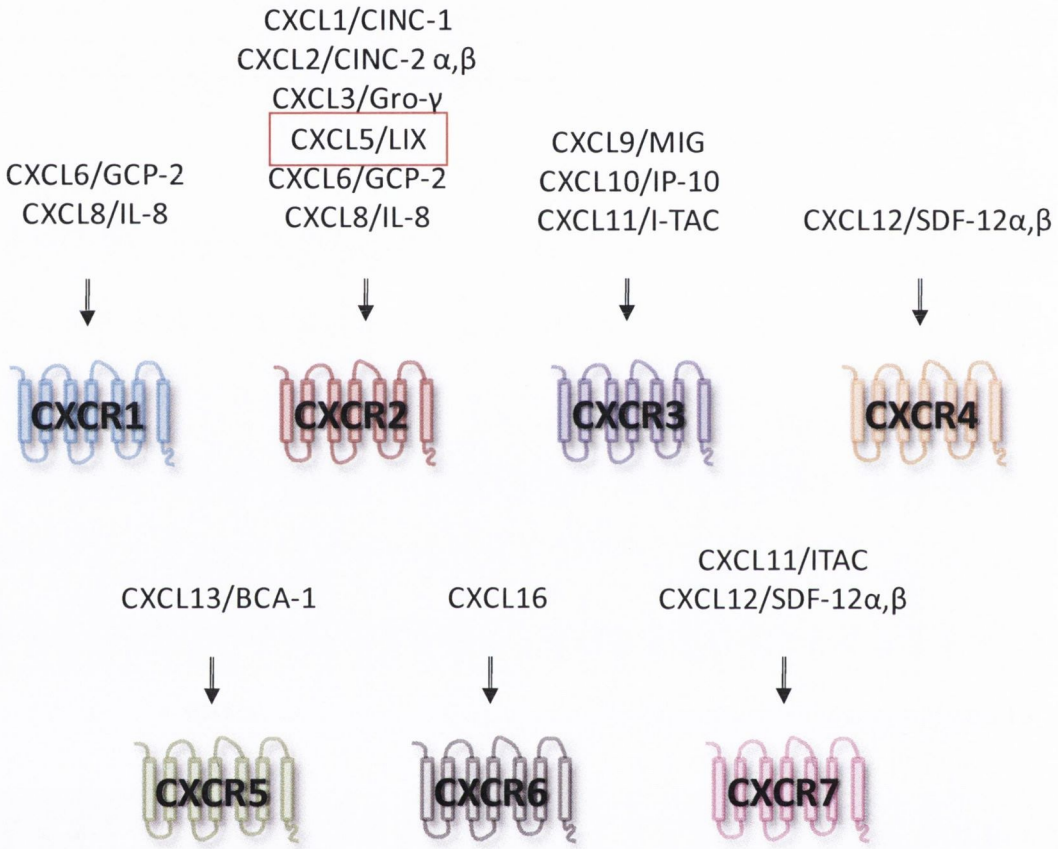

FIGURE 5.2. CXC RECEPTORS AND LIGANDS. There are seven CXC receptors. The CXCR2 receptor binds the most ligands of the CXC family of chemokines, one of these ligands is LIX (CXCL5).

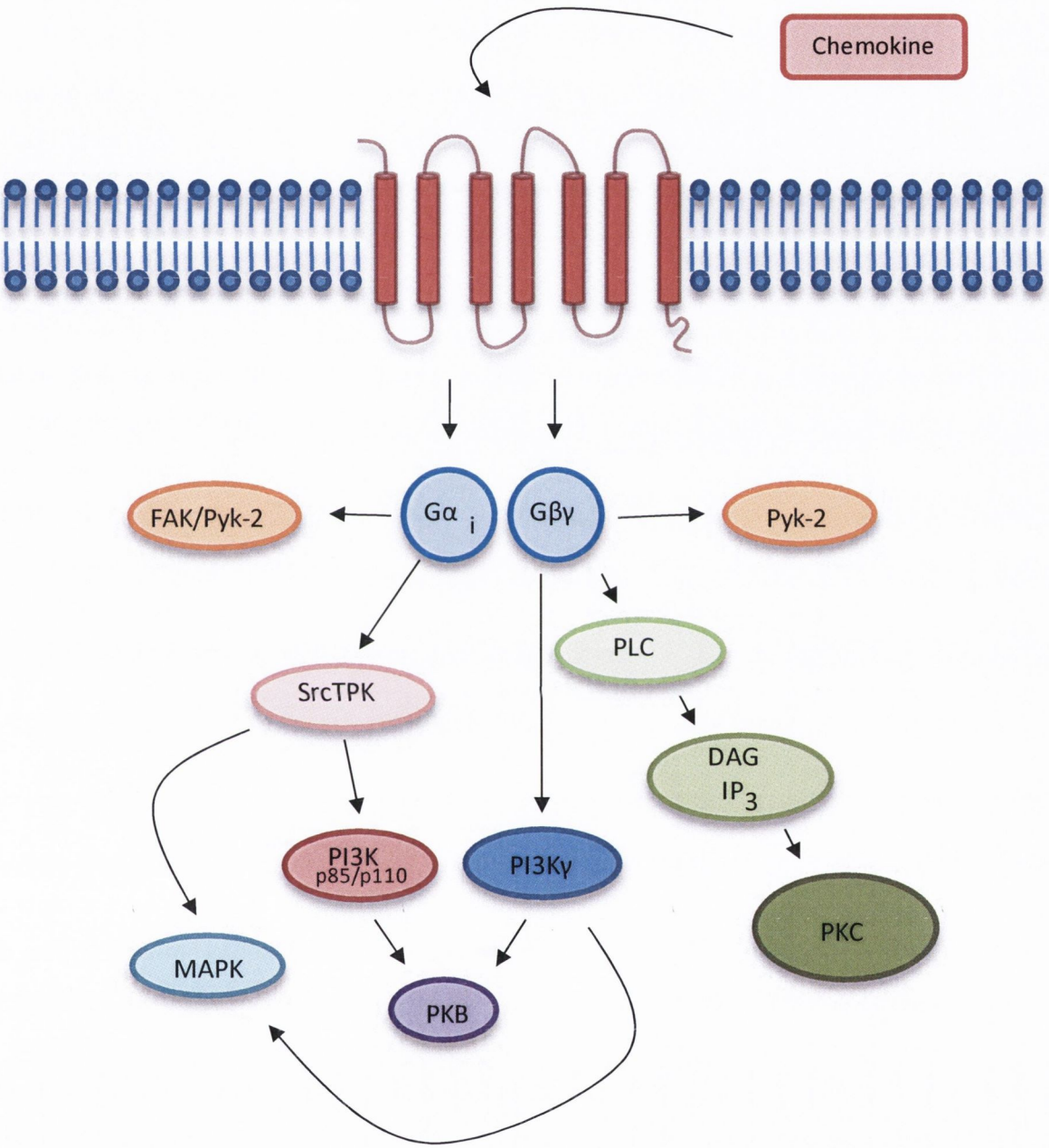

FIGURE 5.3. CHEMOKINE RECEPTOR ACTIVATION AND SIGNALLING. The chemokine binds to the chemokine receptor, a GPCR, on the surface of the cell. Receptor activation causes uncoupling of the $G\alpha_i$ and Gβγ subunits, which are free to activate many downstream secondary messengers. The βγ subunit causes increases in intracellular calcium levels via PLC (phospholipase C) and Pyk-2 (protein tyrosine kinase 2) signalling and can also cause changes in phosphorylation via PI3K (Phosphatidylinositol 3-kinase) and MAPK (mitogen activated protein kinase). The α subunit also triggers changes in phosphorylation via FAK (focal adhesion kinase) PKB (protein kinase B).

5.4.0 RESULTS

5.4.1 MIXED CORTICAL PRIMARY CULTURES ARE COMPRISED OF 68% NEURONS

In order to identify the cell types responsible for changes in the chemokine profile following U18666a treatment the composition of the mixed primary cortical cultures (hereafter called neuronal cultures) was established. The neurons were cultured on coverslips in 24 well plates for one week, then fixed and stained with anti-neurofillament, anti-GFAP, anti-CNPase or anti-CD11b as markers for neurons, astrocytes, oligodendrocytes and microglia respectively alongside hoescht the nuclear marker (**Figure 5.4a-d**). Confocal images were taken of each staining and to quantify the composition of the culture, the total fluorescence level of each cellular marker was calculated as was the total fluorescence of hoescht for each image (Image J). An average ratio of cell marker : hoescht was then calculated for all images. This was then converted into a percentage and plotted as a graph (**Figure 5.4e and f).** The culture comprised of 68.5% neurons, 17.6% astrocytes, 10.5% oligodendrocytes and 3.4% microglia, with the percentage of neurons being significantly higher than all the other cell types present (n=3, one way ANOVA, Bonferroni post hoc test, $p<0.001$). The composition of the cell content of mixed neuronal cultures allows better characterisation of the resultant changes in cytokine and chemokine levels following U18666a treatment.

5.4.2 U18666A TREATMENT INCREASES CHEMOKINE RELEASE FROM NEURONAL CULTURES

As previously discussed NPC disease has been suggested to display an aberrant immune reponse, with several pro-inflammatory molecules raised (Wu et al., 2005). In order to further elucidate the role of inflammation in NPC Disease neuronal cultures were treated with U18666a (1 µg/ml for 48 hours), and the conditioned media was collected. A commercial rat cytokine array (R and D Biosystems) was used to detect any changes in cytokine and chemokine release from control levels. The blot detects 29 different cytokines and chemokines, of which some levels changed dramatically following U18666a treatment (**Figure 5.5a**). Specifically, 7 of the 29 targets were changed significantly (n=2, Students T-test). Overall there was no noted change in cytokine levels, but marked changes in some chemokine levels (**Figure 5.5b**). This data suggests that the chemotactic profile of chemokines is important in the inflammatory response triggered by U18666a.

5.4.3 U18666A Treatment Increases CXC and CCL Chemokine Release

We specifically focused on the effects of U18666a on CXC chemokine release from neurons. Members of the CXCR2 activating sub-family of chemokines were seen to be significantly increased in the media of cells treated with U18666a. LIX (359 % ± 32 %, n=2, Students T-test, $p < 0.001$) and CINC-1 (421 % ± 45 %, n=2, Students T-test, $p < 0.001$) were both observed to increase at least 3 fold following U18666a treatment (**Figure 5.6**). The CXCR3 receptor activating chemokines were also observed to increase, specifically IP-10 levels showed an 11 fold increase (1175 % ± 67 %, n=2, Students T-test, $p < 0.001$) in treated media (**Figure 5.7**). Another member of this family, MIG was present at 7 times (733 % ± 370 %, n=2, Students T-test, $p < 0.01$) the level in treated media compared to control (**Figure 5.7**). Activation of both CXCR2 and CXCR3 are known to stimulate neutrophil and leukocyte migration to sites of inflammation, indicating a role for immune cell infiltration following U18666a treatment. Next, we examined the effect of U18666a on the CCL subfamily of chemokines. We found that two members of the CCL sub-family of chemokines that activated receptors CCR1, CCR3, CCR5 and GPR 75 increased following treatment with U18666a; RANTES (1254 % ± 147 %, n=2, Students T-test, $p < 0.001$) and MIP-1α (118 % ± 41 %, n=2, Students T-test, $p < 0.001$) were significantly elevated from control levels (**Figure 5.8**). Finally, MIP-3α an activator of the CCR6 receptor, was all seen to increase at 10 fold in treated media (1035 % ± 123 %, n=2, Students T-test, $p < 0.001$) (**Figure 5.8**). CCL chemokines induce the migration of monocytes from the periphery and activated glia within the CNS to sites of inflammation further highlighting chemotaxis as a critical process in U18666a treated conditions.

5.4.4 U18666A Treatment Increases LIX Release In A Time And Concentration Dependent Manner

Following identification of the initial hit in the cytokine array the U18666a stimulated release profile of one specific chemokine was further investigated. Previously, LIX release from cerebellar slice cultures was altered following treatment with a modulator of sphingolipid metabolism (Sheridan and Dev, 2012; Shermak et al., 1998). As sphingolipid is found to accumulate alongside cholesterol in NPC disease LIX levels was further explored. Neuronal cultures were treated with 1 µg/ml U18666a for different periods of time (1 hr, 2 hrs, 4 hrs, 8 hrs, 16 hrs, 24 hrs and 48 hrs, and a control of 48 hrs untreated) and LIX levels quantified using an ELISA kit (**Figure 5.9a**). After 1 and 2 hours U18666a treatment LIX levels were slightly increased from control levels, this was then reversed at 4 and 8 hours, with LIX levels returning to nearer control values. At 16 hours a significant increase in LIX was detected (n=3, one way ANOVA, Dunnetts post hoc test, $p < 0.001$). At 24 hours, LIX levels were still

significantly higher than control levels (n=3, one way ANOVA, Dunnetts post hoc test, p <0.01), but slightly decreased when compared to the 16 hour treatment timepoint. LIX levels at 48 hours U18666a treatment were very similar to control levels (**Figure 5.9a**) which contradicts the initial cytokine blot data (**Figure 5.7**) which found LIX to be significantly increased from control levels following U18666a treatment. The ELISA data may be seen to be more reliable as there were more experiments performed with greater n numbers than the initial cytokine array. The Information collected from the ELISA data indicates U18666a causes a time dependent increase in LIX levels. At 48 hours LIX levels were reduced back to control levels in the ELISA experiments which may be due to an increase in cell death at this extended time point. After determining LIX levels are most significantly increased at 16 hours of U18666a treatment, a concentration response curve of U18666a mediated LIX release was generated. Using 16 hours as the treatment time, neurons were treated with varying concentrations of U18666a. The concentrations 0.5 μg/ml, 1 μg/ml and 2 μg/ml all caused a significant increase in LIX levels (n=3, way ANOVA, Dunnetts post hoc test $p < 0.05$, $p < 0.001$, $p < 0.01$ respectively). The greatest increase in LIX levels was observed following treatment with 1 μg/ml U18666a. LIX levels were seen to be significantly decreased (n=3, one way ANOVA, Dunnetts post hoc test $p < 0.05$) from control levels following 5 ug/ml U18666a treatment (**Figure 5.9b**), which may again be due to cell death at this high concentration.

5.4.5 Analysis of U18666a treatment on cell survival

Following the finding that LIX release from mixed cultures decreases after 48 hours of U18666a treatment, it was hypothesized that the cells may be dying at this long an exposure. Thereafter, a cell survival assay was carried out to determine the quantity cell death at each U18666a treatment time point. Neurons were treated with 1 μg/ml U18666a for differing time points (1, 2, 4, 8, 16, 24 and 48 hours) as per the LIX release time point experiment. The cells were then fixed and stained with hoescht as a marker for nuclei and propridium iodide, as a marker for cell death. The overall propridium iodide fluorescence was divided by the overall hoescht fluorescence to give a ratio of cell death. U18666a was found to increase cell death from control levels at 24 hours and 48 hours (n=3, one way ANOVA, Dunnetts post hoc test $p < 0.001$) (**Figure 5.10a**). Notably, this is later than the 16 hour time point that LIX release is found to be significantly increased. Moreover, this death of cells at 24 and 48 hours mirrors the U18666a mediated decrease of LIX at these timepoints. Taken together the decrease in LIX release at 24 and 48 hours seems to be caused by the death of cells at these time points. As LIX release was also found to be significantly reduced from control levels following treatment with 5 μg/ml U18666a, it remained to be determined if this concentration of the

compound induced cell death in neuronal cultures. As previously described, propridium iodide staining was carried out to ascertain the level of cell death at each dose of U18666a. Cell death was observed to be significantly higher than control after treatment with 4 μg/ml and 5 μg/ml U18666a (n=3, one way ANOVA, Dunnetts post hoc test $p < 0.001$) (**Figure 5.10b**). The increase in propridium iodide staining at 5 μg/ml, combined with the information that LIX release is decreased at this concentration indicates the reduction in chemokine release is most likely due U18666a-induced cell death at this concentration.

5.4.6 U18666a Mediated Release Of LIX Is Astrocyte Independent

To determine the cell type responsible for the changes in U18666a mediated LIX release from mixed neuronal cultures, enriched astrocytes cultures were treated with U18666a. The culture purity was first examined (**Figure 5.11**). After determining the purity of astrocyte cultures, they were treated with 1 μg/ml U18666a for the same time points as neuronal cultures (1, 2, 4, 8, 16, 24 and 48 hours). LIX release was not increased from control levels at any times. At 24 and 48 hours LIX release was found to be significantly decreased (n=3, one way ANOVA, Dunnetts post hoc test, $p < 0.01$, $p < 0.001$) (**Figure 5.12a**). Following the results from the propridium iodide staining (**Figure 5.10a**), it can be hypothesised that this decrease is due to an increase in cell death. As baseline levels of astrocyte mediated LIX release were found to be around 600 pg/ml, and 17 percent of the mixed cultures are comprised of astrocytes (**Figure 5.4**), it can be hypothesized that baseline LIX levels in mixed cultures may be due to astrocytes and these are not altered by U18666a treatment. To further ascertain whether U18666a mediated release of LIX in neuronal cultures is due to neurons or glial cells, enriched astrocytes cultures were treated with increasing concentrations of U18666a (0.5 μg/ml, 1 μg/ml, 1.5 μg/ml, 2.0 μg/ml, 3 μg/ml, 4 μg/ml, 5 μg/ml) for 16 hours. Astrocyte mediated LIX release was found not to change following treatment with any concentration of U18666a after 16 hrs treatment(n=3, one way ANOVA, Dunnetts post hoc test, $p < 0.05$) (**Figure 5.12b**). This finding identifies astrocytes are not responsible for the changes in U18666a mediated release of LIX in neuronal cultures. Thus the data suggests that U18666a may induce release of LIX from neurons or other cell types of the CNS.

5.4.7 The Statin Mevinolin Reverses U18666a Increases In mRNA Levels Of CXC Chemokines

As U18666a was found to increase CXC chemokine release (**Figure 5.6 and 5.7**), it remained to be determined whether differing cholesterol environments had any effect on CXC chemokine synthesis,

at the mRNA level. To investigate this, neuronal cultures were treated for 3 hours with with 2 μg/ml cholesterol, 1 μg/ml U18666a, mevinolin (0.25 μM), or U18666a and mevinolin combined and qPCR performed with two different primers (LIX and IP-10). Firstly, LIX mRNA levels (a CXCR2 activating chemokine) in differing cholesterol environments was investigated. mRNA levels were found to increase four times that of control levels following U18666a treatment (n=4, one-way ANOVA, Dunnets post hoc test, $p<0.05$), but were not altered significantly in the presence of cholesterol or mevinolin (**Figure 5.13a**). Interestingly, the combined treatement of neurons with U18666a and mevinolin was not significantly different from control levels, indicating mevinolin was able to reverse the U18666a mediated increase in LIX mRNA levels. In order to investigate whether these changes in mRNA synthesis were specific to LIX, IP-10 mRNA levels (a CXCR3 activating chemokine) were also investigated under the same conditions. Again, high cholesterol levels or mevinolin-induced low cholesterol levels did not alter IP-10 mRNA synthesis whereas a six fold increase was observed following U18666a treatment alone. Combinational treatment of mevinolin along with U18666a was found to decrease the U18666a mediated changes in IP-10 mRNA back to baseline (**Figure 5.13b**). This data indicates U18666a mediated increase in chemokine release in previous experiments is induced by an upregulation of mRNA synthesis.

5.4.8 The Statin Mevinolin Reverses The U18666a-Mediated Increase In LIX Release

The data above showed that U18666a mediated increases in LIX mRNA synthesis was reversed by additional treatment with mevinolin. In order to investigate whether these changes at the mRNA level were translated to LIX release at the protein level, neuronal cultures were treated for 3 hours with cholesterol, mevinolin, U18666a and mevinolin combined, as in the previous experiment (2 μg/ml cholesterol, 1 μg/ml U18666a, mevinolin (0.25 μM), or U18666a and mevinolin combined) and the level of LIX in the media was examined by LIX ELISA. Neither cholesterol nor mevinolin treatment had any effect on LIX release from neuronal cultures. U18666a was found to significantly increase LIX release (n=4, one-way ANOVA, Dunnets post hoc test, $p<0.01$)(**Figure 5.14**). As observed at the mRNA level, addition of mevinolin to U18666a treated neuronal cultures was found to decrease levels of LIX back to baseline levels. The action of mevinolin to decrease U18666a mediated LIX release is an interesting finding as it may implicate the use of statins to modulate the neuroinflammation observed in NPC disease.

5.4.9 U18666A Mediated LIX Release Is Coupled To NFκB Signalling

In order to elucidate the signaling pathway involved in U18666a mediated release of LIX from neuronal cultures, cells were treated with 1 μg/ml U18666a for 16 hours and the cell lysates collected for western blotting. The membrane was probed with IκBα antibody, stripped and reprobed with actin antibody which allowed IκBα levels to be quantified. U18666a treatment was found to significantly decrease IκBα expression in mixed cultures (n=4, Students T-test, $p<0.05$)(**Figure 5.16a and b**). Probing with pIκBα identified U18666a treatment caused an increase in pIκBα expression (**Figure 5.16c and d**). The finding that IκBα is both phosphorylated and reduced in mixed cultured following U18666a treatment highlights the changes in chemokine release observed may be due to the activation of the NFκB pathway.

5.4.10 U18666A Treatment Causes Demyelination In Cerebellar Slice Cultures

Widespread demyelination of cerebellar neurons has been observed in a mouse model of NPC disease (Loftus et al., 1997). As yet it has not been investigated whether U18666a (the cellular model of NPC disease) is able to trigger the demyelination observed in the animal model. Mouse organotypic cerebellar slices were treated with 1 μg/ml U18666a for 24 hours. Following this, the slices were fixed and stained with neurofillament and MBP (myelin basic protein) antibodies (**Figure 5.17a and b**). The slices were imaged and the staining quantified using EBI Image. The software quantifies the amount of MBP staining overlapping the neurofillament staining (**Figure 5.17c**). Analysis of staining revealed U18666a treatment significantly decreased the level of myelination in mouse organotypic cerebellar slice cultures. This data confirms U18666a mimics the effects of NPC disease.

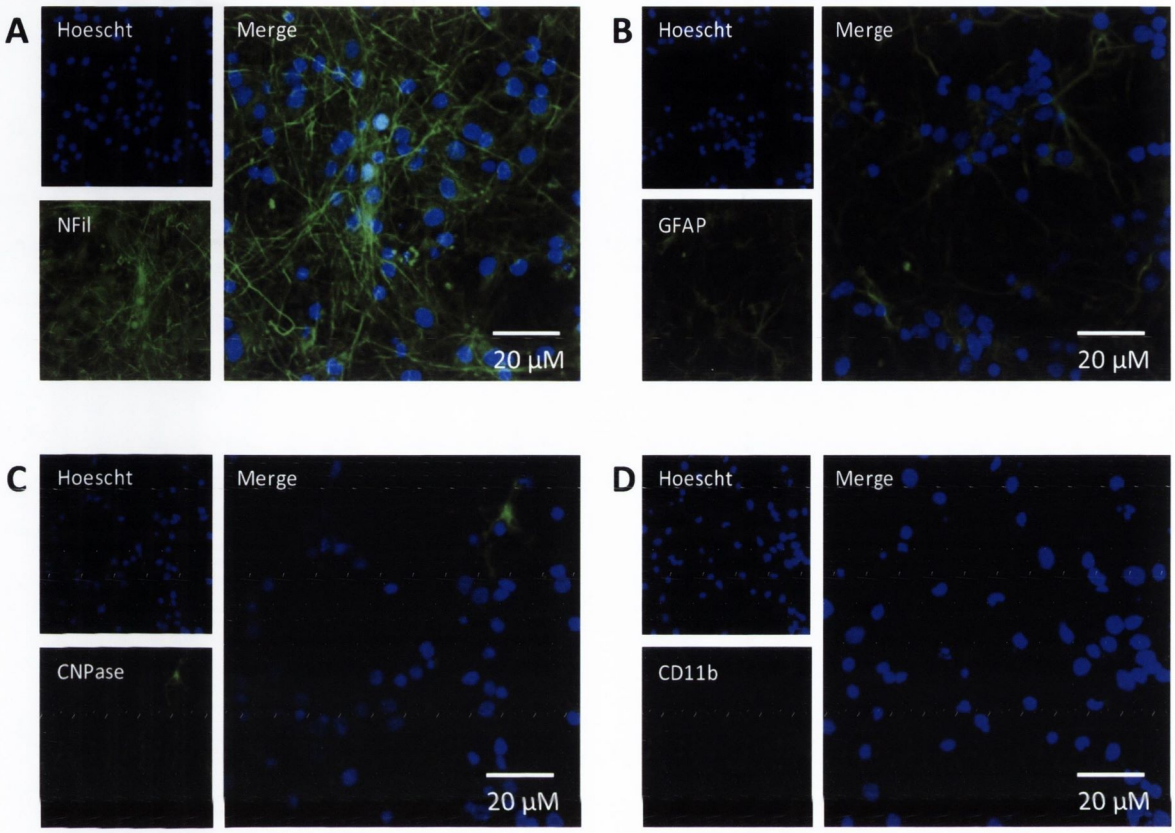

E

		Percentage of Culture
Average Neuron Ratio	3.105	68.46
Average Astrocyte Ratio	0.796	17.55
Average Oligodendrocyte Ratio	0.480	10.58
Average Microglia Ratio	0.154	3.40
Total	**4.535**	**100**

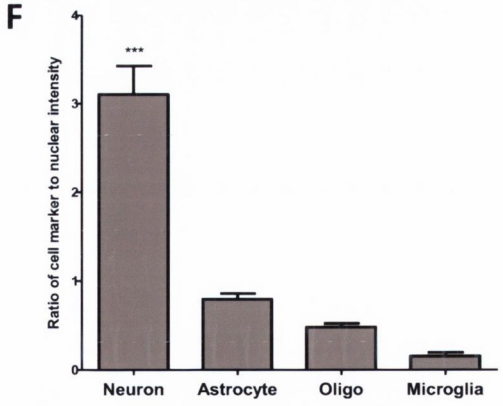

FIGURE 5.4. MIXED CORTICAL PRIMARY CULTURES ARE COMPRISED OF 68% NEURONS. Culture stained with **A.** neurofillament (green) as a marker for neurons **B.** GFAP (green) as a marker for astrocytes **C.** CNPase (green) as a marker for oligodendrocytes **D.** CD11b (green) as a marker for microglia and hoescht (blue). **E.** Following calculation of average fluorescence of each marker and hoescht the percentage culture was calculated. **F.** Graph showing the composition of the culture with neurons being significantly higher in number than all other cell type (n=3, One-way ANOVA, Bonferroni Post hoc test, $p < 0.001$).

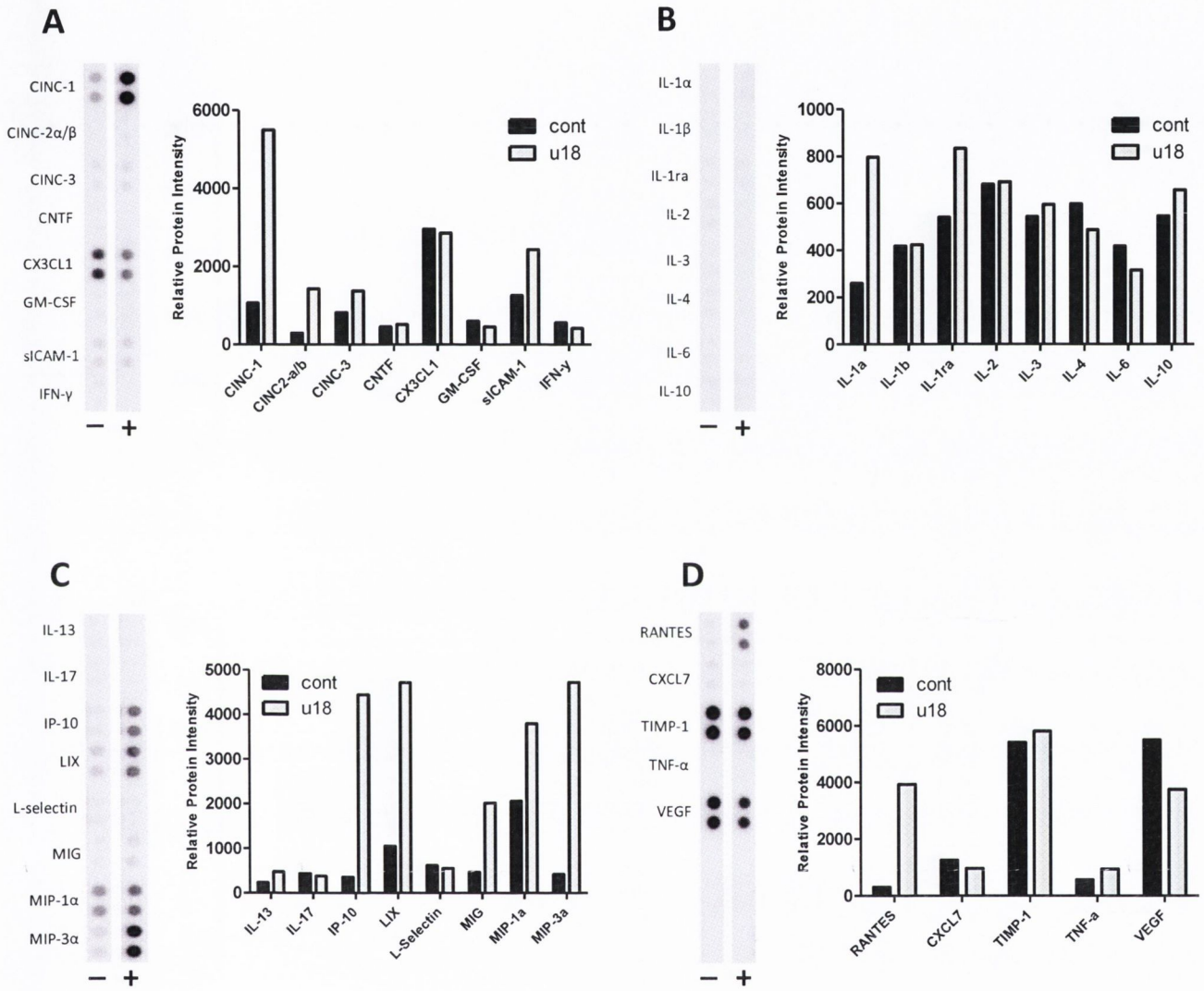

FIGURE 5.5. U18666A CAUSES CHANGES IN CHEMOKINE LEVELS IN MIXED CULTURES. Raw data for cytokine array blots. The control blot is the panel on the right and the treated blot is the left panel for all columns (indicated by – and + respectively). Large scale increases can be seen for chemokines but not for cytokines **B.** Graph of all cytokine and chemokines analysed. The graph shows the average intensity of each dot compared between control and 48 hr U18666a treated (n=2). Control values are shown in black and U18666a treated in grey.

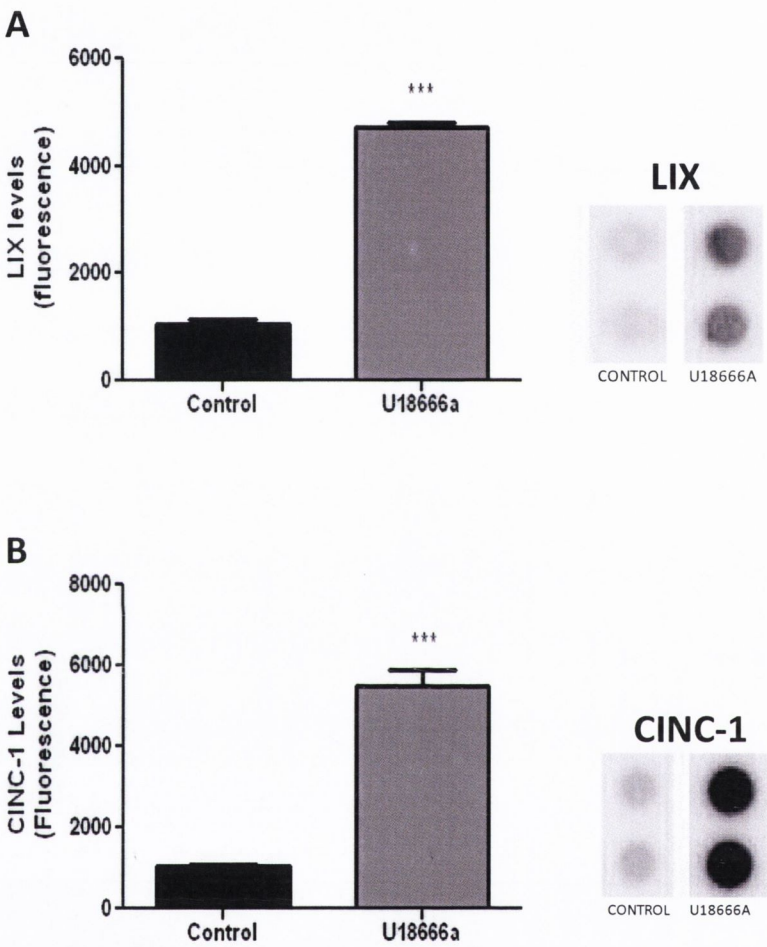

FIGURE 5.6. U18666A CAUSES AN INCREASE IN CXCR2 ACTIVATING CHEMOKINE RELEASE IN MIXED CULTURES Graph showing an increase in **A.** LIX levels and **B.** CINC-1 levels present in media following 48 hr U18666a treatment (n=2, Students T-test, $p < 0.001$), the right panels show the raw blots.

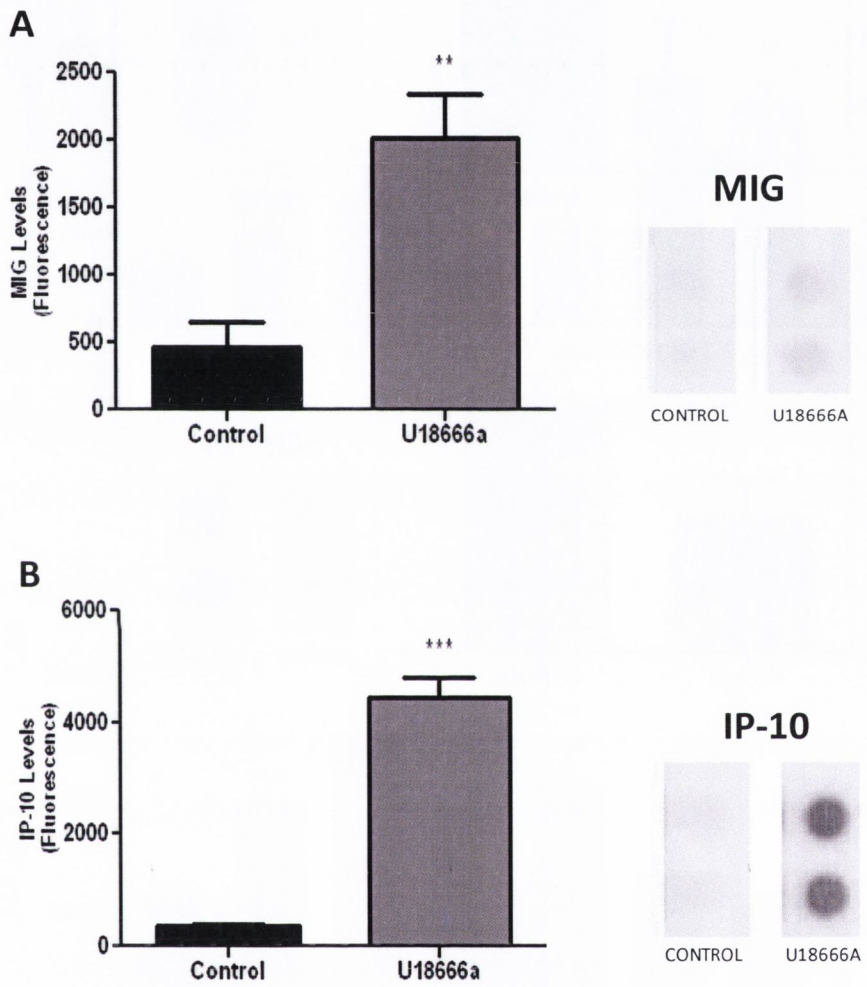

FIGURE 5.7. U18666A CAUSES AN INCREASE IN CXCR3 ACTIVATING CHEMOKINE RELEASE IN MIXED CULTURES
Graph showing an increase in **A.** MIG levels (n=2, Students T-test, $p < 0.01$) and **B.** IP-10 levels (n=2, students t-test, $p < 0.001$) present in media following 48 hr U18666a treatment, the right panel shows the raw data.

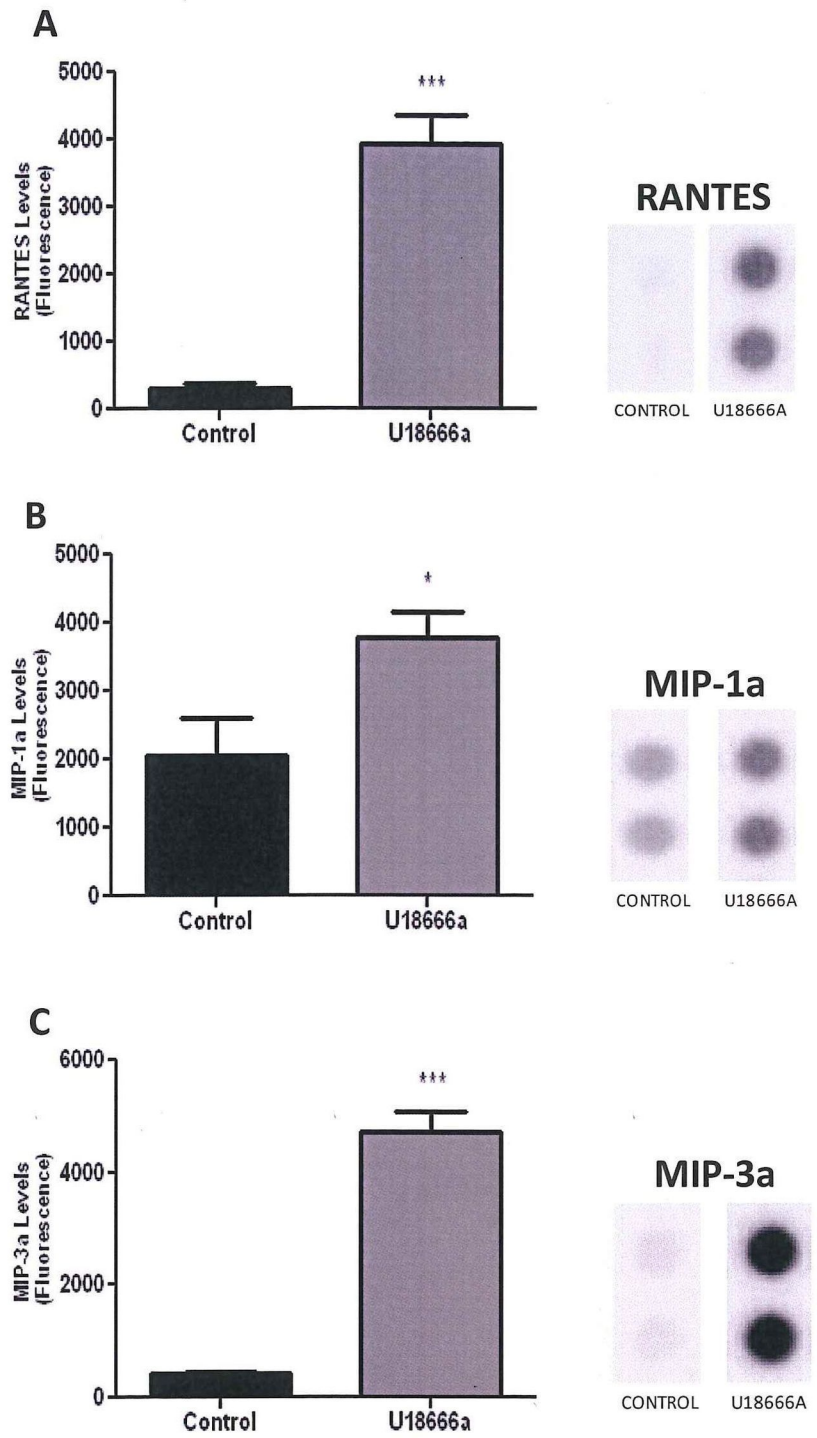

FIGURE 5.8. U18666A CAUSES AN INCREASE IN CCL CHEMOKINES IN MIXED CULTURES Graph showing an increase in **A.** RANTES levels (n=2, students t-test, $p < 0.001$) **B.** MIP-1α levels (n=2, students t-test, $p < 0.05$) **C.** LIX levels (n=2, Students T-test, $p < 0.001$)present in media following 48 hr U18666a treatment, the right panel shows the raw data.

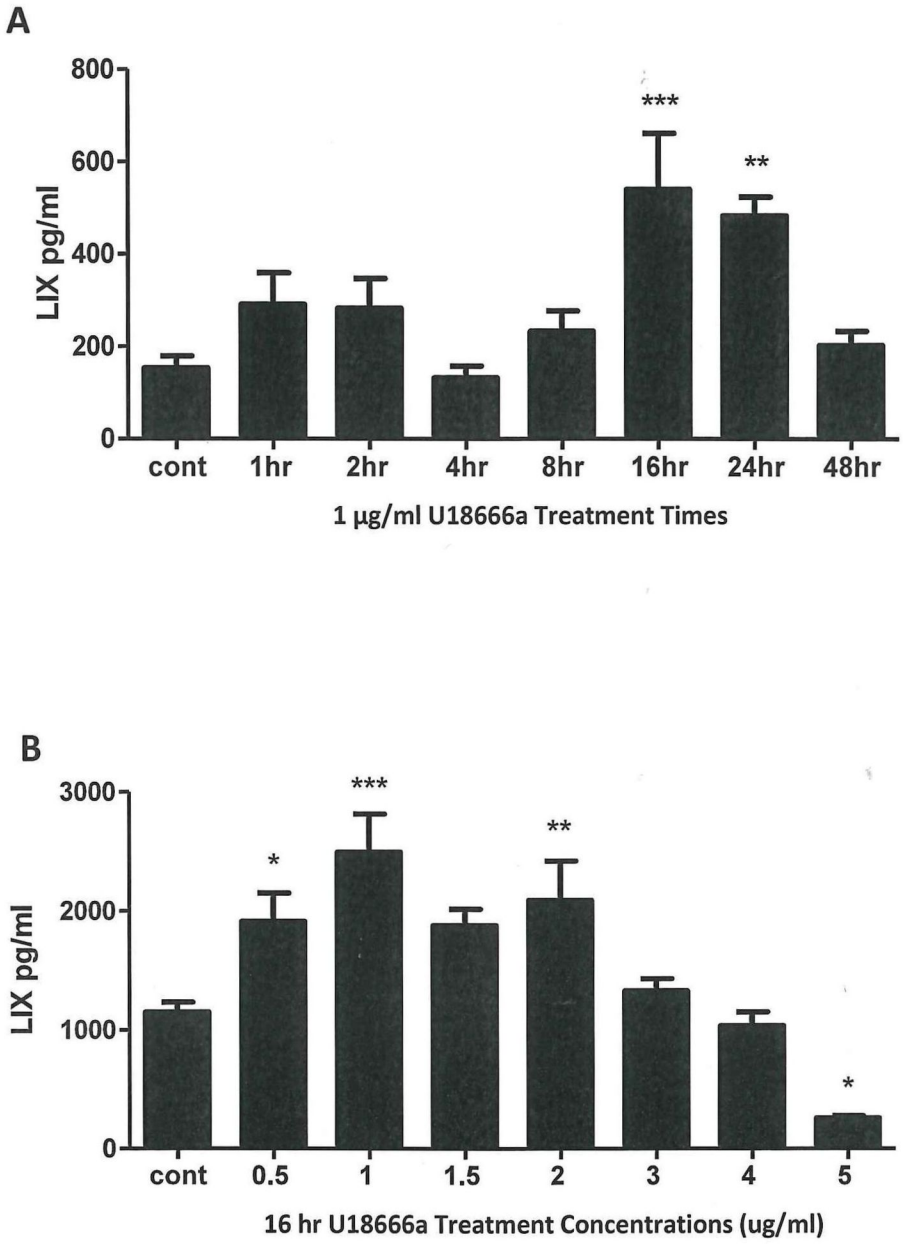

FIGURE 5.9. U18666A TREATMENT CAUSES INCREASES IN LIX RELEASE FROM MIXED CULTURES. A. Quantification of LIX ELISA revealed LIX release was significantly increased after 16 and 24 hour 1 µg/ml U18666a treatment (n=3, One way ANOVA, Dunnets post hoc test, $p<0.001$ and $p<0.01$ respectively). **B.** LIX release was significantly increased from control at 0.5 µg/ml, 1 µg/ml and 2 µg/ml (n=3, One way ANOVA, Dunnets post hoc test, $p<0.05$, $p<0.001$ and $p<0.01$ respectively.) LIX release was significantly decreased from control levels when treated with 5 µg/ml U18666a for 16 hrs (n=3, One way ANOVA, Dunnets post hoc test, $p<0.05$).

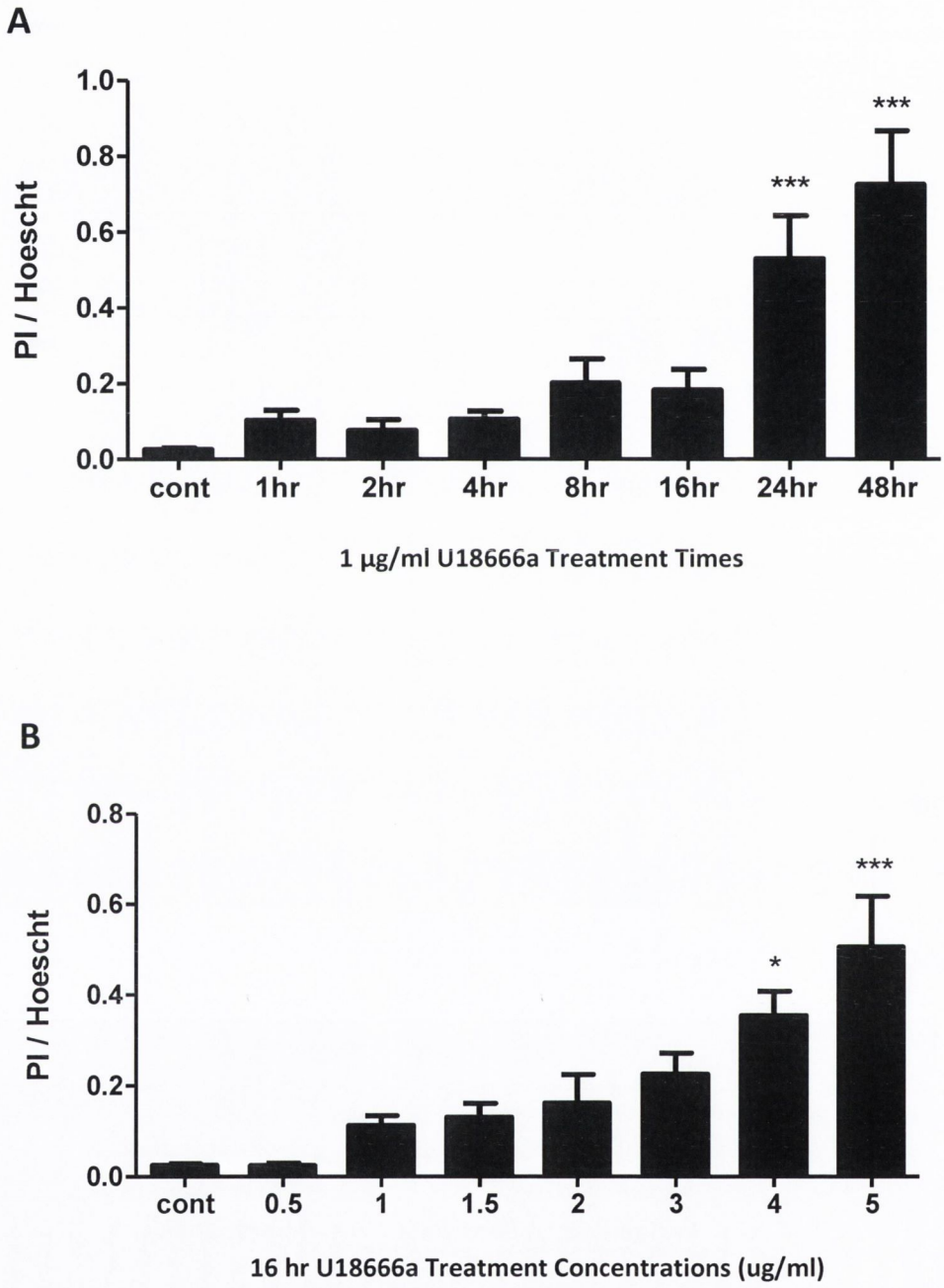

FIGURE 5.10. CELL SURVIVAL IS AFFECTED BY U18666A IN A TIME AND CONCENTRATION DEPENDANT MANNER. **A.** Graph showing quantification of propridium iodide staining following 1µg/ml U18666a for 1, 2, 4, 8, 16, 24 and 48 hours. A significant increase in cell death was observed at 24 hours and 48 hours (n=3, One way ANOVA, Dunnets post hoc test, $p < 0.001$). **B.** Propridium iodide staining following treatment with differing concentrations of U18666a for 16 hours revealed significant increases in cell death at 4 µg/ml and 5 µg/ml hours (n=3, One way ANOVA, Dunnets post hoc test, $p < 0.05$ and $p < 0.001$ respectively)

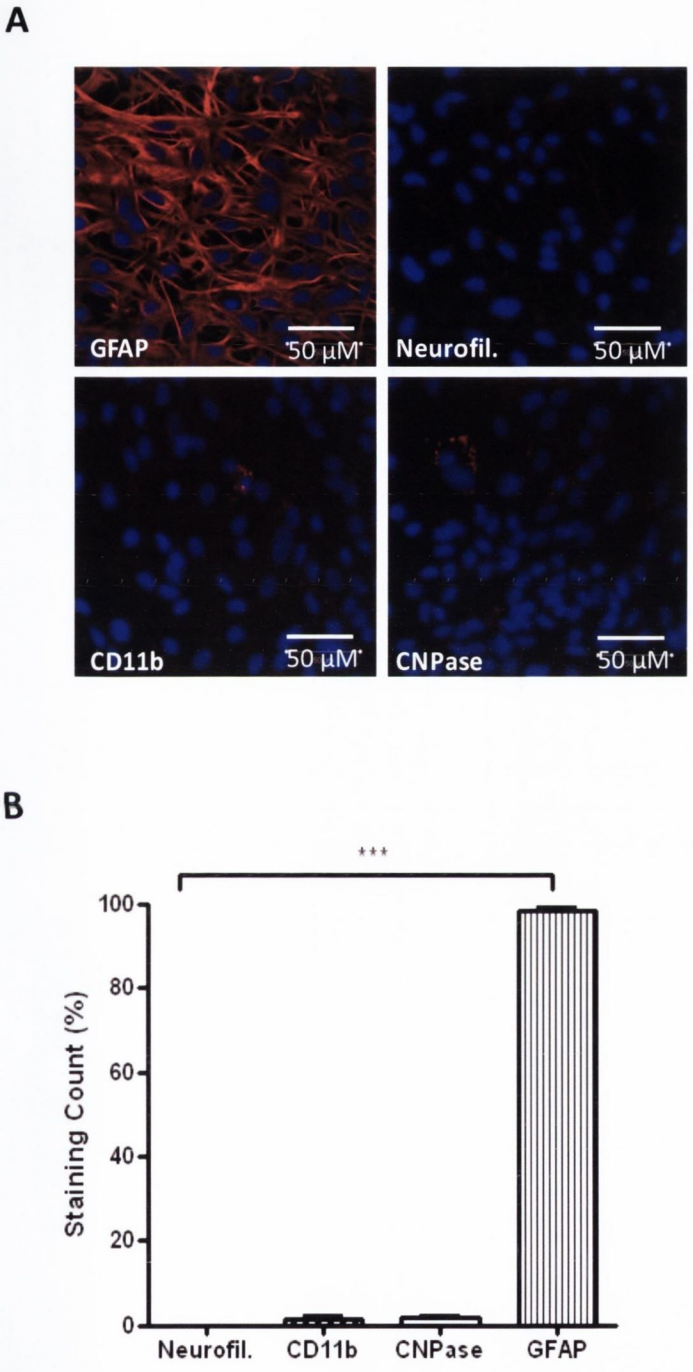

FIGURE 5.11. DETERMINATION OF THE PURITY OF ASTROCYTE CULTURES A. Pure astrocyte preparation stained for GFAP (astrocytes), neurofilament H (neurons), CD11b (microglia) and CNPase (oligodendrocytes). Cell nuclei appear as blue (Hoescht). A total of 24 images were analysed (6 images per group). **B.** Average percentage of positively stained cells for each group was as follows: GFAP 98.58% +/- 0.57, CD11b 1.35% **+/-** 0.77 and CNPase 1.83% **+/-** 0.48. No neurofilament H positive cells were observed. (n=3, One way ANOVA, Dunnets post hoc test, $p>0.05$.). Data provided by Luke Healy

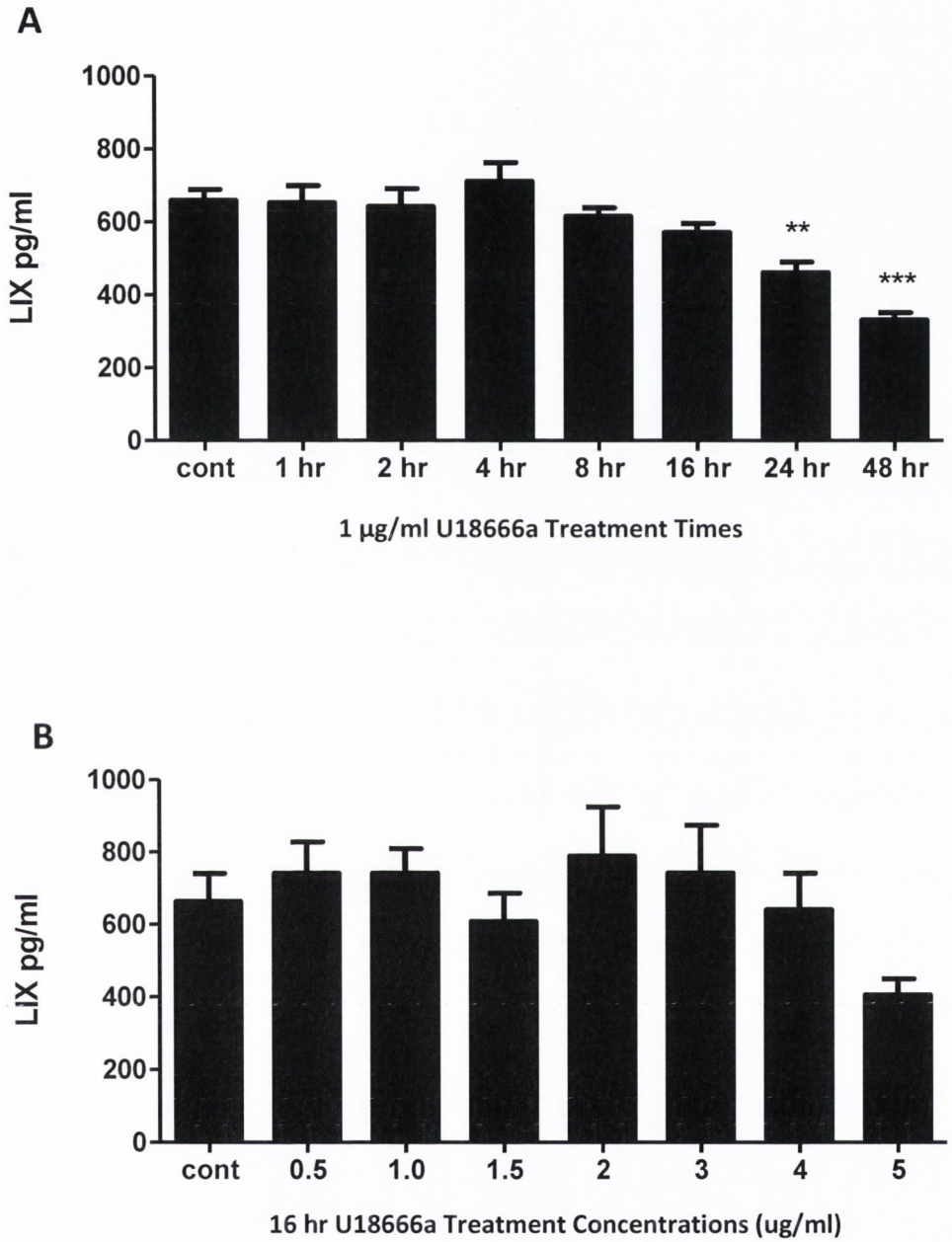

FIGURE 5.12. LIX RELEASE FROM ASTROCYTES IS NOT INCREASED BY U18666A. A. LIX ELISA shows U18666a treatment does not cause an increase in LIX release, but a significant decrease at 24 and 48 hours (n=3, One way ANOVA, Dunnets post hoc test, $p < 0.01$ and $p < 0.001$ respectively). **B.** LIX release was not significantly increased from control levels following treatment with increasing concentrations of U18666a (n=3, One way ANOVA, Dunnets post hoc test, $p > 0.05$.)

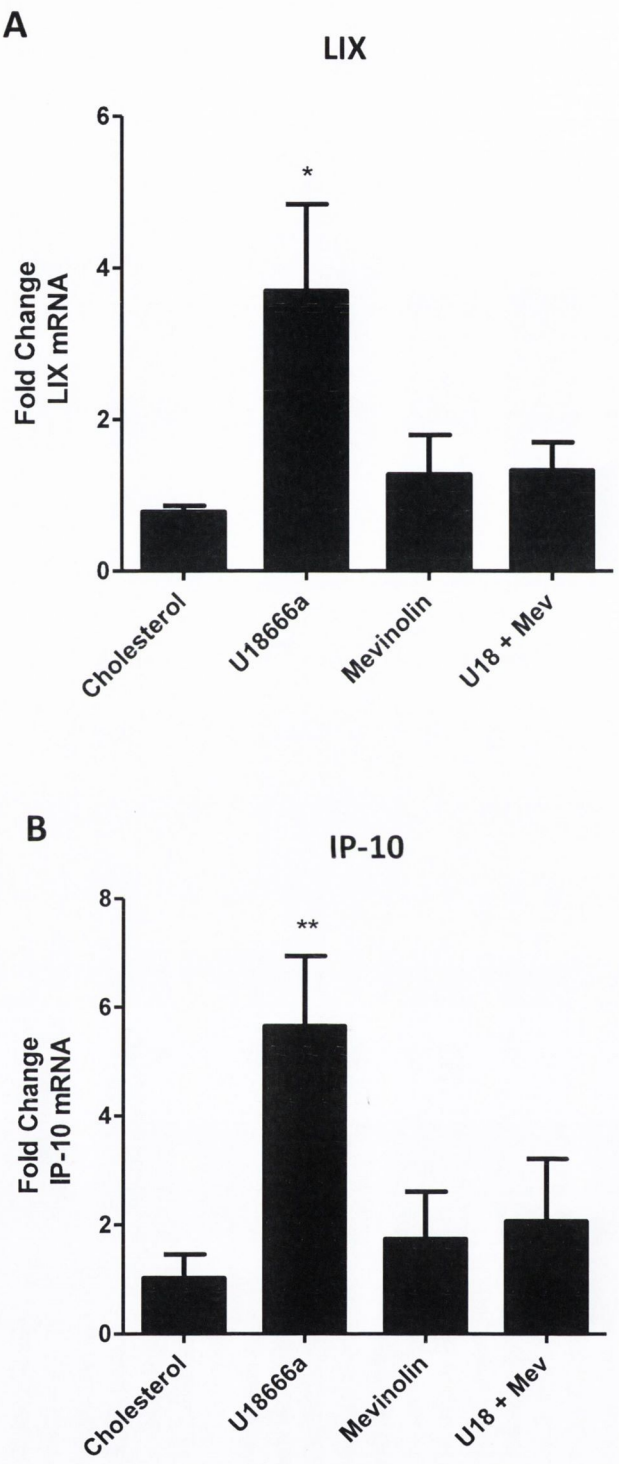

FIGURE 5.13. U18666A TREATMENT CAUSES CHANGES IN CXC CHEMOKINE MRNA LEVELS. Mixed cultures were treated with with 2 µg/ml cholesterol, 1 µg/ml U18666a, mevinolin (0.25 µM), or U18666a and mevinolin combined for 3 hours and rtPCR performed, when co-administered with mevinolin, U18666a induced changes in LIX mRNA were reversed. **A.** U18666a treatment caused a fourfold significant increase in LIX mRNA ($p<0.05$) **B.** U18666a treatment also caused caused a six fold increase in IP-10 mRNA levels. Again, mevinolin in addition to U18666a was found to be not significantly altered from control levels. (n=4, one way ANOVA, Dunnets post hoc test)

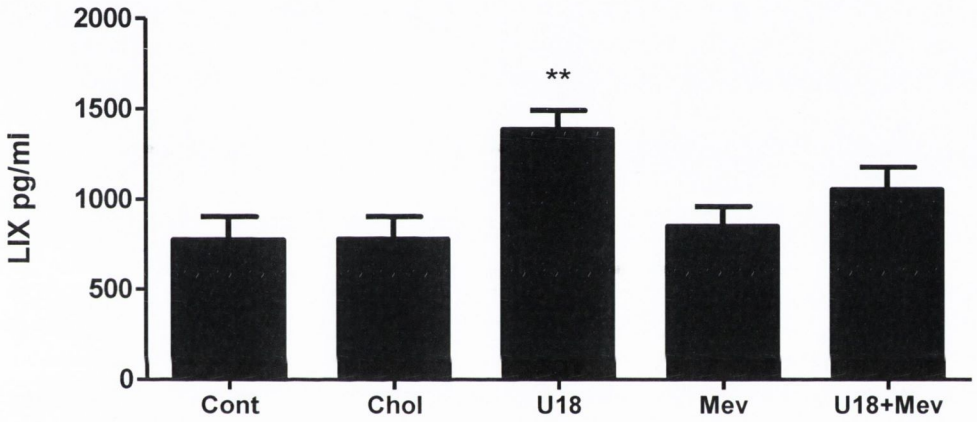

FIGURE 5.14. LIX RELEASE FROM MIXED CULTURES IS MODULATED IN DIFFERING CHOLESTEROL ENVIRONMENTS. LIX release is not altered following treatment with 2 μg/ml cholesterol, nor mevinolin (0.25 μM) for 3 hrs. As previously shown 1 μg/ml U18666a increases LIX release (n=4, One way ANOVA, Dunnets post hoc test, $p<0.01$). Interestingly, the co-administration of U18666a and mevinolin was found to decrease U18666a mediated LIX release back to control levels.

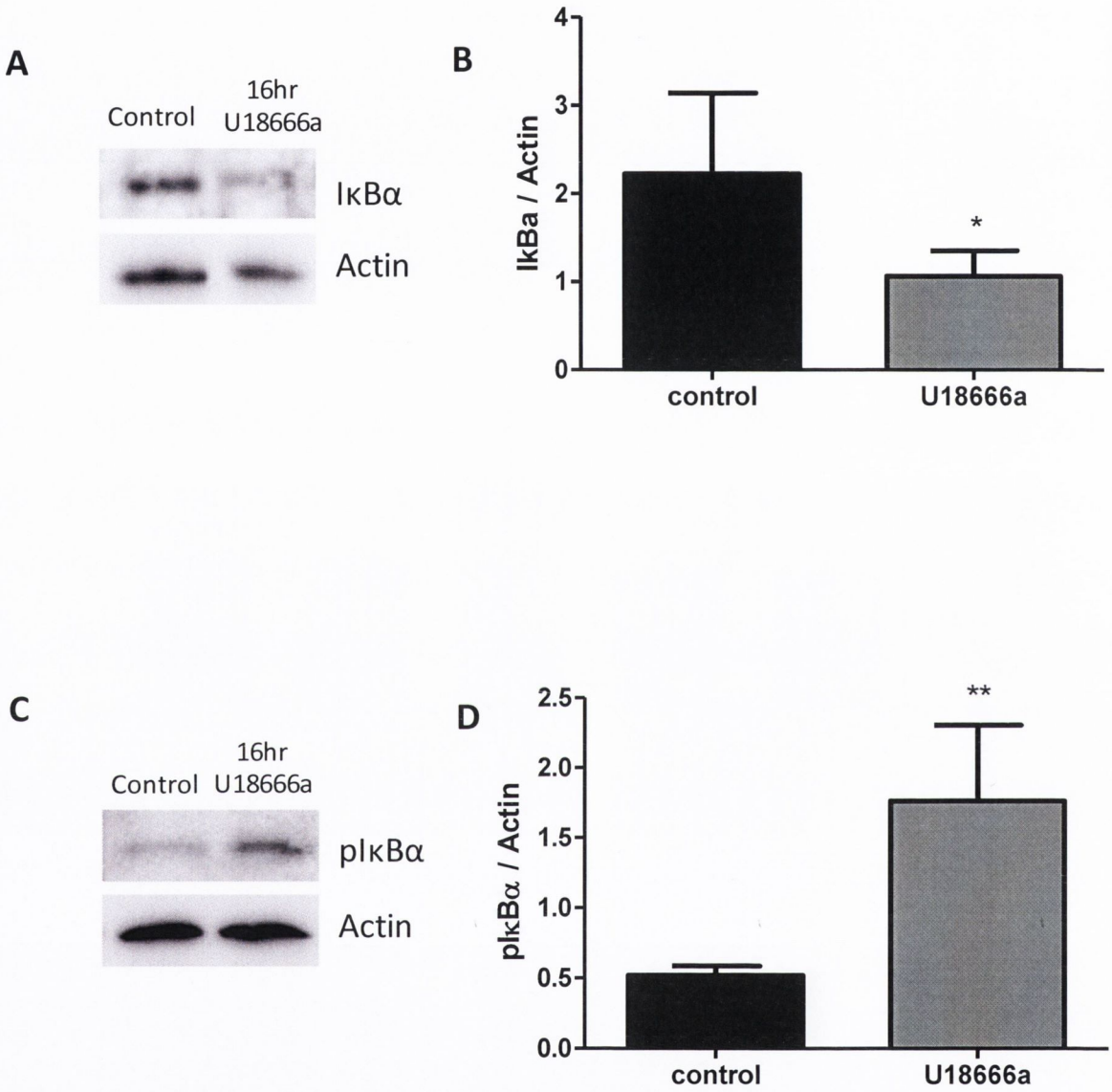

FIGURE 5.15. U18666A TREATMENT OF NEURONS CAUSES PHOSPHORYLATION AND REDUCTION OF IκBA. A. Western blot showing reduction in total IκBα levels following 16 hr U18666a treatment in neurons. **B.** Graph of western blot IκBα/actin ratio, showing significant decrease in total IκBα levels (n=4. Students T-test, $p<0.05$). **C.** Western blot showing increase in phosphoIκBα (Ser 32) following U18666a treatment. **D.** Graph of western blot phosphpIκBα/actin ratio, showing significant increase in phosphorylation of IκBα (n=4, Students T-test, $p<0.01$)

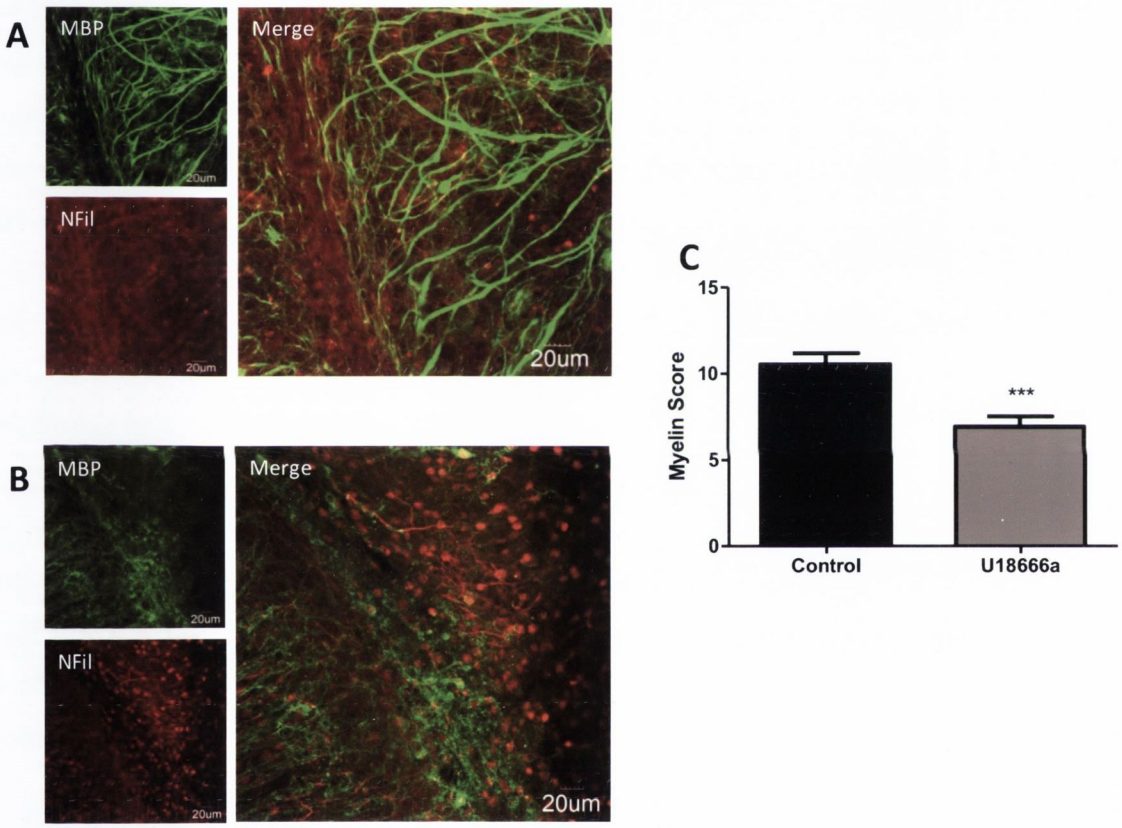

FIGURE 5.16. U18666A TREATMENT CAUSES DEMYELINATION IN CEREBELLAR SLICES. A. Image showing control cerebellar slice stained with MBP antibody to detect myelin and neurofilament antibody to detect neurons. MBP can be seen to colocalise with neurofilament staining where axons are myelinated. **B.** Image showing cerebellar slice treated with 1µg/ml U18666a for 24 hours, changes in myelination can be observed. **C.** When quantified U18666a was found to significantly decrease the level of myelination from control levels (n=3, Students T-test, $p < 0.001$).

5.5.0 DISCUSSION

5.5.1 U18666A TREATMENT INCREASES LEVELS OF CHEMOKINE IN NEURONAL CULTURES

It has been recently shown that the pathogenesis of NPC disease may not be restricted to defects in cholesterol trafficking, but an inflammatory mechanism may play a role in disease progression. At a cellular level, increased levels of Toll-like receptor 4 (TLR4) were found to be co-localised with accumulated cholesterol within the endosomal/lysosomal compartment of human NPC fibroblasts and siRNA knockdown of TLR4 successfully decreased the release of both IL-6 and IL-8 (Suzuki et al., 2007). The compound U18666a is widely used to mimic the cholesterol accumulation observed in NPC disease and has also been found to increase TNF-α release from macrophages (Iftakhar et al., 2009). Combining this data, it remained to be investigated whether U18666a treatment changed the inflammatory profile via changes in cytokine and chemokine release in the CNS environment. A cytokine array (able to detect changes in 29 cytokine/chemokines) was performed using the media from mixed neuronal cultures treated with 1 μg/ml U18666a for 48 hours. Signficant increases were identified in seven chemokines (LIX, CINC-1, MIG, IP-10, RANTES, MIP-1α and MIP-3α), whereas no significant change was noted in cytokine levels. We note that the effect of chemokines specifically, with limited effect on cytokines may be due to the timepoint that the conditioned media was analysed. We analysed levels of cytokines after 48 hours of treatment with U18666a. At this timepoint, levels of cytokines may have returned to normal, whereas chemokine effects are longer lasting. Nevertheless, the specific effects of U18666a on chemokines but not cytokines is of interest when considering the role of the chemokines in chemotactic attraction of neutrophils into the CNS in NPC disease.

At 48 hrs the CC chemokines RANTES, MIP-1α and MIP-3α were found to significantly increase following 48 hr U18666a treatment. These chemokines act on a variety of CCR receptors, namely CCR1, CCR3, CCR5, CCR6 and GPR75, and are known to primarily recruit monocyte/macrophages within inflamed tissue (Montecucco et al., 2008). More recently CC chemokines have been found to induce neutrophil migration, which in turn can further stimulate the infiltration of other inflammatory cell types from blood vessels (Steffens et al., 2009). The CCR5, activated by both RANTES and MIP-1α, is expressed by immune cells (monocytes, macrophages, T lymphocytes, NK cells and immature dendritic cells) and also by astrocytes, microglia and a subset of neurons in mammals (Westmoreland et al., 2002). Within the CNS, CCR5 is expressed on activated microglia and infiltrating T cells in MS and CCR5 expression is also observed on microglia at sites of beta-amyloid deposits in AD (Bajetto et al., 2002). NPC disease and AD have some pathological similarities (NFTs

are observed to form in both NPC disease and AD) indicting a possible shared underlying mechanism (Koh and Cheung, 2006). High cholesterol levels have been associated with the development of AD and patients treated with statins were found to have a lower prevalence of AD indicating cholesterol homeostasis plays a role in both diseases (Jick et al., 2000; Wolozin et al., 2000). This information highlights that increased CC chemokine release from mixed neuronal primary cultures following U18666a treatment may be as a response to altered cholesterol within the cell as is observed in AD and NPC.

Four CXC chemokines were seen to be significantly increased following U18666a treatment; MIG, IP-10 (activators of the CXCR3 receptor), CINC-1 and LIX (activators of the CXCR2 receptor). CXC chemokines have been described as classical neutrophil chemoattractants (Ransohoff et al., 2007). However aside from their inflammatory role, more recently CXC chemokines and their receptors have been found to regulate a variety of processes in the CNS such as neurotransmitter release and neurogenesis (Peng et al., 2007) Both the CXCR2 and CXCR3 receptors are expressed in the CNS, and have been implicated both in normal and pathological processes (Ambrosini and Aloisi, 2004). CXCR2 and its ligand CINC-1 are dynamically regulated in astrocytes within the developing rat spinal cord to stimulate cell differentiation and survival whereas the same receptor-ligand interaction has been detected in reactive astrocytes after exposure to various inflammatory stimuli (Filipovic et al., 2003; Kielian et al., 2001) This indicates the increase in CXC chemokines observed in this experiment may not be restricted to an inflamamatory role and may have wider ranging effects such as stimulating growth and survival within cells of the CNS environment. This highlights that manipulation of chemokine levels may be useful in the treatment of CNS disorders.

5.5.2 U18666A Treatment Causes Time And Concentration Dependant Changes In LIX Levels

We have previously shown LIX release from astrocytes is reduced following treatment with FTY720-P. FTY720 is a pro-drug that is phosphorylated to FTY720-P *in vivo* to functionally antagonise the S1P receptor. FTY720 is phosphorylated by two conserved enzymes, sphingosine kinase 1 and 2 (SphK1 and SphK2) both of which play a major role in sphingolipid metabolism. Abberant sphingolipid metabolism has been implicated in NPC disease, in particular it has been hypothesized that the initial build up of sphingolipid within the lysosome triggers the accumulation of cholesterol leading to the phenotype observed in NPC disease (Lloyd-Evans et al., 2008). This indicated LIX release may be linked to sphingosine regulation and therefore NPC disease. Following the observation that U18666a induces increases in levels of seven chemokines, it was decided to focus on LIX, and

investigate the mechanism behind U18666a mediated release of this chemokine. Neuronal cultures were treated with U18666a for varying timepoints and concentrations. It was found in the ELISA experiments that LIX release was significantly increased at 16 and 24 hours, then decreased back to control levels at 48 hours which contradicts the initial finding that LIX levels were increased at 48 hours in the cytokine array. It has previously been shown that 1 μg/ml U18666a treatment caused increases in TNF-α release at 48 and 72 hours but not at 24 hours in a mouse macrophage macrophage cell line (RAW 264.7 cells) (Iftakhar et al., 2009). This data indicates U18666a treatment may vary within different cell types and under different conditions. Propridium iodide staining at the same timepoints and concentrations of U18666a used in the LIX release experiments showed an increase in cell death at the two highest time and concentrations of U18666a treatment, which correlated with decreased levels of LIX observed in these conditions. This data indicated the decrease in LIX levels may be due to the lack of viable cells in the culture. These experiments allowed the characterization of the optimal time point and concentration of U18666a mediated LIX release to be used in future experiments. In all subsequent experiments 1 μg/ml U18666a for a time of either 16 or 24 hours was used.

5.5.3 Astrocytes Do Not Increase Levels Of LIX In Response To U18666a

Conventionally it is thought that glial cells within the CNS are the main producer of cytokines and chemokines (Bajetto et al., 2001). A large proportion of studies investigating the release of cytokines or chemokines within the CNS are carried out using glial cultures. Initially the levels of LIX from U18666a treated neuronal cultures was characterised. As levels of LIX were significantly increased in U18666a treated mixed cultures, it remained to be elucidated the cell type responsible for this change. Therefore, enriched astrocyte cultures were treated with U18666a for the same timepoint and concentrations as neuronal cultures. There was no significant increase in LIX release from astrocytes in any of the timepoints or concentrations used. However, there was a significant decrease following 24 and 48 hour U18666a treatment, and when compared to the propridium iodide staining data it can be extrapolated that astrocytes may be undergoing significant cell death at these timepoints. The results from both the time and concentration experiments reveal that U18666a is not acting directly on astrocytes to mediate LIX levels. As 17% of neuronal cultures were comprised of astrocytes and baseline LIX release from enriched astrocytes is around 600 pg/ml it can be theorised that baseline levels of LIX in mixed cultures may be due to astrocytes. It was previously found that ELR chemokines were endogenously released by a cell line with characteristics of astrocytes, but not by a cell line with characteristics of immature neurons (Lu et al., 2005). However,

in the same study LIX was not found to be released from either cell type, contrary to the findings shown here. Two hypotheses can be drawn from the experimental findings thus far; (i) U18666a treatment acts directly on neurons to increase the release of LIX from this cell type, (ii) U18666a treatment acts on neurons, which via an intermediate signal triggers the release of LIX from astrocytes (**Figure 5.18**). To further investigate the role of a neuron-astrocyte cell cross talk in the release of LIX compounds that specifically disrupt LIX release in astrocytes would be useful in future studies. As microglia are also known to release LIX, it would be of value to investigate changes in LIX levels in this cell type following U18666a stimulation. This information would give a definitive conclusion as to the cell type responsible for the oscillations in LIX levels following U18666a treatment. Pharmacological block of the CXCR2 receptor alongside U18666a treatment would reveal whether the changes in LIX levels were due to receptor stimulation, allowing elucidation of whether changes in LIX levels contribute to NPC disease pathology.

5.5.4 U18666a Induced Increases In mRNA Of LIX/IP-10 Were Reversed With Mevinolin Treatment

LIX mRNA levels were found to be increased following three hours treatment with U18666a and unchanged following treatment with cholesterol and mevinolin. Co-treatment with both U18666a and mevinolin was found to decrease U18666a mediated changes in the synthesis of LIX back to control levels (**Figure 5.13)**. In order to investigate whether these changes were specific to LIX, IP-10 mRNA levels were also analysed in these conditions with the same results observed (**Figure 5.14**). IP-10 was chosen as the chemokine also stimulates the CXCR2 receptor, and was found to be significantly increased in neuronal cultures following U18666a treatment in the initial dot blot experiments. Previously it has been shown that U18666a and pravastatin co-treatment significantly decreased caspase-3 activity compared to the effects of U18666a alone (Koh et al., 2006b). In the same study this co-treatment was also found to reverse MTT reduction caused by U18666a treatment alone. These data correlate with the reduction in IP-10 and LIX mRNA levels following mevinolin and U18666a co-treatment, by indicating statins play a protective role in reversing the damaging effects of U18666a. The same co-treatment was found to reduce U18666a mediated increase in levels of LIX back to baseline levels as analysed by LIX ELISA, showing mevinolin treatment influences chemokine production at the point of mRNA synthesis.

5.5.5 U18666A Stimulated The NFκB Pathway

Western blotting showed overall IκBα levels decreased and phosphorylated IκBα (ser32) levels increased in U18666a treated neuronal cultures, indicating activation of NFκB signalling due to U18666a (**Figure 5.16**). NFκB is constitutively active in some regions of the CNS, stimulating antioxidant enzymes and BDNF (Marini et al., 2004; Mattson and Camandola, 2001). The deregulation of NFκB has been observed in NPC disease (Bi et al., 2005). Neuronal nuclear p65 levels were reduced as was DNA binding in a mouse model of NPC disease. However, in the same study p65 levels within glia were found to be increased. Decreases in NFκB activity in neurons would decrease the transcription of neuroprotective factors (e.g BDNF), whereas increases in glial NFκB would increase inflammatory responses, when combined both would contribute to neurodegeneration. The discovery that NFκB was decreased within neurons in NPC is somewhat contradictory to the finding in this experiment. However this discrepancy may be explained by the results from another study; LIX was found to amplify proinflammatory cytokine response in rat cardiac-derived endothelial cells (CDEC), by its effects on NFκB (Chandrasekar et al., 2003). Exposure of CDEC cells to LIX activated NFκB, and pharmacological blocking of the CXCR2 receptor attenuated this LIX mediated activation. Overexpression of IKK was also found to inhibit LIX mediated NFκB activation (Chandrasekar et al., 2003). This data may account for the increase in NFκB signaling observed following U18666a treatment. The increase in levels of LIX may overcome the decreases in NFκB activation observed in NPC disease.

5.5.6 U18666A Treatment Causes Significant Demyelination Of Cerebellar Neurons

Previous studies with Npc1−/− mice revealed a time-dependent accumulation of unesterified cholesterol in every organ except the brain (Patterson et al., 1993). Subsequently, it was found that the brain's apparent failure to accumulate cholesterol was due to a balance of neuronal accumulation and non-neuronal loss resulting from demyelination (Dietschy and Turley, 2001). However, it had not been elucidated whether U18666a mimics this loss of myelination. In this chapter, cerebellar slices treated with U18666a were found to have a significantly lower level of myelination than non-treated controls. This, combined with the knowledge that U18666a causes cholesterol to accumulate within neurons, suggests that U18666a can be used to generate a slice culture model of NPC disease which may be useful for further drug discovery efforts.

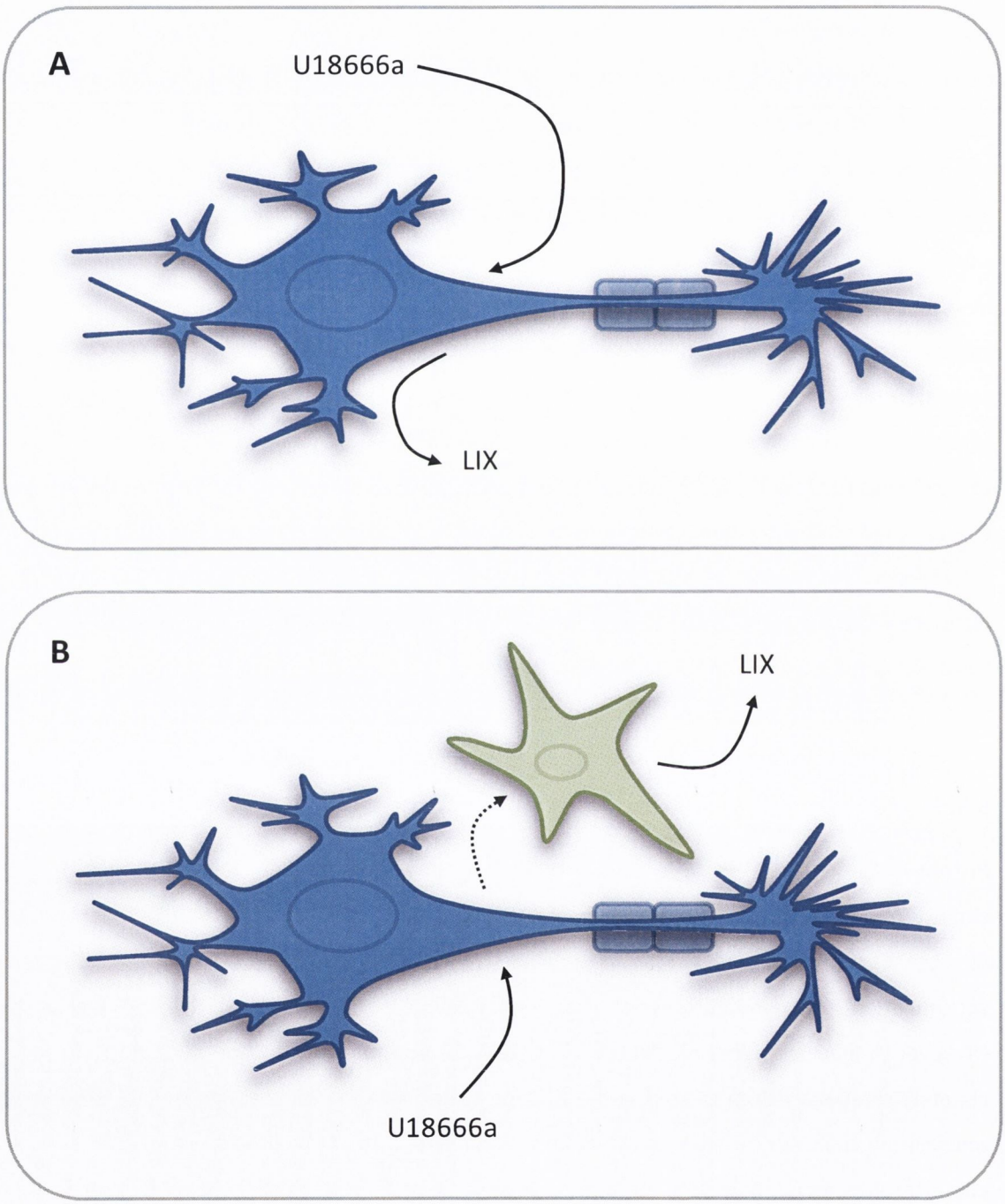

FIGURE 5.18. U18666A MEDIATED LIX RELEASE HYPOTHESIS. A. The first hypothesis for U18666a mediated increase of LIX levels is U18666a acts directly on neurons without communication with any other cell type. **B.** The second hypothesis for U18666a induced LIX release involves U18666a action on neurons, a second messenger then stimulates LIX to be released from astrocytes. Thus in pure astrocyte cultures U18666a has no effect on levels of LIX.

CHAPTER 6. DISCUSSION

6.1.0 DISCUSSION

6.1.1 OPENING REMARKS

Little is known of the specific expression and particular function of SNX8, with only two publications directly addressing these topics (Chatterjee et al., 2009; Dyve et al., 2009). SNX8 was found to co-localise with the early endosome and components of the retromer, indicating a possible role for the protein in retrograde sorting. To support this, SNX8 knockdown was found to alter retrograde trafficking of ricin and shiga toxin in an opposing manner. Following SNX8 knockdown, shiga toxin transport from the early endosome to trans-golgi network was increased, whereas ricin toxin trafficking was slightly decreased (Dyve et al., 2009). In a separate study SNX8 had been identified as a novel activator of the SREBP pathway of cholesterol homeostasis. Overexpression of SNX8 was found to overcome the insig-mediated block of the SCAP-SREBP complex, allowing SREBP to become transcriptionally active and initiate transcription of genes to upregulate cholesterol production (Chatterjee et al., 2009). Efficient endosomal sorting and cholesterol homeostasis are critical for correct brain function. Particularly, within neurons, endosomal sorting is essential for neuronal function during activation and plasticity (Sadowski et al., 2009) and disruption of cholesterol synthesis, trafficking and metabolism at the neuronal level has been implicated in a variety of neurodegenerative disorders, such as AD and NPC disease (Karten et al., 2002; Koudinov and Koudinova, 2001). With this initial information it was hypothesised that SNX8 may play a role in neuronal function via either its function as a modulator of the SREBP pathway, or by its actions on endosomal sorting. To investigate SNX8 function within the CNS, a lentivirus was generated with the addition of a GFP to the N-terminus of the protein. Endogenous SNX8 expression was first investigated and the lentivirus then used to overexpress SNX8 in varying cholesterol conditions (physiological cholesterol, high cholesterol, accumulated cholesterol and low cholesterol) to investigate SNX8 expression in relation to SREBP function. The overall findings in this thesis are summarised in (**Figure 6.1**).

6.1.2 IS DIFFERENTIAL SNX8 EXPRESSION INDICATIVE OF DIFFERENCES IN FUNCTION?

Staining of hippocampal and cerebellar slice cultures with SNX8 primary antibody indicated differences in the distribution of the protein within these two structures. Staining of dissociated neuronal cultures from both regions allowed clarification of these differences first observed in slice cultures. Within hippocampal neurons SNX8 expression was observed both in the soma and processes, whereas within cerebellar neurons SNX8 localisation was restricted to the soma (**Figure**

4.5 and 4.6). The differential expression of SNX8 within different cell types indicates a possible variance in function of SNX8. Sorting nexin expression has been explored in neurons, with members of this group found to be involved in neurite outgrowth, axonal elongation and presynaptic trafficking (Mizutani et al., 2009; Shin et al., 2007). However, only one study to date has investigated SNX expression in glia and found expression to be restricted to neurons (the SNX^{PX} member SNX12 was found to be expressed by cerebral cortex neurons and not by glia) (Mizutani et al., 2012). This information leads to the conclusion that sorting nexins (SNX8 in particular) play specific roles in the functioning of neurons within the CNS. Astrocytes synthesise the majority of cholesterol within the mature brain, thus the lack of SNX8 expression within this cell type in this thesis indicates SNX8 is not involved in regulating the SREBP pathway of cholesterol homeostasis within astrocytes. However, neurons are still able to synthesise small quantities of cholesterol once they reach maturity. Thus, it may be that SNX8 specifically modulates this pathway of cholesterol homeostasis. The finding that SNX8 expression is differentially expressed in neuronal subsets also lends the hypothesis that not only does SNX8 play a specific role within neurons to regulate cholesterol, but this function may be altered in specific neuronal types. Cerebellar neurons are highly myelinated, a process closely linked to cholesterol homeostasis, and accumulation of cholesterol within lysosomes in NPC disease results in widespread cerebellar demyelination, as well as resultant cerebellar neuron degeneration (Higashi et al., 1993). These specific cerebellar neuron functions in relation to cholesterol may account for the differential expression of SNX8 within neuronal subtypes. Further study into the role of SNX8 within cerebellar neurons, such as targeted knockdown may provide insight into the regulation of cholesterol in this environment.

6.1.3 Low And Accumulated Cholesterol Decreases SNX8 Expression; Implications For NPC

Neurons treated with mevinolin and U18666a were found to show decreased SNX8 expression from control levels (**Figure 4.9 and 4.10**). However, overexpression of GFP-SNX8 was not found to alter cholesterol localisation or levels in either mevinolin or U18666a treated neurons. This data indicates that whilst low cholesterol levels can initiate decreases in SNX8 expression, increasing SNX8 expression does feedback to directly affect cholesterol in these low cholesterol conditions. As SNX8 is an activator of the SREBP pathway, the decrease in SNX8 in both low and accumulated cholesterol conditions would lead to the downregulation of SREBP signalling, leading to a further reduction in cholesterol synthesis. The finding that SNX8 levels are decreased in an *in vitro* cellular model of NPC disease (induced by U18666a) initially lead to the hypothesis that SNX8 may be involved in disease pathology, due to its role in the SREBP pathway, and possible role in trafficking. However, the

overexpression of GFP-SNX8 did not alter U18666a mediated cholesterol accumulation, therefore indicating the decrease of SNX8 expression in this model is not directly linked to cholesterol accumulation (**Figure 6.2**).

6.1.4 Does SNX8 Overexpression In High Cholesterol Conditions Cause Changes in Trafficking?

Overexpression of SNX8 in neurons (in a high cholesterol environment) was found to both decrease levels and alter localisation of unesterified cholesterol (**Figure 4.15**), whereas high cholesterol levels had no direct influence on endogenous SNX8 levels (**Figure 4.8**). The changes in unesterified cholesterol localisation following U18666a treatments were observed to be similar to that of the staining observed in U18666a treated cells. Previously, the knockdown of SNX8 in HeLa cells was found to alter the trafficking of Shiga and Ricin toxin (Dyve et al., 2009), therefore it may be hypothesised that the overexpression of SNX8 specifically in high cholesterol levels may tigger changes in cholesterol trafficking. As SNX8 was implicated in retrograde sorting via its colocalisation with the early endosome and retromer components (Dyve et al., 2009), it may be postulated that SNX8 overexpression influences the trafficking of cholesterol via the retrograde pathway. Further elucidation of the specific function of SNX8 within sorting pathways may provide more information into the accumulation of cholesterol obseved in this study.

6.1.5 Why Are Chemokine Levels Increased In A Neuronal Model Of NPC Disease?

Chemokines attract leukocytes to sites of inflammation, CC chemokines specifically attract monocytes and T cells, where as CXC chemokines have a higher affinity for neutrophils (Steinke and Borish, 2006). In order for chemokine release in the CNS to influence leukocyte infiltration, the blood-brain barrier must be breached, and as yet to our knowledge the permeability of the BBB in NPC disease has not been investigated. Chemokine receptors are also expressed by cells of the CNS, and both astrocytes and microglia are known to secrete chemokines (Aravalli et al., 2005; Sheridan and Dev, 2012). This information leads to the hypothesis that chemokines act within the CNS in NPC disease to stimulate glial activation and neurodegeneration. Activated glia have been observed in several brain regions of $NPC^{-/-}$ mice, preceding the onset of neurodegeneration (Baudry et al., 2003). This was coupled with an increase in IL-1β levels, suggesting that glial activation may be causally related to neuronal degeneration. The accumulation of sphingolipids and cholesterol within the lysosome of neuronal cells in NPC disease results in neurodegeneration via a currently unknown

mechanism (Higashi et al., 1993). Recently focus has shifted away from direct cholesterol effects of NPC disease to the hypothesis that neuroinflammation may be contributing to the cell death observed (Iftakhar et al., 2009). In this thesis the compound U18666a was used to treat neuronal cultures to generate an *in vitro* cell model of NPC disease, and changes in chemokine levels were observed. Following 48 hours treatment with U18666a, neuronal cultures were found to have increased levels of seven chemokines (RANTES, IP-10, MIP-1α, MIP-3α, CINC-1, MIG and LIX) (**Figure 5.6-5.8**). No cytokines were found to be increased at this timepoint, whereas TNF-α levels were found to be increased following the same time and concentration of U18666a in a mouse macrophage cell line (Iftakhar et al., 2009). This data indicates the inflammatory profile elicited by U18666a treatment is cell and environment specific. Future studies investigating cytokine and chemokine release following different treatment times with U18666a as in the case of LIX would provide greater characterisation of the inflammatory signals produced in an NPC model, thus may highlight potential therapeutic targets for the treatment of the inflammatory symptoms of NPC disease, such as the pharmacological blocking of a specific chemokine receptor.

6.1.6 How May An Increase In Levels Of LIX Be Linked To Neurodegeneration?

The time and dose dependent increases in neuronal LIX levels following U18666a treatment indicate a role for this chemokine in NPC disease. Augmented LIX levels have been observed in human pancreatic cancer, where LIX levels were found to be directly correlated with shorter patient survival times (Li et al., 2011). Interestingly, LIX levels were found also to be elevated in the serum of patients with hypercholesterolemia (Yang et al., 2010). This association was found to be independent of percentage body fat and body mass index (BMI), indicating that LIX may not just be increased as a direct effect of the low-level chronic inflammation associated with obesity, but may be related to the rise in cholesterol within the blood. In the CNS, LIX has been found to be increased in the CSF of children with bacterial meningitis as well as patients with ischaemic stroke where LIX levels correlated with the size of early brain damage detected by computed tomography (CT) (Zaremba et al., 2006; Zwijnenburg et al., 2003). These studies demonstrate LIX levels to be increased in cases of inflammation and neurodegeneration. However, recently it has been observed that decreases in LIX can also be detrimental to neuron survival. Reduced expression of CXCL5/LIX by rat oligodendrocytic cells activated neuronal mitogen-activated protein kinases (MAPK) and glycogen synthase kinase (GSK3) pathways resulting in neuronal apoptosis in response to the depletion of CXCL5/LIX signaling (Merabova et al., 2012). Taken together this data suggests that LIX is critical for

neuronal survival, but high levels as observed in U18666a treated neurons can contribute to neurodegeneration.

6.1.7 Which CNS Cell Type Is Contributing To U18666a Mediated LIX Release?

LIX levels were not observed to change following U18666a treatment of enriched astrocyte cultures (**Figure 5.12**). These glial cells may account for the baseline levels of LIX present in neuronal cultures, or it may also be possible that U18666a acts on neurons and via a second messenger to cause LIX release from astrocytes (**Figure 6.1**). Microglia have been observed to release LIX via the activation of the TLR2 receptor (Aravalli et al., 2005) and as approximately 3% of the neuronal cultures prepared in this thesis were comprised of microglia, the contribution of this cell type to LIX levels remains to be characterised. As previously mentioned oligodendrocytes are known to release LIX (Merabova et al., 2012). Oligodendrocytes are the cells responsible for myelination, a process heavily regulated by cholesterol homeostasis (both of which are defective in NPC disease). The contribution of oligodendrocytes to U18666a mediated LIX release would provide further insight into the inflammatory aspect of NPC disease. Neuronal cultures show increased LIX levels following U18666a treatment. CXCR2 receptors are known to be expressed at high levels by neurons and oligodendrocytes in various brain regions (Horuk et al., 1997; Omari et al., 2005). It may be hypothesised that in NPC disease, LIX release is increased from glia, as a direct result of inflammation. This released LIX can then act on neurons and oligodendrocytes via interaction with the CXCR2 receptor to trigger the demyelination and neurodegeneration observed in NPC disease.

6.1.8 Why Is NFκB Signalling Activated By U18666a In Neurons?

U18666a was found to decrease total IκBα levels and increase phosphorlyated IκBα levels in neurons (**Figure 5.16**). This data led to the hypothesis that the NFκB pathway is activated following U18666a treatment. Further exploration of U18666a effects on other aspects of NFκB signalling, such as p65 translocation would allow full corroboration that the NFκB pathway is activated in this model of NPC disease. Exposure of CDEC cells to LIX was found to stimulate pro-inflammatory cytokine production (Chandrasekar et al., 2003). LIX was found to upregulate mRNA expression of TNF-α and IL-1β, and treatment with IL-10 was found to reverse LIX mediated increases in cytokine production. Levels of TNF-α have also been observed to increase in U18666a treated mouse macrophage cells. This increase may now be attributed to the possible action of LIX (Iftakhar et al., 2009). It may be further hypothesised that IL-10 treatment may decrease the inflammatory response observed following

U18666a treatment. LIX was found to directly stimulate NFκB via interaction with the CXCR2 receptor (Iftakhar et al., 2009). Pharmacological blockade of the CXCR2 receptor and inhibition of G_i protein signalling attenuated the LIX mediated NFκB activation. The same tools would be of use in U18666a treated neurons to distinguish if the upregulation of NFκB is mediated by LIX.

6.1.9 How Does Statin Treatment Decrease Chemokine mRNA Synthesis?

Mevinolin treatment was found to reverse the U18666a mediated increases in IP-10 and LIX mRNA levels, as well as LIX release (**Figure 5.13 and 5.14**). Previously, pravastatin was found to reduce neuronal death following U18666a treatment via caspase-3 reduction (Koh et al., 2006a). Together, these data suggest a role for statins in the control of neuroinflammation. In a mouse model of EAE, lovastatin treatment was found to inhibit leukocyte infiltration into the CNS due to a reduction in endothelial cell adhesion molecules (Stanislaus et al., 2001). This information combined with the discovery that mevinolin treatment inhibits chemokine production, illustrates a twofold mechanism for the reduction in leukocyte infiltration in neuroinflammation. Statin induced attenuation of disease in a relapsing and remitting mouse model of EAE was found to be partially reversed by addition of exogenous mevalonate (statin treatment reduces mevalonate). This indicates it is via direct function on the pathway of cholesterol production that statins exert their neuroprotective qualities.

6.2.0 Closing Remarks

The data in this thesis has contributed to unravelling the role of SNX8 in cholesterol homeostasis. Endogenous SNX8 levels are modulated in low cholesterol conditions and overexpression of SNX8 can itself alter cholesterol localisation in high cholesterol conditions. This finding shows promise for the manipulation of SNX8 (as a modulator of the SREBP pathway) to explore cholesterol homeostasis within neurons, and further exploration into the role of SNX8 in NPC disease. Chemokine levels were found to be increased in a U18666a model of NPC disease, combined with activation of the NFκB pathway of signalling at 16 hrs, further contributing to the inflammatory aspect of NPC disease. Further investigation into the trafficking role of SNX8 would provide insight into the specific function of the protein within cholesterol homeostasis, and manipulation of this function may be useful in diseases with defects in cholesterol homeostasis. The finding that LIX levels are increased in a model of NPC disease indicates a potential therapeutic target for the treatment of the inflammatory symptoms through either inhibiting LIX production pharmacologically blocking the LIX receptor

CXCR2. Taken together, this data highlights the role of SNX8 in cholesterol homeostasis, a process that is disregulated in NPC disease, and the role of chemokines in this neurodegenerative disease.

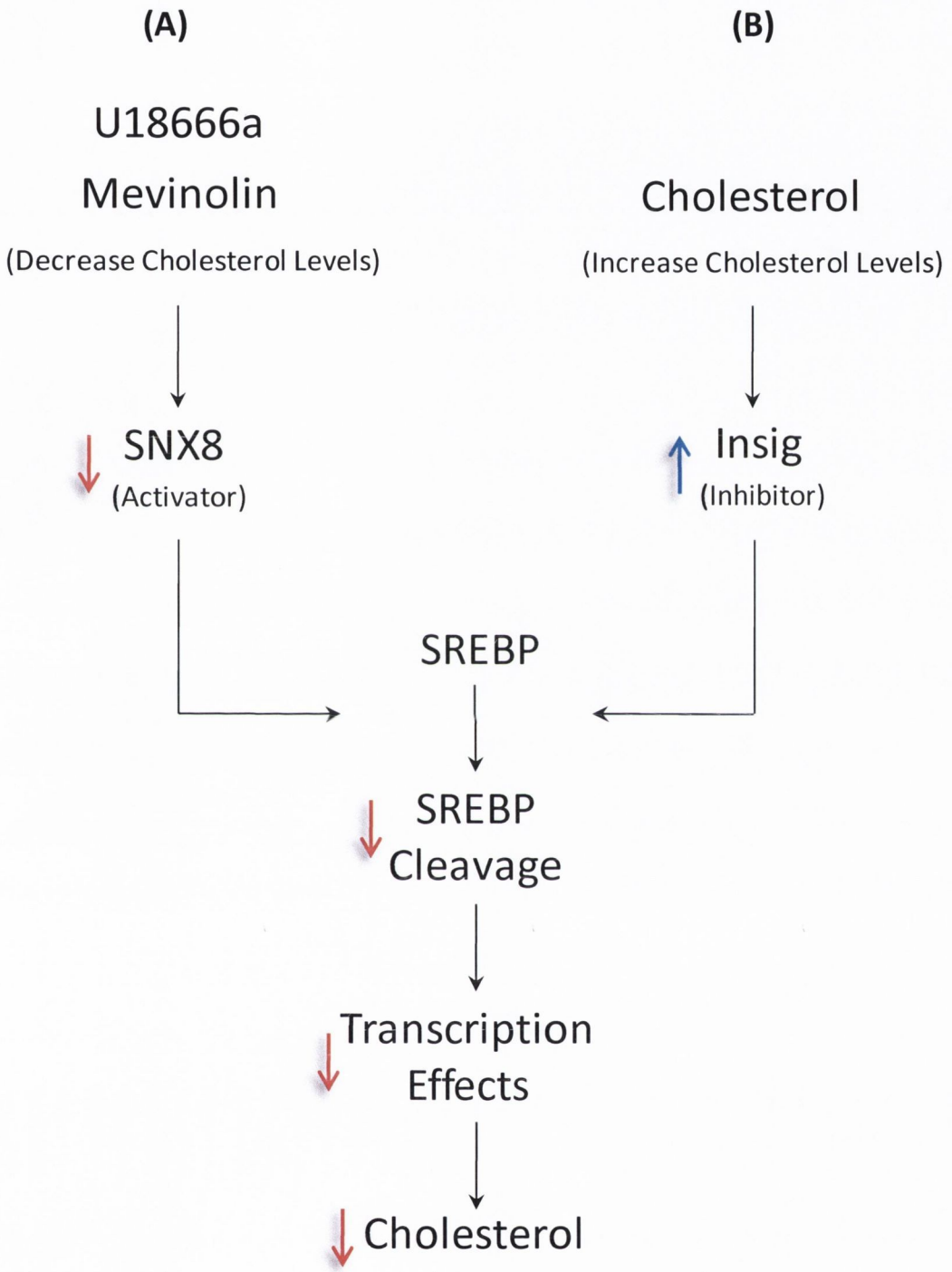

FIGURE 6.1. HYPOTHESIS OF SNX8 EXPRESSION AND SREBP FUNCTION. Pathway **(A)** demonstrates U18666a and mevinolin both act to decrease cholesterol levels, which in turn decreases SNX8 levels. This then leads to a decreased level of SREBP cleavage, a decrease of transcriptionally active SREBP, and finally a decrease in cholesterol production. **(B)** An increase in intracellular cholesterol causes Insig to interact with SCAP decreasing SREBP cleavage, resulting in reduced cholesterol production. This pathway is independent of SNX8 function.

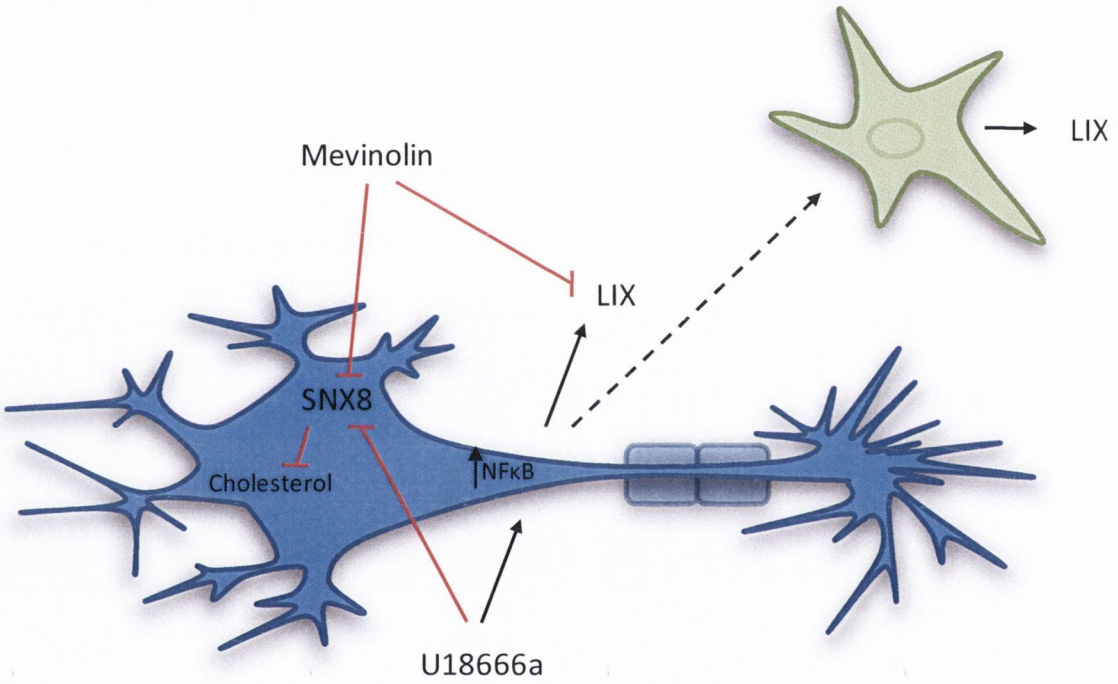

FIGURE 6.2. THE FUNCTION OF SNX8 AND LIX IN A CELLULAR MODEL OF NPC DISEASE. U18666a acts on neurons to cause a decrease in SNX8 expression and an increase in NFκB activity and LIX release (via either direct release, or via second messenger mediated release from astrocytes). Mevinolin acts to both decrease SNX8 expression in neurons and decrease LIX levels. In high cholesterol conditions overexpression of SNX8 causes the accumulation and overall decrease of unesterified cholesterol. This data combined highlights the role of SNX8 in cholesterol homeostasis within neurons, a process that when disturbed may result in changes in chemokine release.

BIBLIOGRAPHY

Adachi, M., Volk, B. W., Schneck, L., 1976. Animal model of human disease: Niemann-Pick Disease type C. Am J Pathol 85, 229-232.

Akira, S., Taga, T., Kishimoto, T., 1993. Interleukin-6 in biology and medicine. Adv Immunol 54, 1-78.

Ambrosini, E., Aloisi, F., 2004. Chemokines and glial cells: a complex network in the central nervous system. Neurochem Res 29, 1017-1038.

Aravalli, R. N., Hu, S., Rowen, T. N., Palmquist, J. M., Lokensgard, J. R., 2005. Cutting edge: TLR2-mediated proinflammatory cytokine and chemokine production by microglial cells in response to herpes simplex virus. J Immunol 175, 4189-4193.

Bajetto, A., Bonavia, R., Barbero, S., Florio, T., Schettini, G., 2001. Chemokines and their receptors in the central nervous system. Front Neuroendocrinol 22, 147-184.

Bajetto, A., Bonavia, R., Barbero, S., Schettini, G., 2002. Characterization of chemokines and their receptors in the central nervous system: physiopathological implications. J Neurochem 82, 1311-1329.

Bargmann, C. I., Horvitz, H. R., 1991. Control of larval development by chemosensory neurons in Caenorhabditis elegans. Science 251, 1243-1246.

Bascunan-Castillo, E. C., Erickson, R. P., Howison, C. M., Hunter, R. J., Heidenreich, R. H., Hicks, C., Trouard, T. P., Gillies, R. J., 2004. Tamoxifen and vitamin E treatments delay symptoms in the mouse model of Niemann-Pick C. J Appl Genet 45, 461-467.

Baudry, M., Yao, Y., Simmons, D., Liu, J., Bi, X., 2003. Postnatal development of inflammation in a murine model of Niemann-Pick type C disease: immunohistochemical observations of microglia and astroglia. Exp Neurol 184, 887-903.

Bengoechea-Alonso, M. T., Ericsson, J., 2007. SREBP in signal transduction: cholesterol metabolism and beyond. Curr Opin Cell Biol 19, 215-222.

Bhalla, A., Vetanovetz, C. P., Morel, E., Chamoun, Z., Di Paolo, G., Small, S. A., 2012. The location and trafficking routes of the neuronal retromer and its role in amyloid precursor protein transport. Neurobiol Dis 47, 126-134.

Bhatia, V. K., Madsen, K. L., Bolinger, P. Y., Kunding, A., Hedegard, P., Gether, U., Stamou, D., 2009. Amphipathic motifs in BAR domains are essential for membrane curvature sensing. EMBO J.

Bi, X., Liu, J., Yao, Y., Baudry, M., Lynch, G., 2005. Deregulation of the phosphatidylinositol-3 kinase signaling cascade is associated with neurodegeneration in Npc1-/- mouse brain. Am J Pathol 167, 1081-1092.

Bjorkhem, I., Meaney, S., 2004. Brain cholesterol: long secret life behind a barrier. Arterioscler Thromb Vasc Biol 24, 806-815.

Block, M. L., Zecca, L., Hong, J. S., 2007. Microglia-mediated neurotoxicity: uncovering the molecular mechanisms. Nat Rev Neurosci 8, 57-69.

Blomer, U., Naldini, L., Kafri, T., Trono, D., Verma, I. M., Gage, F. H., 1997. Highly efficient and sustained gene transfer in adult neurons with a lentivirus vector. J Virol 71, 6641-6649.

Boersma, M. C., Dresselhaus, E. C., De Biase, L. M., Mihalas, A. B., Bergles, D. E., Meffert, M. K., 2011. A requirement for nuclear factor-kappaB in developmental and plasticity-associated synaptogenesis. J Neurosci 31, 5414-5425.

Bonanomi, D., Benfenati, F., Valtorta, F., 2006. Protein sorting in the synaptic vesicle life cycle. Prog Neurobiol 80, 177-217.

Bonifacino, J. S., Rojas, R., 2006. Retrograde transport from endosomes to the trans-Golgi network. Nat Rev Mol Cell Biol 7, 568-579.

Bowers, K., Stevens, T. H., 2005. Protein transport from the late Golgi to the vacuole in the yeast Saccharomyces cerevisiae. Biochim Biophys Acta 1744, 438-454.

Braun, V., Wong, A., Landekic, M., Hong, W. J., Grinstein, S., Brumell, J. H., 2010. Sorting nexin 3 (SNX3) is a component of a tubular endosomal network induced by Salmonella and involved in maturation of the Salmonella-containing vacuole. Cell Microbiol 12, 1352-1367.

Bravo, J., Karathanassis, D., Pacold, C. M., Pacold, M. E., Ellson, C. D., Anderson, K. E., Butler, P. J., Lavenir, I., Perisic, O., Hawkins, P. T., Stephens, L., Williams, R. L., 2001. The crystal structure of the PX

domain from p40(phox) bound to phosphatidylinositol 3-phosphate. Mol Cell 8, 829-839.

Brown, D. E., Thrall, M. A., Walkley, S. U., Wenger, D. A., Mitchell, T. W., Smith, M. O., Royals, K. L., March, P. A., Allison, R. W., 1994. Feline Niemann-Pick disease type C. Am J Pathol 144, 1412-1415.

Burger, C., Nash, K., Mandel, R. J., 2005. Recombinant adeno-associated viral vectors in the nervous system. Hum Gene Ther 16, 781-791.

Burton, E. A., Fink, D. J., Glorioso, J. C., 2005. Replication-defective genomic HSV gene therapy vectors: design, production and CNS applications. Curr Opin Mol Ther 7, 326-336.

Byrnes, A. P., Rusby, J. E., Wood, M. J., Charlton, H. M., 1995. Adenovirus gene transfer causes inflammation in the brain. Neuroscience 66, 1015-1024.

Cai, L., Loo, L. S., Atlashkin, V., Hanson, B. J., Hong, W., 2011. Deficiency of Sorting Nexin 27 (SNX27) Leads to Growth Retardation and Elevated Levels of N-methyl-D-aspartate (NMDA) Receptor 2C (NR2C). Mol Cell Biol.

Carlton, J., Bujny, M., Peter, B. J., Oorschot, V. M., Rutherford, A., Mellor, H., Klumperman, J., McMahon, H. T., Cullen, P. J., 2004. Sorting nexin-1 mediates tubular endosome-to-TGN transport through coincidence sensing of high- curvature membranes and 3-phosphoinositides. Curr Biol 14, 1791-1800.

Cavallini, G., Massarani, E., 1951. [Relation between chemical constitution and biological activity; new vasodilators and curare-simulants derived from sex hormones]. Farmaco 6, 291-299.

Cavazzana-Calvo M, H.-B. S., de Saint Basile G et al, 2000. Gene therapy of human severe combined immunodeficiency (SCID)-X1 disease Science 288, 669-672.

Cenedella, R. J., 1980. Concentration-dependent effects of AY-9944 and U18666A on sterol synthesis in brain. Variable sensitivities of metabolic steps. Biochem Pharmacol 29, 2751-2754.

Cenedella, R. J., 1980. Concentration-dependent effects of AY-9944 and U18666A on sterol synthesis in brain. Variable sensitivities of metabolic steps. Biochem Pharmacol 29, 2751-2754.

Cenedella, R. J., 2009. Cholesterol synthesis inhibitor U18666A and the role of sterol metabolism and trafficking in numerous pathophysiological processes. Lipids 44, 477-487.

Cenedella, R. J., Bierkamper, G. G., 1979. Mechanism of cataract production by 3-beta(2-diethylaminoethoxy) androst-5-en-17-one hydrochloride, U18666A: an inhibitor of cholesterol biosynthesis. Exp Eye Res 28, 673-688.

Chandel, N. S., Trzyna, W. C., McClintock, D. S., Schumacker, P. T., 2000. Role of oxidants in NF-kappa B activation and TNF-alpha gene transcription induced by hypoxia and endotoxin. J Immunol 165, 1013-1021.

Chandrasekar, B., Melby, P. C., Sarau, H. M., Raveendran, M., Perla, R. P., Marelli-Berg, F. M., Dulin, N. O., Singh, I. S., 2003. Chemokine-cytokine cross-talk. The ELR+ CXC chemokine LIX (CXCL5) amplifies a proinflammatory cytokine response via a phosphatidylinositol 3-kinase-NF-kappa B pathway. J Biol Chem 278, 4675-4686.

Chang, J. Y., Phelan, K. D., Chavis, J. A., 1998. Neurotoxicity of 25-OH-cholesterol on sympathetic neurons. Brain Res Bull 45, 615-622.

Charo, I. F., Ransohoff, R. M., 2006. The many roles of chemokines and chemokine receptors in inflammation. N Engl J Med 354, 610-621.

Chatterjee, S., Szustakowski, J. D., Nanguneri, N. R., Mickanin, C., Labow, M. A., Nohturfft, A., Dev, K. K., Sivasankaran, R., 2009. Identification of Novel Genes and Pathways Regulating SREBP Transcriptional Activity. PLoS One 4, -.

Cheung, N. S., Koh, C. H., Bay, B. H., Qi, R. Z., Choy, M. S., Li, Q. T., Wong, K. P., Whiteman, M., 2004. Chronic exposure to U18666A induces apoptosis in cultured murine cortical neurons. Biochem Biophys Res Commun 315, 408-417.

Cho, W. J., Jeremic, A., Jin, H., Ren, G., Jena, B. P., 2007. Neuronal fusion pore assembly requires membrane cholesterol. Cell Biol Int 31, 1301-1308.

Choi, D. Y., Lee, J. W., Lin, G., Lee, Y. K., Lee, Y. H., Choi, I. S., Han, S. B., Jung, J. K., Kim, Y. H.,

Kim, K. H., Oh, K. W., Hong, J. T., Lee, M. S., 2012. Obovatol attenuates LPS-induced memory impairments in mice via inhibition of NF-kappaB signaling pathway. Neurochem Int 60, 68-77.

Chotard, C., Salecker, I., 2004. Neurons and glia: team players in axon guidance. Trends Neurosci 27, 655-661.

Coil DA, M. A., 2004. Phosphatidylserine is not the cell surface receptor for vesicular stomatitis virus. J Virol 78, 10920-10926.

Conibear, E., Stevens, T. H., 1998. Multiple sorting pathways between the late Golgi and the vacuole in yeast. Biochim Biophys Acta 1404, 211-230.

Cozier, G. E., Carlton, J., McGregor, A. H., Gleeson, P. A., Teasdale, R. D., Mellor, H., Cullen, P. J., 2002. The phox homology (PX) domain-dependent, 3-phosphoinositide-mediated association of sorting nexin-1 with an early sorting endosomal compartment is required for its ability to regulate epidermal growth factor receptor degradation. J Biol Chem 277, 48730-48736.

Cullen, P. J., 2008. Endosomal sorting and signalling: an emerging role for sorting nexins. Nat Rev Mol Cell Biol 9, 574-582.

Davidson, B. L., Stein, C. S., Heth, J. A., Martins, I., Kotin, R. M., Derksen, T. A., Zabner, J., Ghodsi, A., Chiorini, J. A., 2000. Recombinant adeno-associated virus type 2, 4, and 5 vectors: transduction of variant cell types and regions in the mammalian central nervous system. Proc Natl Acad Sci U S A 97, 3428-3432.

Dawson, J. C., Legg, J. A., Machesky, L. M., 2006. Bar domain proteins: a role in tubulation, scission and actin assembly in clathrin-mediated endocytosis. Trends Cell Biol 16, 493-498.

Demer, L., Tintut, Y., 2011. The roles of lipid oxidation products and receptor activator of nuclear factor-kappaB signaling in atherosclerotic calcification. Circ Res 108, 1482-1493.

Dietschy, J. M., Turley, S. D., 2001. Cholesterol metabolism in the brain. Curr Opin Lipidol 12, 105-112.

Dietschy, J. M., Turley, S. D., 2004. Thematic review series: brain Lipids. Cholesterol metabolism in the central nervous system during early development and in the mature animal. J Lipid Res 45, 1375-1397.

Dyve, A. B., Bergan, J., Utskarpen, A., Sandvig, K., 2009. Sorting nexin 8 regulates endosome-to-Golgi transport. Biochem Biophys Res Commun 390, 109-114.

Ekena, K., Stevens, T. H., 1995. The Saccharomyces cerevisiae MVP1 gene interacts with VPS1 and is required for vacuolar protein sorting. Mol Cell Biol 15, 1671-1678.

Escors D, B. K., 2010. Lentiviral vectors in gene therapy: their current status and future potential. Arch Immunol Ther Exp 58, 107-119.

Fan, Q. W., Yu, W., Senda, T., Yanagisawa, K., Michikawa, M., 2001. Cholesterol-dependent modulation of tau phosphorylation in cultured neurons. J Neurochem 76, 391-400.

Fassbender, K., Simons, M., Bergmann, C., Stroick, M., Lutjohann, D., Keller, P., Runz, H., Kuhl, S., Bertsch, T., von Bergmann, K., Hennerici, M., Beyreuther, K., Hartmann, T., 2001. Simvastatin strongly reduces levels of Alzheimer's disease beta -amyloid peptides Abeta 42 and Abeta 40 in vitro and in vivo. Proc Natl Acad Sci U S A 98, 5856-5861.

Filipovic, R., Jakovcevski, I., Zecevic, N., 2003. GRO-alpha and CXCR2 in the human fetal brain and multiple sclerosis lesions. Dev Neurosci 25, 279-290.

Flier, J., Boorsma, D. M., van Beek, P. J., Nieboer, C., Stoof, T. J., Willemze, R., Tensen, C. P., 2001. Differential expression of CXCR3 targeting chemokines CXCL10, CXCL9, and CXCL11 in different types of skin inflammation. J Pathol 194, 398-405.

Fonseca, A. C., Resende, R., Oliveira, C. R., Pereira, C. M., 2010. Cholesterol and statins in Alzheimer's disease: current controversies. Exp Neurol 223, 282-293.

Fraefel, C., Jacoby, D. R., Breakefield, X. O., 2000. Herpes simplex virus type 1-based amplicon vector systems. Adv Virus Res 55, 425-451.

Frost, A., Unger, V. M., De Camilli, P., 2009. The BAR Domain Superfamily: Membrane-Molding Macromolecules. Cell 137, 191-196.

Gerdes, C. A., Castro, M. G., Lowenstein, P. R., 2000. Strong promoters are the key to

highly efficient, noninflammatory and noncytotoxic adenoviral-mediated transgene delivery into the brain in vivo. Mol Ther 2, 330-338.

Gibbs, J. S., Regier, D. A., Desrosiers, R. C., 1994. Construction and in vitro properties of HIV-1 mutants with deletions in "nonessential" genes. AIDS Res Hum Retroviruses 10, 343-350.

Glabinski, A. R., Ransohoff, R. M., 1999. Sentries at the gate: chemokines and the blood-brain barrier. J Neurovirol 5, 623-634.

Grace, P. M., Rolan, P. E., Hutchinson, M. R., 2011. Peripheral immune contributions to the maintenance of central glial activation underlying neuropathic pain. Brain Behav Immun 25, 1322-1332.

Griffin, L. D., Gong, W., Verot, L., Mellon, S. H., 2004. Niemann-Pick type C disease involves disrupted neurosteroidogenesis and responds to allopregnanolone. Nat Med 10, 704-711.

Griffiths, G., Simons, K., 1986. The trans Golgi network: sorting at the exit site of the Golgi complex. Science 234, 438-443.

Haft, C. R., de la Luz Sierra, M., Bafford, R., Lesniak, M. A., Barr, V. A., Taylor, S. I., 2000. Human orthologs of yeast vacuolar protein sorting proteins Vps26, 29, and 35: assembly into multimeric complexes. Mol Biol Cell 11, 4105-4116.

Harms, A. S., Barnum, C. J., Ruhn, K. A., Varghese, S., Trevino, I., Blesch, A., Tansey, M. G., 2011. Delayed dominant-negative TNF gene therapy halts progressive loss of nigral dopaminergic neurons in a rat model of Parkinson's disease. Mol Ther 19, 46-52.

Hayashi, H., Campenot, R. B., Vance, D. E., Vance, J. E., 2004. Glial lipoproteins stimulate axon growth of central nervous system neurons in compartmented cultures. J Biol Chem 279, 14009-14015.

Hayden, M. S., Ghosh, S., 2012. NF-kappaB, the first quarter-century: remarkable progress and outstanding questions. Genes Dev 26, 203-234.

Herrup, K., Yang, Y., 2007. Cell cycle regulation in the postmitotic neuron: oxymoron or new biology? Nat Rev Neurosci 8, 368-378.

Hierro, A., Rojas, A. L., Rojas, R., Murthy, N., Effantin, G., Kajava, A. V., Steven, A. C., Bonifacino, J. S., Hurley, J. H., 2007. Functional architecture of the retromer cargo-recognition complex. Nature 449, 1063-1067.

Higashi, Y., Murayama, S., Pentchev, P. G., Suzuki, K., 1993. Cerebellar degeneration in the Niemann-Pick type C mouse. Acta Neuropathol 85, 175-184.

Horuk, R., Martin, A. W., Wang, Z., Schweitzer, L., Gerassimides, A., Guo, H., Lu, Z., Hesselgesser, J., Perez, H. D., Kim, J., Parker, J., Hadley, T. J., Peiper, S. C., 1997. Expression of chemokine receptors by subsets of neurons in the central nervous system. J Immunol 158, 2882-2890.

Horvath, L., van Marion, I., Tai, K., Nielsen, T. T., Lundberg, C., 2011. Knockdown of GAD67 protein levels normalizes neuronal activity in a rat model of Parkinson's disease. J Gene Med 13, 188-197.

Hua, X., Nohturfft, A., Goldstein, J. L., Brown, M. S., 1996. Sterol resistance in CHO cells traced to point mutation in SREBP cleavage-activating protein. Cell 87, 415-426.

Huang, X., Warren, J. T., Buchanan, J., Gilbert, L. I., Scott, M. P., 2007. Drosophila Niemann-Pick type C-2 genes control sterol homeostasis and steroid biosynthesis: a model of human neurodegenerative disease. Development 134, 3733-3742.

Iftakhar, E. K. I., Koide, N., Hassan, F., Noman, A. S., Dagvadorj, J., Tumurkhuu, G., Naiki, Y., Komatsu, T., Yoshida, T., Yokochi, T., 2009. Novel mechanism of U18666A-induced tumour necrosis factor-alpha production in RAW 264.7 macrophage cells. Clin Exp Immunol 155, 552-558.

Ikeda, Y., Iguchi, H., Nakata, M., Ioka, R. X., Tanaka, T., Iwasaki, S., Magoori, K., Takayasu, S., Yamamoto, T. T., Kodama, T., Yada, T., Sakurai, T., Yanagisawa, M., Sakai, J., 2005. Identification of N-arachidonylglycine, U18666A, and 4-androstene-3,17-dione as novel insulin Secretagogues. Biochem Biophys Res Commun 333, 778-786.

Imanifooladi, A. A., Yazdani, S., Nourani, M. R., 2010. The role of nuclear factor-kappaB in inflammatory lung disease. Inflamm Allergy Drug Targets 9, 197-205.

Irisawa, M., Inoue, J., Ozawa, N., Mori, K., Sato, R., 2009. The sterol-sensing endoplasmic reticulum (ER) membrane protein TRC8 hampers ER to Golgi transport of sterol regulatory element-binding protein-2 (SREBP-2)/SREBP cleavage-activated protein and reduces SREBP-2 cleavage. J Biol Chem 284, 28995-29004.

Jeyakumar, M., Smith, D. A., Williams, I. M., Borja, M. C., Neville, D. C., Butters, T. D., Dwek, R. A., Platt, F. M., 2004. NSAIDs increase survival in the Sandhoff disease mouse: synergy with N-butyldeoxynojirimycin. Ann Neurol 56, 642-649.

Jick, H., Zornberg, G. L., Jick, S. S., Seshadri, S., Drachman, D. A., 2000. Statins and the risk of dementia. Lancet 356, 1627-1631.

Johannes, L., Wunder, C., 2011. The SNXy flavours of endosomal sorting. Nat Cell Biol 13, 884-886.

Jones, L. L., Banati, R. B., Graeber, M. B., Bonfanti, L., Raivich, G., Kreutzberg, G. W., 1997. Population control of microglia: does apoptosis play a role? J Neurocytol 26, 755-770.

Joubert, L., Hanson, B., Barthet, G., Sebben, M., Claeysen, S., Hong, W., Marin, P., Dumuis, A., Bockaert, J., 2004. New sorting nexin (SNX27) and NHERF specifically interact with the 5-HT4a receptor splice variant: roles in receptor targeting. J Cell Sci 117, 5367-5379.

Karten, B., Hayashi, H., Francis, G. A., Campenot, R. B., Vance, D. E., Vance, J. E., 2005. Generation and function of astroglial lipoproteins from Niemann-Pick type C1-deficient mice. Biochem J 387, 779-788.

Karten, B., Peake, K. B., Vance, J. E., 2009. Mechanisms and consequences of impaired lipid trafficking in Niemann-Pick type C1-deficient mammalian cells. Biochim Biophys Acta 1791, 659-670.

Karten, B., Vance, D. E., Campenot, R. B., Vance, J. E., 2002. Cholesterol accumulates in cell bodies, but is decreased in distal axons, of Niemann-Pick C1-deficient neurons. J Neurochem 83, 1154-1163.

Kielian, T., Barry, B., Hickey, W. F., 2001. CXC chemokine receptor-2 ligands are required for neutrophil-mediated host defense in experimental brain abscesses. J Immunol 166, 4634-4643.

Klug, A., Borst, J. G., Carlson, B. A., Kopp-Scheinpflug, C., Klyachko, V. A., Xu-Friedman, M. A., 2012. How do short-term changes at synapses fine-tune information processing? J Neurosci 32, 14058-14063.

Koh, C. H., Cheung, N. S., 2006. Cellular mechanism of U18666A-mediated apoptosis in cultured murine cortical neurons: bridging Niemann-Pick disease type C and Alzheimer's disease. Cell Signal 18, 1844-1853.

Koh, C. H., Qi, R. Z., Qu, D., Melendez, A., Manikandan, J., Bay, B. H., Duan, W., Cheung, N. S., 2006a. U18666A-mediated apoptosis in cultured murine cortical neurons: role of caspases, calpains and kinases. Cell Signal 18, 1572-1583.

Koh, C. H., Whiteman, M., Li, Q. X., Halliwell, B., Jenner, A. M., Wong, B. S., Laughton, K. M., Wenk, M., Masters, C. L., Beart, P. M., Bernard, O., Cheung, N. S., 2006b. Chronic exposure to U18666A is associated with oxidative stress in cultured murine cortical neurons. J Neurochem 98, 1278-1289.

Koudinov, A. R., Koudinova, N. V., 2001. Essential role for cholesterol in synaptic plasticity and neuronal degeneration. FASEB J 15, 1858-1860.

Lattanzi, A., Neri, M., Maderna, C., di Girolamo, I., Martino, S., Orlacchio, A., Amendola, M., Naldini, L., Gritti, A., 2010. Widespread enzymatic correction of CNS tissues by a single intracerebral injection of therapeutic lentiviral vector in leukodystrophy mouse models. Hum Mol Genet 19, 2208-2227.

Laudanna, C., Kim, J. Y., Constantin, G., Butcher, E., 2002. Rapid leukocyte integrin activation by chemokines. Immunol Rev 186, 37-46.

Le Doux JM, D. H., Morgan JR et al, 1999. Kinetics of retrovirus production and decay. Biotechnol Bioeng 63, 654-662.

Le Gal La Salle, G., Robert, J. J., Berrard, S., Ridoux, V., Stratford-Perricaudet, L. D., Perricaudet, M., Mallet, J., 1993. An adenovirus vector for gene transfer into neurons and glia in the brain. Science 259, 988-990.

Lee, J., Retamal, C., Cuitino, L., Caruano-Yzermans, A., Shin, J. E., van Kerkhof, P.,

Marzolo, M. P., Bu, G., 2008. Adaptor protein sorting nexin 17 regulates amyloid precursor protein trafficking and processing in the early endosomes. J Biol Chem 283, 11501-11508.

Lewis PF, E. M., 1994. Passage through mitosis is required for oncoretroviruses but not for human immunodeficiency virus. J Virol 68, 510-516.

Li, A., King, J., Moro, A., Sugi, M. D., Dawson, D. W., Kaplan, J., Li, G., Lu, X., Strieter, R. M., Burdick, M., Go, V. L., Reber, H. A., Eibl, G., Hines, O. J., 2011. Overexpression of CXCL5 is associated with poor survival in patients with pancreatic cancer. Am J Pathol 178, 1340-1349.

Liao, G., Cheung, S., Galeano, J., Ji, A. X., Qin, Q., Bi, X., 2009. Allopregnanolone treatment delays cholesterol accumulation and reduces autophagic/lysosomal dysfunction and inflammation in Npc1-/- mouse brain. Brain Res 1270, 140-151.

Liscum, L., Faust, J. R., 1989. The intracellular transport of low density lipoprotein-derived cholesterol is inhibited in Chinese hamster ovary cells cultured with 3-beta-[2-(diethylamino)ethoxy]androst-5-en-17-one. J Biol Chem 264, 11796-11806.

Liu, B., Turley, S. D., Burns, D. K., Miller, A. M., Repa, J. J., Dietschy, J. M., 2009. Reversal of defective lysosomal transport in NPC disease ameliorates liver dysfunction and neurodegeneration in the npc1-/- mouse. Proc Natl Acad Sci U S A 106, 2377-2382.

Liu, B. H., Wang, X., Ma, Y. X., Wang, S., 2004. CMV enhancer/human PDGF-beta promoter for neuron-specific transgene expression. Gene Ther 11, 52-60.

Liu, L., Belkadi, A., Darnall, L., Hu, T., Drescher, C., Cotleur, A. C., Padovani-Claudio, D., He, T., Choi, K., Lane, T. E., Miller, R. H., Ransohoff, R. M., 2010. CXCR2-positive neutrophils are essential for cuprizone-induced demyelination: relevance to multiple sclerosis. Nat Neurosci 13, 319-326.

Lloyd-Evans, E., Morgan, A. J., He, X., Smith, D. A., Elliot-Smith, E., Sillence, D. J., Churchill, G. C., Schuchman, E. H., Galione, A., Platt, F. M., 2008. Niemann-Pick disease type C1 is a sphingosine storage disease that causes deregulation of lysosomal calcium. Nat Med 14, 1247-1255.

Loftus, S. K., Morris, J. A., Carstea, E. D., Gu, J. Z., Cummings, C., Brown, A., Ellison, J., Ohno, K., Rosenfeld, M. A., Tagle, D. A., Pentchev, P. G., Pavan, W. J., 1997. Murine model of Niemann-Pick C disease: mutation in a cholesterol homeostasis gene. Science 277, 232-235.

Loo, M. A., Jensen, T. J., Cui, L., Hou, Y., Chang, X. B., Riordan, J. R., 1998. Perturbation of Hsp90 interaction with nascent CFTR prevents its maturation and accelerates its degradation by the proteasome. EMBO J 17, 6879-6887.

Lowenstein, P. R., 2004. Input virion proteins: cryptic targets of antivector immune responses in preimmunized subjects. Mol Ther 9, 771-774.

Lowenstein, P. R., Thomas, C. E., Umana, P., Gerdes, C. A., Verakis, T., Boyer, O., Tondeur, S., Klatzmann, D., Castro, M. G., 2002. High-capacity,helper-dependent, "gutless" adenoviral vectors for gene transfer into brain. Methods Enzymol 346, 292-311.

Lu, W., Maheshwari, A., Misiuta, I., Fox, S. E., Chen, N., Zigova, T., Christensen, R. D., Calhoun, D. A., 2005. Neutrophil-specific chemokines are produced by astrocytic cells but not by neuronal cells. Brain Res Dev Brain Res 155, 127-134.

Lundmark, R., Carlsson, S. R., 2009. SNX9 - a prelude to vesicle release. J Cell Sci 122, 5-11.

Lunn, M. L., Nassirpour, R., Arrabit, C., Tan, J., McLeod, I., Arias, C. M., Sawchenko, P. E., Yates, J. R., 3rd, Slesinger, P. A., 2007. A unique sorting nexin regulates trafficking of potassium channels via a PDZ domain interaction. Nat Neurosci 10, 1249-1259.

Lynch, M. A., 2009. The multifaceted profile of activated microglia. Mol Neurobiol 40, 139-156.

Mailman, T., Hariharan, M., Karten, B., 2011. Inhibition of neuronal cholesterol biosynthesis with lovastatin leads to impaired synaptic vesicle release even in the presence of lipoproteins or geranylgeraniol. J Neurochem 119, 1002-1015.

Mandel, R. J., Burger, C., Snyder, R. O., 2008. Viral vectors for in vivo gene transfer in Parkinson's disease: properties and

clinical grade production. Exp Neurol 209, 58-71.

Mari, M., Bujny, M. V., Zeuschner, D., Geerts, W. J., Griffith, J., Petersen, C. M., Cullen, P. J., Klumperman, J., Geuze, H. J., 2008. SNX1 defines an early endosomal recycling exit for sortilin and mannose 6-phosphate receptors. Traffic 9, 380-393.

Marini, A. M., Jiang, X., Wu, X., Tian, F., Zhu, D., Okagaki, P., Lipsky, R. H., 2004. Role of brain-derived neurotrophic factor and NF-kappaB in neuronal plasticity and survival: From genes to phenotype. Restor Neurol Neurosci 22, 121-130.

Mattson, M. P., Camandola, S., 2001. NF-kappaB in neuronal plasticity and neurodegenerative disorders. J Clin Invest 107, 247-254.

Mauch, D. H., Nagler, K., Schumacher, S., Goritz, C., Muller, E. C., Otto, A., Pfrieger, F. W., 2001. CNS synaptogenesis promoted by glia-derived cholesterol. Science 294, 1354-1357.

Maxfield, F. R., Wustner, D., 2012. Analysis of cholesterol trafficking with fluorescent probes. Methods Cell Biol 108, 367-393.

McMahon, H. T., Gallop, J. L., 2005. Membrane curvature and mechanisms of dynamic cell membrane remodelling. Nature 438, 590-596.

Meffert, M. K., Chang, J. M., Wiltgen, B. J., Fanselow, M. S., Baltimore, D., 2003. NF-kappa B functions in synaptic signaling and behavior. Nat Neurosci 6, 1072-1078.

Mellon, S. H., Gong, W., Schonemann, M. D., 2008. Endogenous and synthetic neurosteroids in treatment of Niemann-Pick Type C disease. Brain Res Rev 57, 410-420.

Merabova, N., Kaminski, R., Krynska, B., Amini, S., Khalili, K., Darbinyan, A., 2012. JCV agnoprotein-induced reduction in CXCL5/LIX secretion by oligodendrocytes is associated with activation of apoptotic signaling in neurons. J Cell Physiol 227, 3119-3127.

Millard, E. E., Gale, S. E., Dudley, N., Zhang, J., Schaffer, J. E., Ory, D. S., 2005. The sterol-sensing domain of the Niemann-Pick C1 (NPC1) protein regulates trafficking of low density lipoprotein cholesterol. J Biol Chem 280, 28581-28590.

Mizutani, R., Nakamura, K., Kato, N., Aizawa, K., Miyamoto, Y., Torii, T., Yamauchi, J., Tanoue, A., 2012. Expression of sorting nexin 12 is regulated in developing cerebral cortical neurons. J Neurosci Res 90, 721-731.

Mizutani, R., Nakamura, K., Yokoyama, S., Sanbe, A., Kusakawa, S., Miyamoto, Y., Torii, T., Asahara, H., Okado, H., Yamauchi, J., Tanoue, A., 2011. Developmental expression of sorting nexin 3 in the mouse central nervous system. Gene Expr Patterns 11, 33-40.

Mizutani, R., Yamauchi, J., Kusakawa, S., Nakamura, K., Sanbe, A., Torii, T., Miyamoto, Y., Tanoue, A., 2009. Sorting nexin 3, a protein upregulated by lithium, contains a novel phosphatidylinositol-binding sequence and mediates neurite outgrowth in N1E-115 cells. Cell Signal 21, 1586-1594.

Montecucco, F., Burger, F., Mach, F., Steffens, S., 2008. CB2 cannabinoid receptor agonist JWH-015 modulates human monocyte migration through defined intracellular signaling pathways. Am J Physiol Heart Circ Physiol 294, H1145-1155.

Munana, K. R., Luttgen, P. J., Thrall, M. A., Mitchell, T. W., Wenger, D. A., 1994. Neurological manifestations of Niemann-Pick disease type C in cats. J Vet Intern Med 8, 117-121.

Nakazawa, S., Gotoh, N., Matsumoto, H., Murayama, C., Suzuki, T., Yamamoto, T., 2011. Expression of Sorting Nexin 18 (SNX18) Is Dynamically Regulated in Developing Spinal Motor Neurons. J Histochem Cytochem 59, 202-213.

Naldini, L., Blomer, U., Gage, F. H., Trono, D., Verma, I. M., 1996a. Efficient transfer, integration, and sustained long-term expression of the transgene in adult rat brains injected with a lentiviral vector. Proc Natl Acad Sci U S A 93, 11382-11388.

Naldini, L., Blomer, U., Gallay, P., Ory, D., Mulligan, R., Gage, F. H., Verma, I. M., Trono, D., 1996b. In vivo gene delivery and stable transduction of nondividing cells by a lentiviral vector. Science 272, 263-267.

Naldini, L., Verma, I. M., 2000. Lentiviral vectors. Adv Virus Res 55, 599-609.

Nelson, D. E., Ihekwaba, A. E., Elliott, M., Johnson, J. R., Gibney, C. A., Foreman, B. E., Nelson, G., See, V., Horton, C. A., Spiller, D. G., Edwards, S. W., McDowell, H. P., Unitt, J. F., Sullivan, E., Grimley, R., Benson, N., Broomhead, D., Kell, D. B., White, M. R., 2004. Oscillations in NF-kappaB signaling control the dynamics of gene expression. Science 306, 704-708.

Nohturfft, A., Yabe, D., Goldstein, J. L., Brown, M. S., Espenshade, P. J., 2000. Regulated step in cholesterol feedback localized to budding of SCAP from ER membranes. Cell 102, 315-323.

Omari, K. M., John, G. R., Sealfon, S. C., Raine, C. S., 2005. CXC chemokine receptors on human oligodendrocytes: implications for multiple sclerosis. Brain 128, 1003-1015.

Palu, G., Parolin, C., Takeuchi, Y., Pizzato, M., 2000. Progress with retroviral gene vectors. Rev Med Virol 10, 185-202.

Panini, S. R., Sexton, R. C., Rudney, H., 1984. Regulation of 3-hydroxy-3-methylglutaryl coenzyme A reductase by oxysterol by-products of cholesterol biosynthesis. Possible mediators of low density lipoprotein action. J Biol Chem 259, 7767-7771.

Park, D. S., So, H. S., Lee, J. H., Park, H. Y., Lee, Y. J., Cho, J. H., Yoon, K. H., Park, C., Yun, K., Park, R., 2009. Simvastatin treatment induces morphology alterations and apoptosis in murine cochlear neuronal cells. Acta Otolaryngol 129, 166-174.

Patel, S. C., Suresh, S., Kumar, U., Hu, C. Y., Cooney, A., Blanchette-Mackie, E. J., Neufeld, E. B., Patel, R. C., Brady, R. O., Patel, Y. C., Pentchev, P. G., Ong, W. Y., 1999. Localization of Niemann-Pick C1 protein in astrocytes: implications for neuronal degeneration in Niemann- Pick type C disease. Proc Natl Acad Sci U S A 96, 1657-1662.

Patterson, M. C., Di Bisceglie, A. M., Higgins, J. J., Abel, R. B., Schiffmann, R., Parker, C. C., Argoff, C. E., Grewal, R. P., Yu, K., Pentchev, P. G., et al., 1993. The effect of cholesterol-lowering agents on hepatic and plasma cholesterol in Niemann-Pick disease type C. Neurology 43, 61-64.

Pease, J. E., 2011. Targeting chemokine receptors in allergic disease. Biochem J 434, 11-24.

Peden, C. S., Burger, C., Muzyczka, N., Mandel, R. J., 2004. Circulating anti-wild-type adeno-associated virus type 2 (AAV2) antibodies inhibit recombinant AAV2 (rAAV2)-mediated, but not rAAV5-mediated, gene transfer in the brain. J Virol 78, 6344-6359.

Peng, H., Kolb, R., Kennedy, J. E., Zheng, J., 2007. Differential expression of CXCL12 and CXCR4 during human fetal neural progenitor cell differentiation. J Neuroimmune Pharmacol 2, 251-258.

Pentchev, P. G., Boothe, A. D., Kruth, H. S., Weintroub, H., Stivers, J., Brady, R. O., 1984. A genetic storage disorder in BALB/C mice with a metabolic block in esterification of exogenous cholesterol. J Biol Chem 259, 5784-5791.

Perlman, S. J., Mar, S., 2012. Leukodystrophies. Adv Exp Med Biol 724, 154-171.

Perry, V. H., 2007. Stress primes microglia to the presence of systemic inflammation: implications for environmental influences on the brain. Brain Behav Immun 21, 45-46.

Peter, B. J., Kent, H. M., Mills, I. G., Vallis, Y., Butler, P. J., Evans, P. R., McMahon, H. T., 2004. BAR domains as sensors of membrane curvature: the amphiphysin BAR structure. Science 303, 495-499.

Phillips, S. E., Woodruff, E. A., 3rd, Liang, P., Patten, M., Broadie, K., 2008. Neuronal loss of Drosophila NPC1a causes cholesterol aggregation and age-progressive neurodegeneration. J Neurosci 28, 6569-6582.

Phillips, W. A., Avigan, J., 1963. Inhibition of cholesterol biosynthesis in the rat by 3 beta-(2-diethylaminoethoxy) androst5-en-17-one hydrochloride. Proc Soc Exp Biol Med 112, 233-236.

Pineda, M., Wraith, J. E., Mengel, E., Sedel, F., Hwu, W. L., Rohrbach, M., Bembi, B., Walterfang, M., Korenke, G. C., Marquardt, T., Luzy, C., Giorgino, R., Patterson, M. C., 2009. Miglustat in patients with Niemann-Pick disease Type C (NP-C): a multicenter observational retrospective cohort study. Mol Genet Metab 98, 243-249.

Platt, F. M., Neises, G. R., Dwek, R. A., Butters, T. D., 1994. N-butyldeoxynojirimycin is a

novel inhibitor of glycolipid biosynthesis. J Biol Chem 269, 8362-8365.

Pluta, K., Kacprzak, M. M., 2009. Use of HIV as a gene transfer vector. Acta Biochim Pol 56, 531-595.

Quan, G., Xie, C., Dietschy, J. M., Turley, S. D., 2003. Ontogenesis and regulation of cholesterol metabolism in the central nervous system of the mouse. Brain Res Dev Brain Res 146, 87-98.

Ransohoff, R. M., Brown, M. A., 2012. Innate immunity in the central nervous system. J Clin Invest 122, 1164-1171.

Ransohoff, R. M., Liu, L., Cardona, A. E., 2007. Chemokines and chemokine receptors: multipurpose players in neuroinflammation. Int Rev Neurobiol 82, 187-204.

Rawson, R. B., 2003. The SREBP pathway--insights from Insigs and insects. Nat Rev Mol Cell Biol 4, 631-640.

Rodal, A. A., Blunk, A. D., Akbergenova, Y., Jorquera, R. A., Buhl, L. K., Littleton, J. T., 2011. A presynaptic endosomal trafficking pathway controls synaptic growth signaling. J Cell Biol 193, 201-217.

Rojas, R., Kametaka, S., Haft, C. R., Bonifacino, J. S., 2007. Interchangeable but essential functions of SNX1 and SNX2 in the association of retromer with endosomes and the trafficking of mannose 6-phosphate receptors. Mol Cell Biol 27, 1112-1124.

Rutishauser, J., 2011. Statins in clinical medicine. Swiss Med Wkly 141, w13310.

Ryan, T. A., 2006. A pre-synaptic to-do list for coupling exocytosis to endocytosis. Curr Opin Cell Biol 18, 416-421.

Sadowski, L., Pilecka, I., Miaczynska, M., 2009. Signaling from endosomes: location makes a difference. Exp Cell Res 315, 1601-1609.

Sakuma, T., Barry, M. A., Ikeda, Y., 2012. Lentiviral vectors: basic to translational. Biochem J 443, 603-618.

Santa-Catalina, M. O., Garcia-Marin, L. J., Bragado, M. J., 2008. Lovastatin effect in rat neuroblasts of the CNS: inhibition of cap-dependent translation. J Neurochem 106, 1078-1091.

Sato, R., Takano, T., 1995. Regulation of intracellular cholesterol metabolism. Cell Struct Funct 20, 421-427.

Seaman, M. N., 2007. Identification of a novel conserved sorting motif required for retromer-mediated endosome-to-TGN retrieval. J Cell Sci 120, 2378-2389.

Seet, L. F., Hong, W., 2006. The Phox (PX) domain proteins and membrane traffic. Biochim Biophys Acta 1761, 878-896.

Sen, R., Smale, S. T., 2010. Selectivity of the NF-{kappa}B response. Cold Spring Harb Perspect Biol 2, a000257.

Seo, E., Kim, S., Jho, E. H., 2009. Induction of cancer cell-specific death via MMP2 promoterdependent Bax expression. BMB Rep 42, 217-222.

Serretti, A., Artioli, P., Quartesan, R., De Ronchi, D., 2005. Genes involved in Alzheimer's disease, a survey of possible candidates. J Alzheimers Dis 7, 331-353.

Sever, N., Yang, T., Brown, M. S., Goldstein, J. L., DeBose-Boyd, R. A., 2003. Accelerated degradation of HMG CoA reductase mediated by binding of insig-1 to its sterol-sensing domain. Mol Cell 11, 25-33.

Sheridan, G. K., Dev, K. K., 2012. S1P1 receptor subtype inhibits demyelination and regulates chemokine release in cerebellar slice cultures. Glia 60, 382-392.

Shermak, M. A., Wolfort, S. F., Thomas, D., Chang, B., 1998. A universal micro-suction mat to optimize TRAM breast reconstruction. Plast Reconstr Surg 102, 2276.

Shin, N., Lee, S., Ahn, N., Kim, S. A., Ahn, S. G., YongPark, Z., Chang, S., 2007. Sorting nexin 9 interacts with dynamin 1 and N-WASP and coordinates synaptic vesicle endocytosis. J Biol Chem 282, 28939-28950.

Singer, O., Marr, R. A., Rockenstein, E., Crews, L., Coufal, N. G., Gage, F. H., Verma, I. M., Masliah, E., 2005. Targeting BACE1 with siRNAs ameliorates Alzheimer disease neuropathology in a transgenic model. Nat Neurosci 8, 1343-1349.

Small, S. A., Kent, K., Pierce, A., Leung, C., Kang, M. S., Okada, H., Honig, L., Vonsattel, J. P., Kim, T. W., 2005. Model-guided microarray implicates the retromer complex in Alzheimer's disease. Ann Neurol 58, 909-919.

Smith, D., Wallom, K. L., Williams, I. M., Jeyakumar, M., Platt, F. M., 2009. Beneficial effects of anti-inflammatory

therapy in a mouse model of Niemann-Pick disease type C1. Neurobiol Dis 36, 242-251.

Snipes, G. J., Orfali, W., 1998. Common themes in peripheral neuropathy disease genes. Cell Biol Int 22, 815-835.

Solomon, D., Winkelman, A. C., Zee, D. S., Gray, L., Buttner-Ennever, J., 2005. Niemann-Pick type C disease in two affected sisters: ocular motor recordings and brain-stem neuropathology. Ann N Y Acad Sci 1039, 436-445.

Somers, K. L., Royals, M. A., Carstea, E. D., Rafi, M. A., Wenger, D. A., Thrall, M. A., 2003. Mutation analysis of feline Niemann-Pick C1 disease. Mol Genet Metab 79, 99-103.

Soriano, S. G., Piva, S., 2008. Central nervous system inflammation. Eur J Anaesthesiol Suppl 42, 154-159.

Spencer, B., Marr, R. A., Rockenstein, E., Crews, L., Adame, A., Potkar, R., Patrick, C., Gage, F. H., Verma, I. M., Masliah, E., 2008. Long-term neprilysin gene transfer is associated with reduced levels of intracellular Abeta and behavioral improvement in APP transgenic mice. BMC Neurosci 9, 109.

Spencer, B., Potkar, R., Trejo, M., Rockenstein, E., Patrick, C., Gindi, R., Adame, A., Wyss-Coray, T., Masliah, E., 2009. Beclin 1 gene transfer activates autophagy and ameliorates the neurodegenerative pathology in alpha-synuclein models of Parkinson's and Lewy body diseases. J Neurosci 29, 13578-13588.

Sriram, K., Matheson, J. M., Benkovic, S. A., Miller, D. B., Luster, M. I., O'Callaghan, J. P., 2006. Deficiency of TNF receptors suppresses microglial activation and alters the susceptibility of brain regions to MPTP-induced neurotoxicity: role of TNF-alpha. FASEB J 20, 670-682.

Stanislaus, R., Singh, A. K., Singh, I., 2001. Lovastatin treatment decreases mononuclear cell infiltration into the CNS of Lewis rats with experimental allergic encephalomyelitis. J Neurosci Res 66, 155-162.

Steffens, S., Montecucco, F., Mach, F., 2009. The inflammatory response as a target to reduce myocardial ischaemia and reperfusion injury. Thromb Haemost 102, 240-247.

Steinke, J. W., Borish, L., 2006. 3. Cytokines and chemokines. J Allergy Clin Immunol 117, S441-445.

Strochlic, T. I., Setty, T. G., Sitaram, A., Burd, C. G., 2007. Grd19/Snx3p functions as a cargo-specific adapter for retromer-dependent endocytic recycling. J Cell Biol 177, 115-125.

Sugimoto, Y., Ninomiya, H., Ohsaki, Y., Higaki, K., Davies, J. P., Ioannou, Y. A., Ohno, K., 2001. Accumulation of cholera toxin and GM1 ganglioside in the early endosome of Niemann-Pick C1-deficient cells. Proc Natl Acad Sci U S A 98, 12391-12396.

Suzuki, M., Sugimoto, Y., Ohsaki, Y., Ueno, M., Kato, S., Kitamura, Y., Hosokawa, H., Davies, J. P., Ioannou, Y. A., Vanier, M. T., Ohno, K., Ninomiya, H., 2007. Endosomal accumulation of Toll-like receptor 4 causes constitutive secretion of cytokines and activation of signal transducers and activators of transcription in Niemann-Pick disease type C (NPC) fibroblasts: a potential basis for glial cell activation in the NPC brain. J Neurosci 27, 1879-1891.

Sym, M., Basson, M., Johnson, C., 2000. A model for niemann-pick type C disease in the nematode Caenorhabditis elegans. Curr Biol 10, 527-530.

Takata, K., Kitamura, Y., 2012. Molecular approaches to the treatment, prophylaxis, and diagnosis of Alzheimer's disease: tangle formation, amyloid-beta, and microglia in Alzheimer's disease. J Pharmacol Sci 118, 331-337.

Tang, Y., Li, H., Liu, J. P., 2009. Niemann-Pick Disease Type C: From Molecule To Clinic. Clin Exp Pharmacol Physiol.

Teasdale, R. D., Collins, B. M., 2012. Insights into the PX (phox-homology) domain and SNX (sorting nexin) protein families: structures, functions and roles in disease. Biochem J 441, 39-59.

Thelen, M., 2001. Dancing to the tune of chemokines. Nat Immunol 2, 129-134.

Thiele, C., Hannah, M. J., Fahrenholz, F., Huttner, W. B., 2000. Cholesterol binds to synaptophysin and is required for biogenesis of synaptic vesicles. Nat Cell Biol 2, 42-49.

Tong, J., Borbat, P. P., Freed, J. H., Shin, Y. K., 2009. A scissors mechanism for stimulation of SNARE-mediated lipid

mixing by cholesterol. Proc Natl Acad Sci U S A 106, 5141-5146.

Trebst, C., Sorensen, T. L., Kivisakk, P., Cathcart, M. K., Hesselgesser, J., Horuk, R., Sellebjerg, F., Lassmann, H., Ransohoff, R. M., 2001. CCR1+/CCR5+ mononuclear phagocytes accumulate in the central nervous system of patients with multiple sclerosis. Am J Pathol 159, 1701-1710.

Vance, J. E., Hayashi, H., Karten, B., 2005. Cholesterol homeostasis in neurons and glial cells. Semin Cell Dev Biol 16, 193-212.

Vanier, M. T., Millat, G., 2003. Niemann-Pick disease type C. Clin Genet 64, 269-281.

Vogt VM, S. M., 1999. Mass determination of rous sarcoma virus virions by scanning transmission electron microscopy. Journal of Virology 73, 7050-7055.

Volin, M. V., Koch, A. E., 2011. Interleukin-18: a mediator of inflammation and angiogenesis in rheumatoid arthritis. J Interferon Cytokine Res 31, 745-751.

Wakabayashi, K., Matsumoto, K., Takayama, K., Yoshimoto, M., Takahashi, H., 1997. NACP, a presynaptic protein, immunoreactivity in Lewy bodies in Parkinson's disease. Neurosci Lett 239, 45-48.

Walkley, S. U., Suzuki, K., 2004. Consequences of NPC1 and NPC2 loss of function in mammalian neurons. Biochim Biophys Acta 1685, 48-62.

Wang, J. T., Kerr, M. C., Karunaratne, S., Jeanes, A., Yap, A. S., Teasdale, R. D., 2010. The SNX-PX-BAR family in macropinocytosis: the regulation of macropinosome formation by SNX-PX-BAR proteins. PLoS One 5, e13763.

Watari, H., Blanchette-Mackie, E. J., Dwyer, N. K., Sun, G., Glick, J. M., Patel, S., Neufeld, E. B., Pentchev, P. G., Strauss, J. F., 3rd, 2000. NPC1-containing compartment of human granulosa-lutein cells: a role in the intracellular trafficking of cholesterol supporting steroidogenesis. Exp Cell Res 255, 56-66.

Westmoreland, S. V., Alvarez, X., deBakker, C., Aye, P., Wilson, M. L., Williams, K. C., Lackner, A. A., 2002. Developmental expression patterns of CCR5 and CXCR4 in the rhesus macaque brain. J Neuroimmunol 122, 146-158.

Wichmann, T., DeLong, M. R., 2003. Pathophysiology of Parkinson's disease: the MPTP primate model of the human disorder. Ann N Y Acad Sci 991, 199-213.

Wolozin, B., Kellman, W., Ruosseau, P., Celesia, G. G., Siegel, G., 2000. Decreased prevalence of Alzheimer disease associated with 3-hydroxy-3-methyglutaryl coenzyme A reductase inhibitors. Arch Neurol 57, 1439-1443.

Worby, C. A., Simonson-Leff, N., Clemens, J. C., Huddler, D., Jr., Muda, M., Dixon, J. E., 2002. Drosophila Ack targets its substrate, the sorting nexin DSH3PX1, to a protein complex involved in axonal guidance. J Biol Chem 277, 9422-9428.

Worby, C. A., Simonson-Leff, N., Clemens, J. C., Kruger, R. P., Muda, M., Dixon, J. E., 2001. The sorting nexin, DSH3PX1, connects the axonal guidance receptor, Dscam, to the actin cytoskeleton. J Biol Chem 276, 41782-41789.

Wraith, J. E., Baumgartner, M. R., Bembi, B., Covanis, A., Levade, T., Mengel, E., Pineda, M., Sedel, F., Topcu, M., Vanier, M. T., Widner, H., Wijburg, F. A., Patterson, M. C., 2009. Recommendations on the diagnosis and management of Niemann-Pick disease type C. Mol Genet Metab 98, 152-165.

Wraith, J. E., Imrie, J., 2009. New therapies in the management of Niemann-Pick type C disease: clinical utility of miglustat. Ther Clin Risk Manag 5, 877-887.

Wu, D., Tang, Y. P., Wade, J., 2010. Co-localization of sorting nexin 2 and androgen receptor in the song system of juvenile zebra finches. Brain Res 1343, 104-111.

Wu, Y. P., Mizukami, H., Matsuda, J., Saito, Y., Proia, R. L., Suzuki, K., 2005. Apoptosis accompanied by up-regulation of TNF-alpha death pathway genes in the brain of Niemann-Pick type C disease. Mol Genet Metab 84, 9-17.

Wu, Y. P., Proia, R. L., 2004. Deletion of macrophage-inflammatory protein 1 alpha retards neurodegeneration in Sandhoff disease mice. Proc Natl Acad Sci U S A 101, 8425-8430.

Xie, C., Lund, E. G., Turley, S. D., Russell, D. W., Dietschy, J. M., 2003. Quantitation of two pathways for cholesterol excretion from the brain in normal mice and mice with

neurodegeneration. J Lipid Res 44, 1780-1789.

Yang, T., Espenshade, P. J., Wright, M. E., Yabe, D., Gong, Y., Aebersold, R., Goldstein, J. L., Brown, M. S., 2002. Crucial step in cholesterol homeostasis: sterols promote binding of SCAP to INSIG-1, a membrane protein that facilitates retention of SREBPs in ER. Cell 110, 489-500.

Yang, Z., Zhang, Z., Wen, J., Wang, X., Lu, B., Zhang, W., Wang, M., Feng, X., Ling, C., Wu, S., Hu, R., 2010. Elevated serum chemokine CXC ligand 5 levels are associated with hypercholesterolemia but not a worsening of insulin resistance in Chinese people. J Clin Endocrinol Metab 95, 3926-3932.

Yanjanin NM, V. J., Gropman A, et al. , 2009. Linear clinical preogression independent of onset, in Niemann-Pick disease Type C. . An J Med Genet B Neuropsychiatr Genet.

Yarar, D., Waterman-Storer, C. M., Schmid, S. L., 2007. SNX9 couples actin assembly to phosphoinositide signals and is required for membrane remodeling during endocytosis. Dev Cell 13, 43-56.

Yu, W., Gong, J. S., Ko, M., Garver, W. S., Yanagisawa, K., Michikawa, M., 2005. Altered cholesterol metabolism in Niemann-Pick type C1 mouse brains affects mitochondrial function. J Biol Chem 280, 11731-11739.

Zampieri, S., Mellon, S. H., Butters, T. D., Nevyjel, M., Covey, D. F., Bembi, B., Dardis, A., 2009. Oxidative stress in NPC1 deficient cells: protective effect of allopregnanolone. J Cell Mol Med 13, 3786-3796.

Zaremba, J., Skrobanski, P., Losy, J., 2006. The level of chemokine CXCL5 in the cerebrospinal fluid is increased during the first 24 hours of ischaemic stroke and correlates with the size of early brain damage. Folia Morphol (Warsz) 65, 1-5.

Zervas, M., Somers, K. L., Thrall, M. A., Walkley, S. U., 2001. Critical role for glycosphingolipids in Niemann-Pick disease type C. Curr Biol 11, 1283-1287.

Zhang, X. Y., La Russa, V. F., Reiser, J., 2004. Transduction of bone-marrow-derived mesenchymal stem cells by using lentivirus vectors pseudotyped with modified RD114 envelope glycoproteins. J Virol 78, 1219-1229.

Zhao, X., Wen, L., Li, G., Ba, Q., Cui, Y., Han, Z., Jia, Y., Xu, Y., 2011. Lentivirus-mediated APP695-RNAi reduces apoptosis in APP transgenic mouse neurons. Neuroreport 22, 804-808.

Zhao, Y., Wang, Y., Yang, J., Wang, X., Zhang, X., Zhang, Y. W., 2012. Sorting nexin 12 interacts with BACE1 and regulates BACE1-mediated APP processing. Mol Neurodegener 7, 30.

Zhong, Q., Lazar, C. S., Tronchere, H., Sato, T., Meerloo, T., Yeo, M., Songyang, Z., Emr, S. D., Gill, G. N., 2002. Endosomal localization and function of sorting nexin 1. Proc Natl Acad Sci U S A 99, 6767-6772.

Zimmerberg, J., McLaughlin, S., 2004. Membrane curvature: how BAR domains bend bilayers. Curr Biol 14, R250-252.

Zwijnenburg, P. J., de Bie, H. M., Roord, J. J., van der Poll, T., van Furth, A. M., 2003. Chemotactic activity of CXCL5 in cerebrospinal fluid of children with bacterial meningitis. J Neuroimmunol 145, 148-153.